

AD-R137 555

EQUATORIAL SCINTILLATION OF SATELLITE SIGNALS AND SOME
DRIFT CHARACTERISTICS OF THE SCINTILLATION(U) NAVAL
OCEAN SYSTEMS CENTER SAN DIEGO CA M R PAULSON

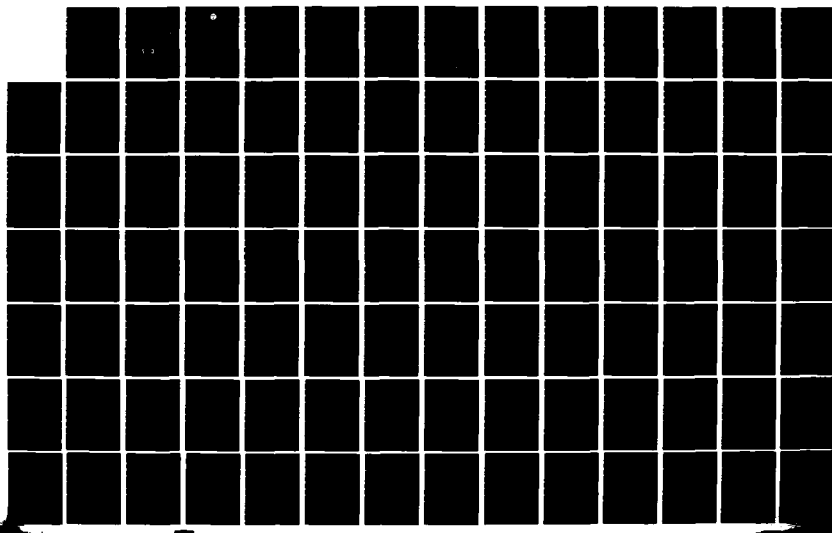
1/3

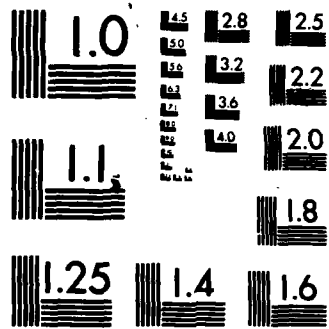
UNCLASSIFIED

15 OCT 83 NOSC/TR-911

F/G 28/14

NL





MICROCOPY RESOLUTION TEST CHART
NATIONAL BUREAU OF STANDARDS-1963-A

(12)

NOSC TR 911
AD A137555

NOSC TR 911

Technical Report 911

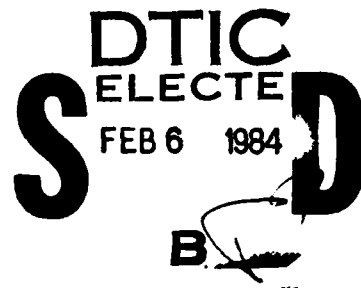
EQUATORIAL SCINTILLATION OF SATELLITE SIGNALS AND SOME DRIFT CHARACTERISTICS OF THE SCINTILLATION

M. R. Paulson

15 October 1983
Final Report
October 1981 — August 1983

Prepared for
Naval Air Systems Command

Approved for public release; distribution unlimited.



DTIC FILE COPY

NOSC

NAVAL OCEAN SYSTEMS CENTER

San Diego, California 92152

84 02 06 009



NAVAL OCEAN SYSTEMS CENTER SAN DIEGO, CA 92152

AN ACTIVITY OF THE NAVAL MATERIAL COMMAND

J.M. PATTON, CAPT, USN

Commander

R.M. HILLYER

Technical Director

ADMINISTRATIVE INFORMATION

The work reported on in this document was funded by the Naval Air Systems Command (NAIR-330) under program element 62759N, project F59551, subproject SF59-551-697, work unit MP33F.

Released by

J.H. Richter, Head

Ocean & Atmospheric Sciences Division

Under authority of

J.D. Hightower, Head

Environmental Sciences Department

ACKNOWLEDGMENTS

The uhf-spaced received data and the L-band data were recorded by personnel of the Satellite Communications Division at the Naval Communication Area Master Station (NAVCAMS) in Guam. We would like to express our appreciation for their assistance. We also appreciate the efforts of ETC C.F. Troy and ET1 G.S. Zeno to keep the equipment working properly.

Our appreciation also goes to the various personnel of Division 34 at the NAVCAMS who have provided the Naval Ocean Systems Center with uhf scintillation data since 1978.

UNCLASSIFIED

SECURITY CLASSIFICATION OF THIS PAGE (When Data Entered)

REPORT DOCUMENTATION PAGE		READ INSTRUCTIONS BEFORE COMPLETING FORM
1. REPORT NUMBER NOSC Technical Report 911 (TR 911)	2. GOVT ACCESSION NO. A137555	3. RECIPIENT'S CATALOG NUMBER
4. TITLE (and Subtitle) EQUATORIAL SCINTILLATION OF SATELLITE SIGNALS AND SOME DRIFT CHARACTERISTICS OF THE SCINTILLATION		5. TYPE OF REPORT & PERIOD COVERED Final October 1981–August 1983
		6. PERFORMING ORG. REPORT NUMBER
7. AUTHOR(s) M.R. Paulson		8. CONTRACT OR GRANT NUMBER(s)
9. PERFORMING ORGANIZATION NAME AND ADDRESS Naval Ocean Systems Center Code 5324 San Diego, CA 92152		10. PROGRAM ELEMENT, PROJECT, TASK AREA & WORK UNIT NUMBERS 62759N, F59551, SF59-551-697, MP33F
11. CONTROLLING OFFICE NAME AND ADDRESS P. Twitchell Naval Air Systems Command (NAIR-330)		12. REPORT DATE 15 October 1983
14. MONITORING AGENCY NAME & ADDRESS (if different from Controlling Office)		13. NUMBER OF PAGES 194
		15. SECURITY CLASS. (of this report) Unclassified
		15a. DECLASSIFICATION/DOWNGRADING SCHEDULE
16. DISTRIBUTION STATEMENT (of this Report) Approved for public release; distribution unlimited.		
17. DISTRIBUTION STATEMENT (of the abstract entered in Block 20, if different from Report)		
18. SUPPLEMENTARY NOTES		
19. KEY WORDS (Continue on reverse side if necessary and identify by block number) Equatorial scintillations Ultrahigh frequency L-band frequencies Equatorial drift Solar activity Drift winds Satellite scintillations Seasonal variations		
20. ABSTRACT (Continue on reverse side if necessary and identify by block number) > Vhf/uhf satellite signals from the Pacific FleetSat have been monitored in Guam from April 1982 through 1 May 1983 to study the drift characteristics of equatorial scintillation. Two receivers spaced 1500 feet (457 metres) apart in an east-west direction were used. In addition, one receiver was used to monitor the L-band signals from the Pacific MariSat. Occurrence and intensity of equatorial scintillation are compared to drift velocities and geomagnetic and solar activity. Drift velocities and geomagnetic activity are also compared.		

SUMMARY

OBJECTIVE

To investigate the drift characteristics of equatorial scintillation of satellite signals to identify the generating mechanism for the ionospheric irregularities which cause the scintillations. Also, to determine how the various solar and geophysical phenomena contribute to the occurrence and intensity of equatorial scintillation.

RESULTS

Comparison of equatorial scintillation and east-west drift during the 1982-83 period is much more complicated than that during 1976. Maximum scintillation intensity frequently occurred long after the maximum drift velocity. However, the amount of delay was quite variable. It could be as little as 10 or 15 minutes or as much as 4 or 5 hours.

The drift velocity showed a consistent eastward drift through most of the night. When scintillation started early in the evening the velocity started at a low value and quickly increased to a maximum, then showed a general decrease through the night. However this pattern varied some, for at times the velocity would increase again later at night.

On three or four nights there was an apparent westward drift for a short while right after sunset, before the drift to the east began. This may have been caused by upward drift, since the spaced receiver technique cannot distinguish between vertical and horizontal movement.

For 19 nights the drift velocity changed to a westward drift at, or near, sunrise and continued into the daylight hours. Average westward drift velocities for these days were compared to the various 3-hour K_p indices for the corresponding days and the K_p index measurements centered around 0300 GMT had a correlation of +0.800. This was about 16 to 18 hours delay between the geomagnetic activity and the drift velocity.

Average drift velocities for the period 1100-1400 GMT (2100-2400 LST) were also calculated for 38 nights and compared with the 3-hour K_p indices for the corresponding nights. These show a correlation of -0.729 with K_p measurements centered around 0600 GMT for a delay of 6 or 7 hours between geomagnetic activity and the drift velocity.

At times, the eleven-day running averages of the scintillation occurrences and of the daily average geomagnetic K_p indices, showed dips in the scintillation occurrence which corresponded to increases in geomagnetic activity. This was particularly evident during the first half of 1979 and on several occasions in 1980. There was more periodic variation in scintillation, however, than accounted for by the variation in geomagnetic activity.

Correlation between the unsmoothed occurrence of scintillation and daily average geomagnetic activity ranged from -0.54 through zero to +0.47, depending on the length of the data sample used and the time of year considered.

Seasonal variation of the scintillation occurrence showed the December-January minimum observed in the Pacific region, with a secondary minimum in June-July for the low-elevation-angle Indian Ocean satellite. This secondary minimum starts to show for the Pacific Ocean satellite (elevation angle 55 degrees) in the 1982 data.

A comparison of the occurrence of scintillation with solar activity on a year-to-year basis using a common 4-month data sample showed the same positive dependence previously observed with shorter common 11-day data samples.

RECOMMENDATIONS .

Probably the greatest limitation of using the spaced receiver technique to study drift characteristics of scintillation is the inability to monitor drift when there is no scintillation and when cross correlations are low. Some method for continuously monitoring drift is needed. A geostationary satellite with several frequencies from about 40 to 1000 MHz might be useful for this purpose if the lowest frequency was sufficiently affected by irregularities in the ionosphere when there was no scintillation on the higher frequencies. The higher frequencies could be used during periods of intense scintillation.

The relationship between drift and equatorial scintillation should be further investigated during the next solar minimum to see if the good agreement observed in 1976 is again evident. It is possible that the greater variability observed in the 1982-83 data was the result of a greatly expanded atmosphere caused by greater solar heating.

CONTENTS

	Page
Introduction.....	1
Description of the Experimental Program.....	2
Data Analysis and Results.....	3
Drift and Intensity Calculations.....	3
Scintillation Intensity Versus Drift Velocity.....	4
L-band Scintillation Versus uhf Scintillation.....	5
Drift Versus Geomagnetic Activity.....	6
East-to-West Drift of Equatorial Scintillation.....	6
Altitude of the Ionospheric Irregularities.....	8
Additional Scintillation Measurements.....	10
Seasonal Variation of Equatorial Scintillation.....	10
Scintillation Versus Geomagnetic Activity.....	10
Scintillation Versus Solar Activity.....	11
Summary.....	13
References.....	14

REF ID: A6491

Accession For	
NTIS GRA&I <input checked="" type="checkbox"/>	
DTIC TAB <input type="checkbox"/>	
Unannounced <input type="checkbox"/>	
Justification.....	
By.....	
Distribution/.....	
Availability Codes	
Dist	Avail and/or Special
A1	

INTRODUCTION

Equatorial scintillation can have very disruptive effects on vhf/uhf satellite communications. This condition has been recognized since operation at equatorial sites began with TACSAT-1 in the early 1970s. As operations of vhf/uhf satellite communications networks have increased, the extent of the problem has become more widely recognized.

The scintillation of radio waves from a satellite is caused by irregularities in the electron density of the ionosphere. These irregularities usually occur in the F-region of the ionosphere, at an altitude of about 200-400 km (Koster, 1972). The electron density irregularities cause corresponding irregularities in the refractive index of the ionosphere. This results in variations in the propagation velocity of the radio wave through different portions of the ionosphere. As the radio waves pass through the ionosphere they are diffracted, or refracted, by these regions. This results in an irregular wave front which emerges from the ionosphere and then propagates to the ground, where a standing wave pattern is set up. As the ionospheric irregularities drift and change, the standing wave pattern moves across the ground, causing the intensity of a signal received on an antenna to fluctuate. Signal enhancements of up to 10 dB and fades of more than 30 dB occur regularly at frequencies around 250 MHz.

There have been many theories proposed for the generation of the irregularities in the electron density in the ionosphere. None of the theories presented so far, however, have been accepted as explanations of all the observed effects.

Farley et al. (1970) reported results that ruled out most theories for the generation of irregularities and stated that gradients of density and drift velocity remain as possible causes.

Koster (1972) considers ways in which ionospheric irregularities could be generated. He finds that the seasonal variation of equatorial scintillation has more of an annual, rather than a semi-annual, variation with a pronounced minimum during the northern solstice month. This, he says, is remarkably similar to the variation in thermospheric temperature observed by Jacchia (1967). He suggests that the velocity of the neutral atmospheric wind at F-region heights is a function of atmospheric temperature and that the production of F-region irregularities is closely associated with the velocity of this wind.

In 1976 some spaced-receiver measurements of equatorial scintillation were made in Guam (Paulson and Hopkins, 1977). Examples of the results of these measurements are shown in figures 1 and 2. These measurements suggested that the east-west component of the scintillation drift velocity might be used as an indication of zonal winds at F-region heights. Because measurements were made for only two months and 1976 was a year of minimum solar activity the available data were quite limited. For this reason an additional measurement program was undertaken to more thoroughly evaluate this idea.

The measurements were begun in late April 1982 and continued to 1 May 1983. While one of the main objectives of the program was to investigate the drift characteristics of equatorial scintillation, other aspects of the scintillation were of equal interest.

DESCRIPTION OF THE EXPERIMENTAL PROGRAM

The measurement equipment was located at the Naval Communication Area Master Station (NAVCAMS) in Guam and was operated by personnel of the Satellite Communications Division (Division 31). Signals from the uhf broadcast channel of the Pacific Fleet Satellite were received on two antennas separated 1500 feet (457 metres) in the magnetic east-west direction. These signals were brought back to a central point on buried coaxial cable and their amplitudes were recorded on two channels of an analog magnetic tape recorder.

Also, at the center, a receiver monitored the L-band beacon of the Pacific Ocean Maritime Satellite and the amplitude of this signal was recorded on a third channel of the tape recorder. An IRIG B time code was recorded on the fourth channel.

Strip-chart recorders paralleled the L-band channel and one of the uhf channels. These charts were used for editing the tapes and for getting some statistical information on the occurrence of scintillation.

The elevation angle to the uhf satellite was about 55 degrees and that to the L-band satellite was about 50 degrees.

Starting in early 1978, personnel of Division 34 at NAVCAMS have provided the Naval Ocean Systems Center with uhf scintillation data. Some of these data were considered and documented in 1979 (Paulson, 1979), but more data have been received since then and also will be considered in this report.

DATA ANALYSIS AND RESULTS

DRIFT AND INTENSITY CALCULATIONS

The analog magnetic tape data were digitized at 12.5 times per second for periods when the uhf strip charts showed scintillations. The standard deviation divided by the mean was calculated for each 5-minute sample of data for both the uhf and the L-band. These were used as a measure of the intensity of the scintillation at the two frequencies.

Cross correlations between the two uhf channels were calculated for each of the 5-minute samples to determine the maximum correlation and its corresponding delay. Figure 3 shows some examples of these cross correlations. In general, the correlations were not plotted, but the computer searched for the maximum positive correlation and its corresponding delay. An east-west drift velocity component was calculated for each of these 5-minute data samples. These drift velocities, along with the corresponding uhf scintillation intensities, are plotted as a function of time for each night (figure 4) and are included in Appendix A. The same thing was done for the velocities and the L-band scintillation intensities and these are included in Appendix B. Figure 5 is an example of these.

The velocity component measured is called the apparent velocity. If all the changes in signal amplitude were caused by drift this would correspond to the true velocity. Because the irregularity structure changes with time as it drifts the measured velocity is somewhat higher than the drift velocity. This phenomenon has been investigated by several workers. Some of the early investigators were Briggs et al. (1950) and their work will be used here. They assume that plots of equal correlation in the space and time domain are ellipses. They then develop several methods for determining the true drift velocity. Rather than reproduce their work, only the results of the method used here will be presented. The reader is referred to the original for details.

For a one-dimensional ground, with distance in an east-west direction, two receiver sites are separated a distance, x_0 . If the time delay for maximum correlation is τ_0 , the apparent drift velocity is

$$v' = \frac{x_0}{\tau_0} \quad (1)$$

The characteristic velocity is given as

$$v_c = \frac{x_0 t_0}{t_0^2 + \tau_0^2} \quad (2)$$

and the true velocity is

$$v = \frac{x_0}{t_0^2 + \tau_0^2} \quad (3)$$

where t_0 is the time delay on the auto correlation at which the correlation equals the maximum cross correlation.

These equations were used to calculate the true east-west component of drift velocity for 17 nights and then compare that component to the apparent velocity. Figure 6 shows plots for 2 nights where the true velocity is shown

on the vertical axis and the apparent velocity is on the horizontal axis. For most of the points plotted the two velocities do not differ by much. Figure 7 shows the velocity difference as a percent of the true velocity plotted as a function of the maximum cross correlation value. From this we see the two velocities do not usually differ greatly for correlation values as low as about 0.7

Most of the time the cross correlations values were on the order of 0.7 or better, but at times, usually soon after scintillation started, the correlations would get so low that no maximum could be determined. This occurred in 1976 as well, even for receiver separations as little as 300 metres. Although the correlations became very low, the drift velocity apparently did not change greatly. The correlations for spaced receivers at L-band, as seen in figure 8, remained high and the time delay did not change much, even though the uhf cross correlation had no definite maximum.

Because the maximum correlations and time delays could not be determined for these periods of low correlation, true drift velocities were not routinely calculated. A much closer receiver separation would probably be needed to make this possible.

SCINTILLATION INTENSITY VERSUS DRIFT VELOCITY

Comparisons of equatorial scintillation with drift velocity for the 1976 data were quite good (figures 1 and 2). Cross correlations between drift velocity and equatorial scintillation were 0.7 and 0.9, respectively, for these two cases with the scintillation lagging behind the drift velocity by a few minutes.

Comparisons of scintillation intensity with drift velocity for the present data are not as simple as the limited results for 1976 would suggest. On nights when scintillation started in the early evening, the eastward component of the drift velocity started low and rapidly increased to a maximum. Then the eastward component usually would show a general decrease through the night, with some variations superimposed on the decrease. During nights when scintillation occurred for extended periods of time, the intensity also tended to decrease through the night.

The uhf scintillation intensity frequently reached a limiting condition. Examples of this can be seen in figure 4. When this occurs the L-band may be a more accurate measure of scintillation intensity.

When there is no scintillation and when cross correlations are low, the inability to measure drift velocity limits the ability to compare scintillation intensity and drift velocity. When scintillation starts early, so that velocities can be measured from initial low values, the scintillation intensity curve can lag the velocity curve by as little as 10 minutes up to 4 or 5 hours, as shown by figure 5 for L-band.

Cross correlations between drift velocity and scintillation intensity were calculated for many of the nights when the scintillation lasted long enough (table 1). In most cases, however, the delay for maximum correlations was too large a percentage of the data sample for the correlations to be trusted.

DAY JULIAN	FROM - GMT	TO GMT	VEL. US CORR.	UHF DELAY(MIN.)	VEL. US L-BAND CORR.	DELAY(MIN.)
113	10:00	18:00	0.66	45	0.62	50
114	10:30	19:40	0.79	45	0.77	50
115	09:45	18:30	0.68	10	0.82	45
140	10:00	19:30	0.62	10	0.65	15
153	11:20	18:40	0.70	30		
159	13:00	19:00	0.63	55		
160	12:30	19:20	0.59	45		
172	13:30	18:00	0.74	15	0.43	25
030	11:20	16:30	0.92	55		
056	11:15	16:30	0.87	50	0.47	60
076	13:20	17:00	0.90	35		

Table 1. Correlation between drift velocity and scintillation intensity. Velocity leads scintillation intensity.

Because the uhf scintillation often reached a limiting condition, it reduced the maximum correlation. This was not a problem with the L-band scintillation. The L-band signal, however, suffered from access modulation. Every time someone accessed another channel the amplitude of the beacon signal would step down a little. When two or three channels were accessed at the same time these steps could be as much as one or two dB. Access modulation had little effect when the L-band scintillation was strong, but was quite limiting for the weak scintillation.

L-BAND SCINTILLATION VERSUS UHF SCINTILLATION

No fade-by-fade correlation would be expected between the uhf and the L-band scintillation because of the great difference between the two frequencies. But, even more important is the fact that the two frequencies were being transmitted from different satellites, with the L-band satellite being about 4.5 degrees to the east of the uhf satellite.

Cross correlations were calculated between the scintillation intensity of the uhf and the L-band using the values of standard deviation divided by the mean for each of the 5-minute samples. This was done for many of the nights when the duration of the scintillation was reasonably long. The results are shown in table 2, where the positive delay times are consistent with a west-to-east drift. The delay times are only approximate, since the sample interval was 5 minutes. Also, because the total sample was on the order of hours, the delay time is the result of the average drift velocity.

DAY JULIAN	FROM GMT	TO GMT	UHF CORR	US L-BAND DELAY(MIN.)
113	10:45	16:40	0.75	4
114	10:05	16:50	0.76	4
116	11:15	14:20	0.85	7
117	11:15	14:40	0.77	8
124	10:30	15:30	0.62	5
125	9:10	12:30	0.82	8
126	11:00	17:00	0.66	10
127	11:00	16:00	0.65	7
128	11:00	18:00	0.74	6
131	10:00	17:00	0.72	5
133	12:55	16:10	0.61	15
140	9:30	15:30	0.60	10
142	12:00	18:00	0.62	15
145	11:30	17:30	0.73	8
146	8:30	15:30	0.82	10
155	10:00	16:00	0.61	10
157	12:45	18:00	0.61	18
169	11:00	17:00	0.64	8
170	10:15	18:15	0.78	10
172	11:00	17:00	0.65	10
173	10:30	18:30	0.61	12
183	12:10	17:30	0.66	10
239	10:10	15:10	0.73	4
240	10:00	16:45	0.60	8
243	11:45	18:45	0.74	4
244	09:30	14:30	0.65	4
245	10:05	18:00	0.71	8
246	09:40	17:00	0.71	3
262	09:30	15:45	0.66	5
265	19:00	24:00	0.80	-7
267	12:50	16:00	0.68	4
268	09:00	15:30	0.62	4
270	09:30	15:30	0.77	5
271	09:50	18:00	0.60	4
273	09:15	16:15	0.62	4

Table 2. Correlation between uhf and L-band scintillation intensities. For positive delays uhf leads L-band.

DRIFT VERSUS GEOMAGNETIC ACTIVITY

The drift velocity calculations were averaged from 2100 to 2400 LST for each night that scintillation activity occurred continuously. These average velocities were then correlated with each of the eight geomagnetic indices for the corresponding night. These correlations are shown in figure 9 as a function of the geomagnetic index measurement time. Here we see that the maximum negative correlation occurred between the second and third index measurement. This correlation was -0.729. A total of 38 nights was used. These data are plotted in figure 10, along with a least square fit to a straight line.

These data would suggest that, if there is a cause-effect relationship between geomagnetic activity and the equatorial drift, that it is negative and, there is about a six or seven hour delay. The data are very limited, however, and further investigation is needed to see if the relationship is continuous and how much variability there might be in the time delay. A continuous measurement of drift velocity would make this much easier.

EAST-TO-WEST DRIFT OF EQUATORIAL SCINTILLATION

Equatorial scintillation is essentially a nighttime phenomenon, with the scintillation starting some time after local sunset. Furthermore, the drift

velocity associated with the scintillation is usually from west to east. At times during our observations, however, the scintillation continued past local sunrise. When this occurred the velocity reversed direction and moved from east to west. Day 115 in figure 4 is an example of this. Here, the velocity reversed direction some time between 0600 and 0700 LST.

Additional days when scintillation and east-to-west drift occurred are listed in table 3. Typical westward velocities ranged from 10 to 100 or more metres/second. On Julian day 061 of 1983, however, a westward drift of 200 to 240 metres/second was observed around 0545-0600 LST. By 0630 LST this had decreased to below 100 metres/second. The previous night, day 060, eastward velocities of 200 to 240 metres/second were observed from about 2000 to 2230 LST.

YEAR 1982-1983		VELOCITY(METRES/SECOND)			
DAY	FROM(GMT)	TO(GMT)	FIRST MEASURABLE	MAX. MEASURABLE	SUM(Kp)
115	20:15	24:00	5	95	37+
145	19:40	23:00	7	33	15+
146	09:10	09:45	47	47	28
146	19:50	21:00	10	37	28
148	19:10	22:00	10	58	42
159	20:00	22:00	14	48	17
173	19:30	22:00	8	40	25-
186	19:45	21:35	14	41	7+
189	20:30	21:30	5	32	18
192	19:00	20:00	16	60	18
200	20:35	21:00	8	13	31-
265	19:00	24:00	24	112	54
341	20:35	21:50	24	32	28+
016	20:35	20:55	18	18	30
029	20:50	21:30	11	24	22+
036	20:20	21:30	36	136	57
038	09:35	09:50	87	197	37
038	13:40	23:00	5	69	37
043	14:40	15:30	11	32	32
052	19:35	20:10	12	22	36
061	19:45	24:00	43	238	
070	09:50	10:00	64	64	
084	18:25	22:00	18	127	
096	14:05	15:50	10	13	
103	14:10	16:15	12	40	
115	09:10	10:10	88	88	

Table 3. Occurrence of east-to-west scintillation drift. First measureable velocity is the first westward drift for which the correlation was good enough to calculate a velocity. Westward drift may have started earlier.

On nights 043, 096, and 103 the drift reversed direction earlier than usual, around 1400 to 1500 GMT, but in the case of day 043 it resumed an eastward drift at 1550 GMT, while for days 096 and 103 scintillation ended at 1550 and 1615 GMT, respectively.

For Julian days 146, 038, 070, and 115, westward drift occurred early in the evening near the onset of scintillation. It is difficult to think of something that would cause westward drift this early in the evening. However, with an elevation angle to the satellite of 55 degrees the spaced receiver technique cannot differentiate between vertical and horizontal drift. For this reason upward drift would look like westward drift.

Woodman (1970), as well as others, has reported upward ionospheric drift around local sunset. This appears to occur quite regularly, with some seasonal variations. There may be quite large night-to-night variations, however. Possibly the reason that the spaced receivers do not observe it more often is that the scintillation usually does not start this early, or that the cross correlations are too low to determine a time delay at these times.

There were probably more nights when east-to-west drift occurred, but because of equipment problems no velocities could be determined from Julian day 214 to day 255 and from day 267 to day 320.

A cross correlation between averaged westward drift velocities from 1900 GMT on and the summed daily geomagnetic K_p indices gave a value of +0.780. These average drift velocities were also correlated with the individual 3-hour K_p indices. A maximum correlation of +0.800 was obtained for K_p indices centered around 0300 GMT. This is about 16 to 18 hours before the center of the drift velocity measurement period. This positive correlation is in contrast with the -0.729 correlation measured for the pre-midnight drift velocities. Correlation maxima were quite broad in both cases, however, so the time of maximum correlation is not very precise.

A plot of these velocities as a function of the corresponding geomagnetic indices is shown in figure 11.

ALTITUDE OF THE IONOSPHERIC IRREGULARITIES

It should be possible to get an estimate of the height of the ionospheric irregularities from these data if we can assume that the height of the irregularities that are affecting the uhf is the same as that of the irregularities causing the L-band scintillation. While this may not seem to be a reasonable assumption, it was shown in 1976 that the drift velocities for the L-band were the same as those for the uhf. Figure 12 compares the cross correlations at uhf and at L-band for one 5-minute time interval. Of course it would be much better if nearly the same frequency were monitored from both satellites.

Data for several nights were taken in 2-minute samples and cross correlations were calculated at uhf for each sample to determine drift velocities. Standard deviations divided by the means were calculated for each sample at both uhf and L-band as an indication of scintillation intensity. Next, a period of time during the night (usually 2 hours or more, when L-band scintillation was significant) was selected and a cross correlation between the uhf and the L-band was calculated using these results. The time delay for maximum correlation was used along with the average drift for the same time period to determine average east-west separation of the propagation paths to the two satellites at the height of the ionospheric irregularities. This distance was used with figure 13, which is a graph of east-west path separation as a function of altitude, to determine the altitude of the irregularities. The results are shown in table 4. These altitudes ranged from 225 to 330 km.

DAY JULIAN	FROM GMT	TO GMT	CORR. 0.81	DELAY MIN.	U(AVE) M/S	DIST. KM	ALT. KM
124	10:30	12:30	0.81	6	127	46	330
126	09:00	11:00	0.82	3	172	31	225
141	14:00	17:00	0.53	6	85	31	225
258	11:00	13:15	0.59	5	138	41	300
265	19:00	24:00	0.80	-7	-90	38	280

Table 4. Average altitudes of ionospheric irregularities causing equatorial scintillations calculated for 5 nights.

Since data for several hours were used in each case, these heights can only be considered as average heights. It is quite possible that the height varied appreciably during the sample period. Also, because of the 2-minute sample length, time resolution was limited. This reduced the accuracy of the altitude determinations, particularly for the higher drift velocities.

The altitude for Julian day 265 was 280 km, even though this was essentially daytime scintillation. Rastogi and Mullen (1981) have also reported daytime scintillation. In their case, they attribute it to intense Sporadic-E which they observed on an ionospheric sounder. Sporadic-E usually occurs around 100 km altitude.

ADDITIONAL SCINTILLATION MEASUREMENTS

Personnel of Division 34 at the Naval Communications Area Master Station in Guam have been recording and sending to the Naval Ocean Systems Center records of the amplitude scintillation of uhf satellite signals since March 1978. Some of these data were discussed in an earlier report (Paulson, 1979). More data have been received since then.

The earlier data included records from both the Pacific Ocean satellite at an elevation angle of about 50 degrees, and the Indian Ocean satellite at an elevation angle of about 10 degrees. At the beginning of 1980 they discontinued monitoring the Pacific Ocean satellite.

SEASONAL VARIATION OF EQUATORIAL SCINTILLATION

The strip charts were read to determine time periods when uhf fading, due to scintillation, exceeded 6 dB. These periods were summed to give the total number of hours each night that scintillation fading exceeded 6 dB. These were then summed on a monthly basis and the percentage of time each month that scintillation occurred was determined. In the case of missing data, gaps were left and the data on either side of the missing data were summed separately. Figure 14 shows the results for the Indian Ocean satellite and figure 15 shows the results for the Pacific Ocean.

These plots show the minimum occurrence during December and January as reported earlier (Paulson, 1980). There is also a lesser decrease in occurrence during June and July for the Indian Ocean satellite. This decrease starts to become evident in the Pacific Ocean satellite data during 1982, as well.

SCINTILLATION VERSUS GEOMAGNETIC ACTIVITY

Eleven-day running averages of the 1979 data were calculated and plotted (Paulson, 1980). These plots showed a periodic variation in the occurrence, particularly for the first 6 months of the year. An 11-day running average of the daily average of the geomagnetic K_p index also shows a periodic variation of scintillation. These data are shown again in figure 16 for the Indian Ocean satellite data. The top graph is the occurrence of scintillation and the middle and bottom graphs are the 11-day running averages of the daily average magnetic K_p indices and of the 2800-MHz solar flux.

We used the same procedure for the Indian Ocean satellite data for the years 1980 and 1982. These are shown in figures 17 and 18. The 1980 data show sharp decreases in scintillation in two or three places which coincide with pronounced increases in geomagnetic activity. However, there are more periodic variations in the occurrence of scintillation than the geomagnetic activity can account for. The 1982 data are even less clear. In fact, there appears to be a positive correlation between geomagnetic activity and scintillation during the January-February period.

When the unsmoothed scintillation data and K_p data are compared for various time periods the correlations can vary from positive values through zero to negative values, depending on the time of year and the length of the data sample used. For the 1979 sample period, Julian days 30 to 180, the

correlation was -0.42. For the corresponding period in 1980, it was -0.34. For Julian days 335 to 365 in 1982 it was +0.47. Correlations for other time periods are shown in table 5.

YEAR	FROM	TO	CORR.	DELAY
1979	030	090	-0.54	0
1979	030	120	-0.51	0
1979	030	180	-0.42	0
1979	030	330	-0.27	0
1979	180	300	-0.20	0
1980	001	031	+0.37	0
1980	030	090	-0.47	0
1980	030	180	-0.34	0
1980	030	330	-0.32	0
1980	180	300	-0.31	0
1980	274	330	-0.43	0
1982	1	45	+0.34	0
1982	110	181	-0.32	0
1982	182	304	-0.11	0
1982	305	365	+0.33	0
1982	335	365	+0.47	0

Table 5. Correlations between occurrence of scintillation and daily average geomagnetic Kp indices for various time periods.

While a connection between equatorial scintillation and geomagnetic activity is generally accepted, it is not known just how they are related. The relationship appears quite complex, sometimes showing positive and sometimes negative correlation (Aarons, 1977). Further, some question arises as to whether a simple cross correlation between the two is a good way to show a relationship.

Aarons et al. (1980) found that pre-midnight scintillation is inhibited by geomagnetic activity while post-midnight geomagnetic activity increases scintillation activity, at least under moderate solar flux conditions (except for May, June, and July in the 0°-70° W sector and in November, December, and January in the 135°-180° E sector). This is similar to observations for the drift velocities reported here. Geomagnetic activity appeared to reduce drift velocities prior to midnight and increased them for late night or early morning periods. Perhaps geomagnetic activity and equatorial scintillation are linked through the east-west drift, or zonal winds.

SCINTILLATION VERSUS SOLAR ACTIVITY

We have noted that when the occurrence of equatorial scintillation is compared on a year-to-year basis with solar activity there is a direct dependence (Paulson, 1980). The greater the solar activity for a given year the greater the occurrence and intensity of the scintillation.

The previous comparison was done using a common 11-day sample for each of the years considered. This short sample was used because it was the only period, common to the various years, when data were available. The comparison has been done again here for the Pacific Ocean satellite data from Julian day 182 to day 304 and is shown in figure 19. This clearly shows the dependence of equatorial scintillation on solar activity. It also shows that the occurrence of scintillation for 1982 has decreased from that observed in 1979.

SUMMARY

Comparison of equatorial scintillation and east-west drift during the 1982-83 period is much more complicated than that during 1976. Maximum scintillation intensity frequently occurred long after the maximum drift velocity. The amount of delay was quite variable, however. It could be as little as 10 or 15 minutes or as much as 4 or 5 hours.

The drift velocity calculations showed a consistently eastward drift through most of the night. When scintillation started early in the evening the velocity began at a low value and quickly increased to a maximum, then showed a general decrease through the night. There were some variations on this, however. The rapid increase after sunset may have been a regular occurrence, but without scintillation it could not be measured.

On 3 or 4 nights there was an apparent westward drift for a short time right after sunset before the drift to the east began. This may have been caused by upward drift, since the spaced receiver technique cannot distinguish between vertical and horizontal movement.

For 19 nights the drift velocity changed to a westward drift at, or near, local sunrise and scintillation continued into the daylight hours. Average westward drift velocities for these days were compared to the various 3-hour K_p indices for the corresponding days and a correlation of +0.800 was found for K_p index measurements centered around 0300 GMT. This was a delay between the magnetic activity and the drift velocity of about 16 to 18 hours.

Average drift velocities for the period 1100-1400 GMT (2100-2400 LST) also were calculated for 38 nights and compared with the 3-hour K_p indices for the corresponding nights. These showed a correlation of -0.729 with K_p measurements centered around 0600 GMT for a delay of 6 or 7 hours between geomagnetic activity and the drift velocity.

Eleven-day running averages of the scintillation occurrences and of the daily average geomagnetic K_p indices, at times, showed dips in the scintillation occurrences which corresponded to increases in geomagnetic activity. This was particularly evident during the first half of 1979 and on several occasions in 1980. However, there was more periodic variation in the occurrence of scintillation than geomagnetic activity could account for.

Correlations between the unsmoothed occurrence of scintillation and daily average geomagnetic activity ranged from -0.54 to +0.47 depending on the length of the data sample used and the time of year considered.

Seasonal variation of scintillation occurrences show the December-January minimum observed in the Pacific region with a secondary minimum in June-July for the low elevation angle satellite. This secondary minimum starts to show for the Pacific Ocean satellite (elevation angle 55 degrees) in the 1982 data.

A comparison of the occurrence of scintillation with solar activity on a year-to-year basis using common 4-month data samples showed the same positive dependence previously observed with shorter common 11-day data samples.

REFERENCES

- Aarons, J. (1977), Equatorial Scintillation: A Review, IEEE Trans. on Antennas and Propagation, AP25, 729-736.
- Aarons, J., J. P. Mullen, J. R. Koster, R. F. DaSilva, J. R. Mendeiros, A. Bushby, J. Pantoja, J. Lanat, and M. R. Paulson (1980), Seasonal and Geomagnetic Control of Equatorial Scintillation in Two Longitudinal Sectors, J. Atmos. Terr. Phys., 42, 861-866.
- Briggs, B. H., G. J. Phillips and D. H. Shinn (1950), The Analysis of Observations on Spaced Receivers of the Fading of Radio Signals, Proc. Phys. Soc. Lond., B, 63, 106-121.
- Farley, D. T., B. B. Balsley, R. F. Woodman, J. P. McClure (1970), Equatorial Spread-F Implications of Radar Observations, J. Geophys. Res., 75, 7199-7216.
- Jacchia, L. G. (1967), Properties of the Upper Atmosphere Determined from Satellite Orbits, Phil. Trans. Roy. Soc. Lond., A262, 157-171.
- Koster, J. R. (1972), Equatorial Scintillation, Planet. Space Sci., 20, 1999-2014.
- Paulson, M. R. and R. U. F. Hopkins (1977), Space Diversity Characteristics of Equatorial Scintillation, Naval Ocean Systems Center Technical Report 113.
- Paulson, M. R. (1979), Scintillation of uhf SatCom Signals, Naval Ocean Systems Center Technical Report 446.
- Paulson, M. R. (1980), Equatorial Scintillation of Satellite Signals at uhf and L-Band for Two Elevation Angles, Naval Ocean Systems Center Technical Report 543.
- Rastogi, R. G. and J. Mullen (1981), Intense Daytime Radio Wave Scintillations and Sporadic E Layer Near the Dip Equator, J. Geophys. Res., 86, 195-198.
- Woodman, Ronald F. (1970), Vertical Drift Velocities and East-West Electric Fields at the Magnetic Equator, J. Geophys. Res., Space Physics, 75, 6249-6259.

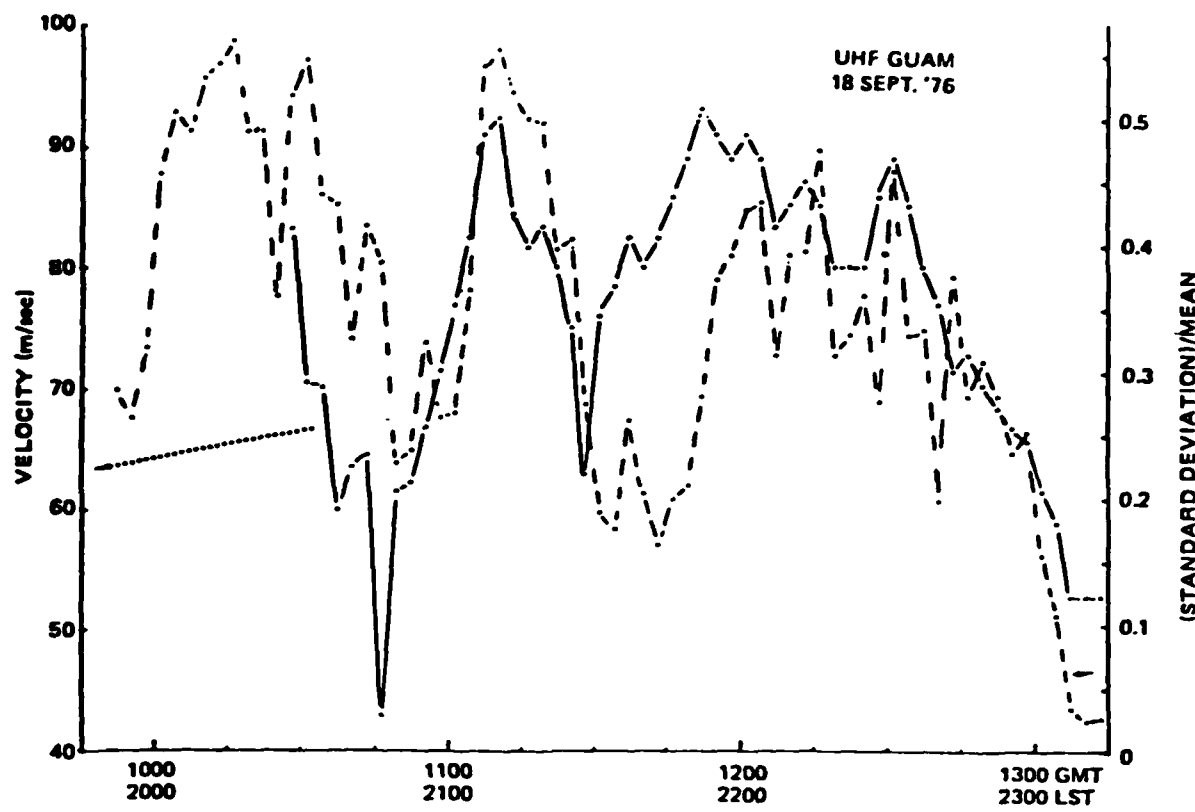


Figure 1. The eastward component of the apparent drift velocity, uncorrected for time decorrelation effects, is shown as a function of time and compared to the scintillation activity, where standard deviation divided by the mean is used as an indication of scintillation intensity.

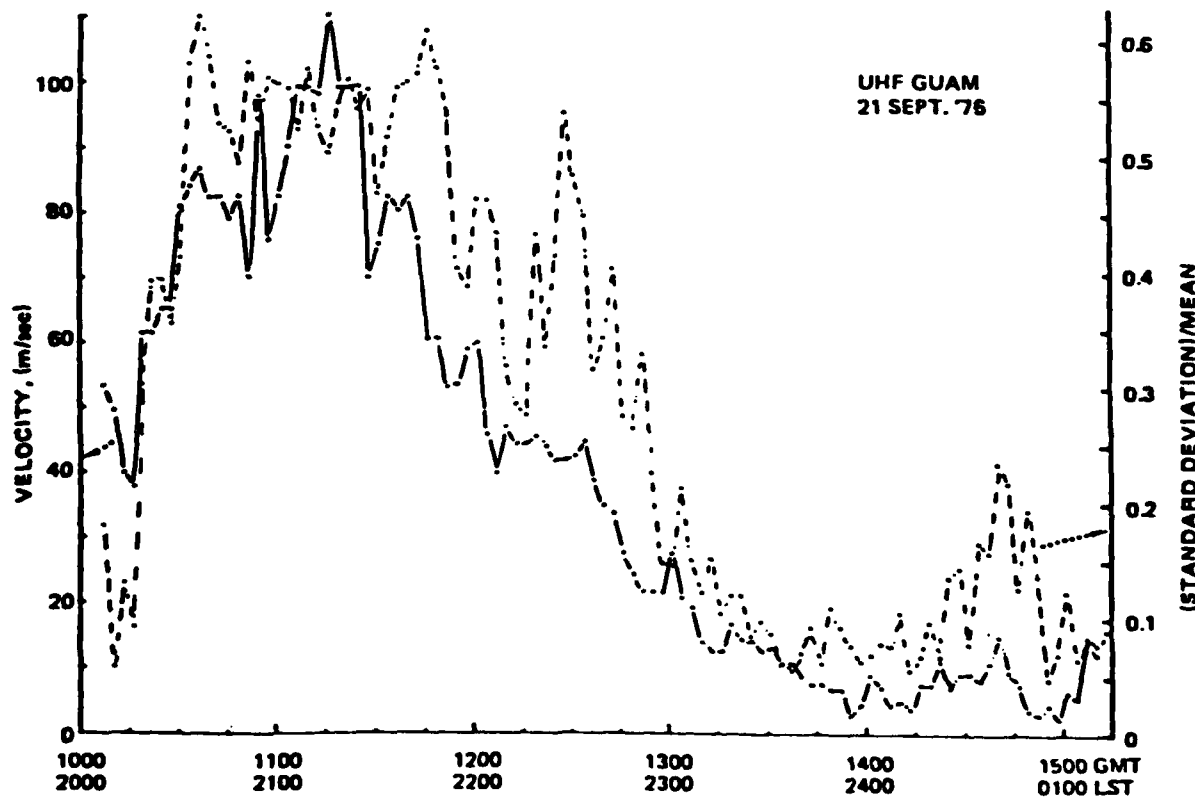


Figure 2. The same as figure 1 but for 21 September 1976.

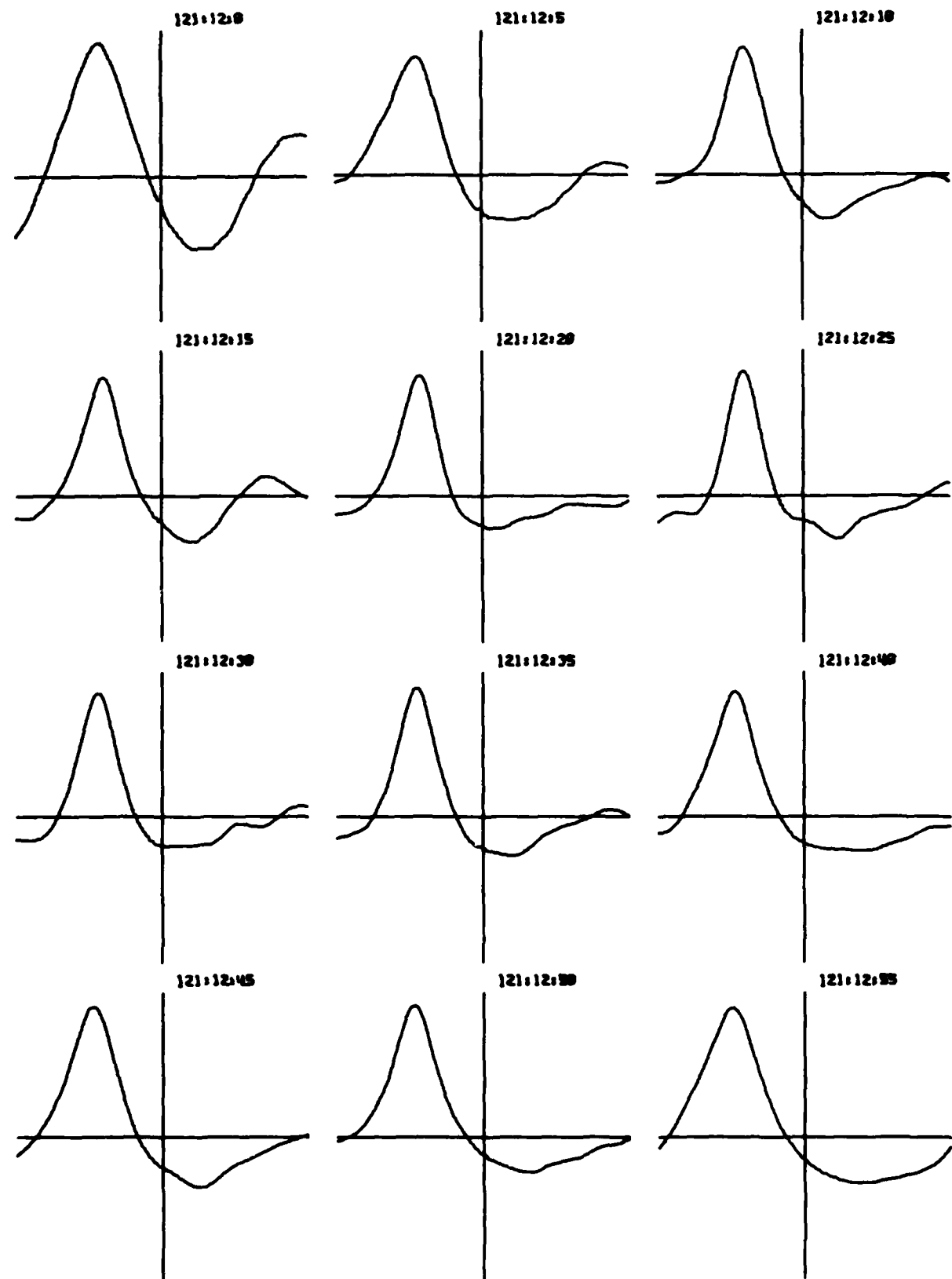


Figure 3. Some examples of cross correlation between the east and west uhf receivers.

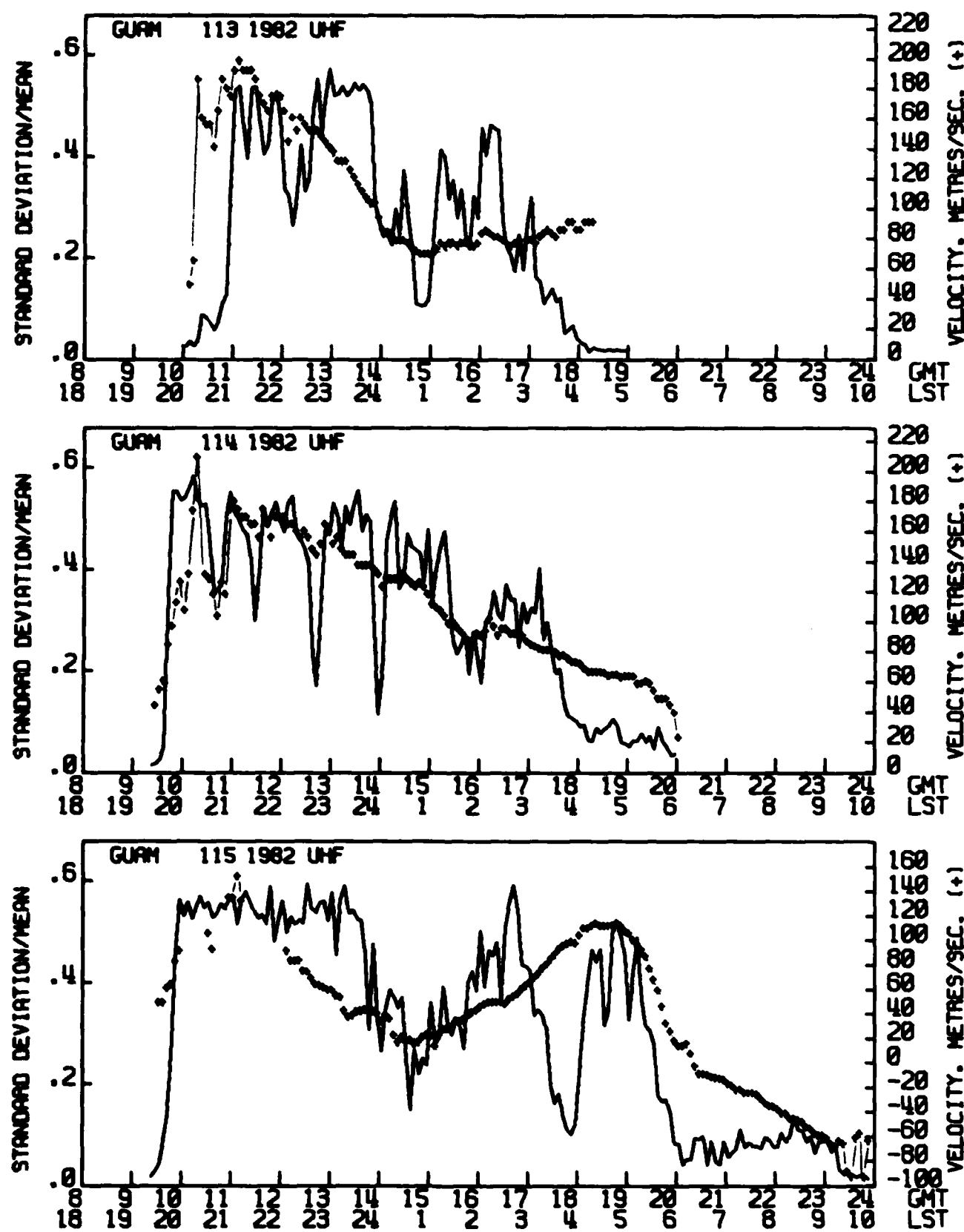


Figure 4. Examples of plots of uhf scintillation intensity and drift velocity. Positive velocities are eastward.

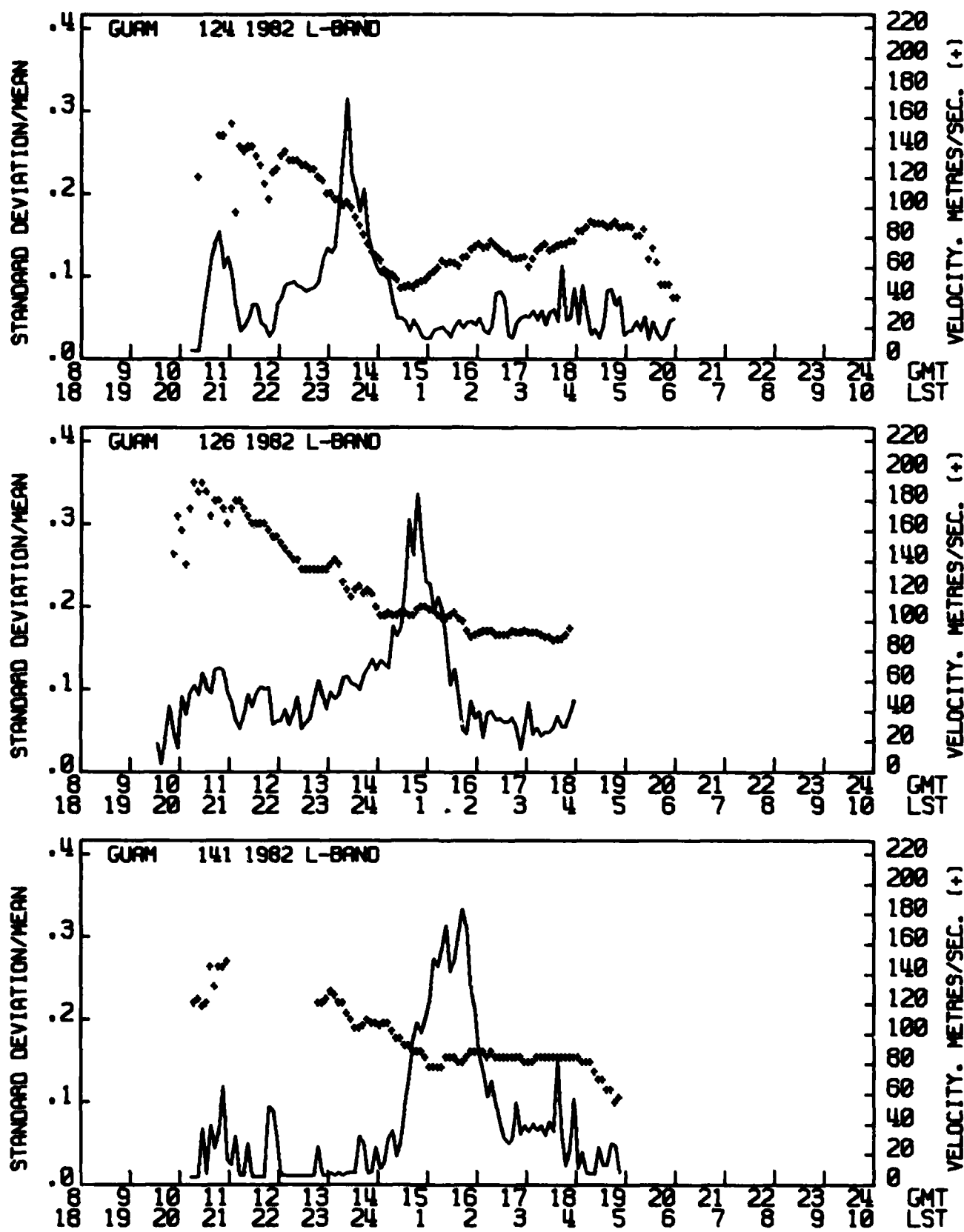


Figure 5. Examples of plots of L-band scintillation intensity and drift velocity. Positive velocities are eastward.

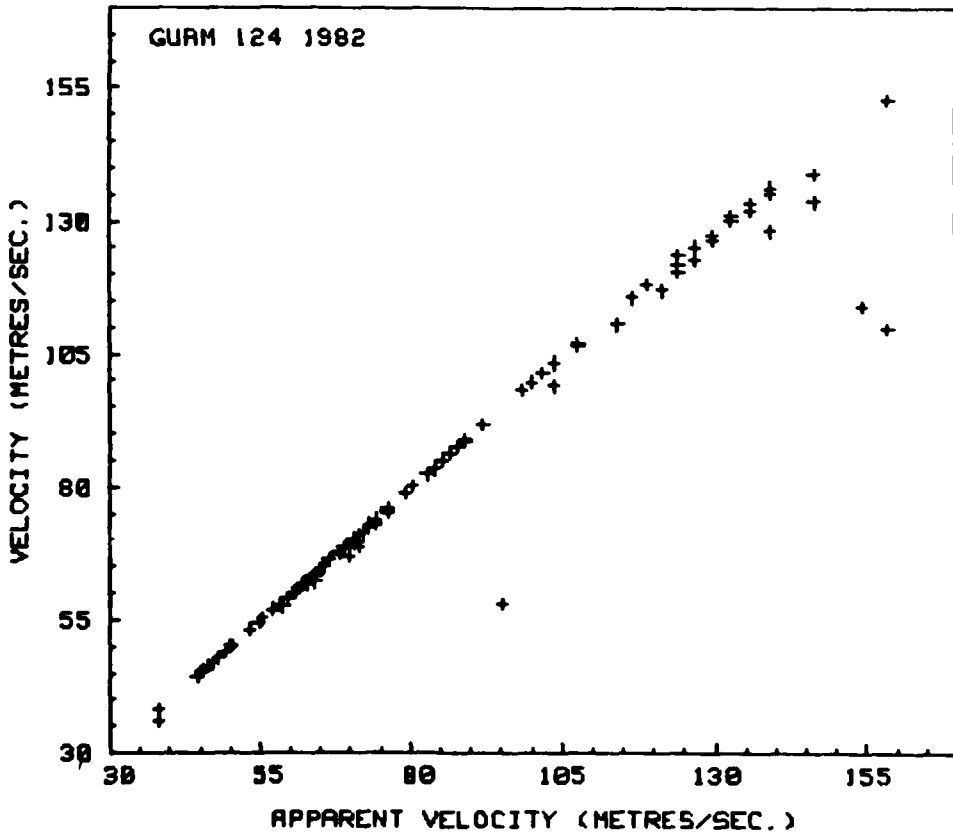
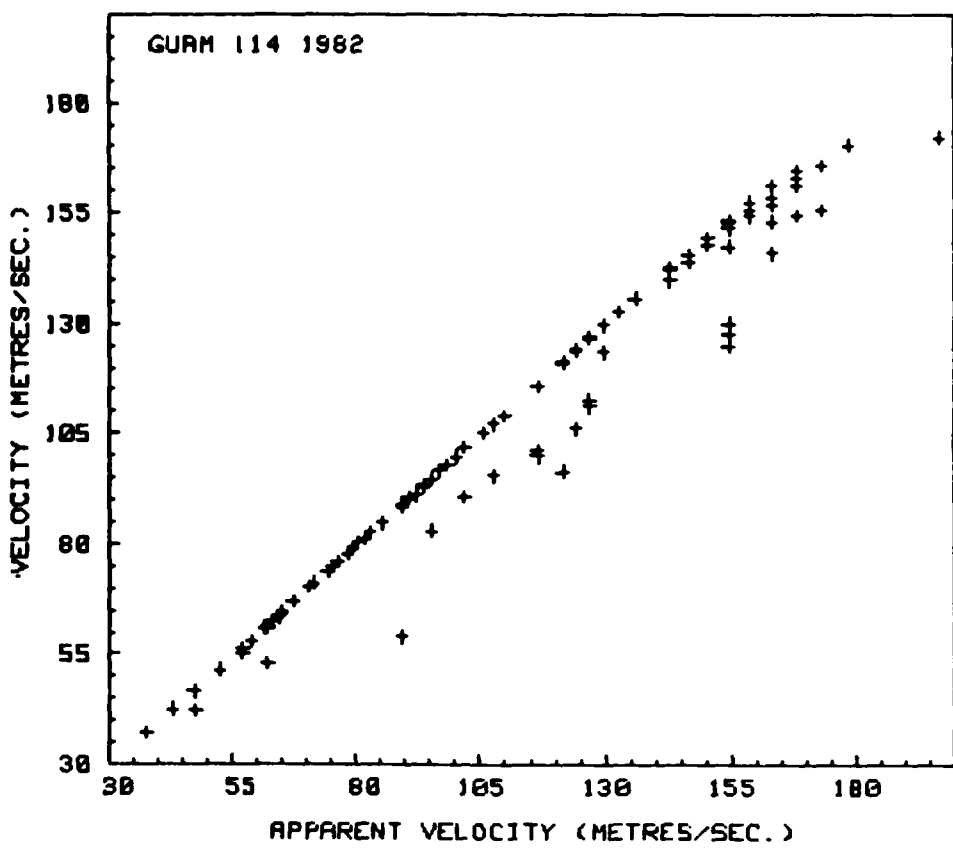


Figure 6. Plots of true velocity as a function of apparent velocity for 2 nights.

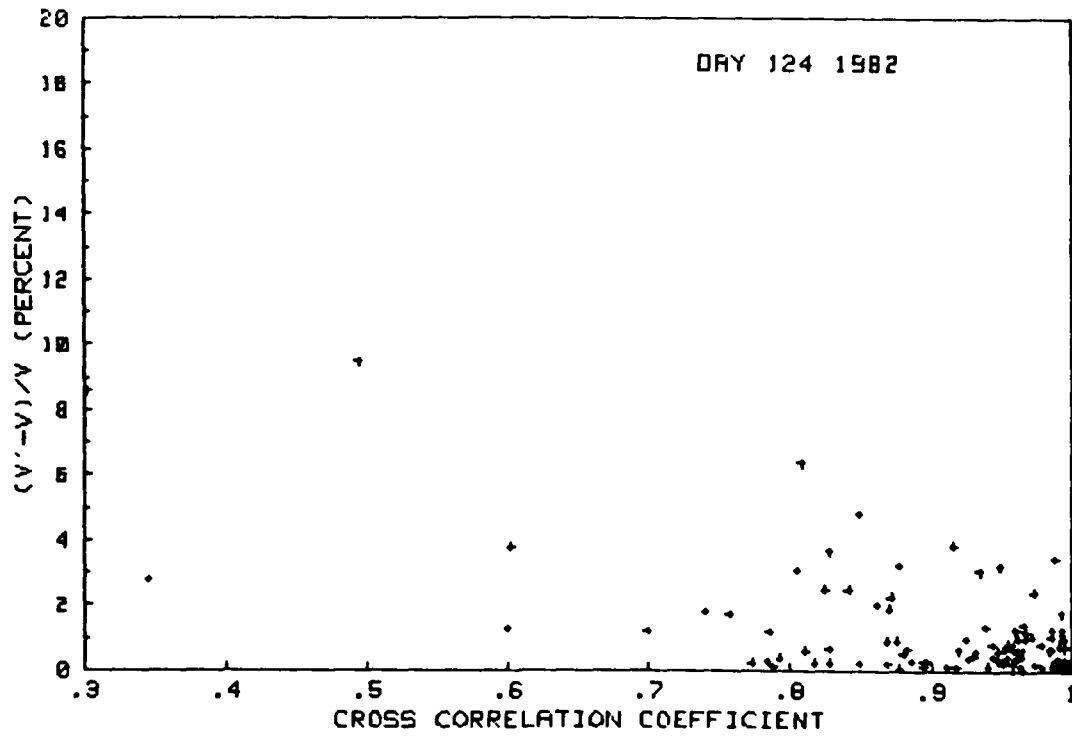
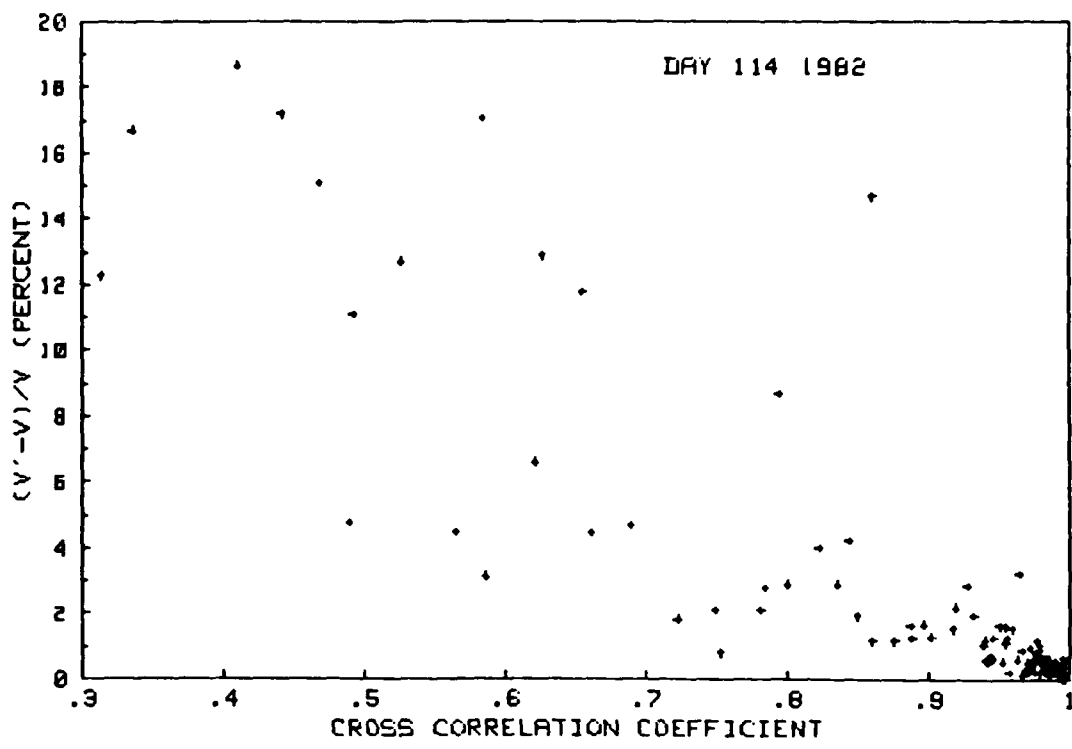


Figure 7. The difference between true velocity and apparent velocity, as a percent of true velocity, shown as a function of the cross correlation coefficient, for the 2 nights shown in figure 6.

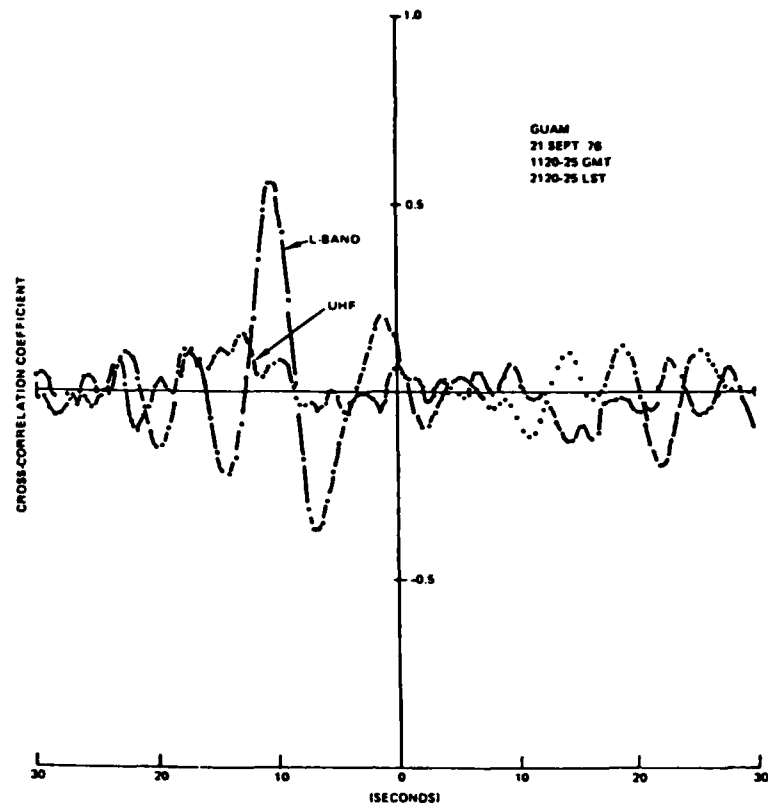


Figure 8. Cross correlations functions for uhf and L-band for a 1000 metre, east-west separation.

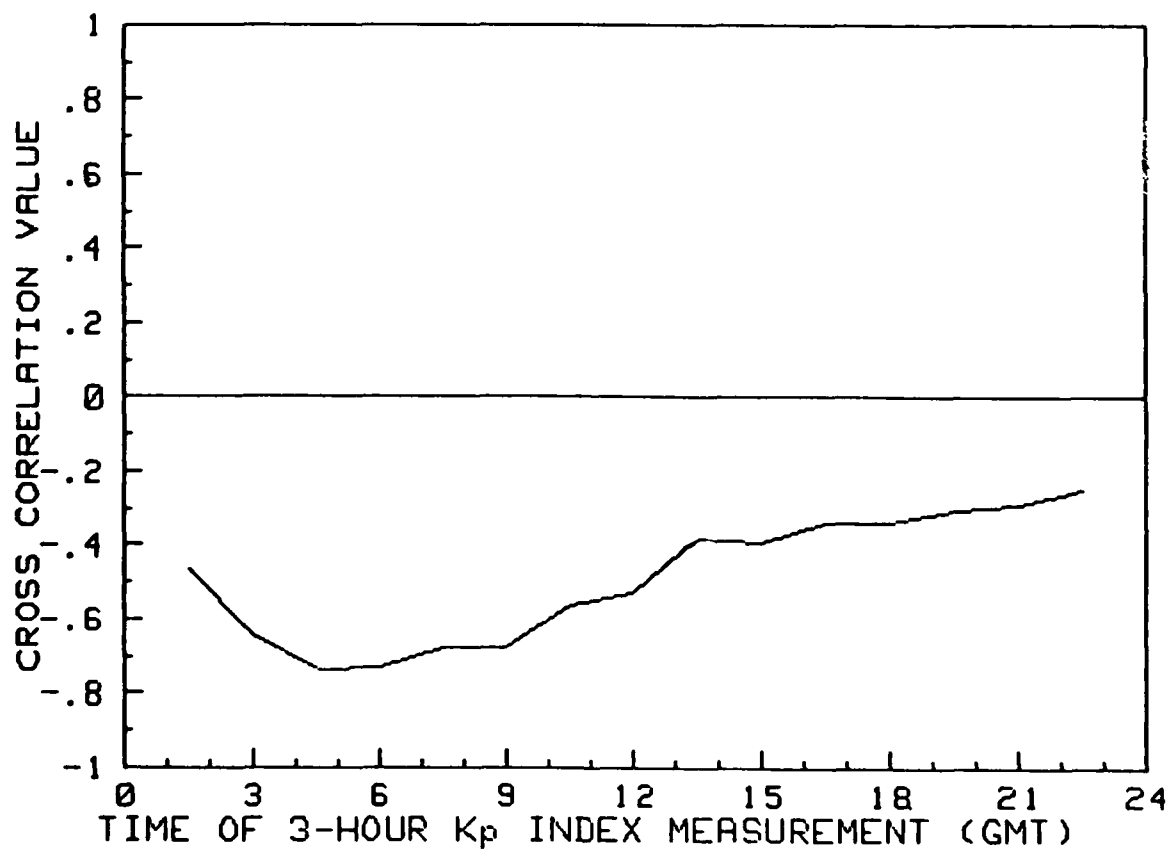


Figure 9. Cross correlations between average eastward drift velocities for the period 1100-1400 GMT (2100-2400 LST) and the eight geomagnetic indices, K_p , shown as a function of the time of the geo-magnetic index measurements.

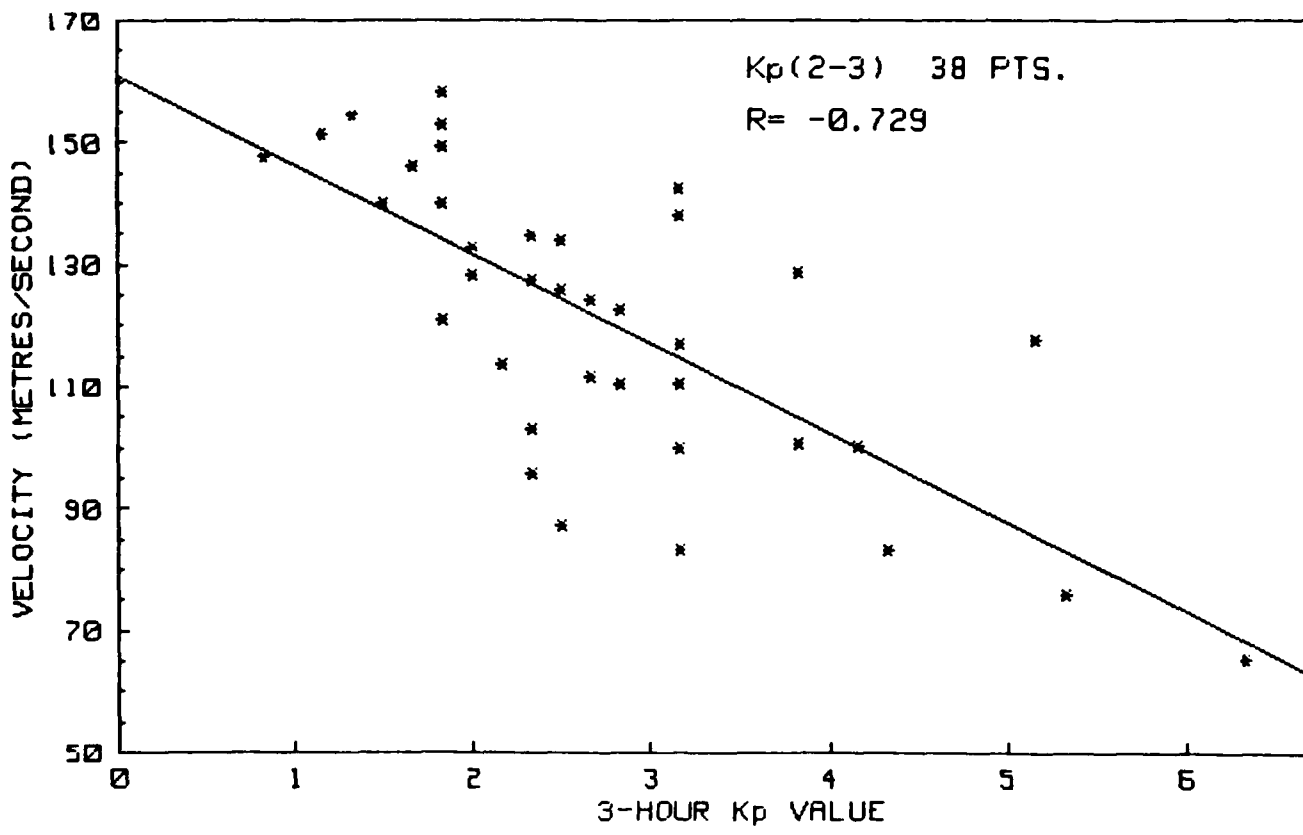


Figure 10. The average eastward drift velocity for the period 1100-1400 GMT shown as a function of the average between the second and third geomagnetic Kp index measurements. The number of points is 38 and the correlation is -0.729.

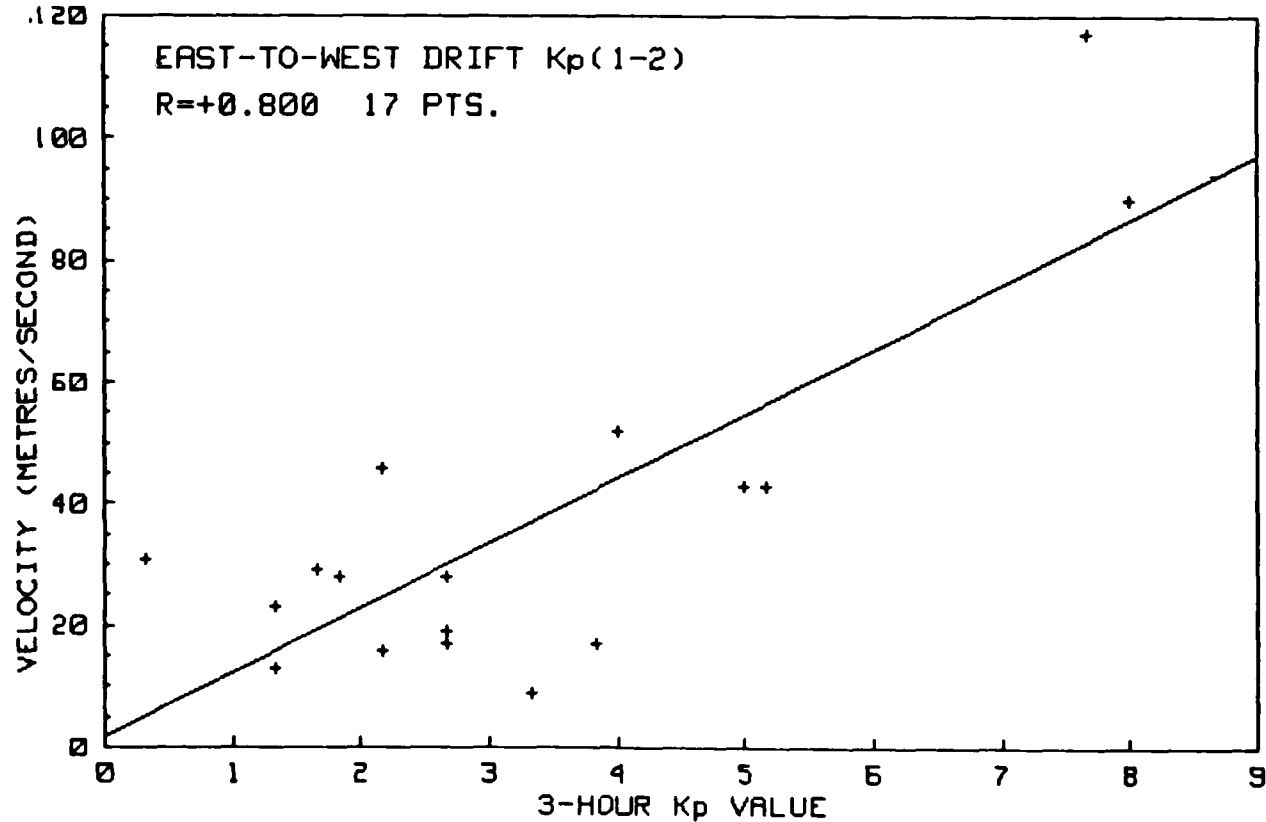


Figure 11. Average westward drift velocity after 1900 GMT (0500 LST) as a function of the average between the first and second geomagnetic Kp index measurements. The number of points is 17 and the correlation is +0.800.

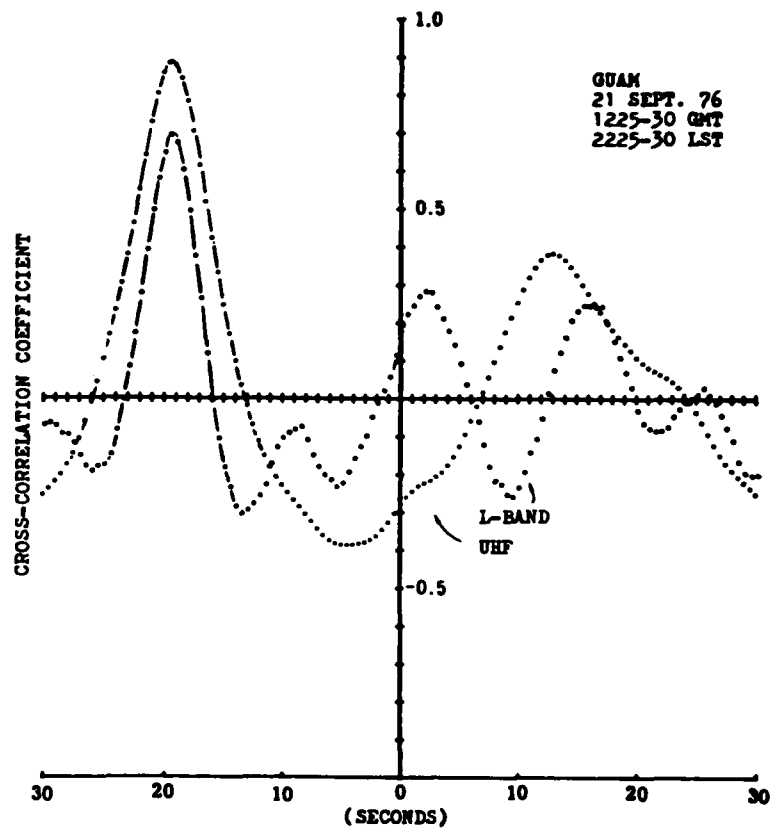


Figure 12. Cross correlations at uhf and at L-band for a 5-minute time sample.

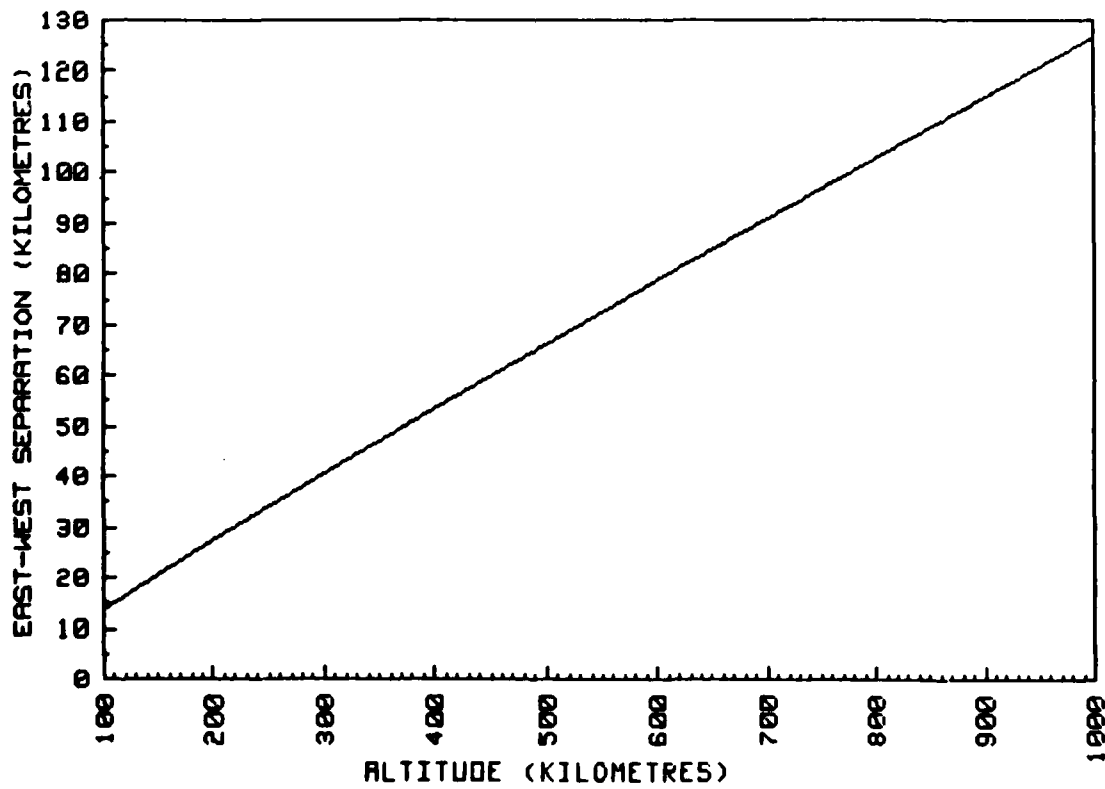


Figure 13. East-west separation of the propagation paths to the two satellites as a function of altitude.

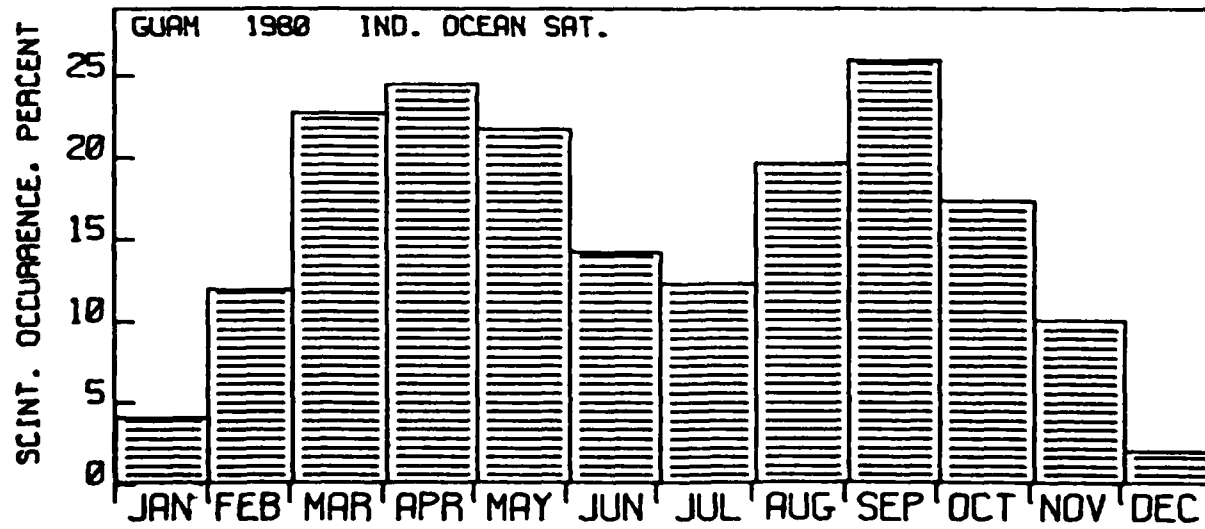
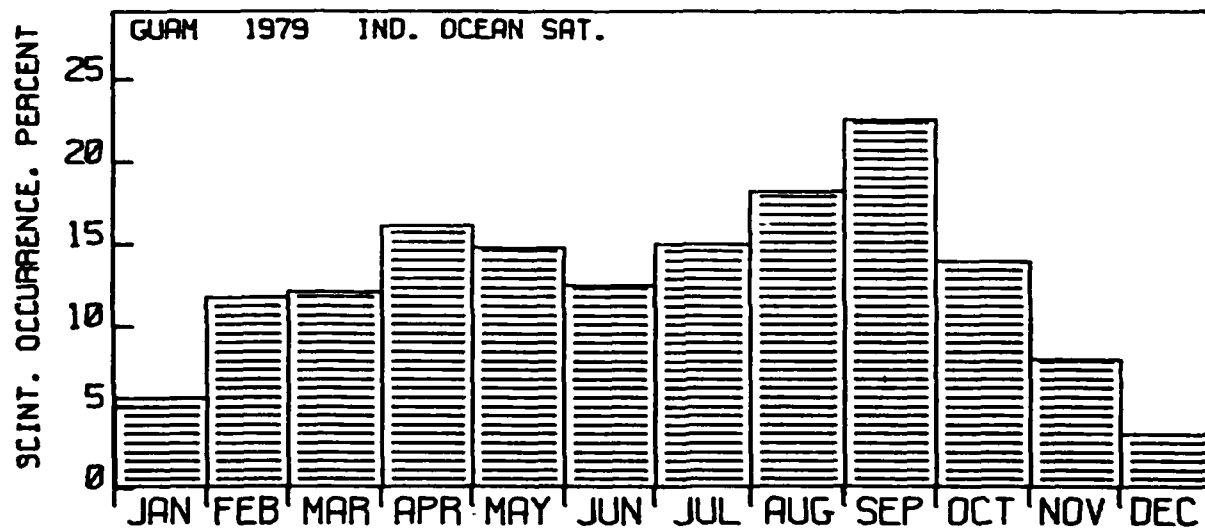
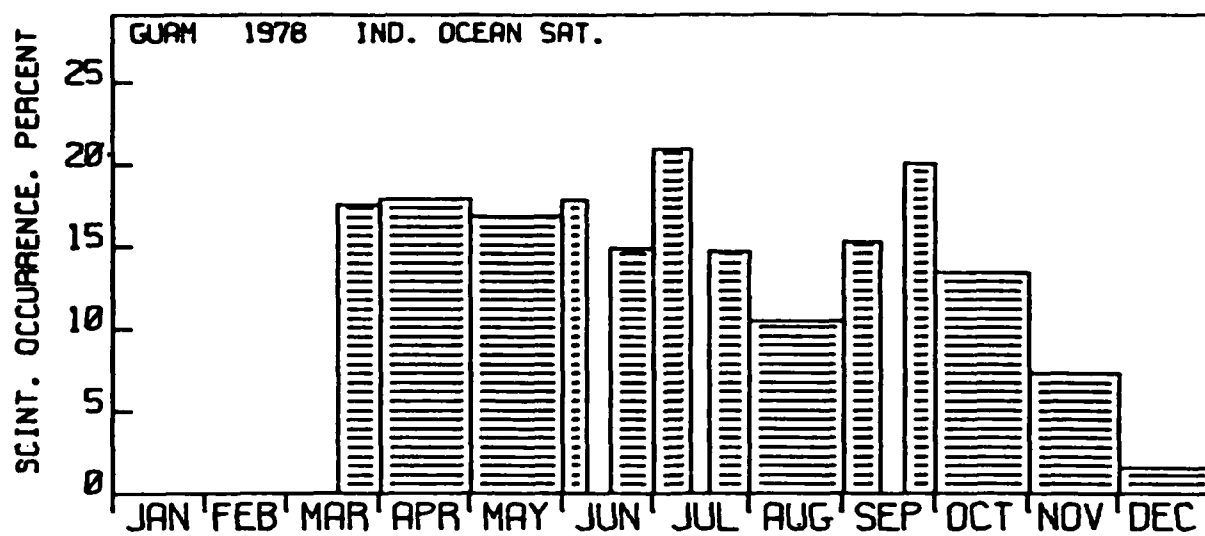


Figure 14. Occurrence of uhf scintillation is shown as the percent of time each month that scintillation with fades greater than 6 dB occurred for the Indian Ocean satellite.

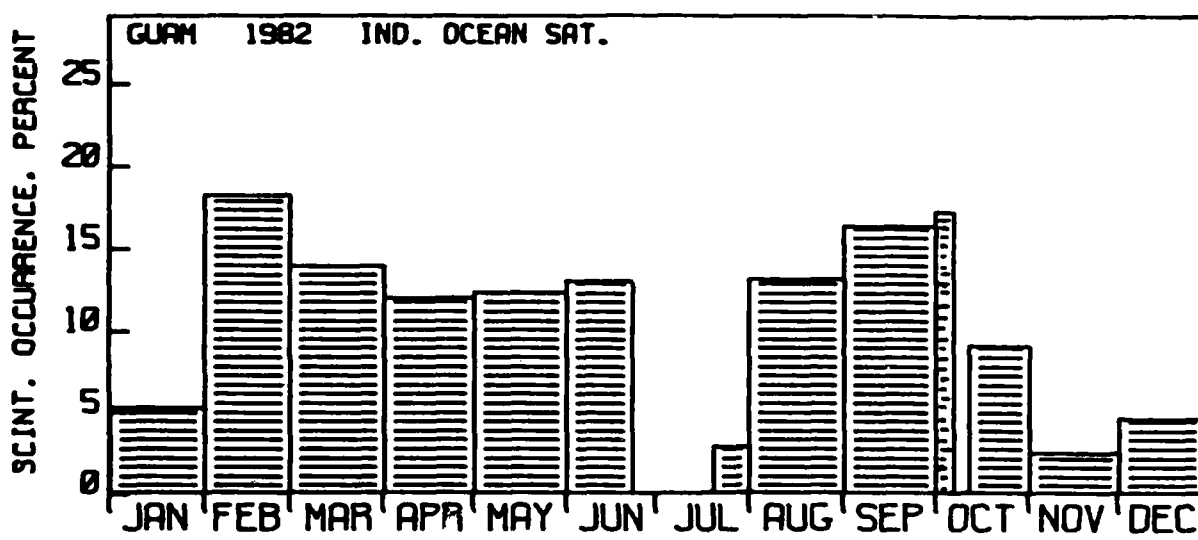
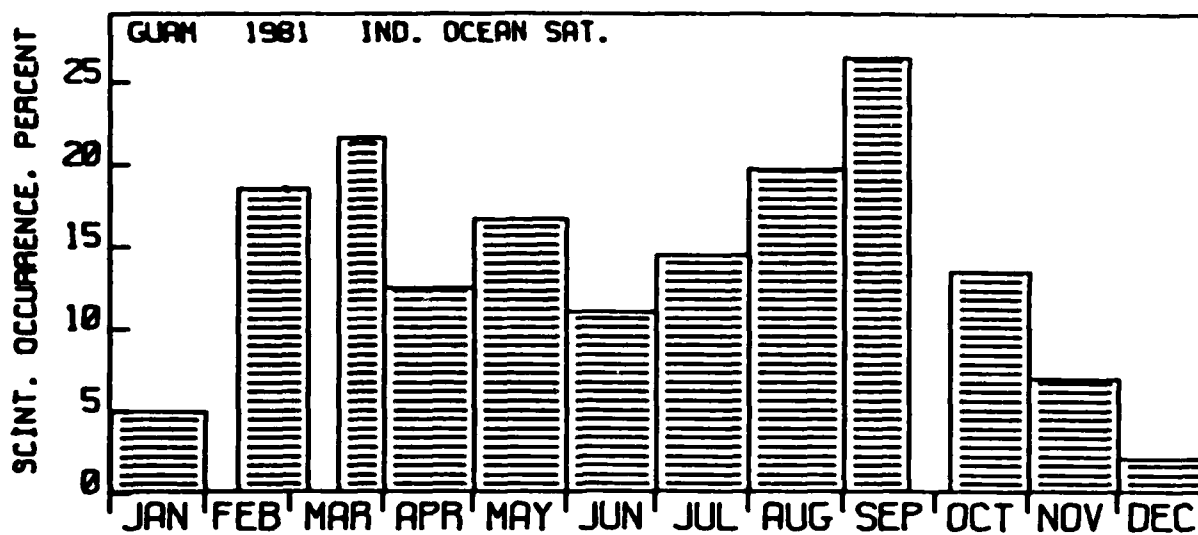


Figure 14. Continued

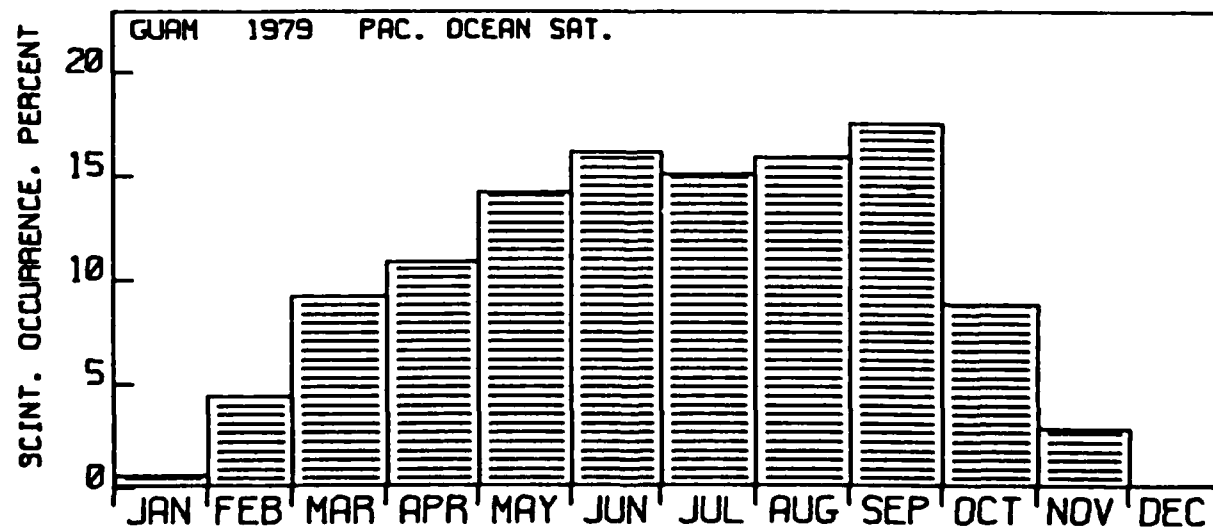
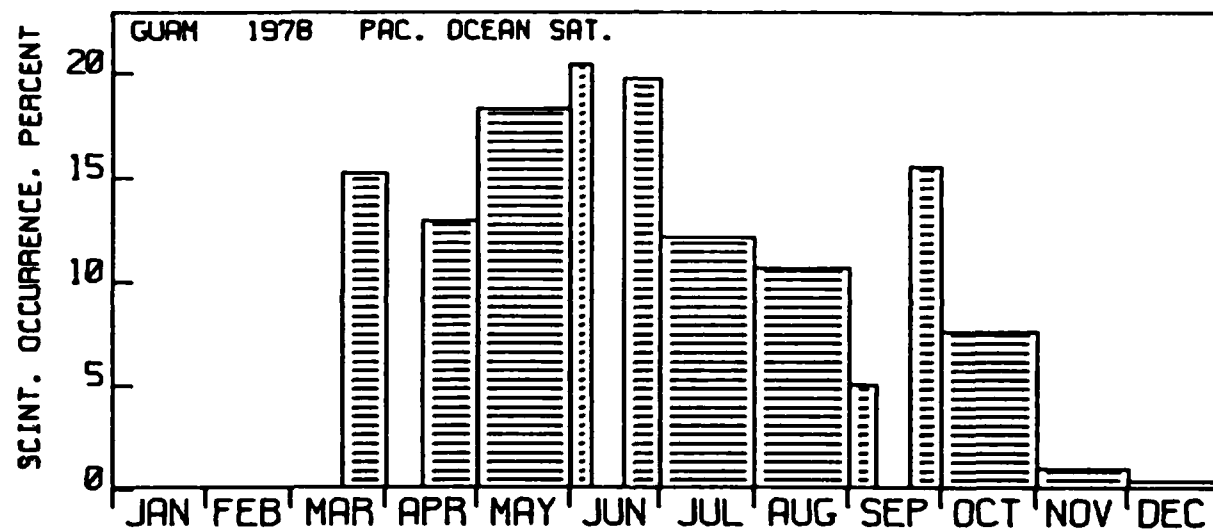
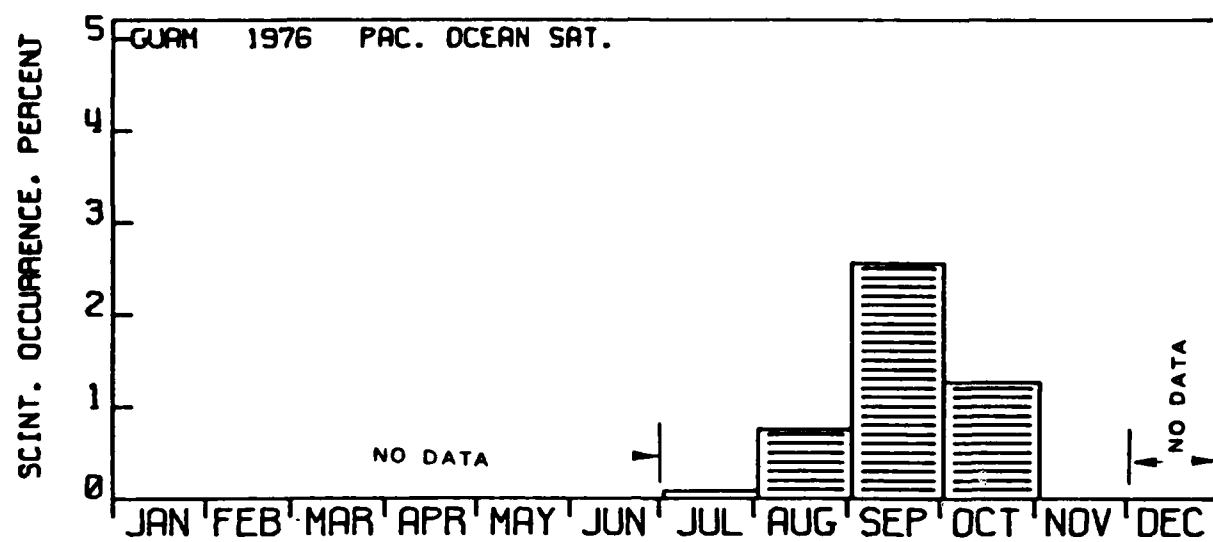


Figure 15. The same as figure 14, but for the Pacific Ocean satellite.

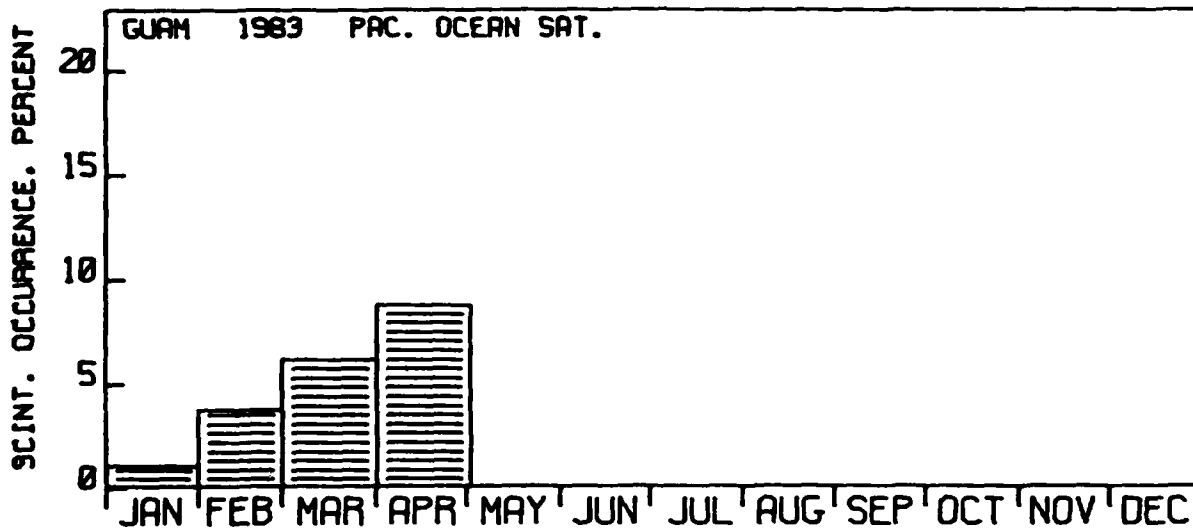
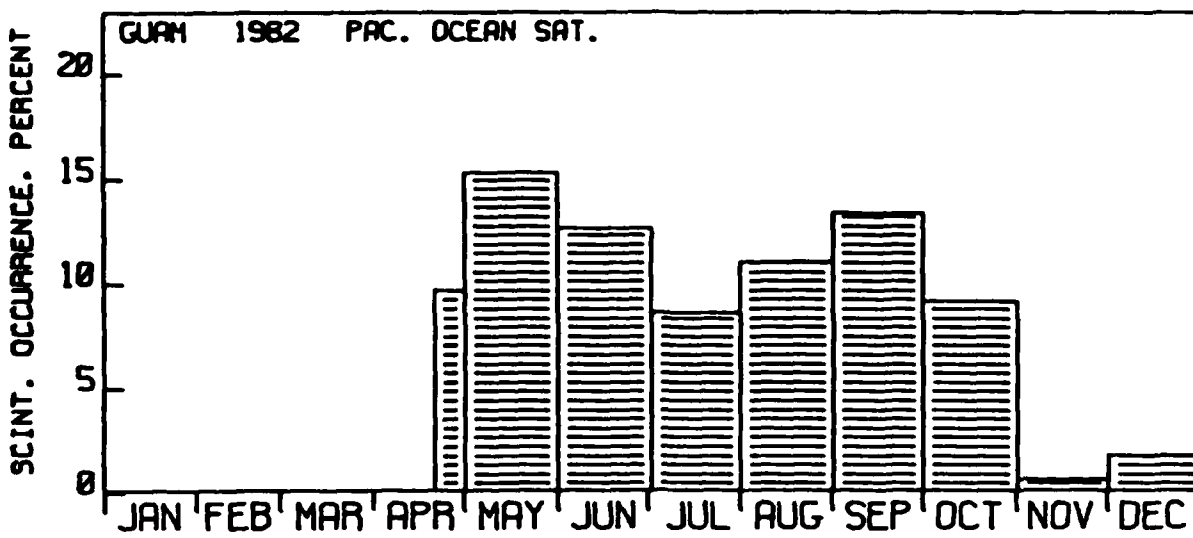


Figure 15. Continued

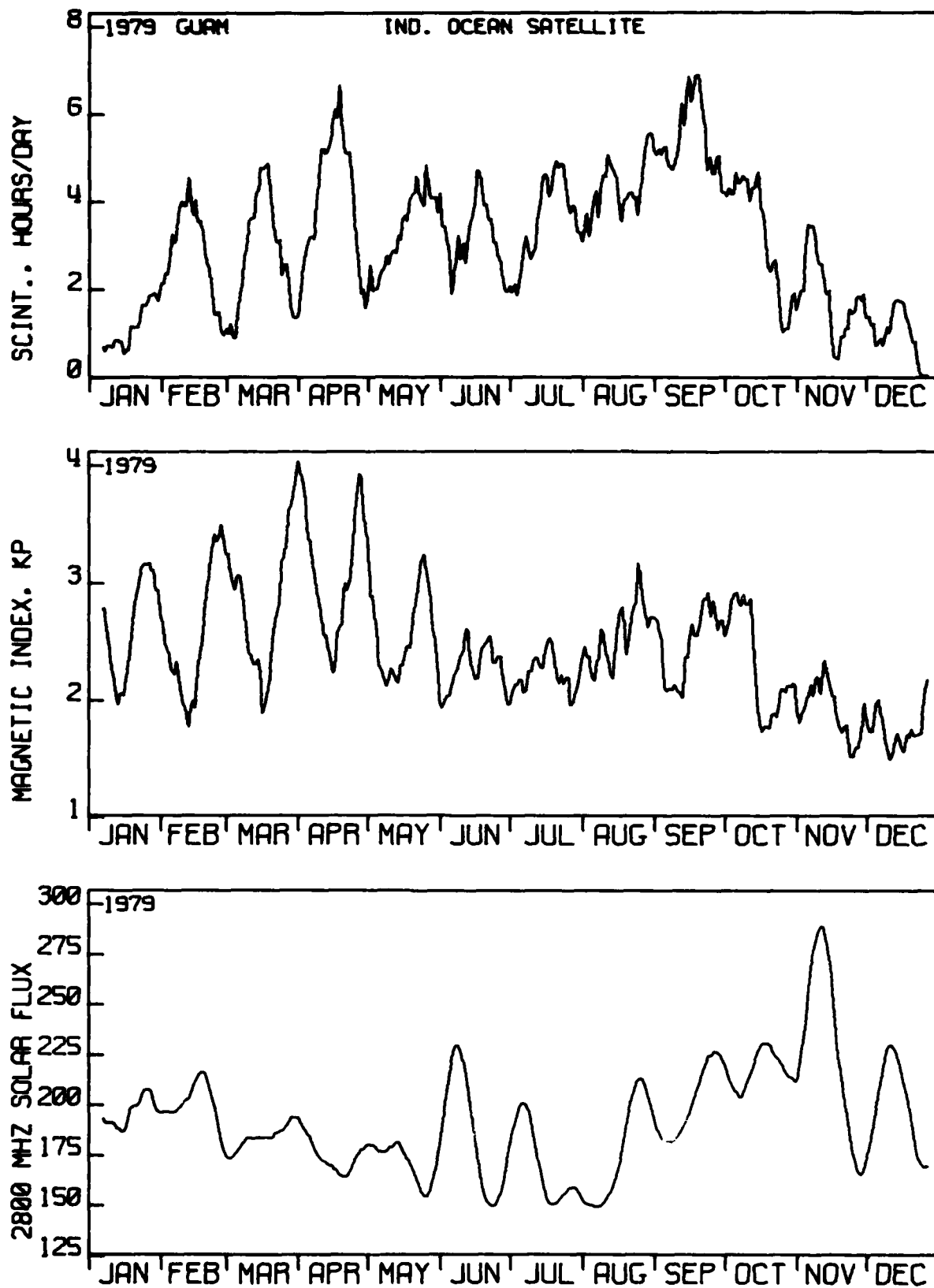


Figure 16. Eleven-day running average for: occurrence of scintillation, top; daily magnetic Kp index, middle; 2800 MHz solar flux, bottom.

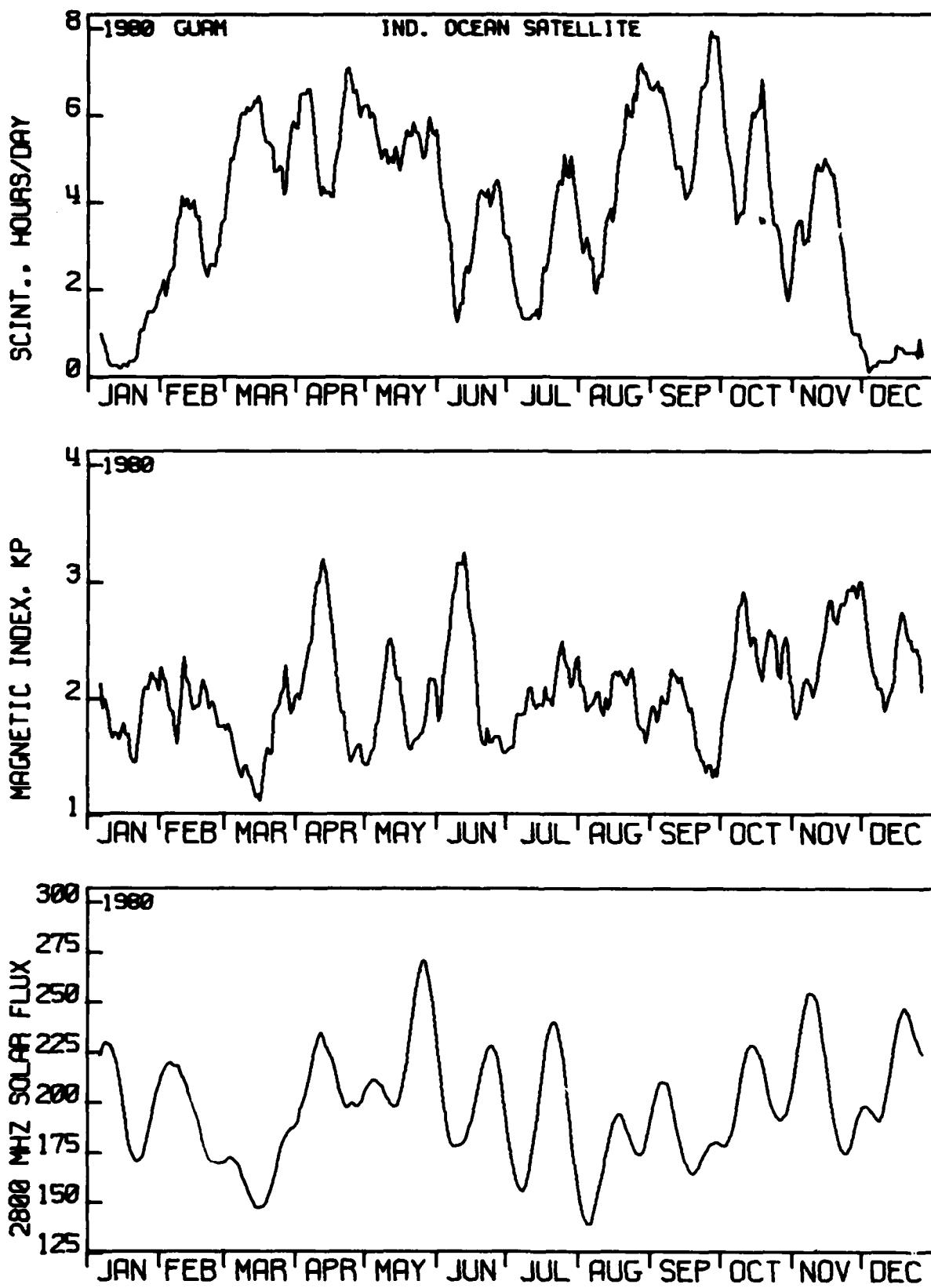


Figure 17. The same as figure 16, but for the year 1980.

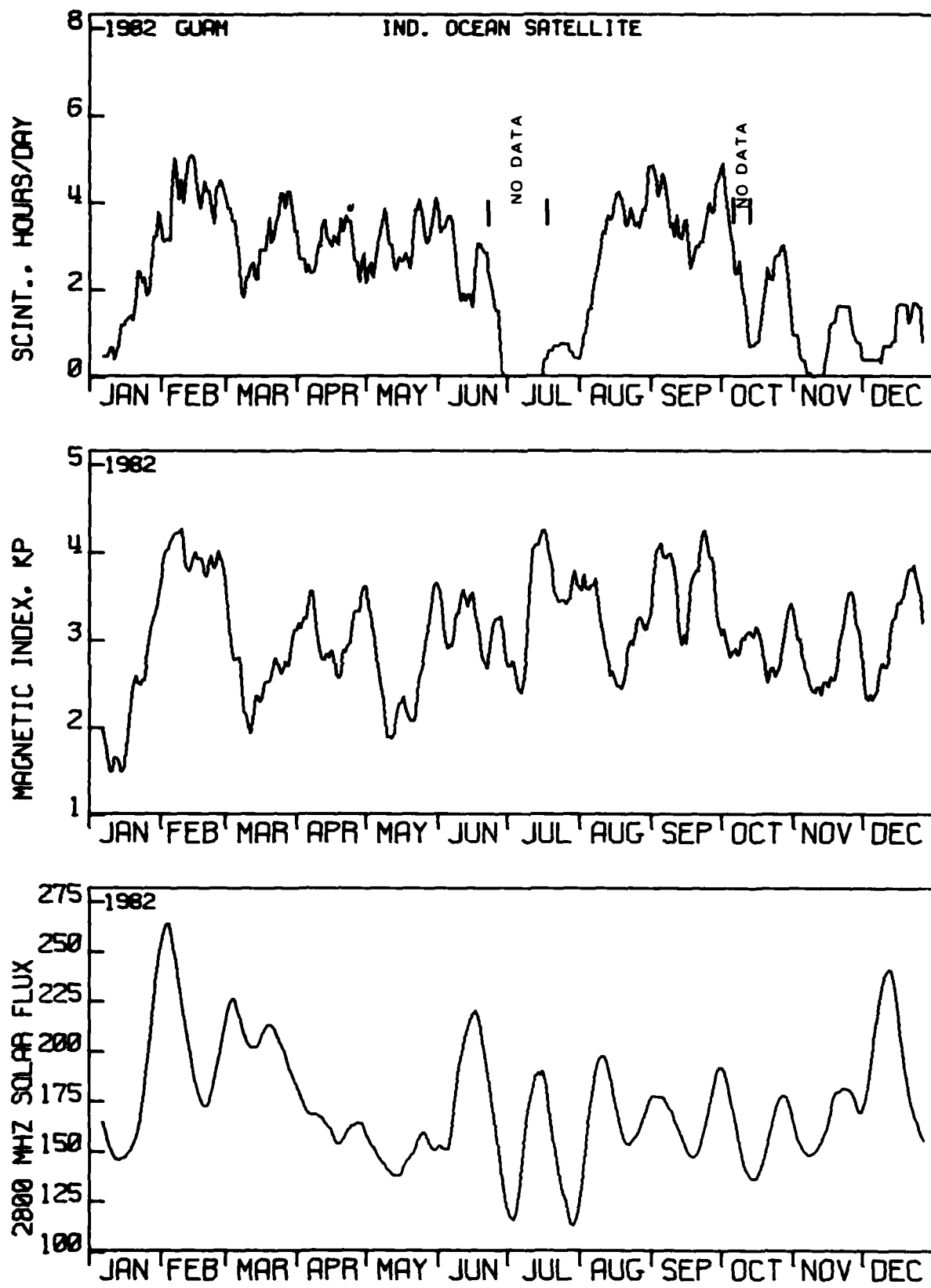


Figure 18. The same as figure 16, but for the year 1982.

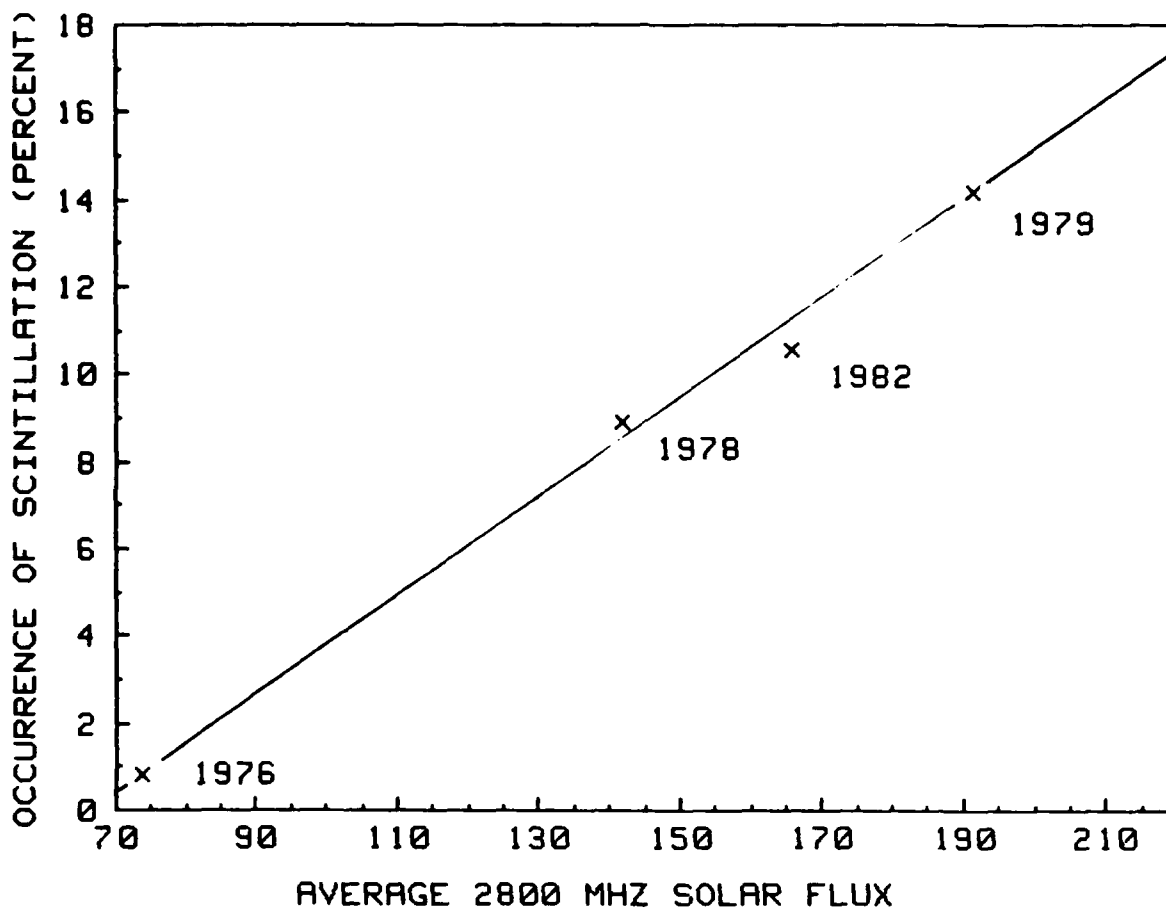
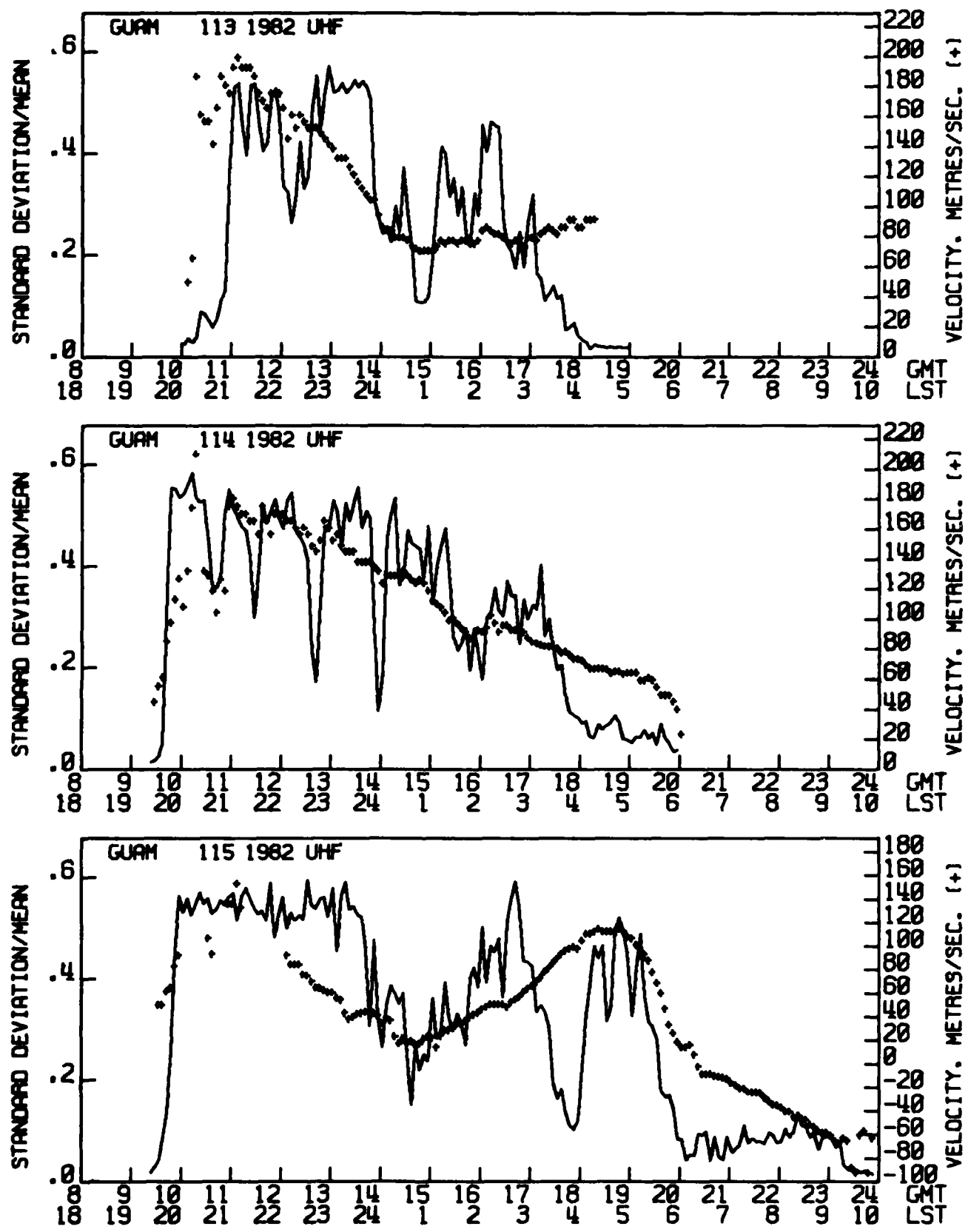


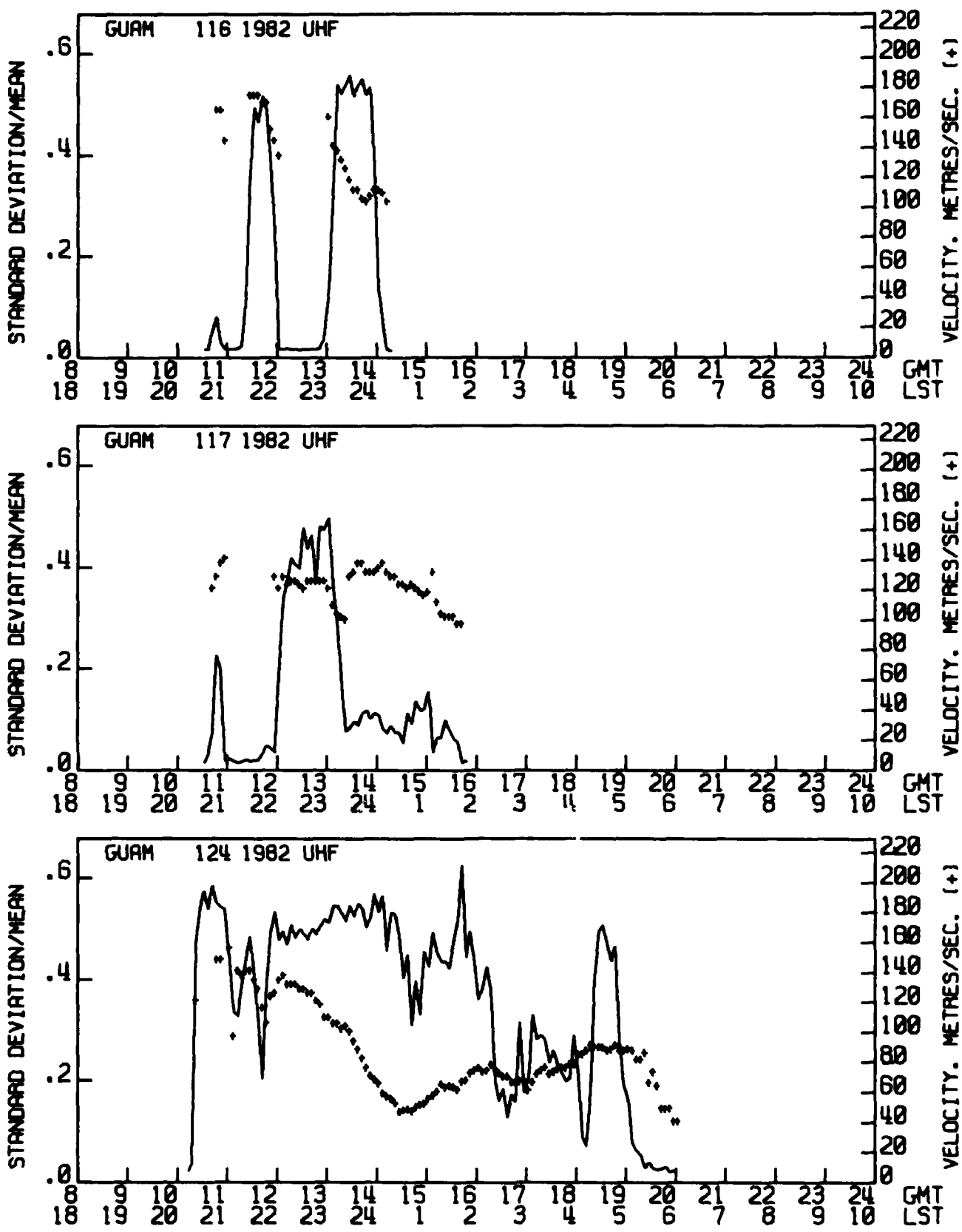
Figure 19. Percent occurrence of equatorial scintillation as a function of the average 2800 MHz solar flux for the period July through October of each of the years indicated.

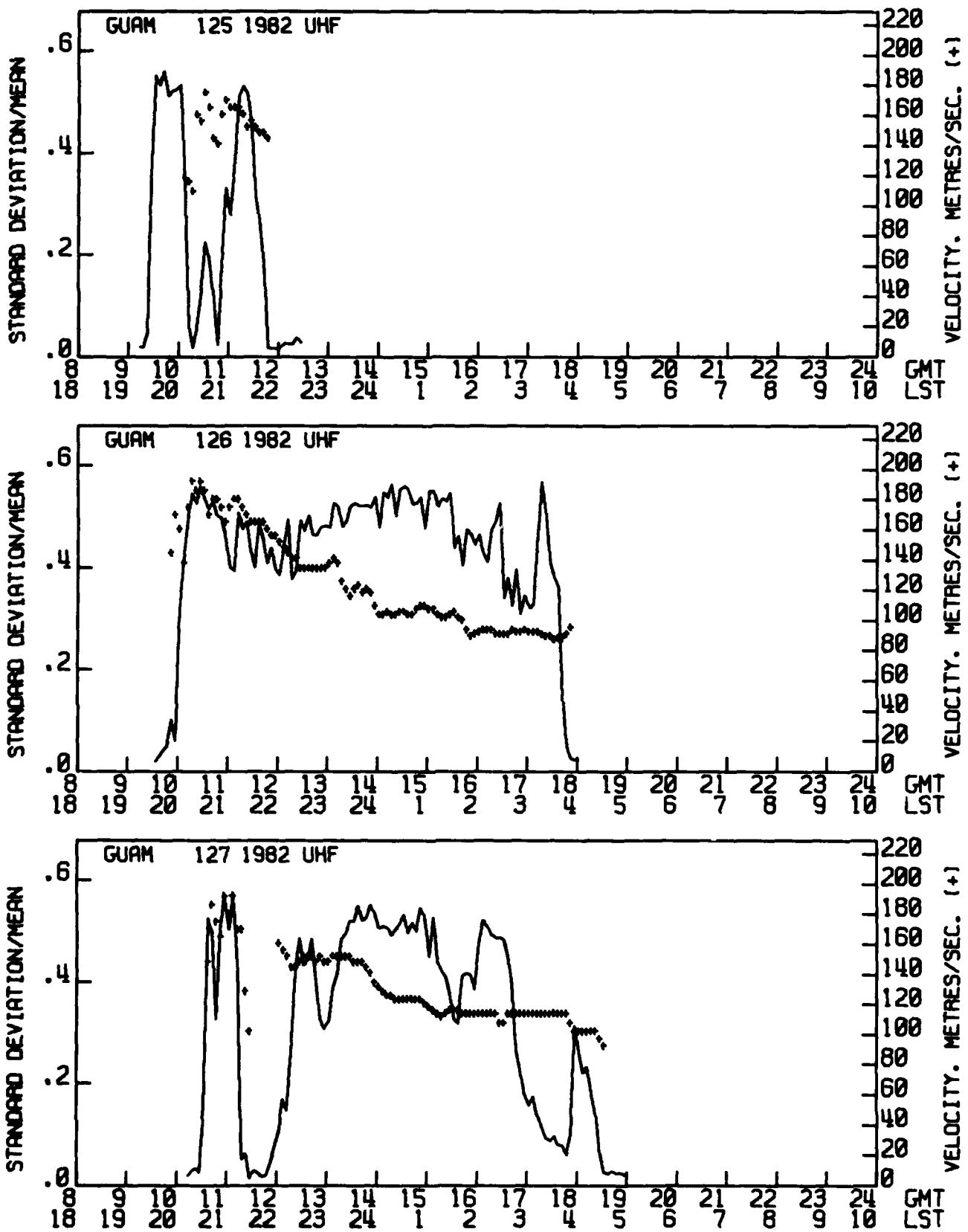
APPENDIX A

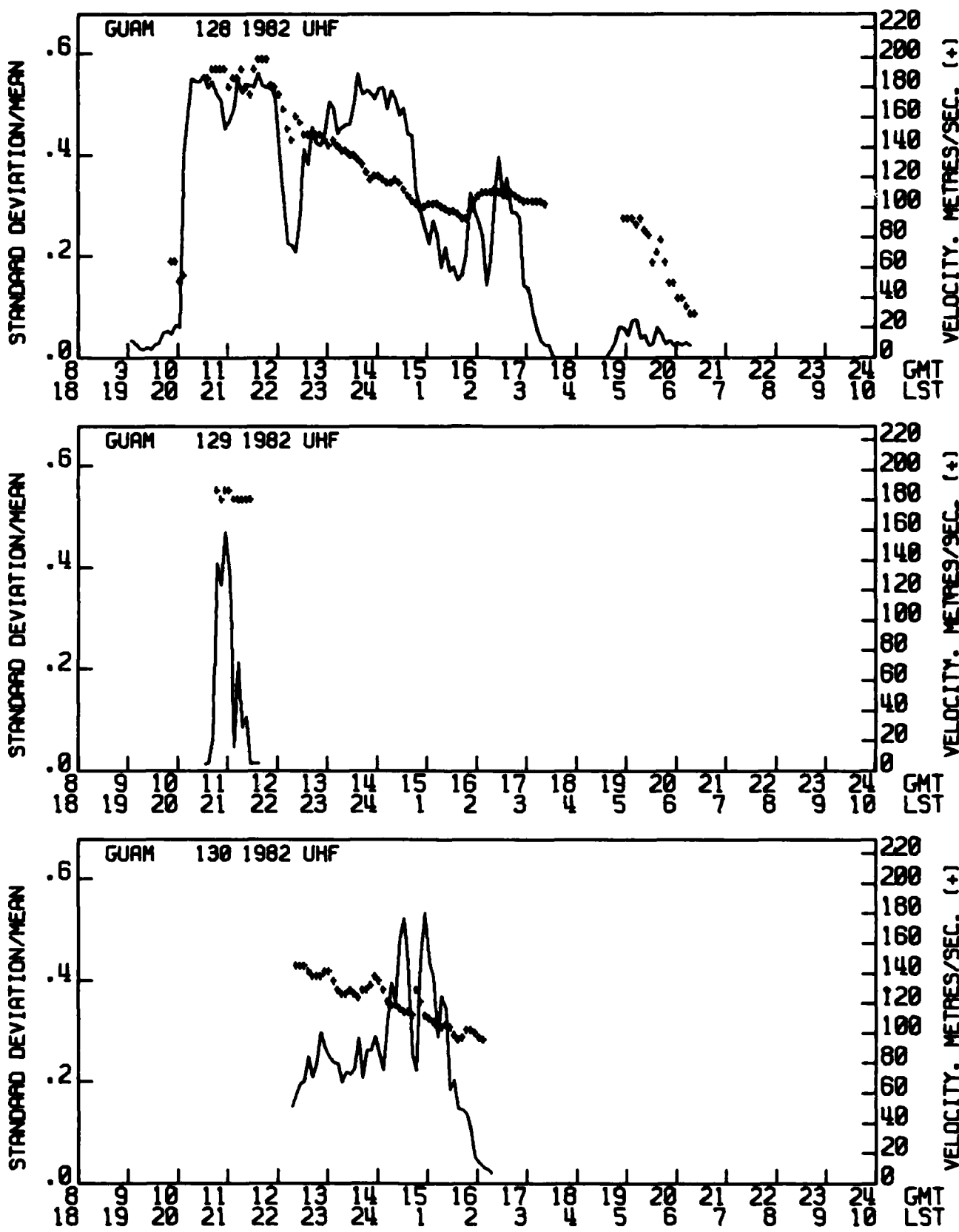
PLOTS OF UHF SCINTILLATION INTENSITIES ALONG
WITH THE EAST-WEST COMPONENT OF DRIFT VELOCITIES
(POSITIVE VELOCITIES ARE EASTWARD DRIFT)

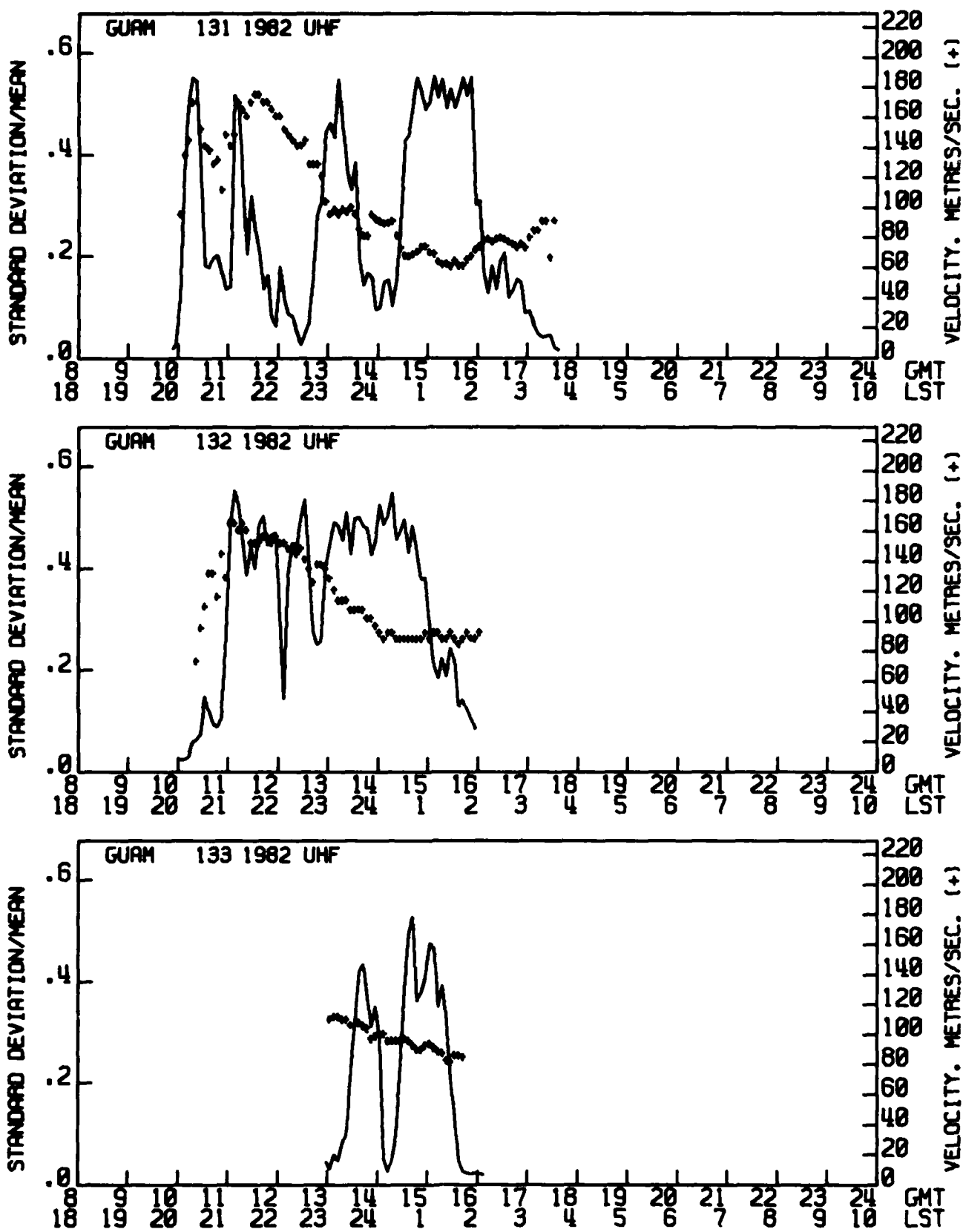


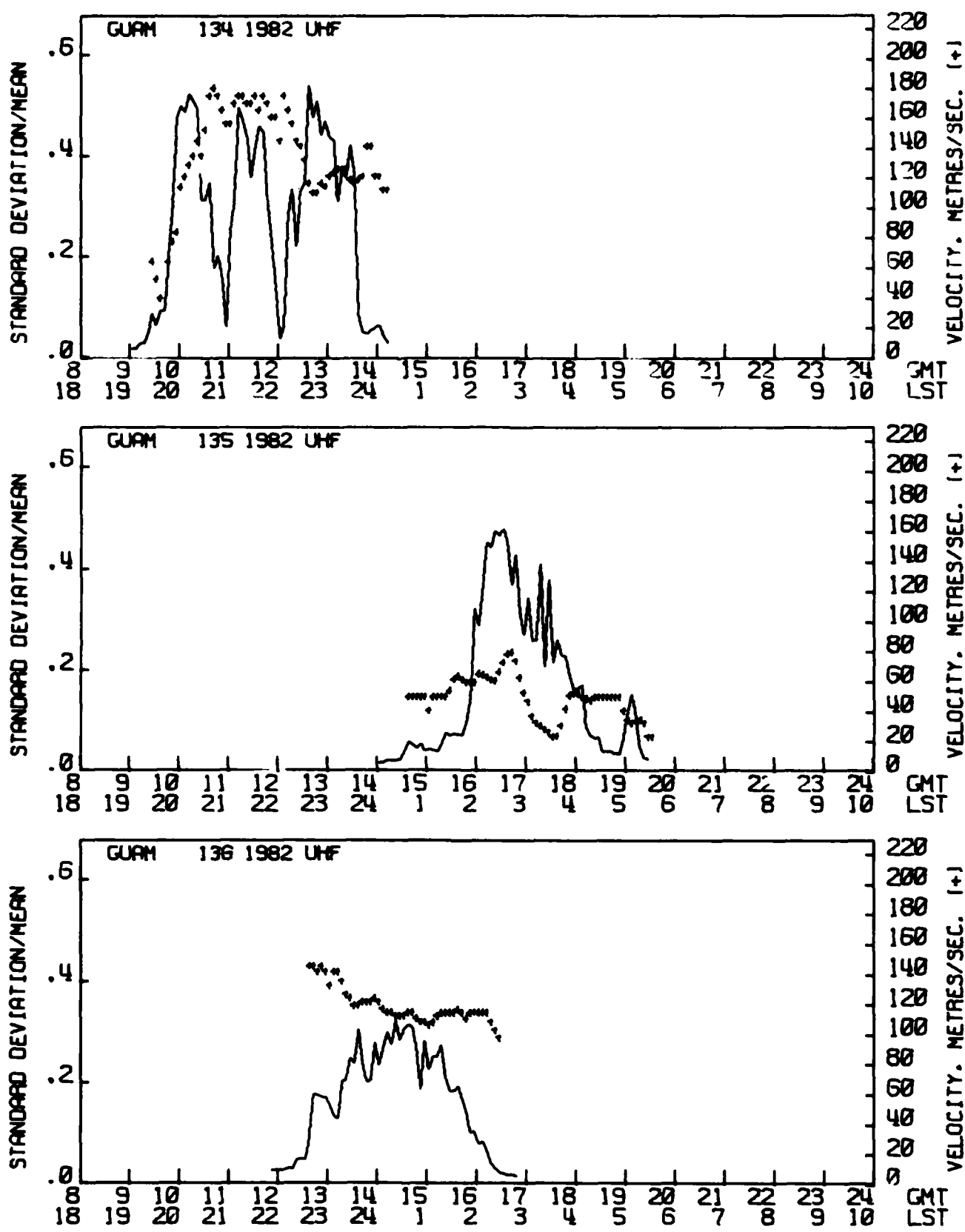
A2

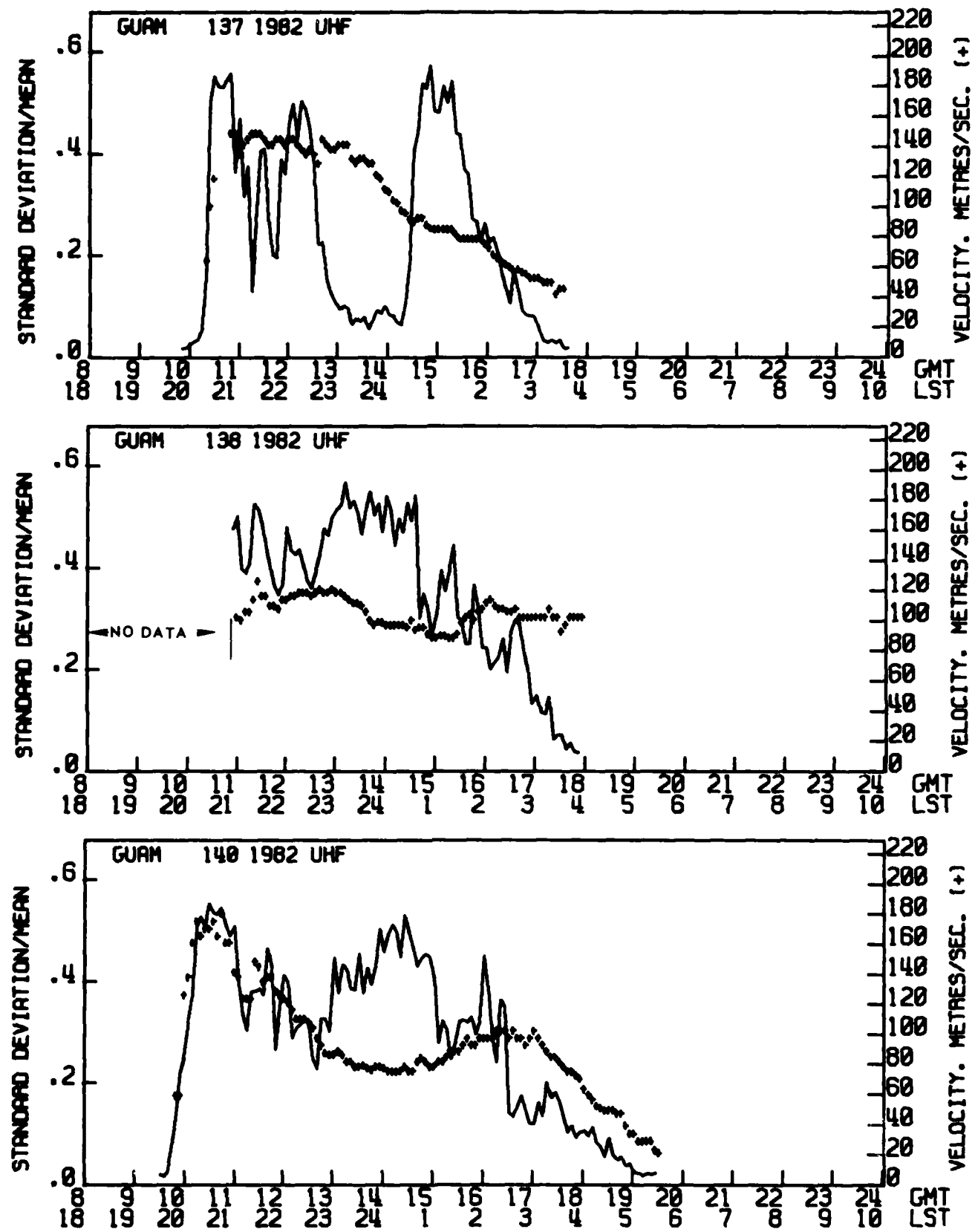


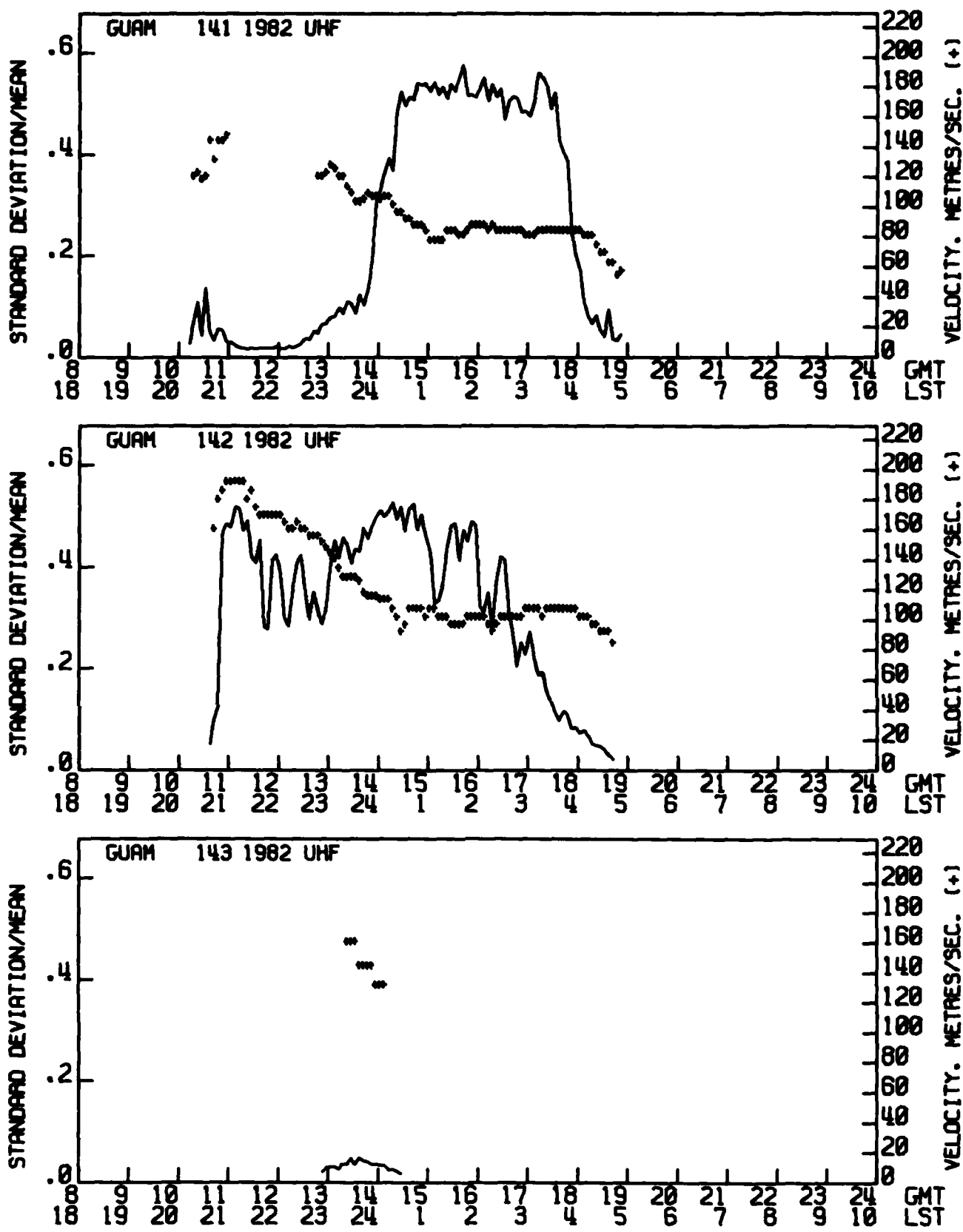


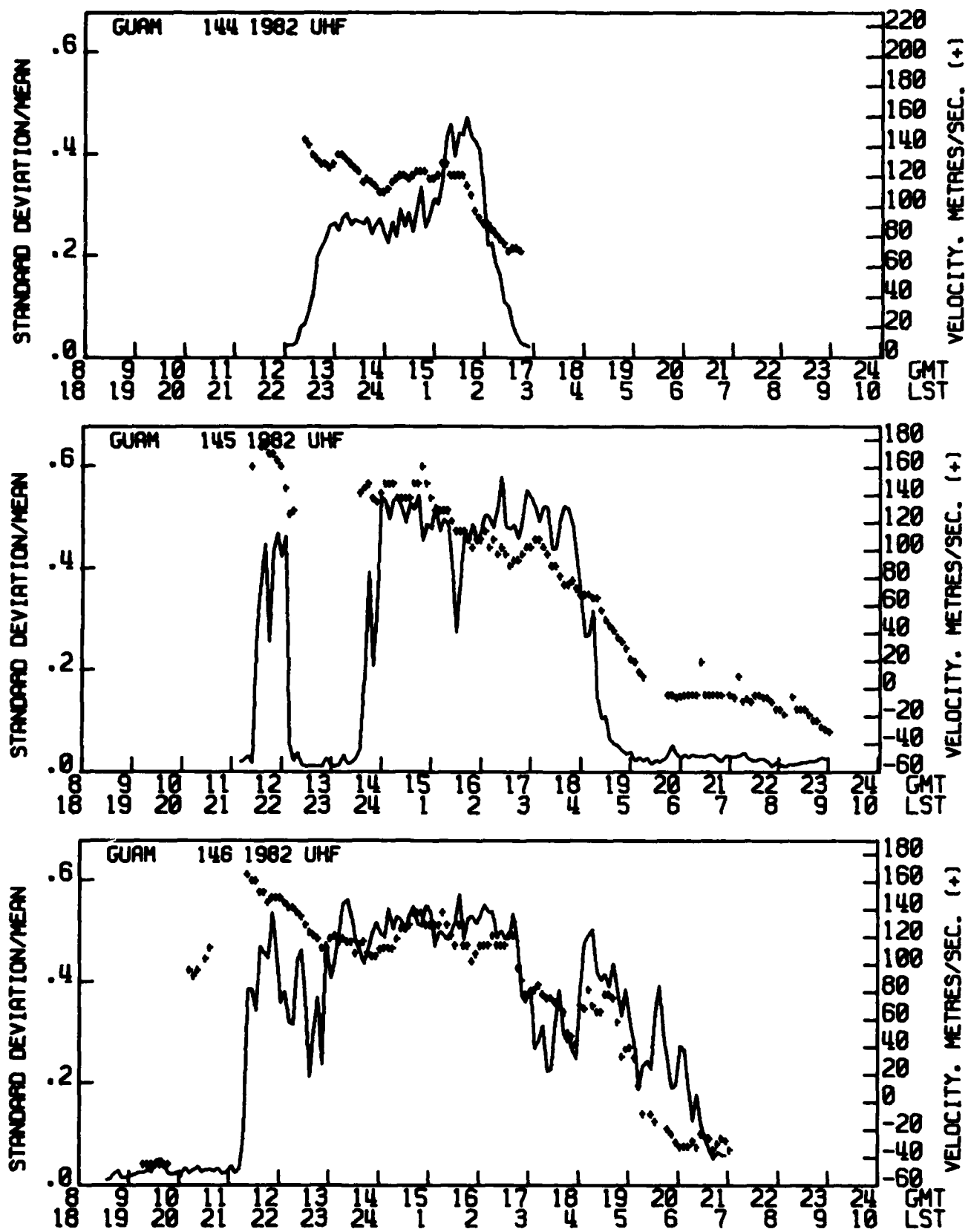


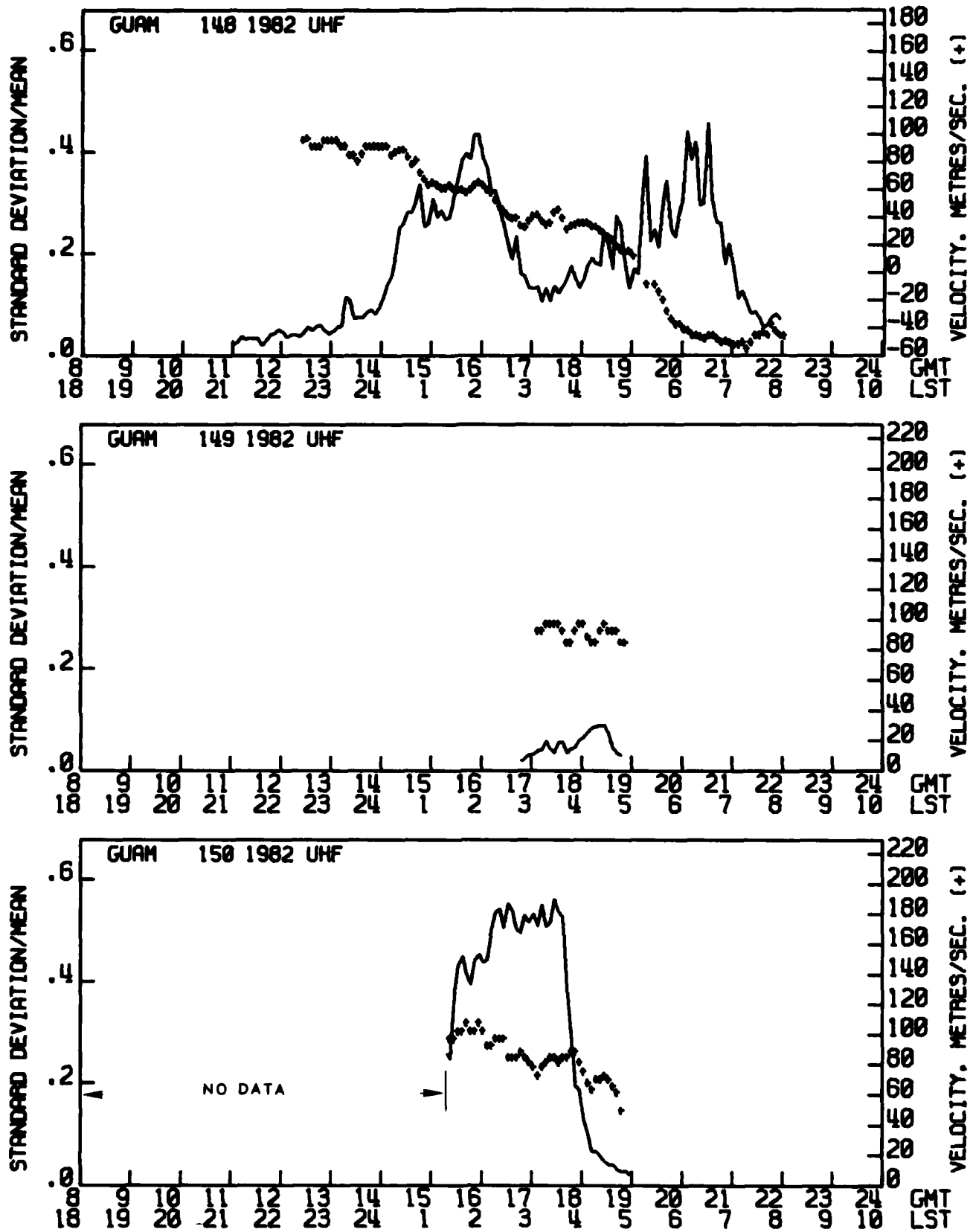


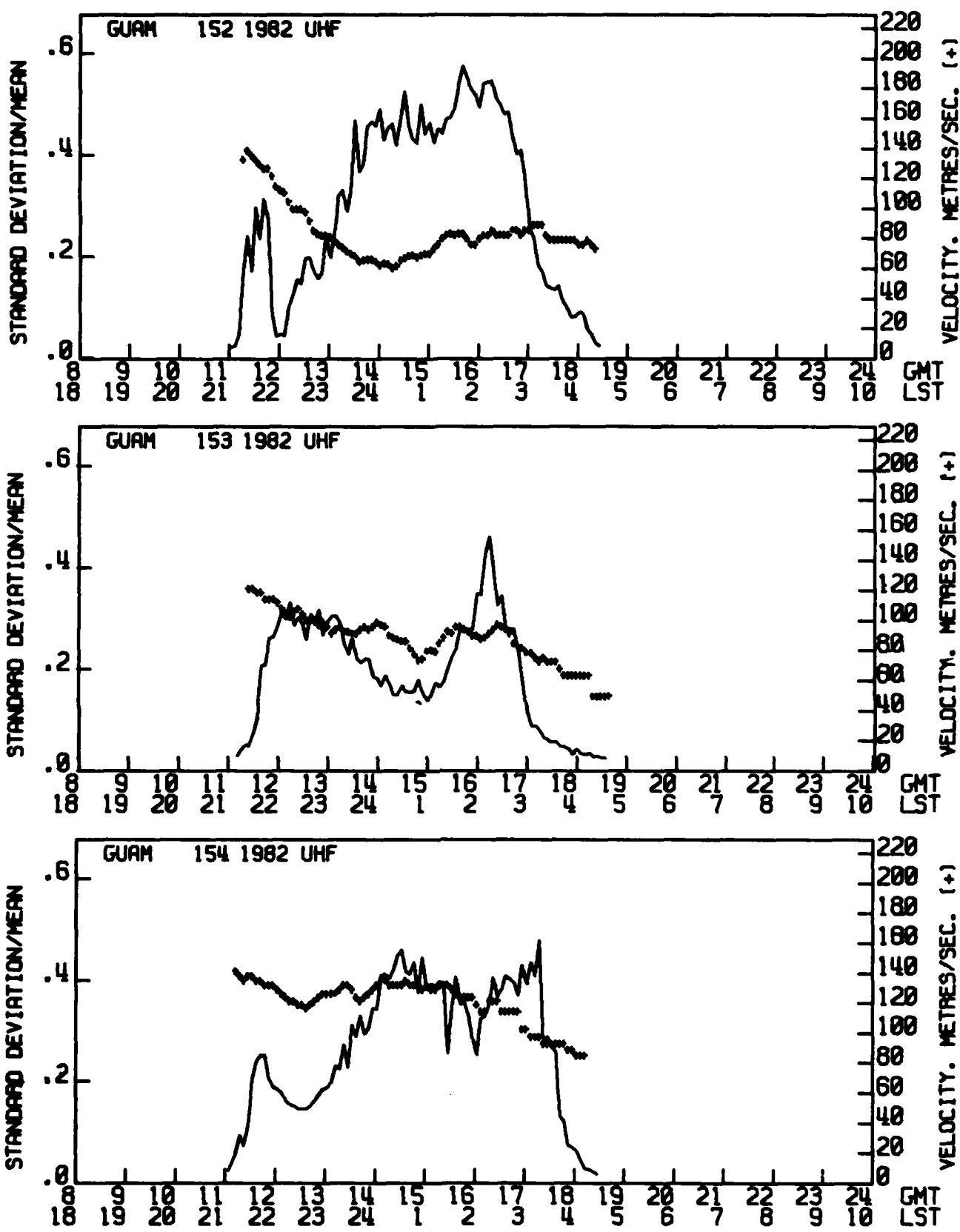


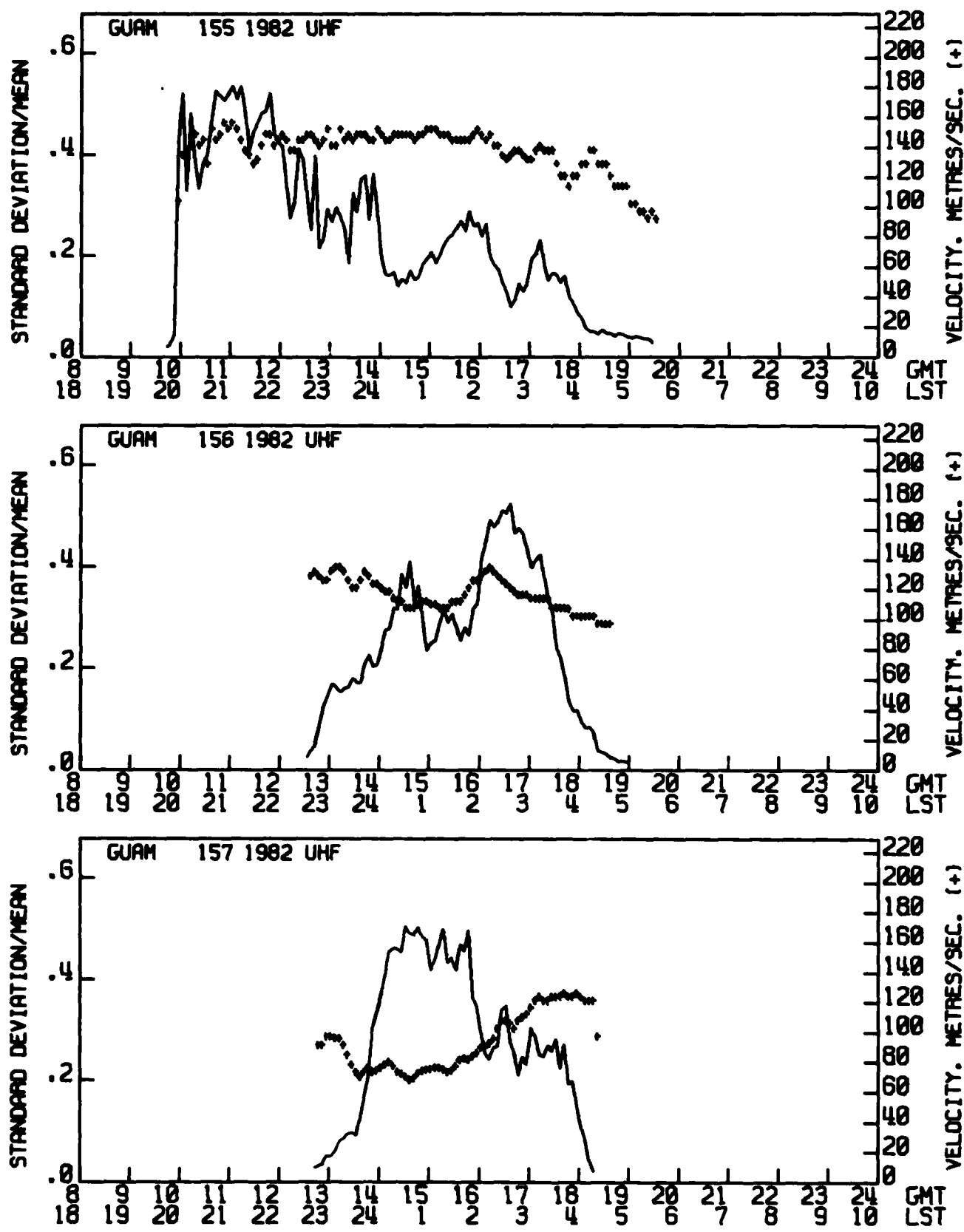


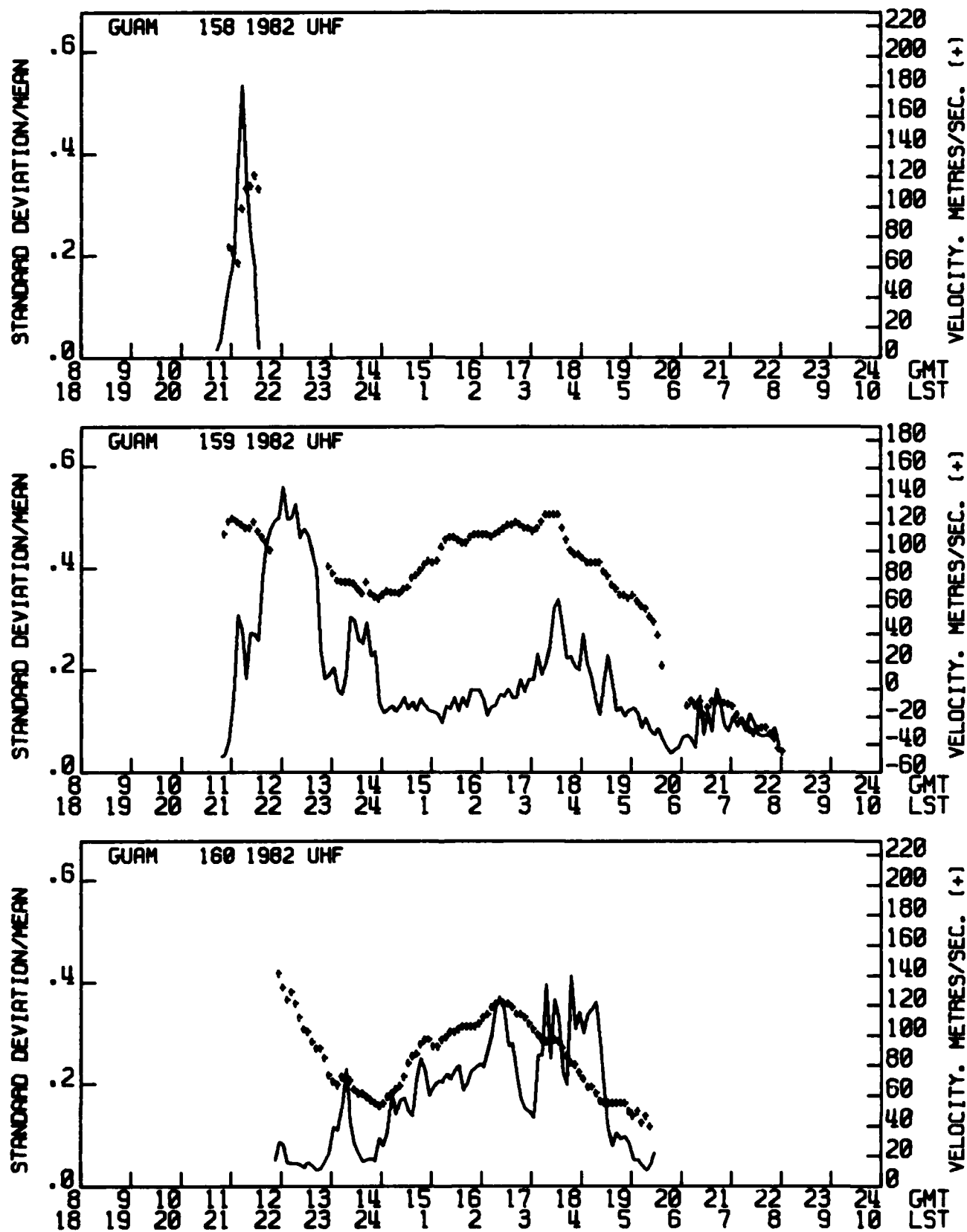


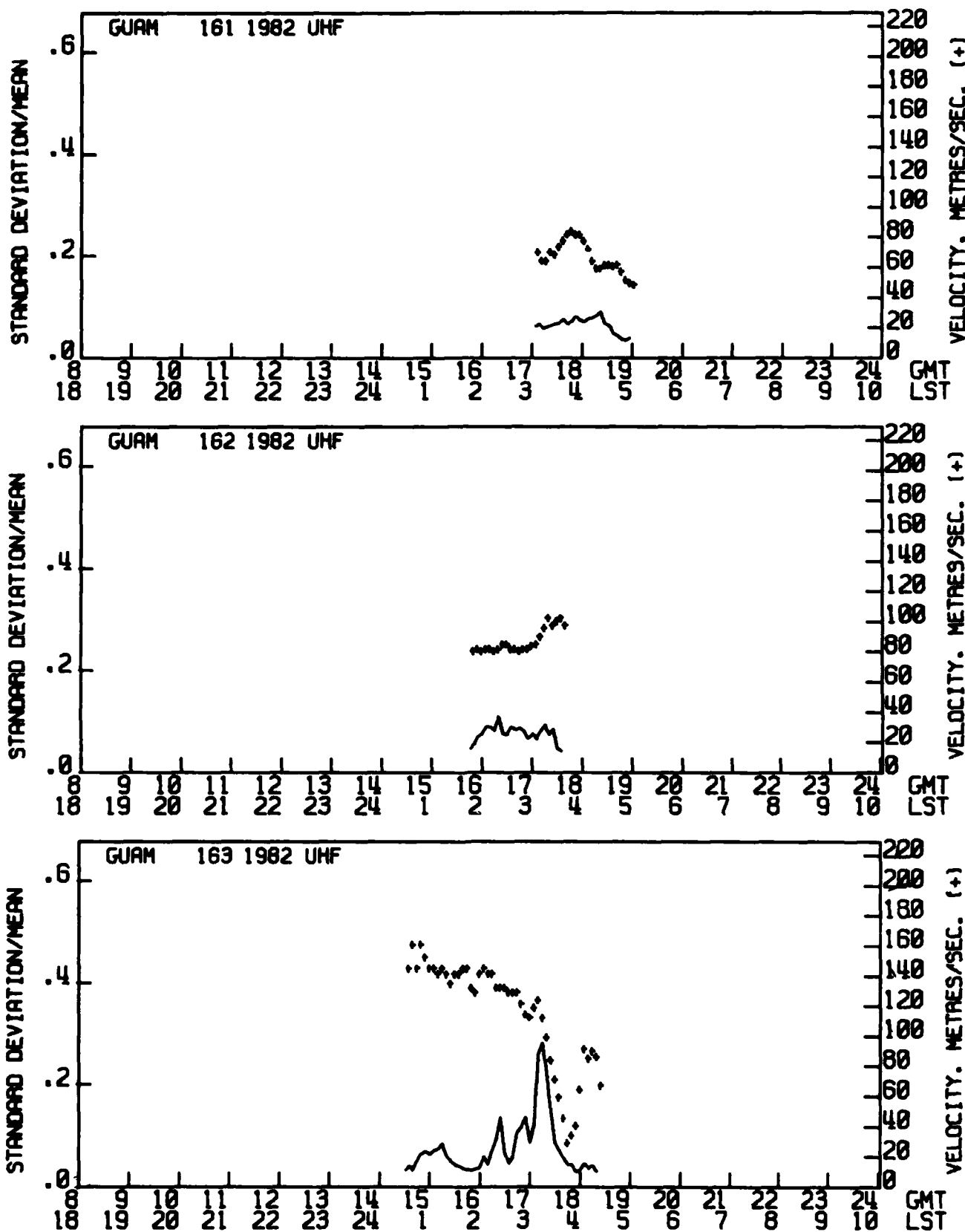


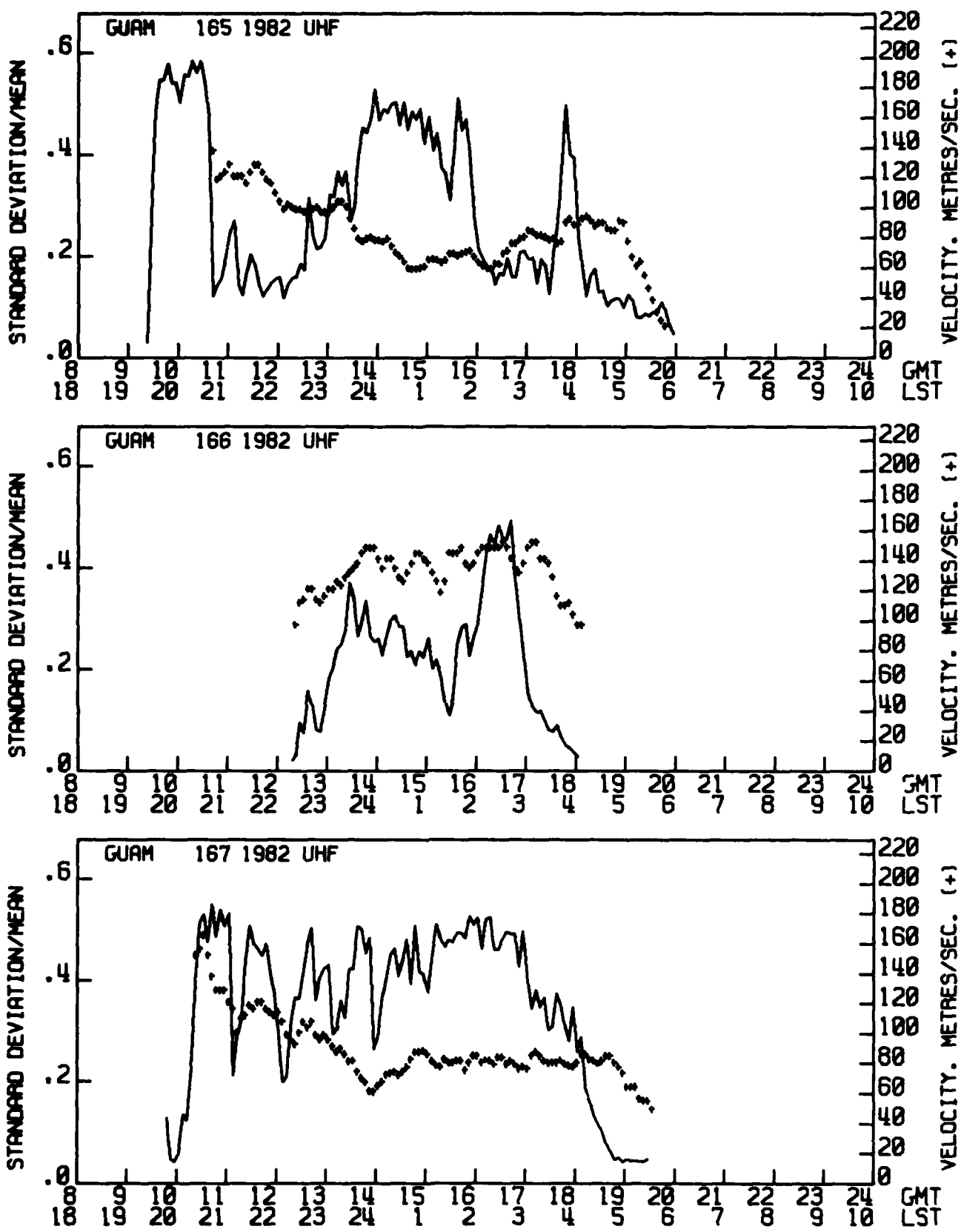


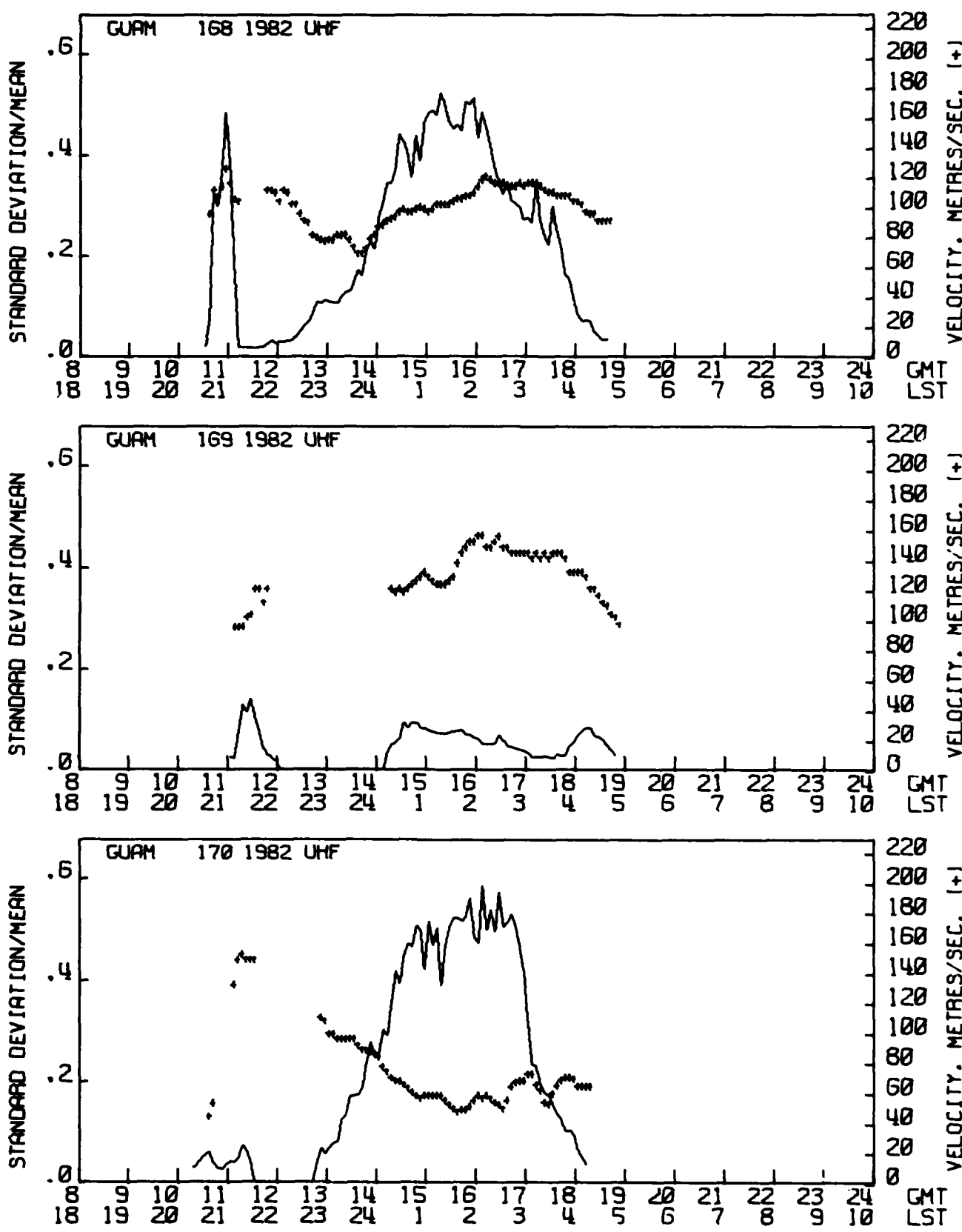


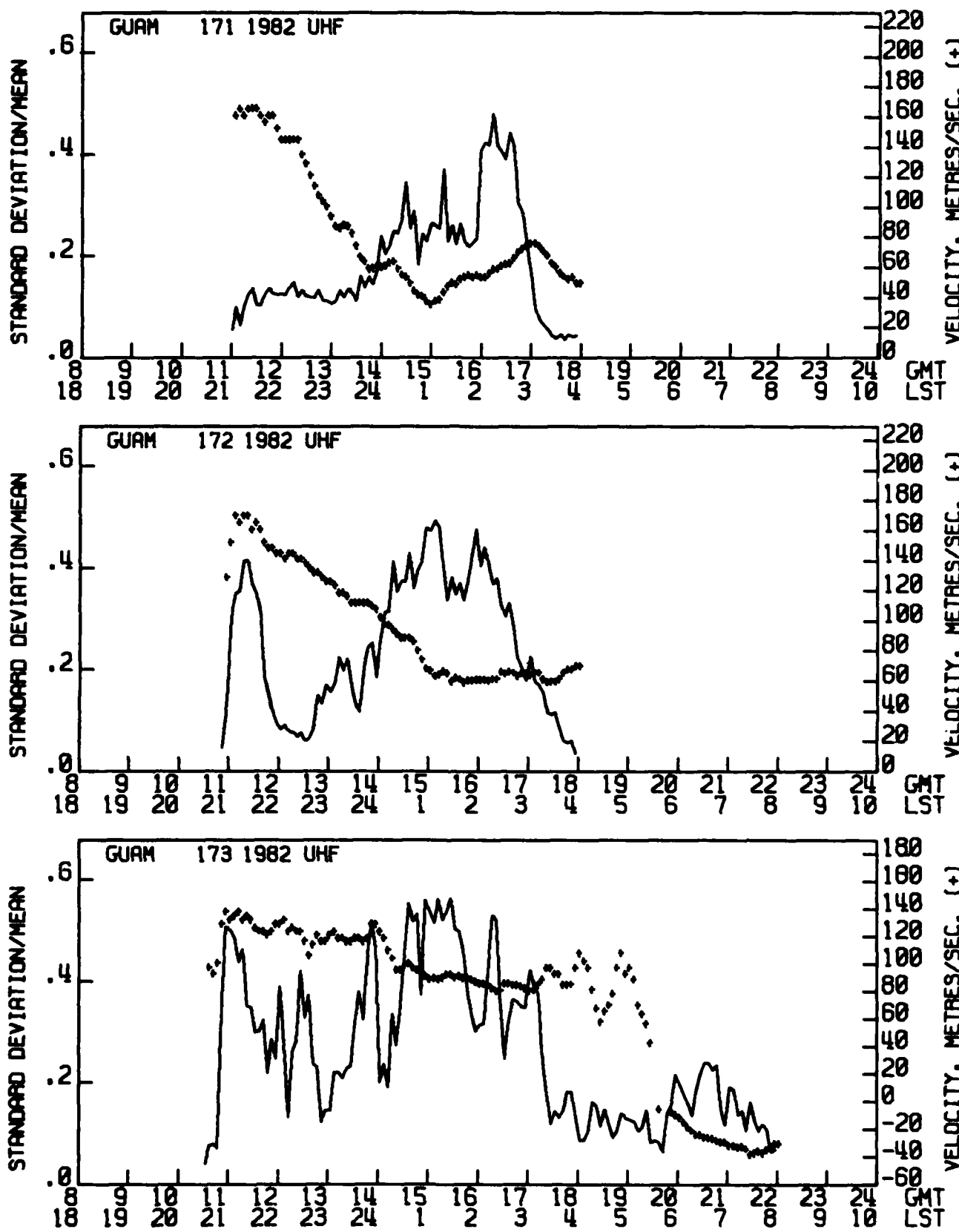


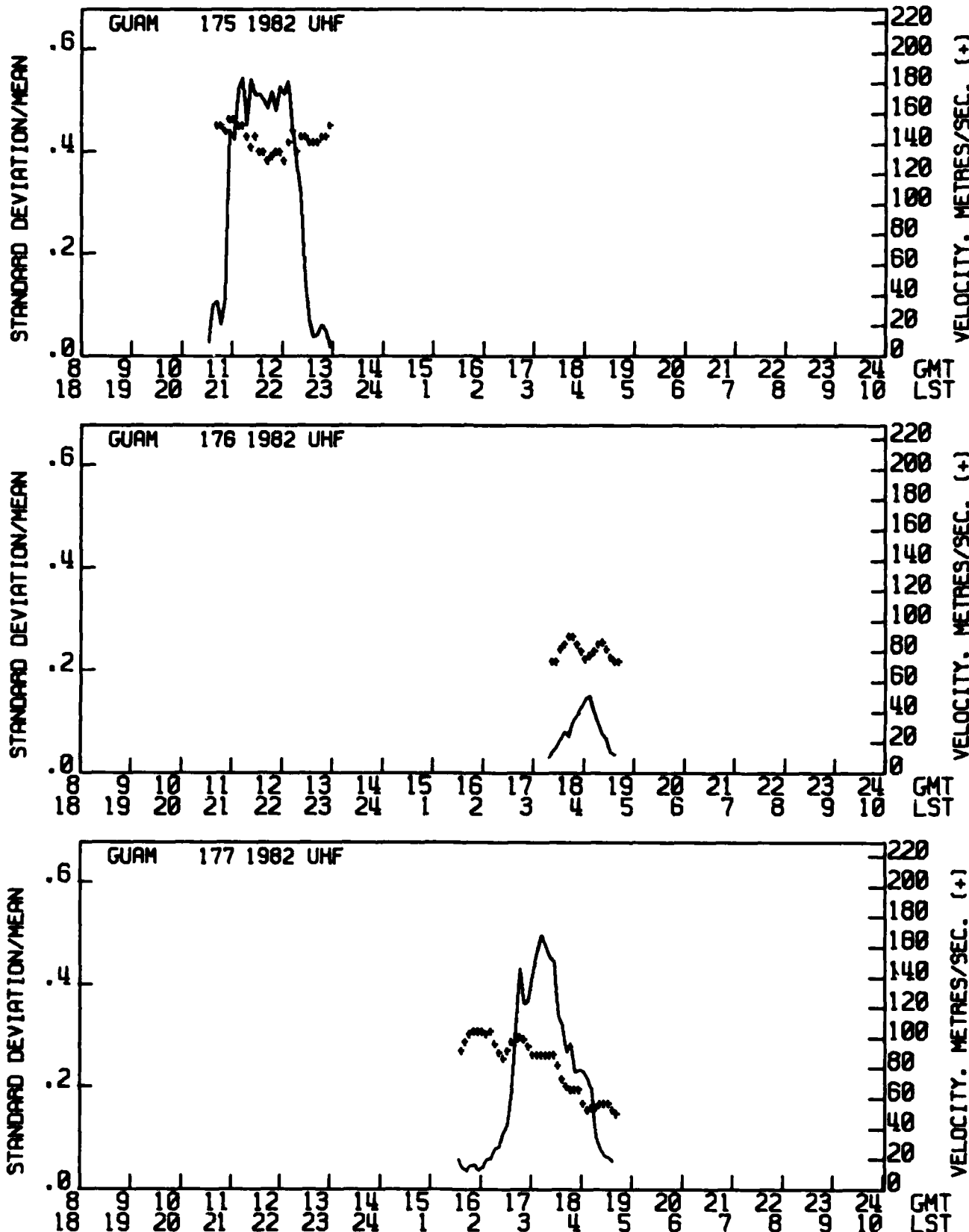


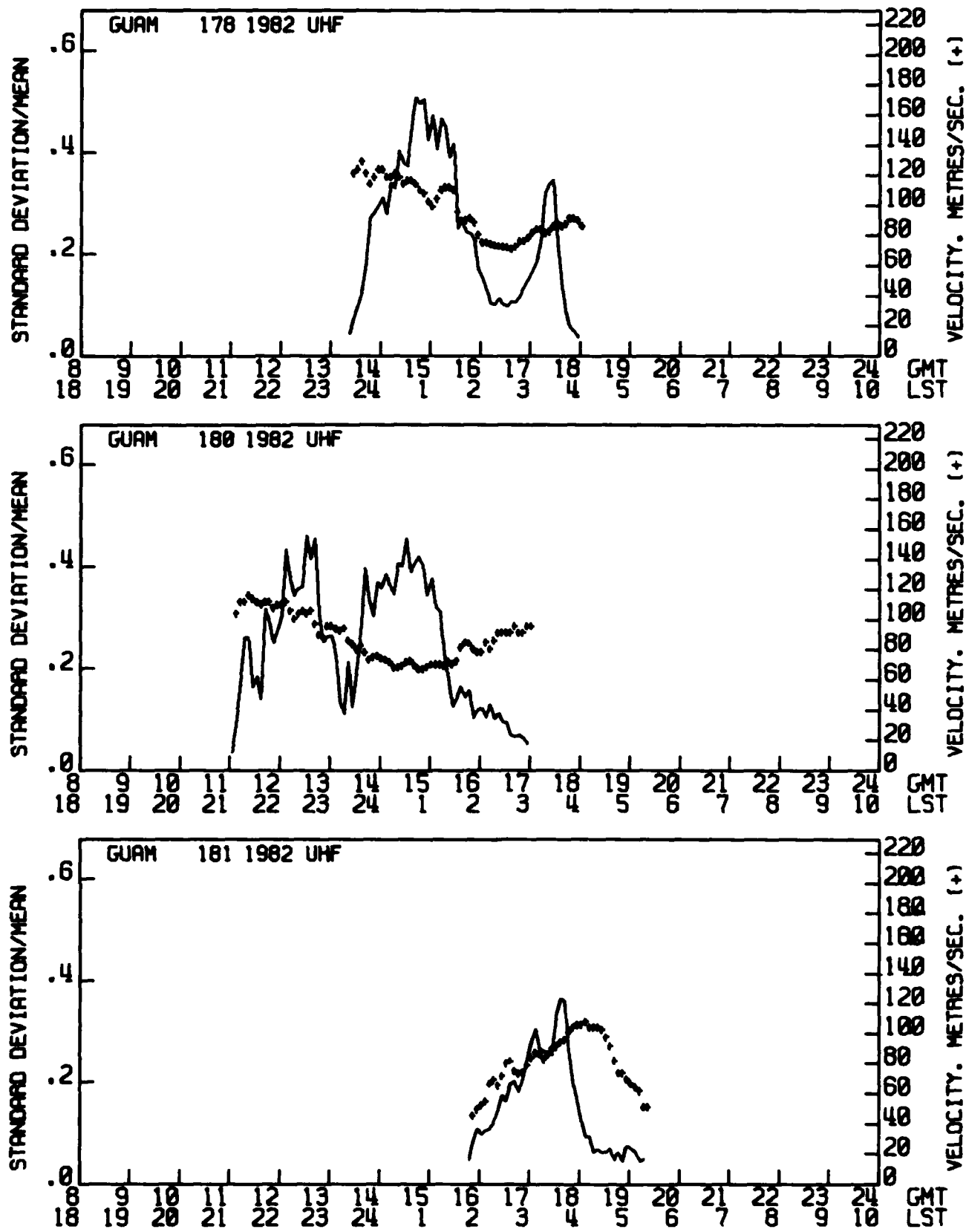


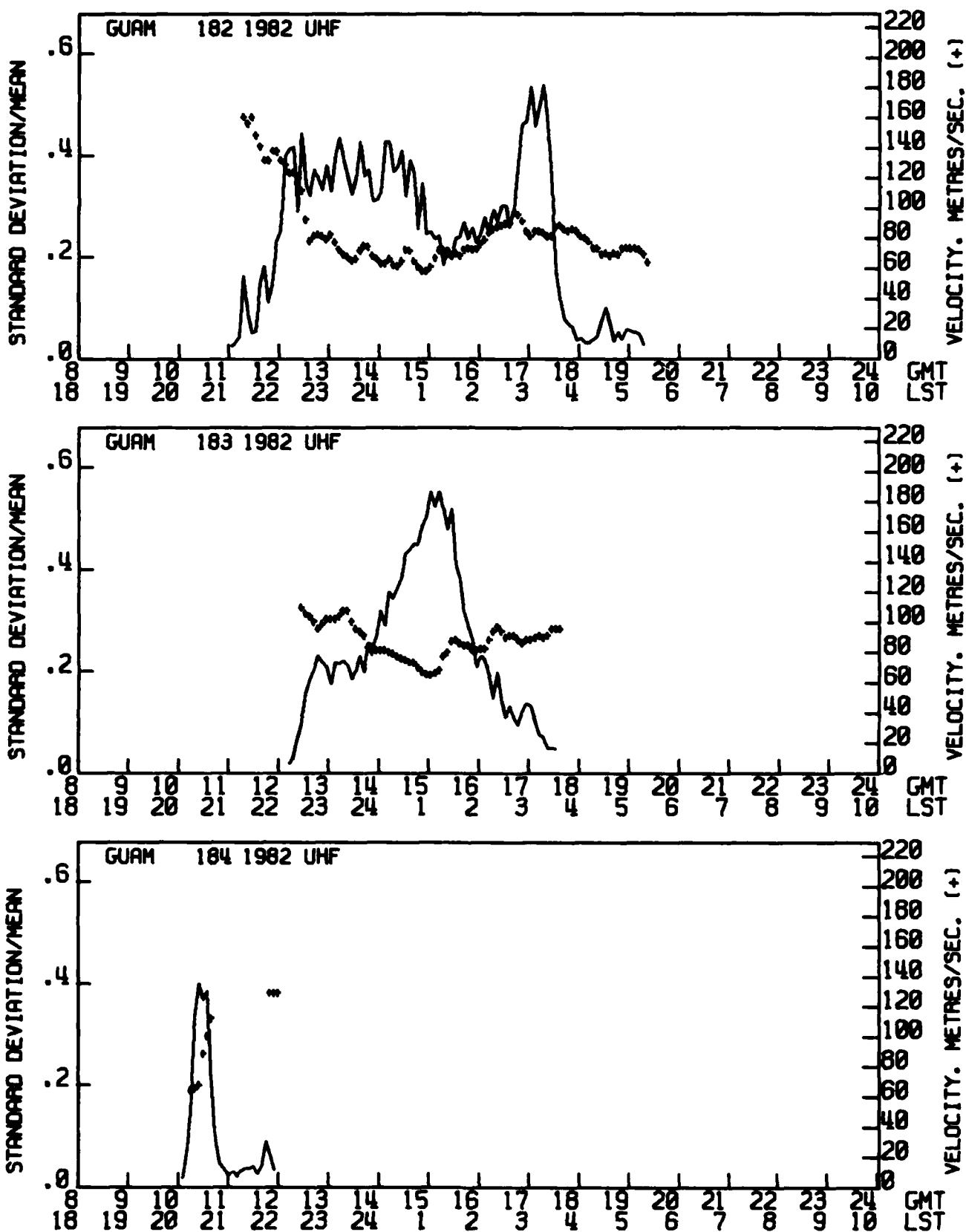


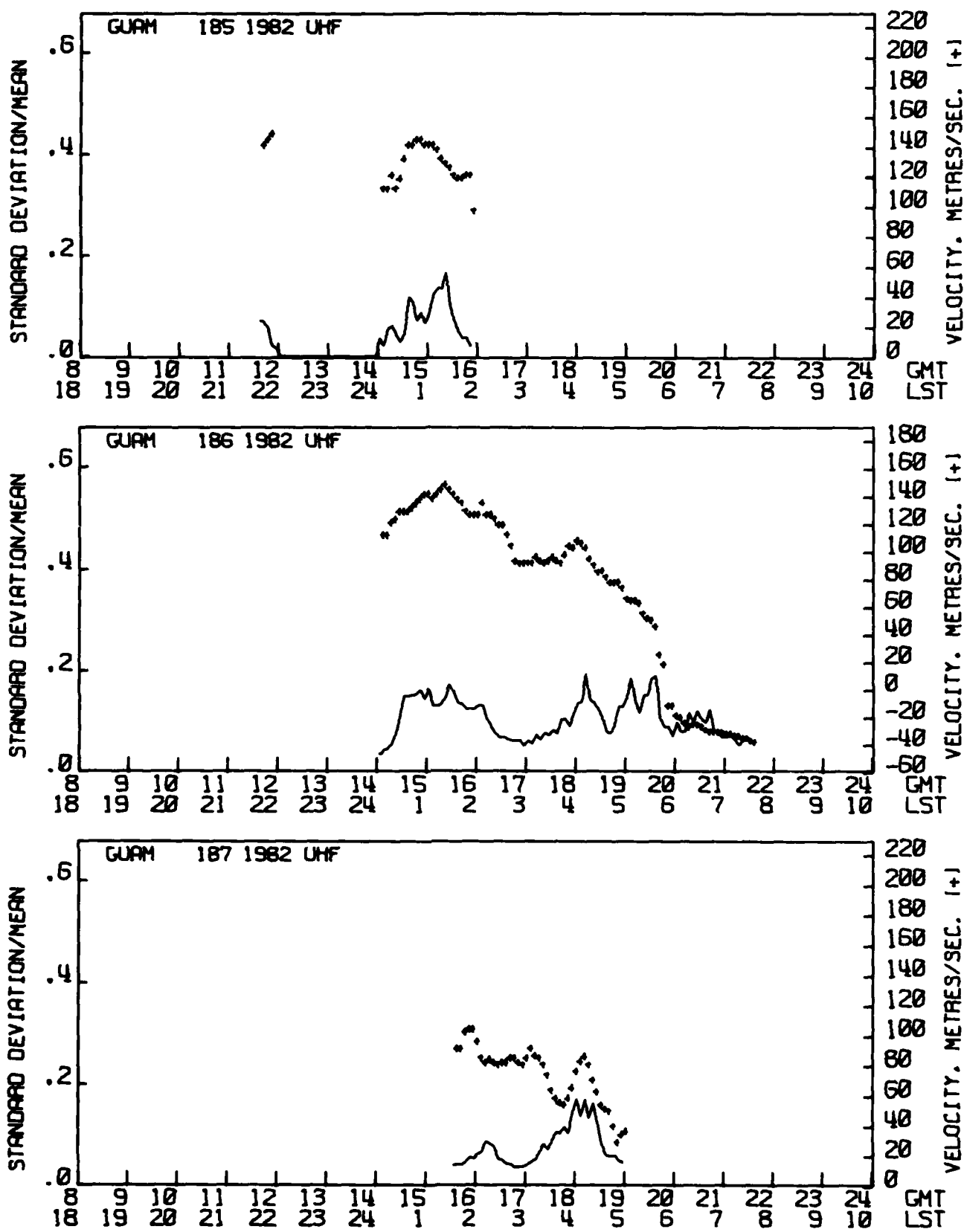


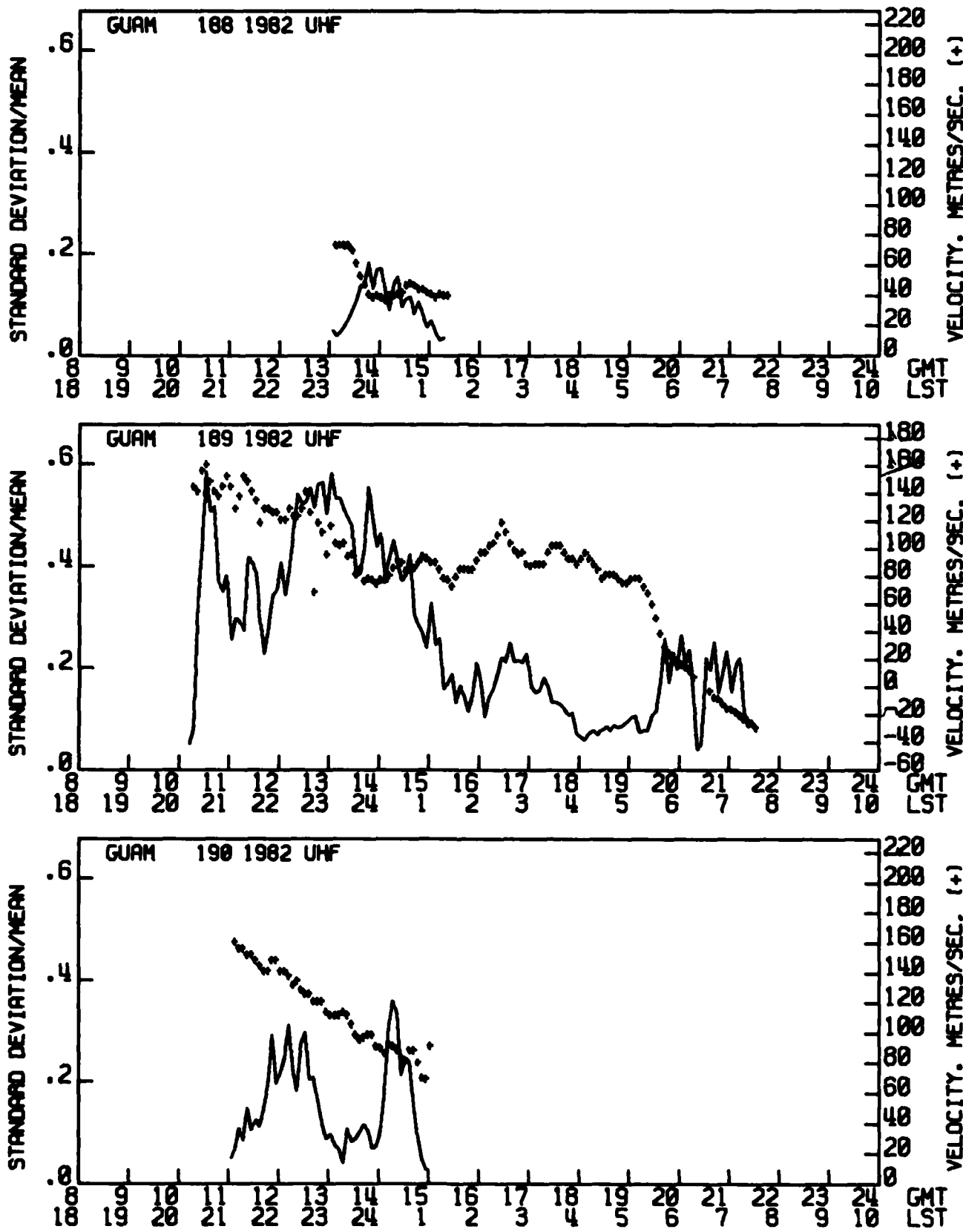


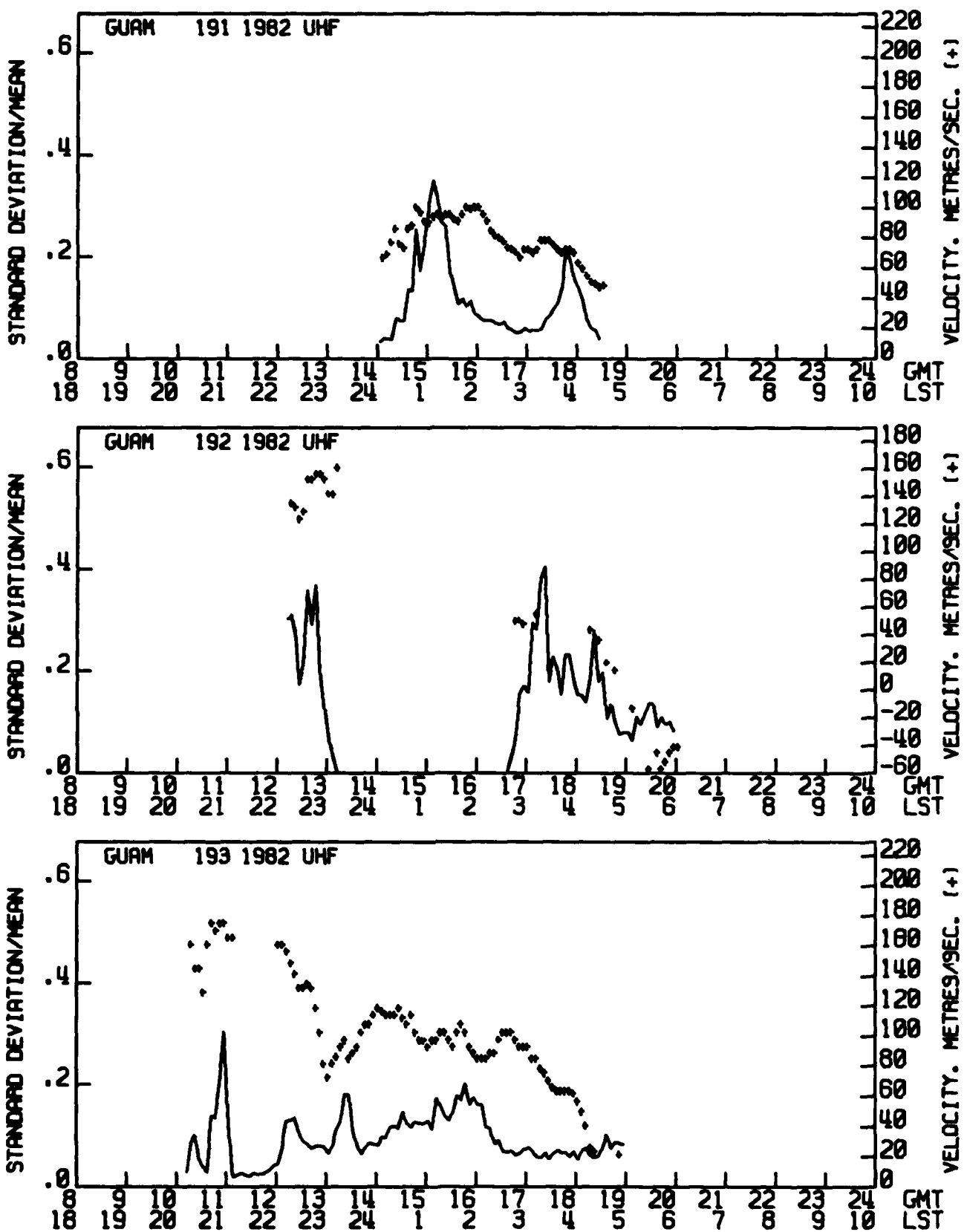


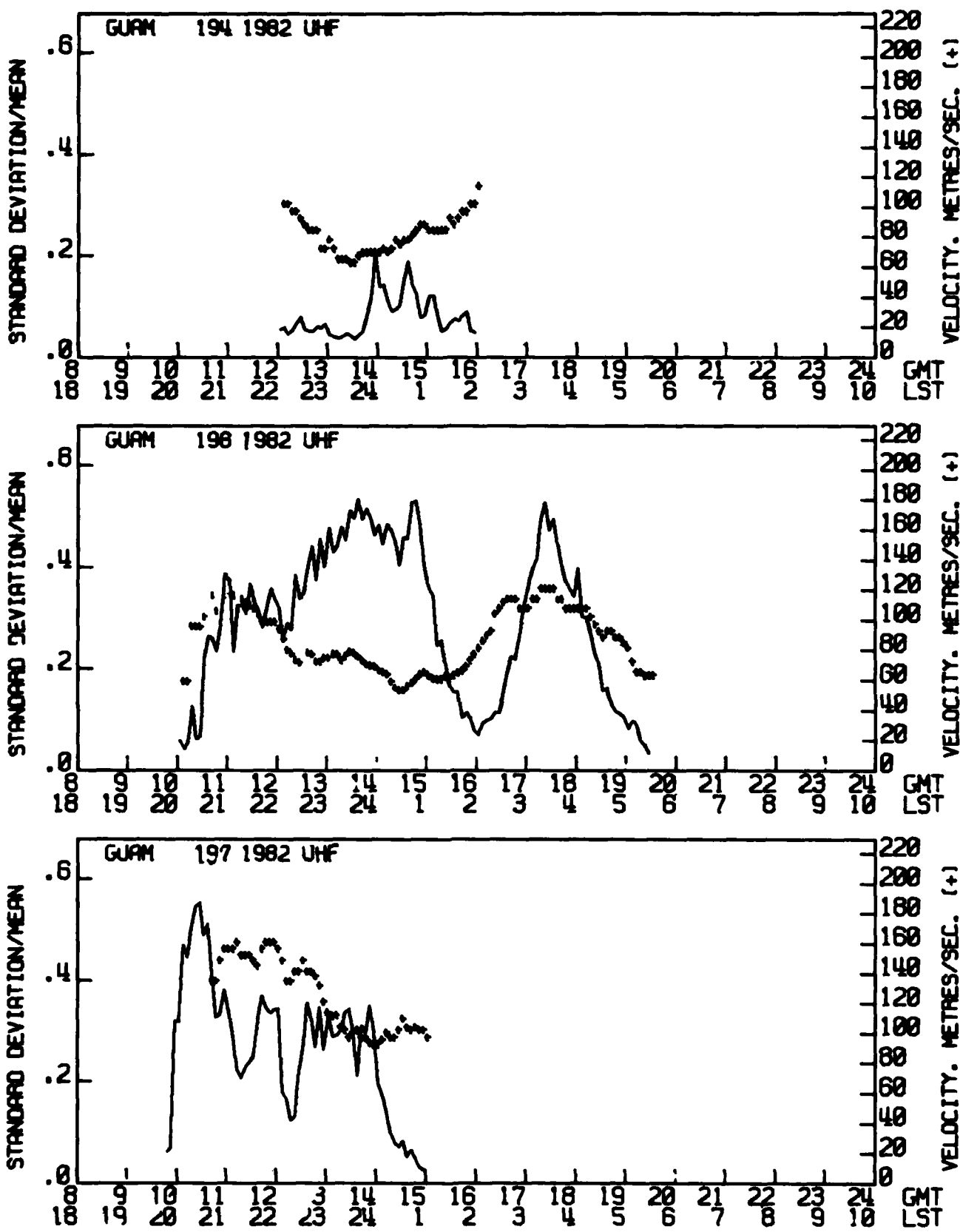


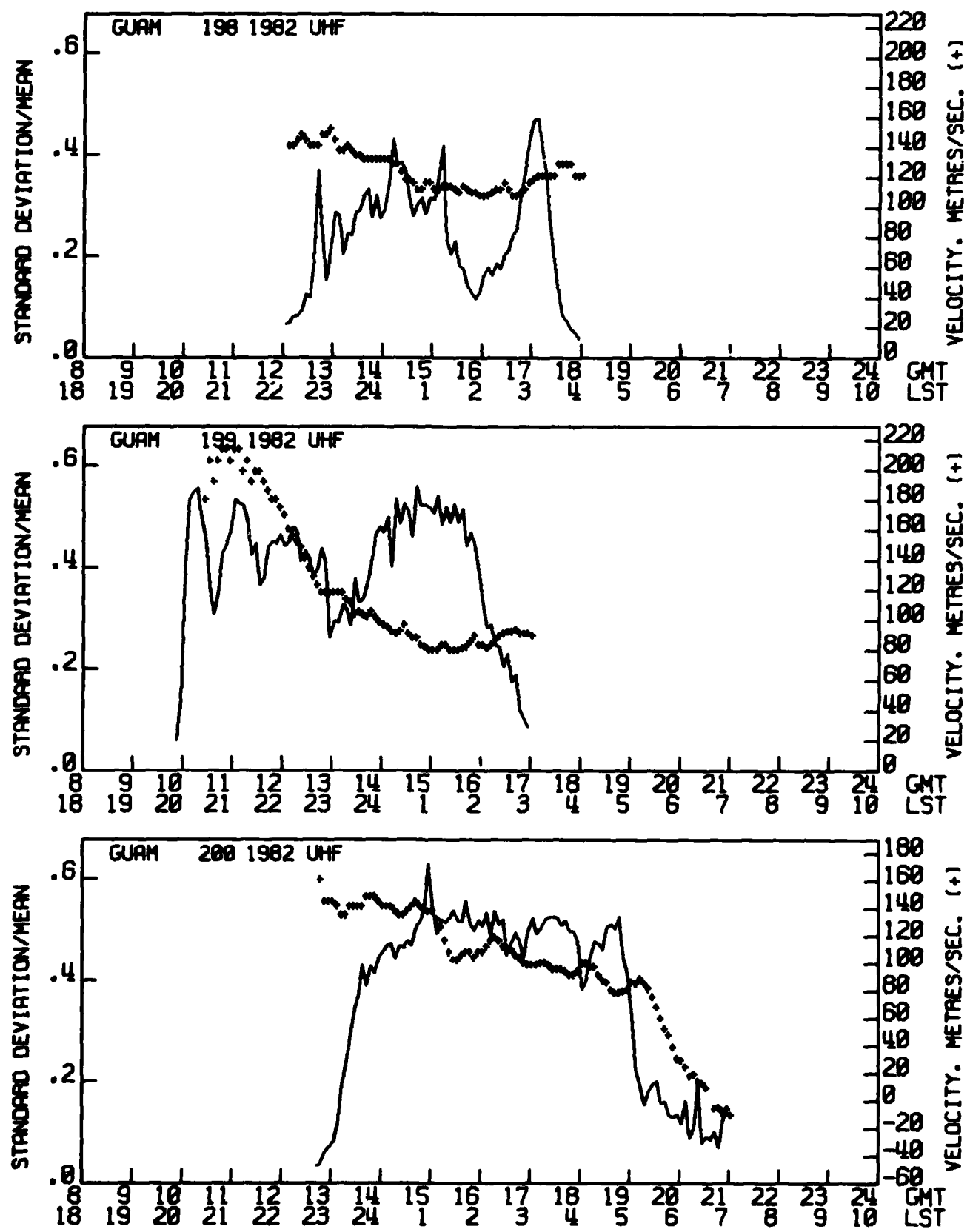


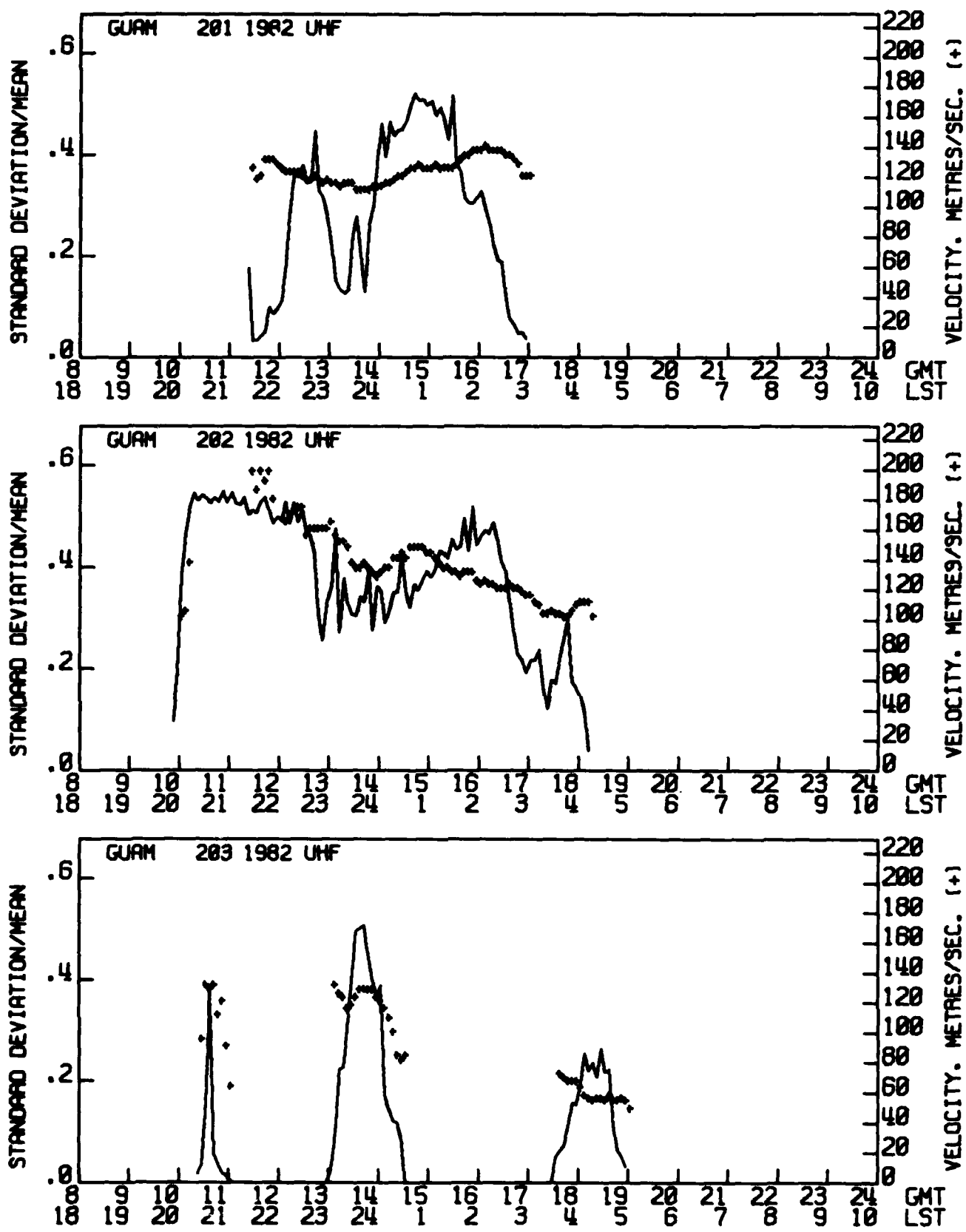


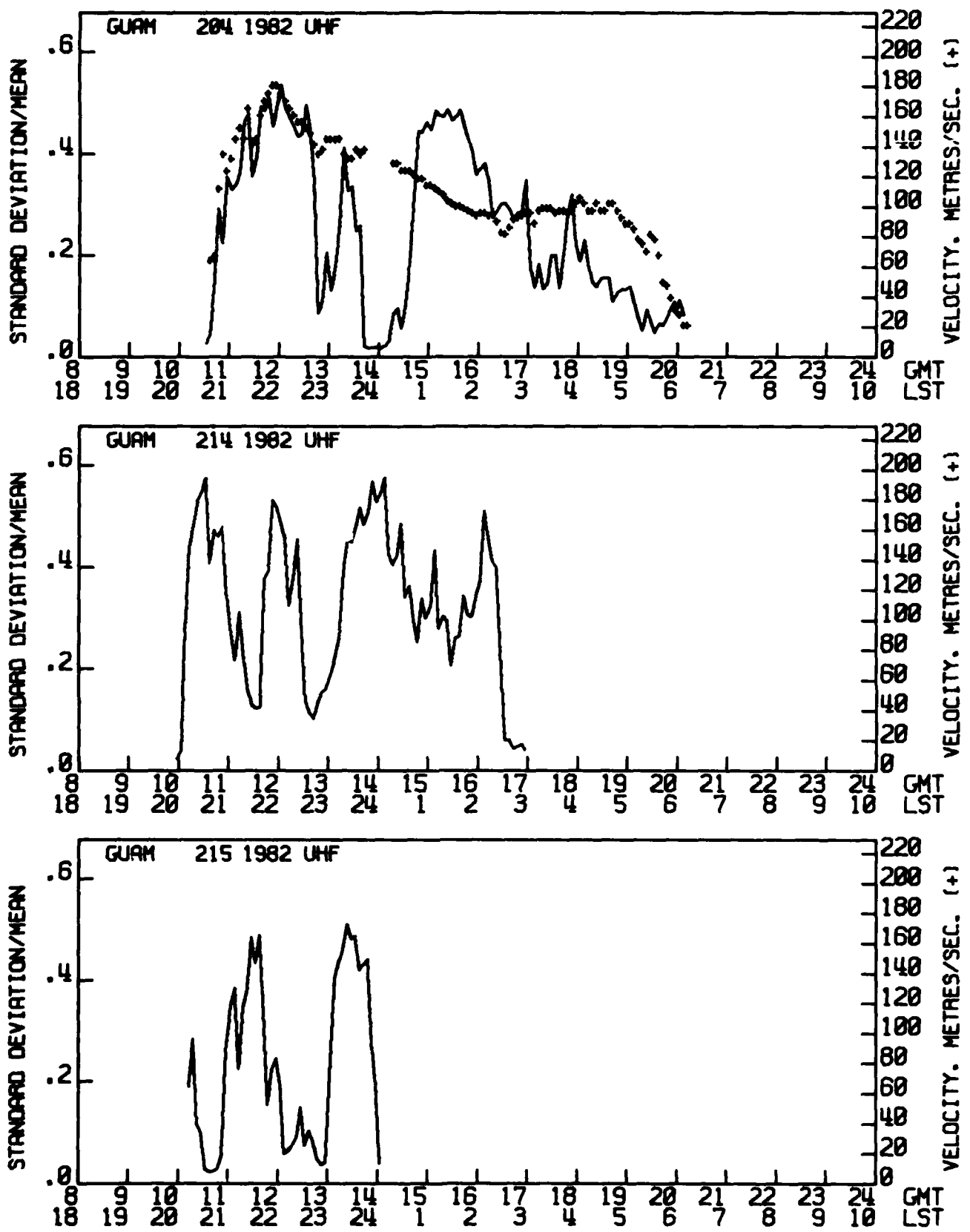


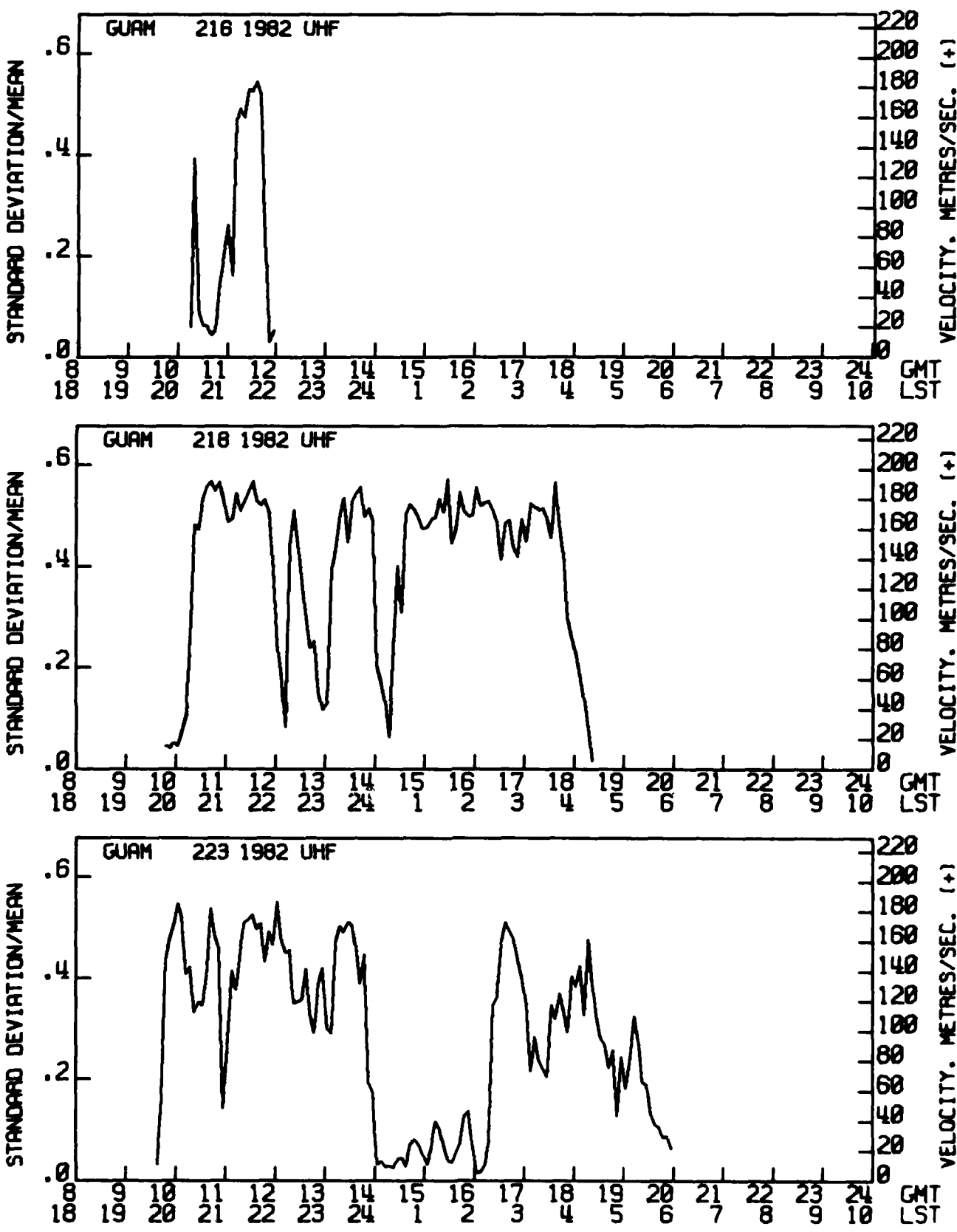


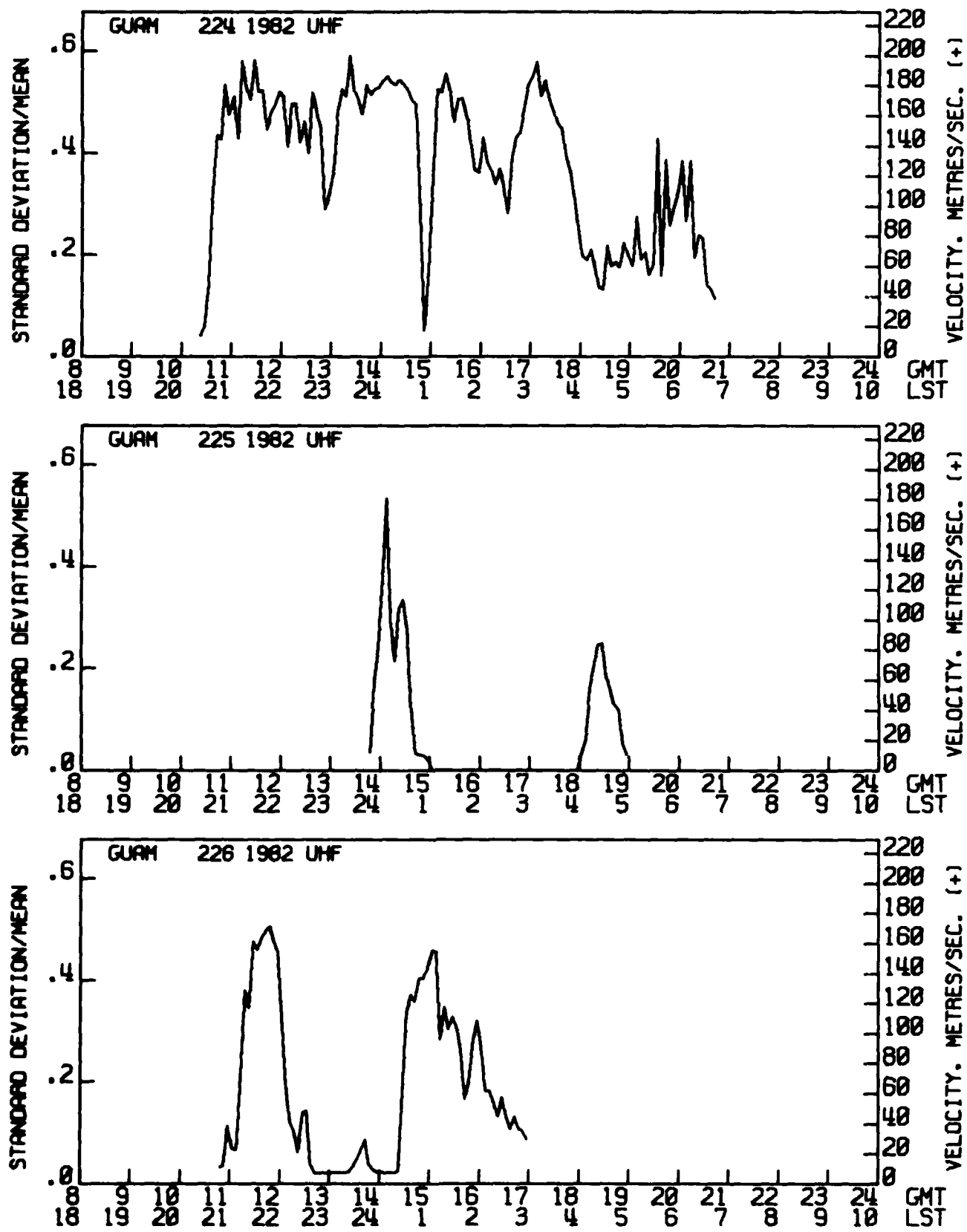


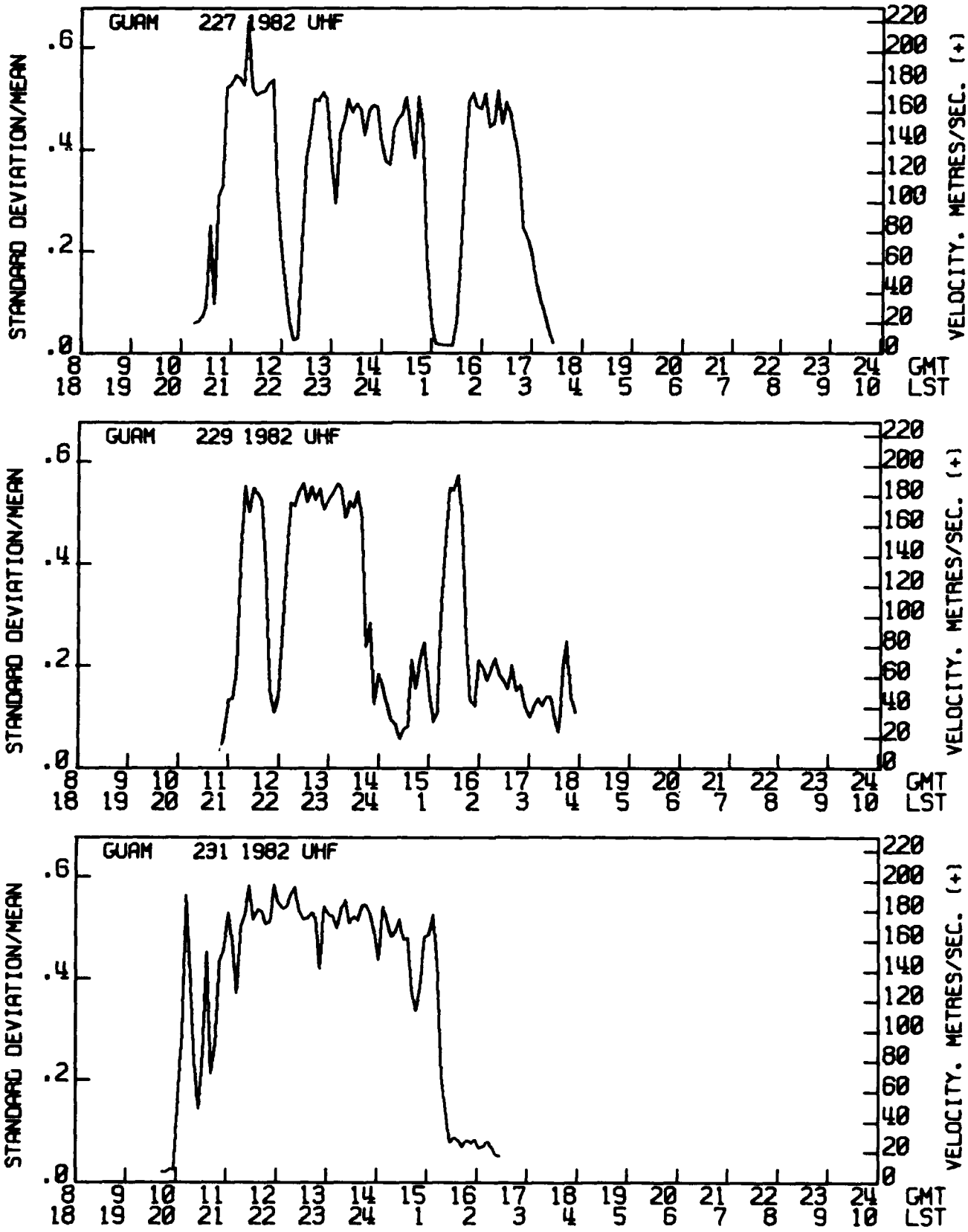


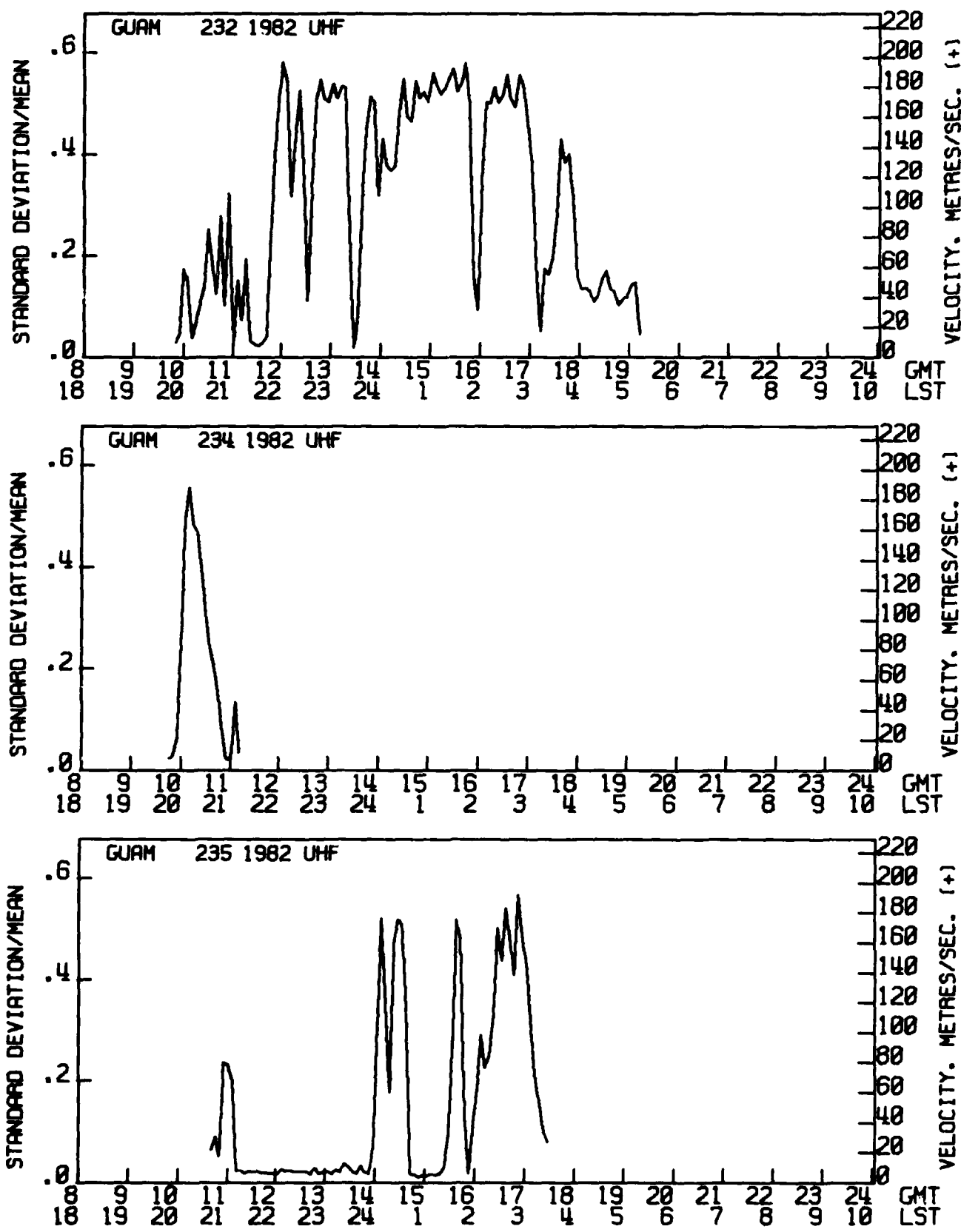


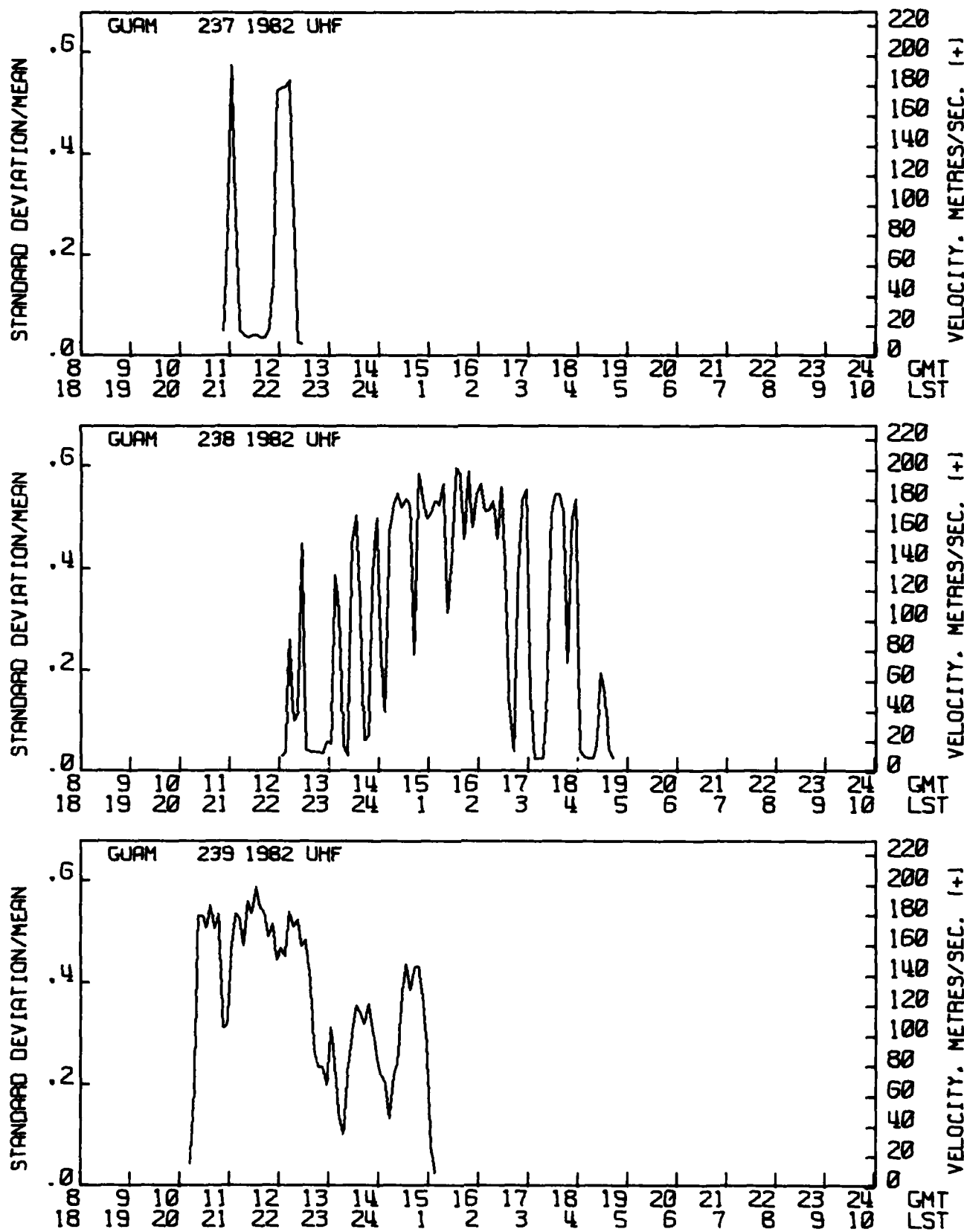


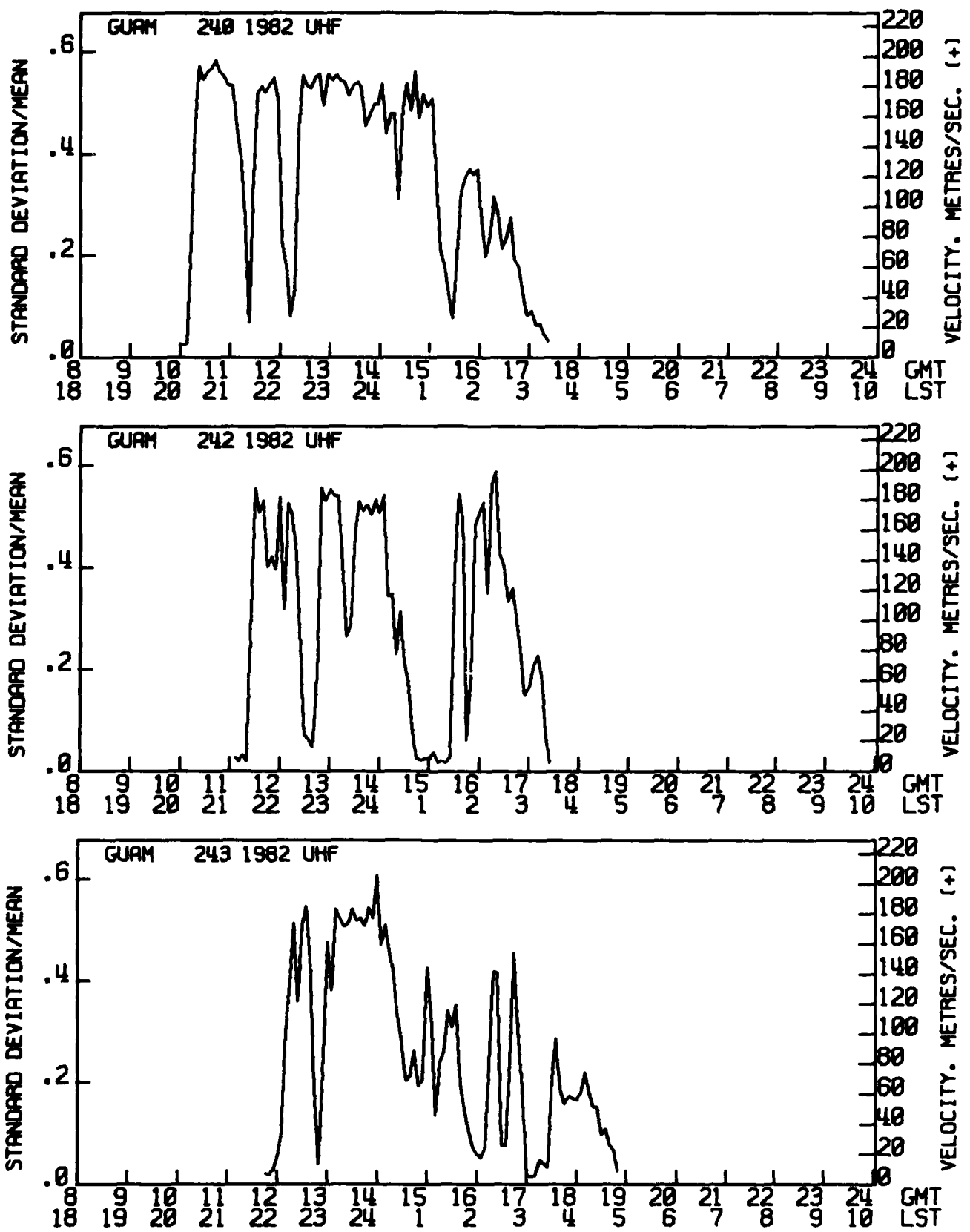


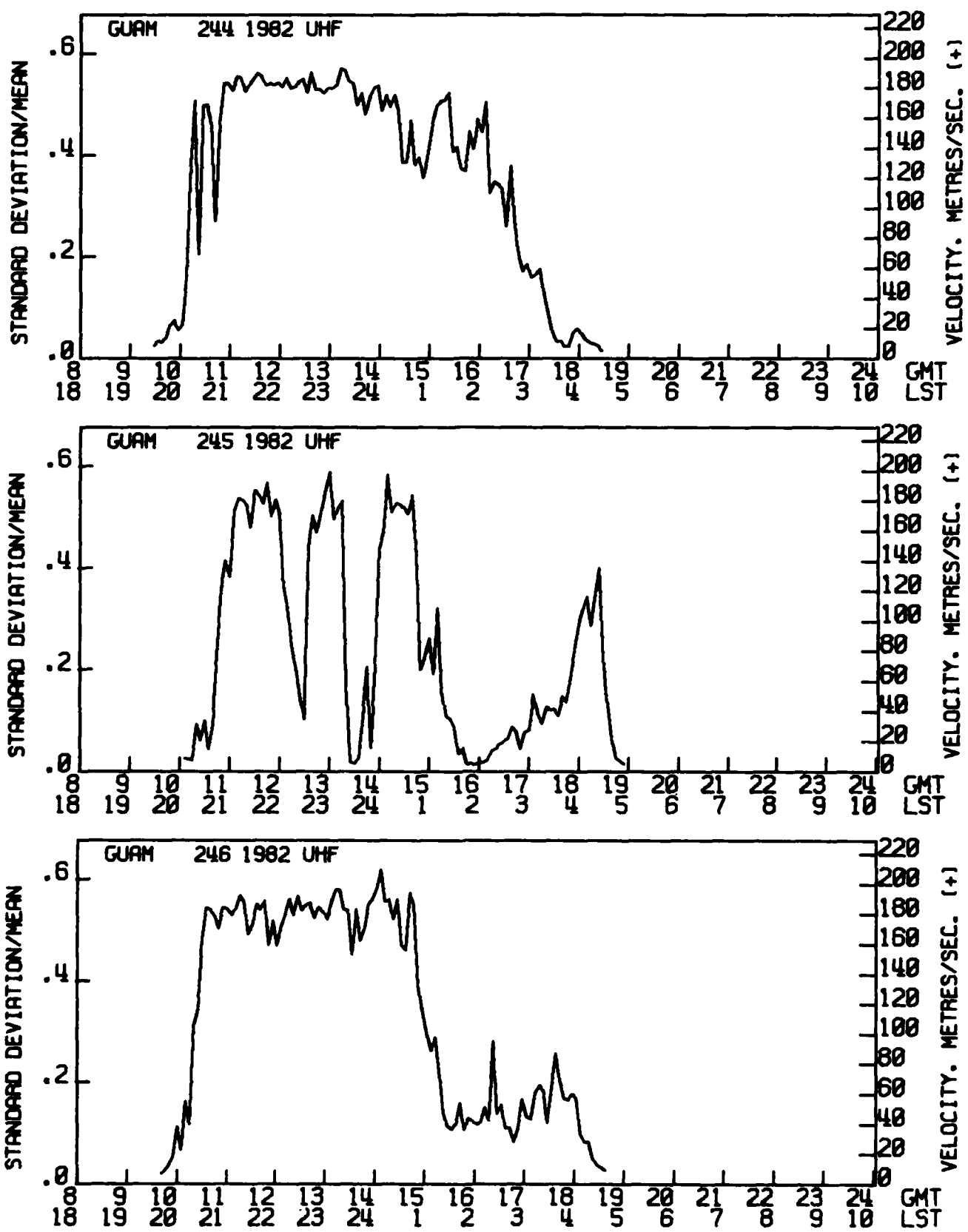


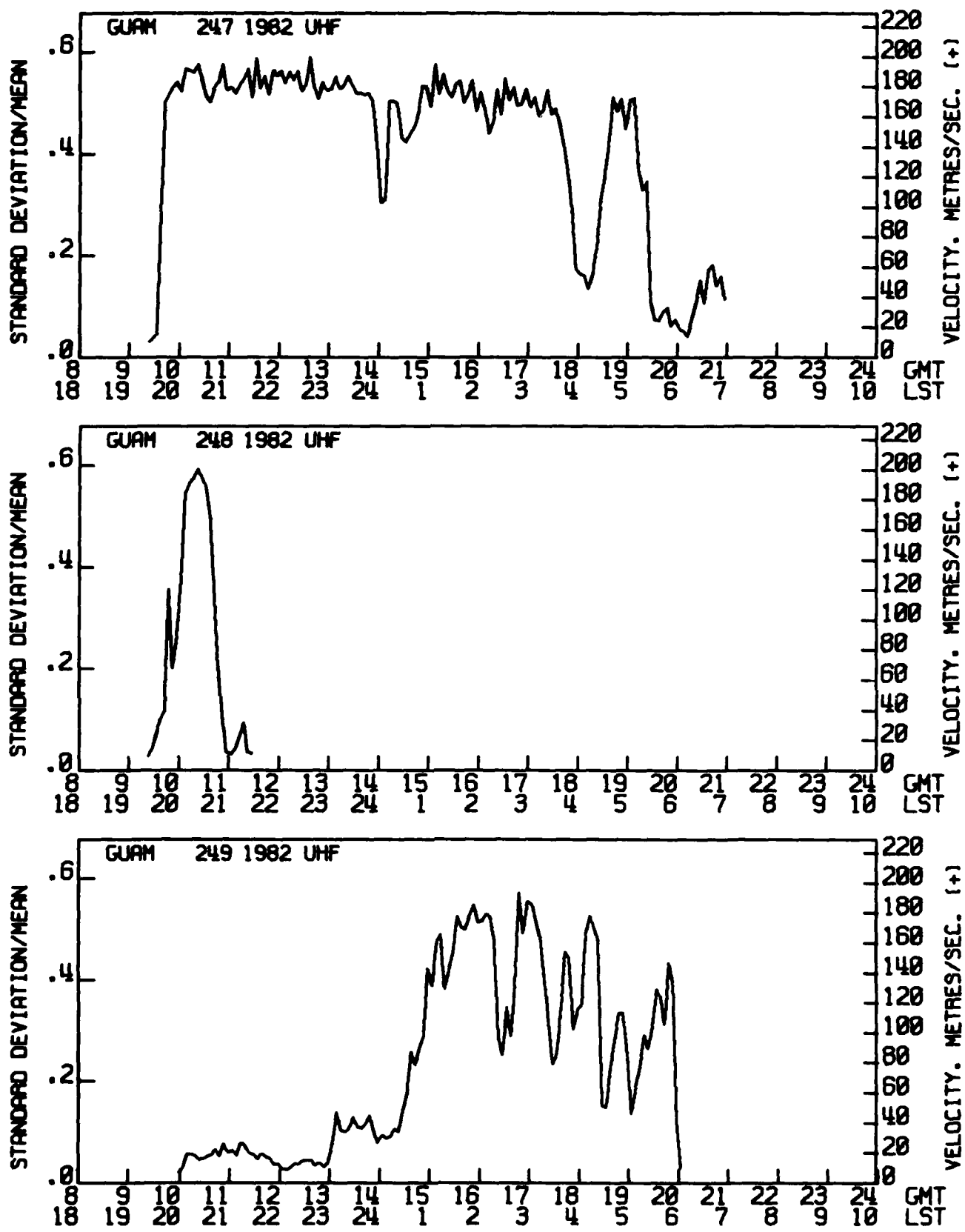


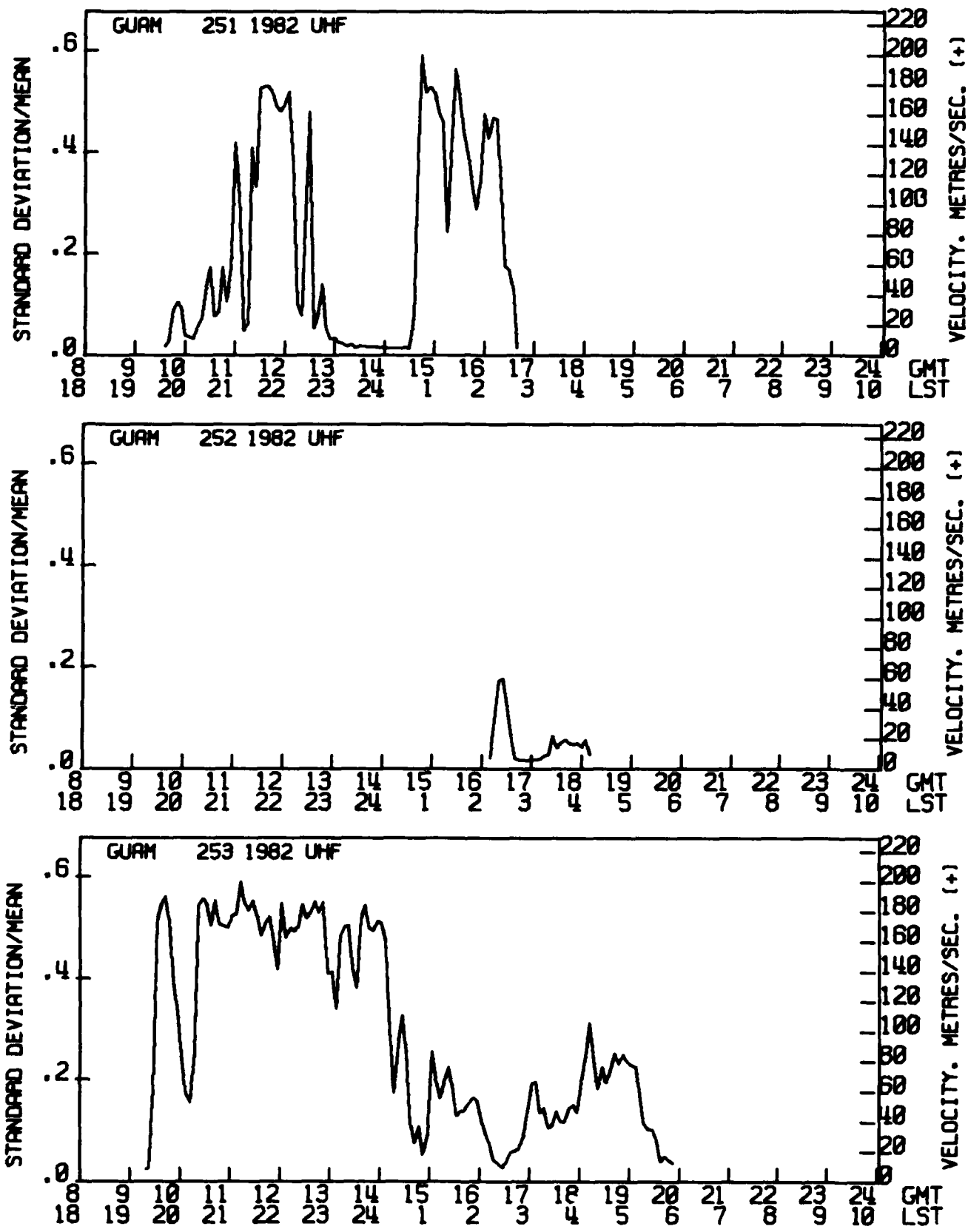


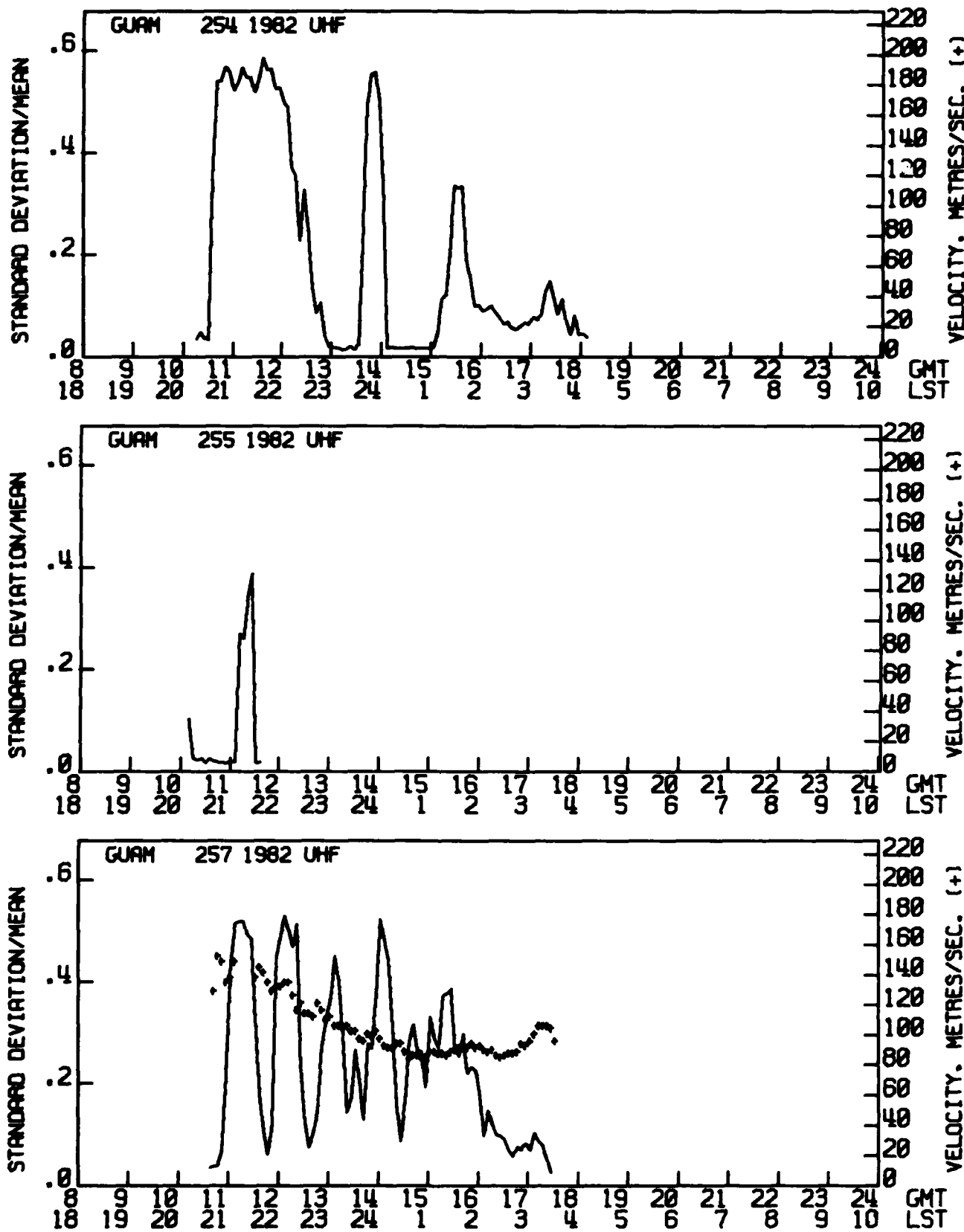


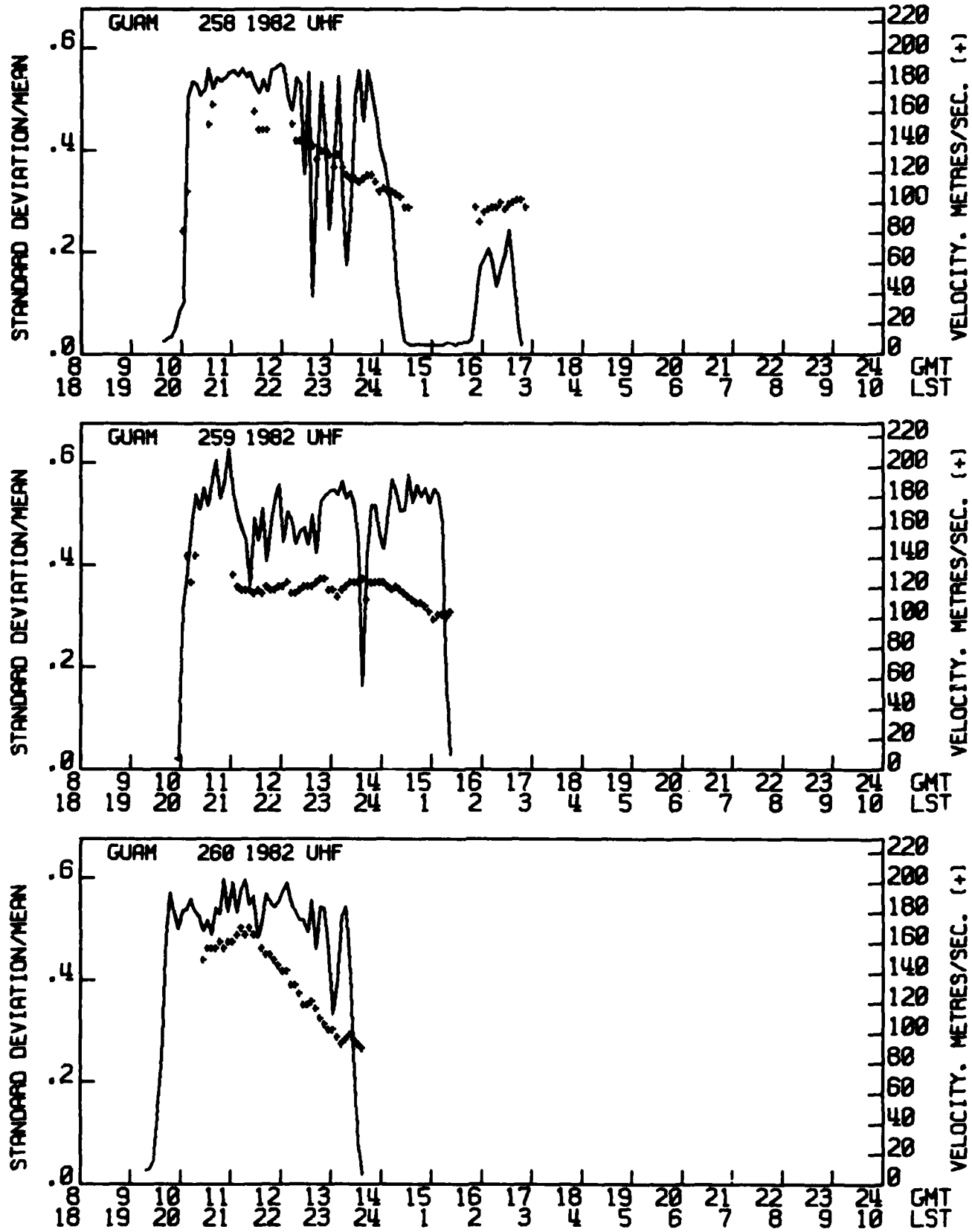


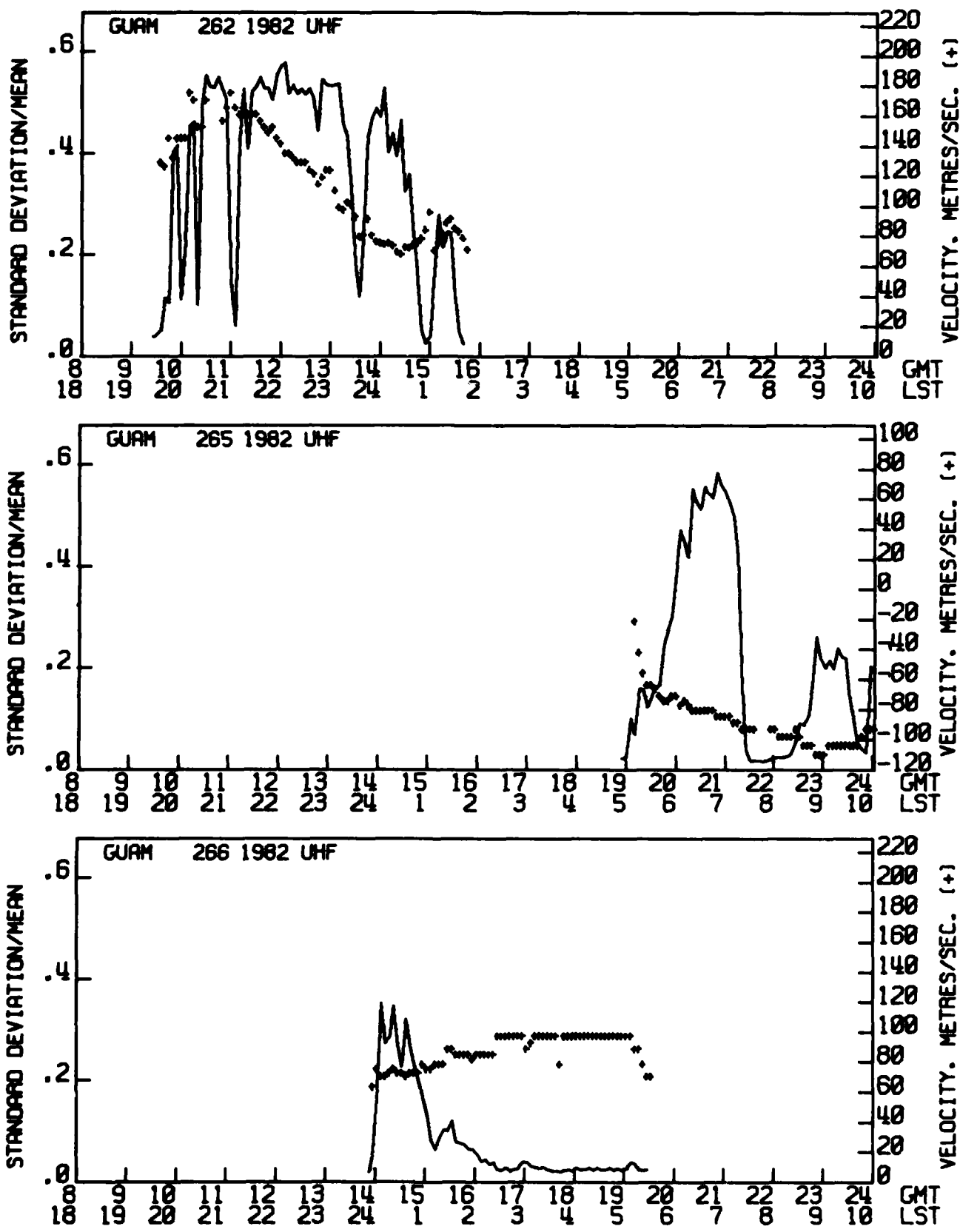


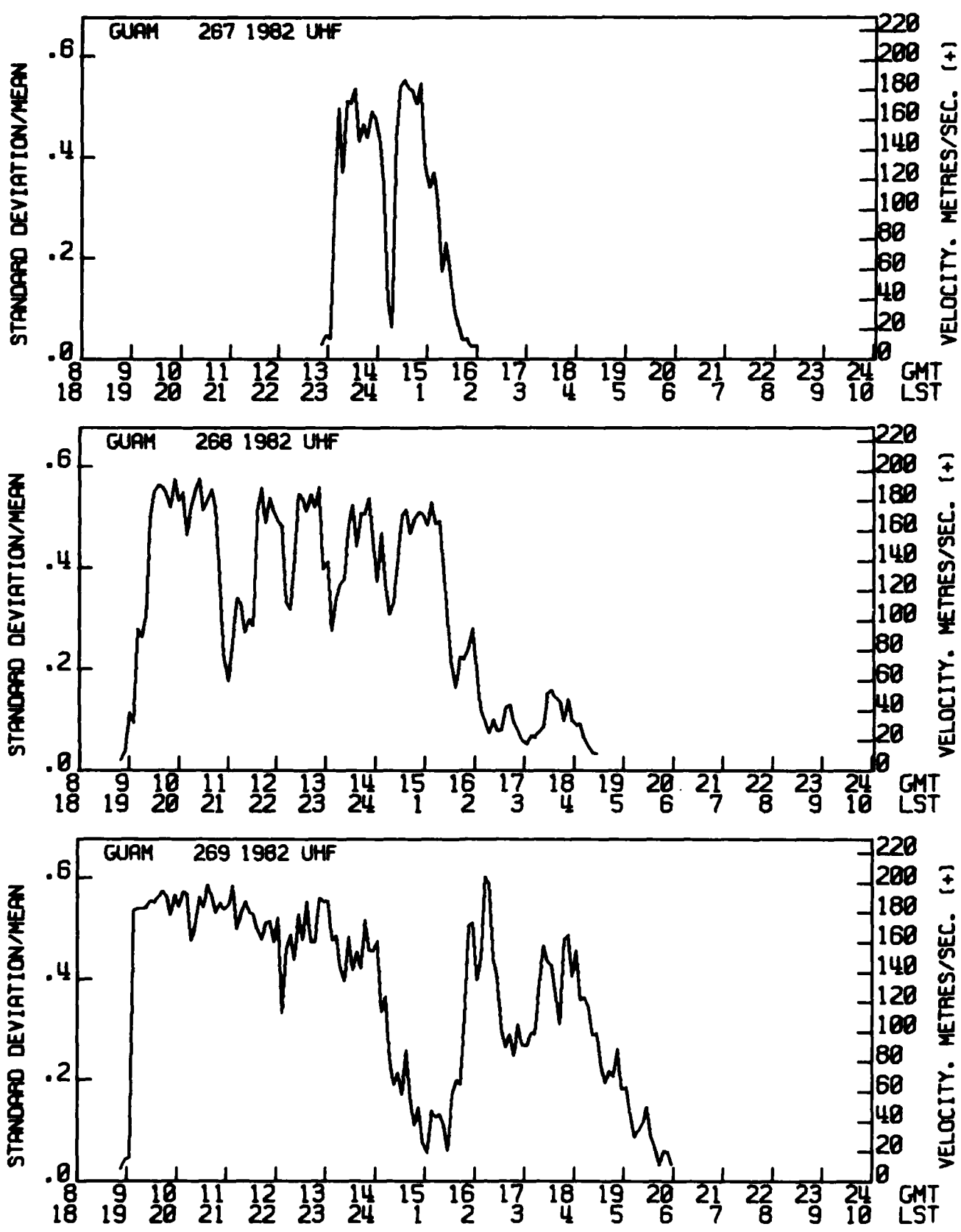


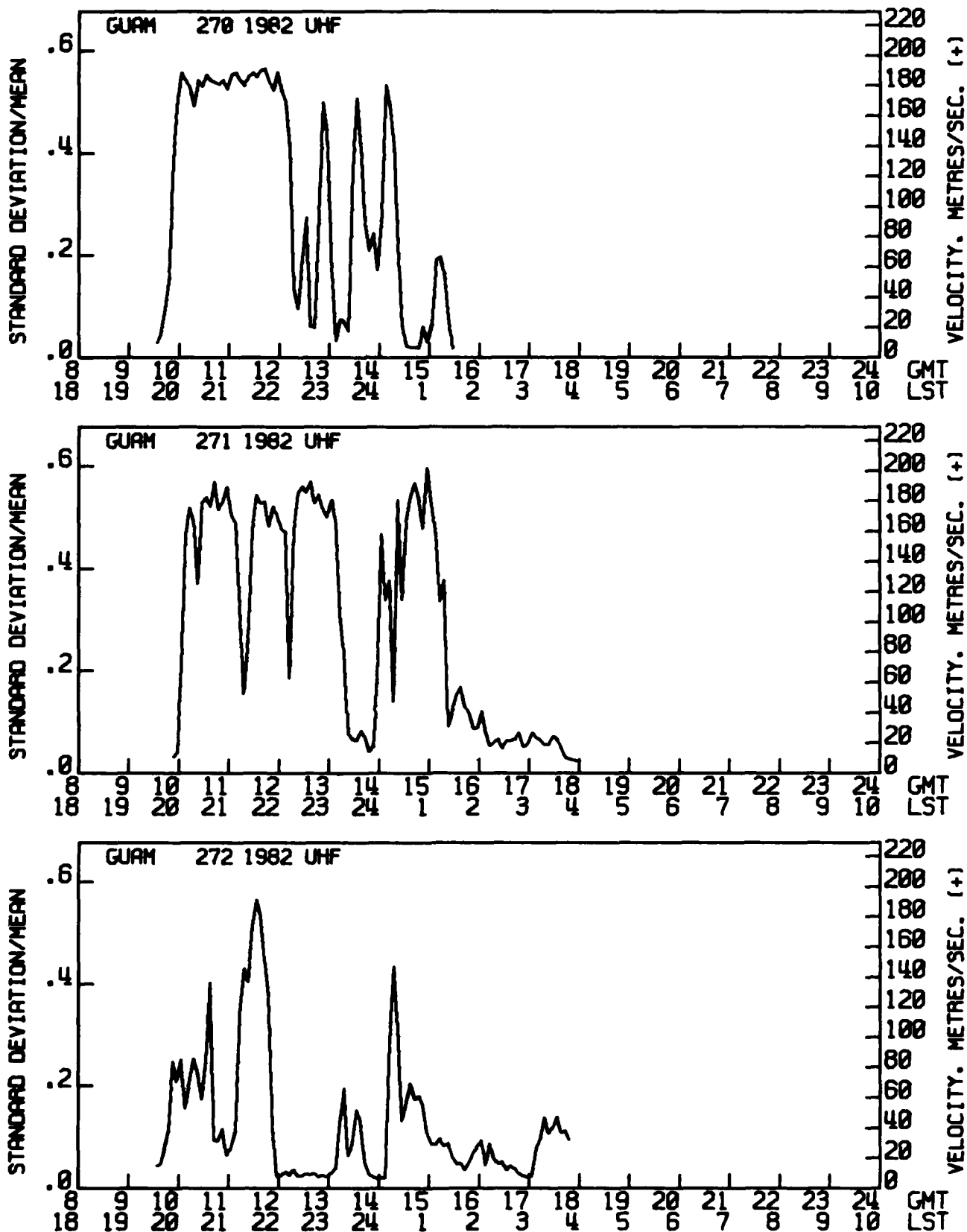


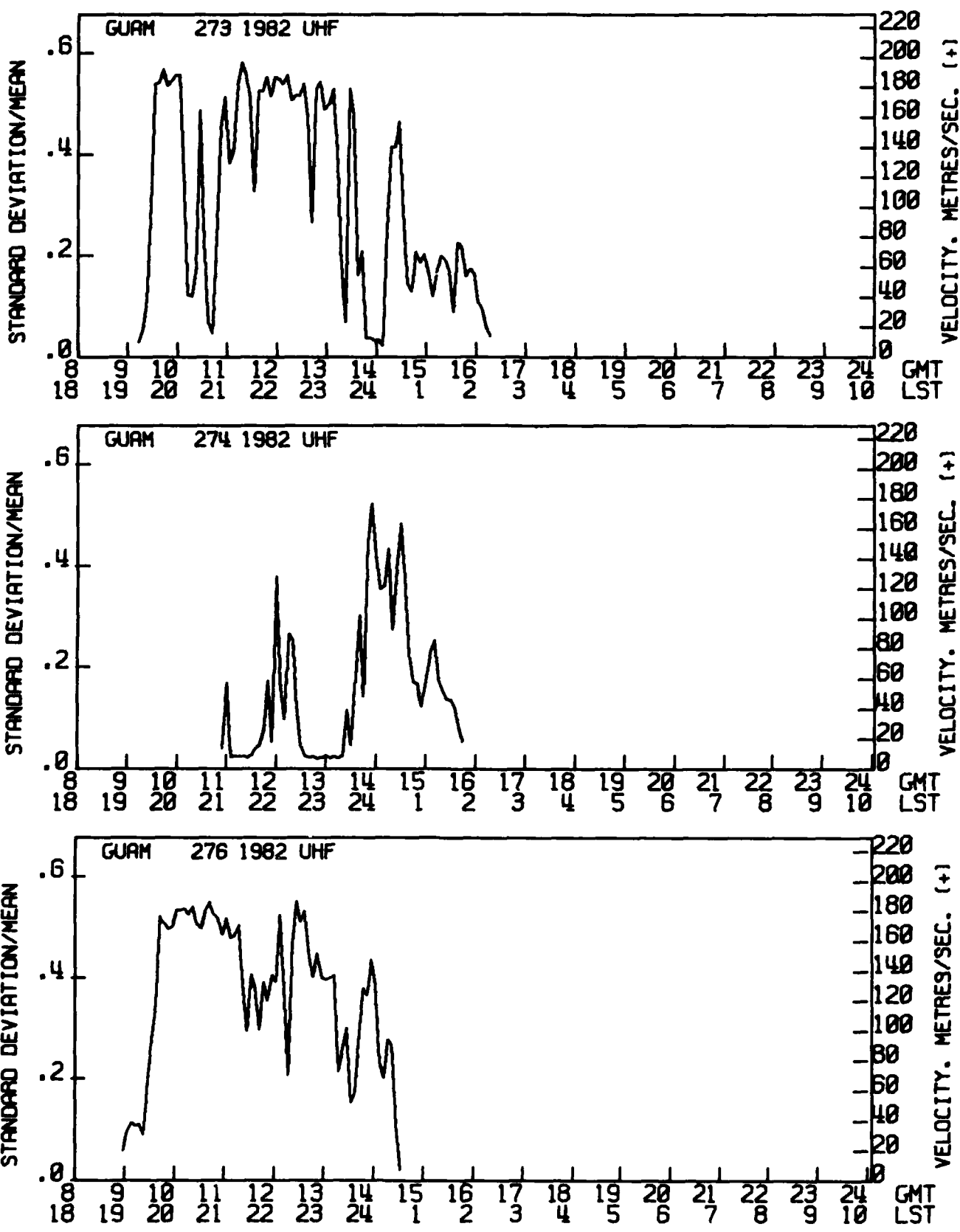


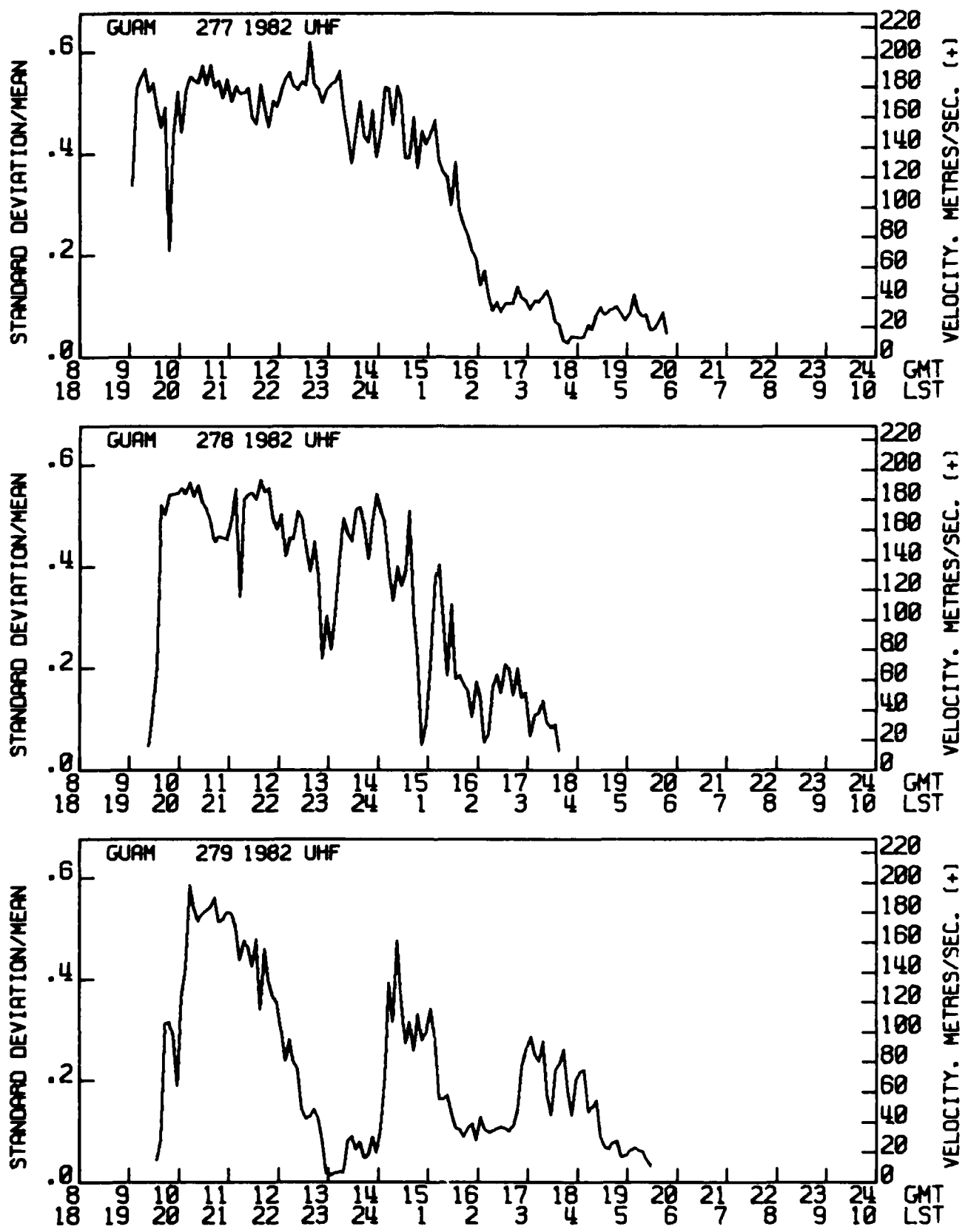


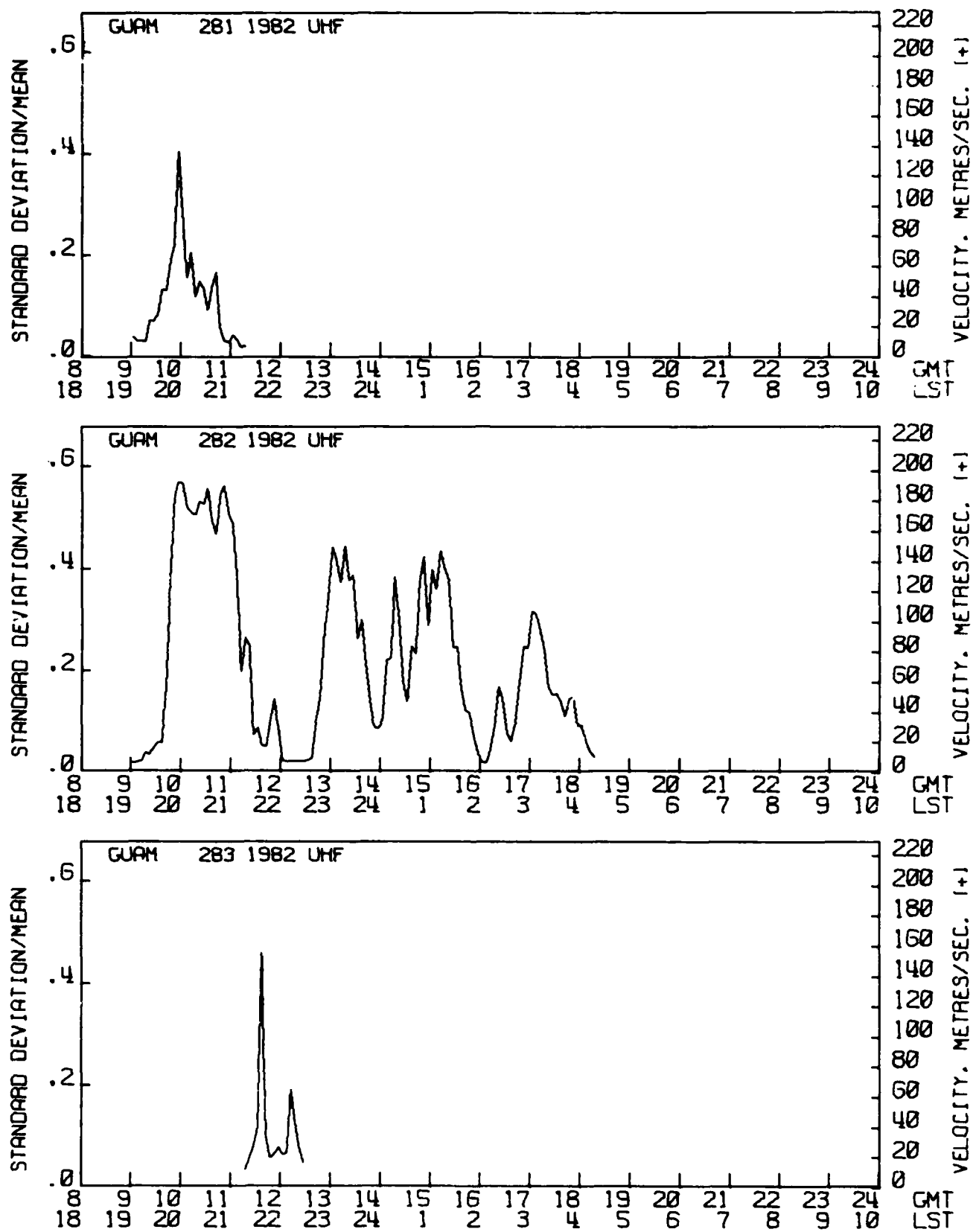


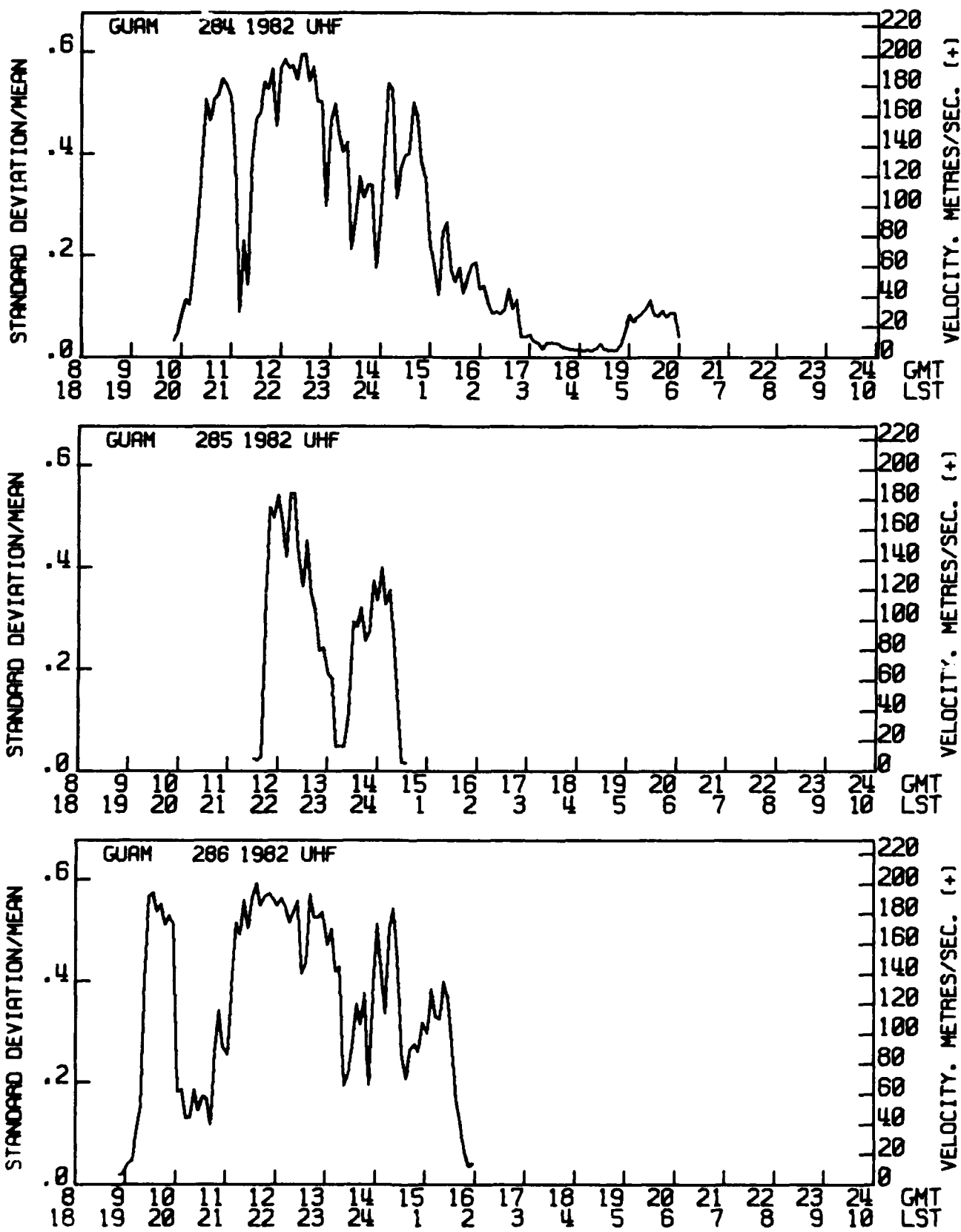


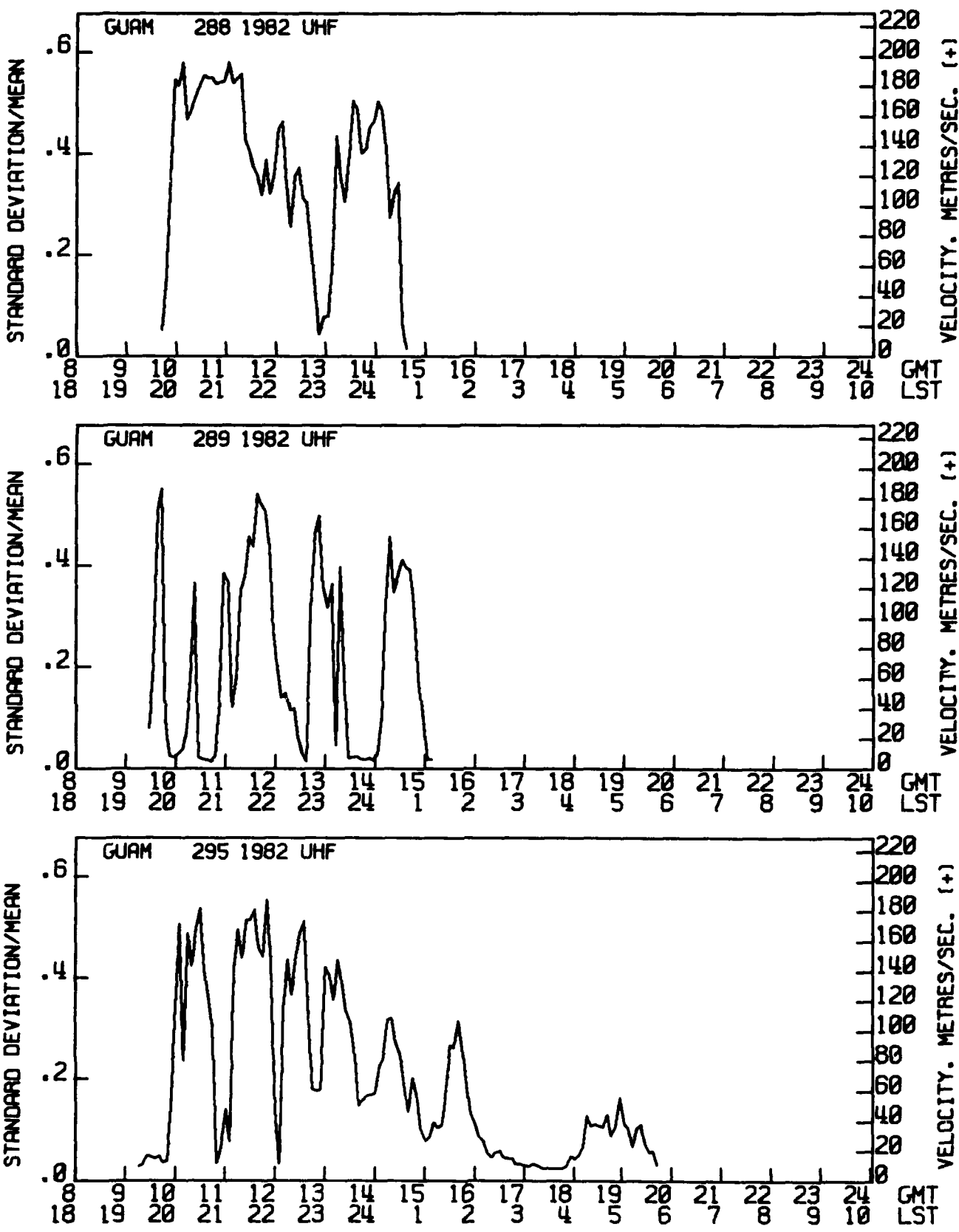


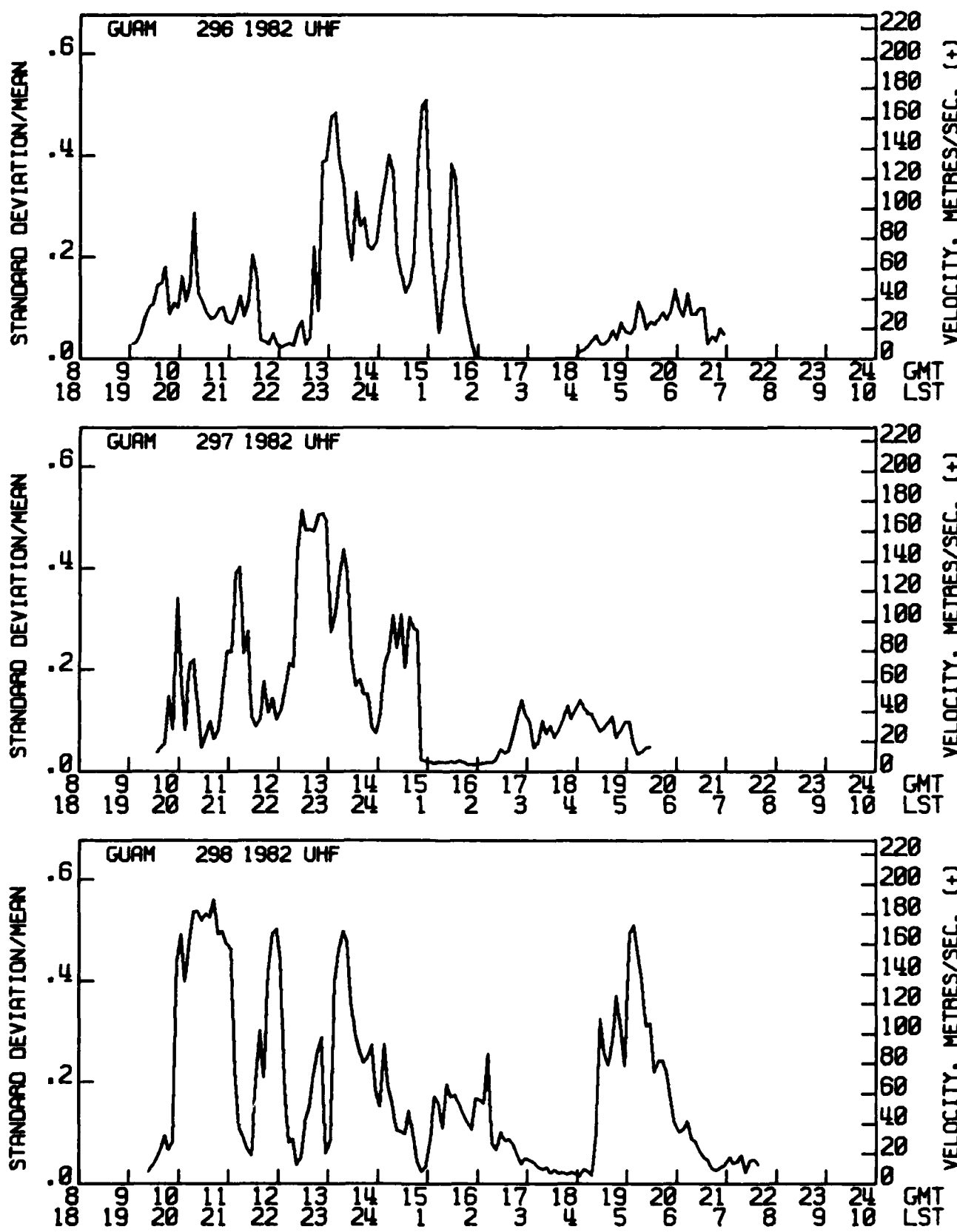


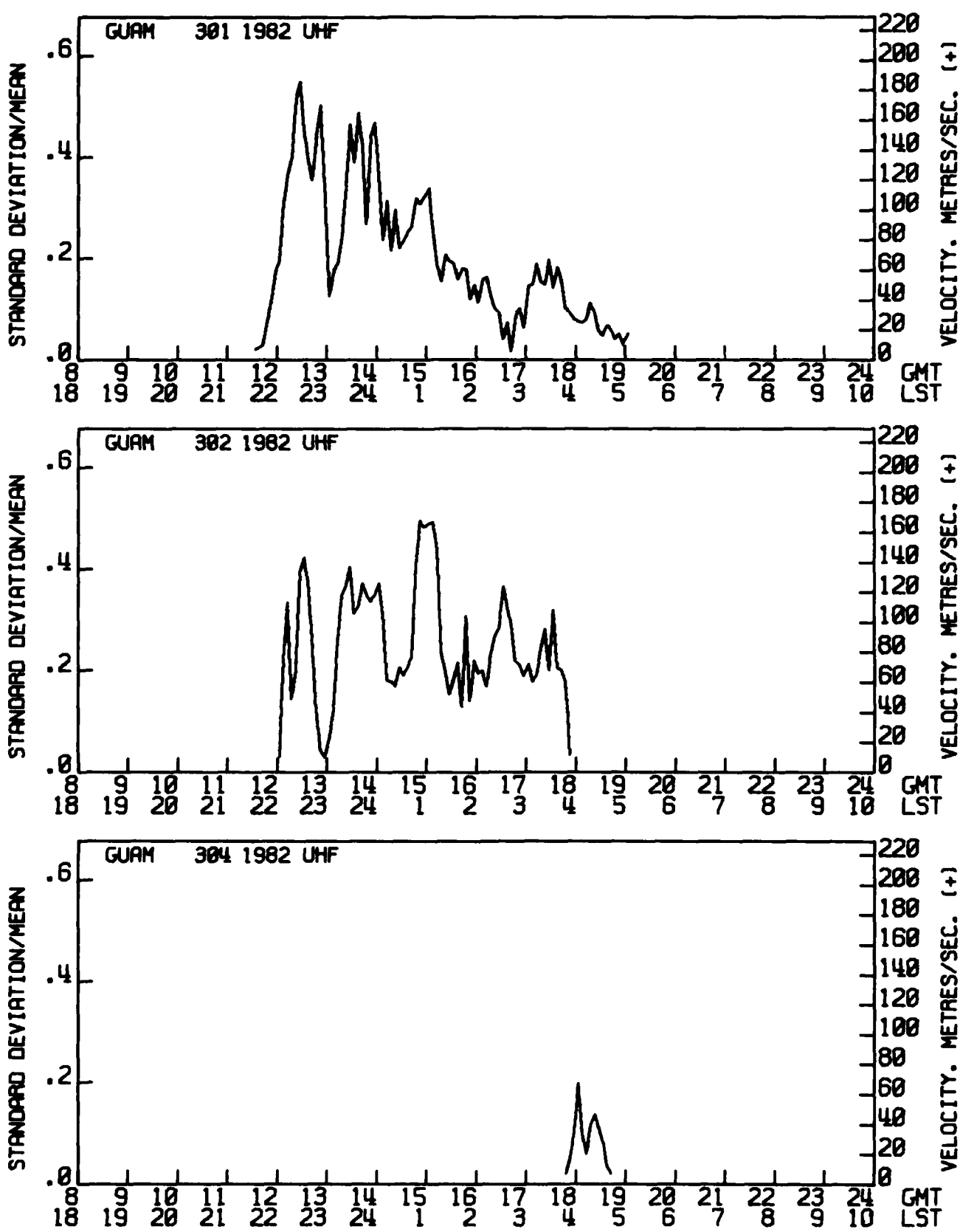


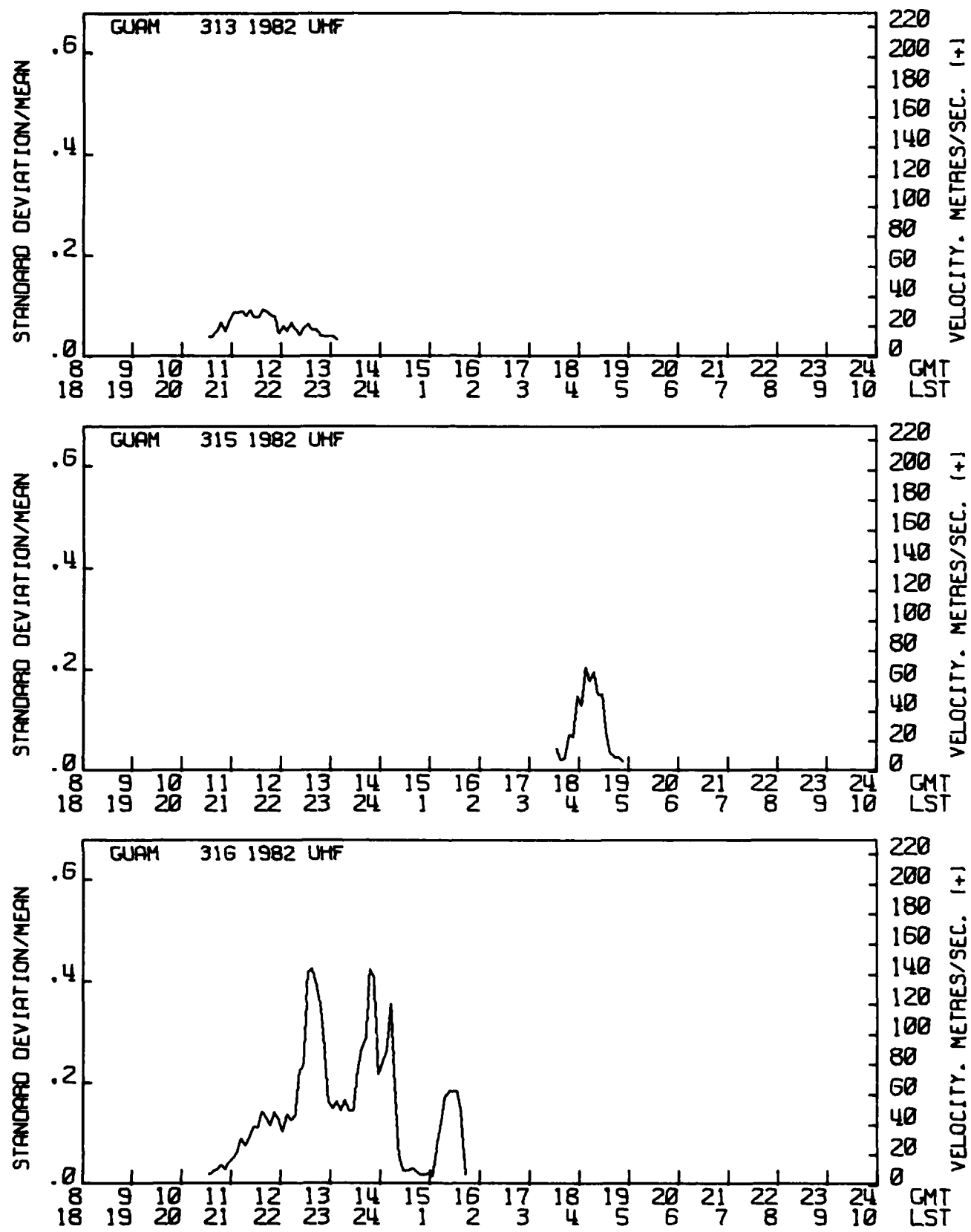


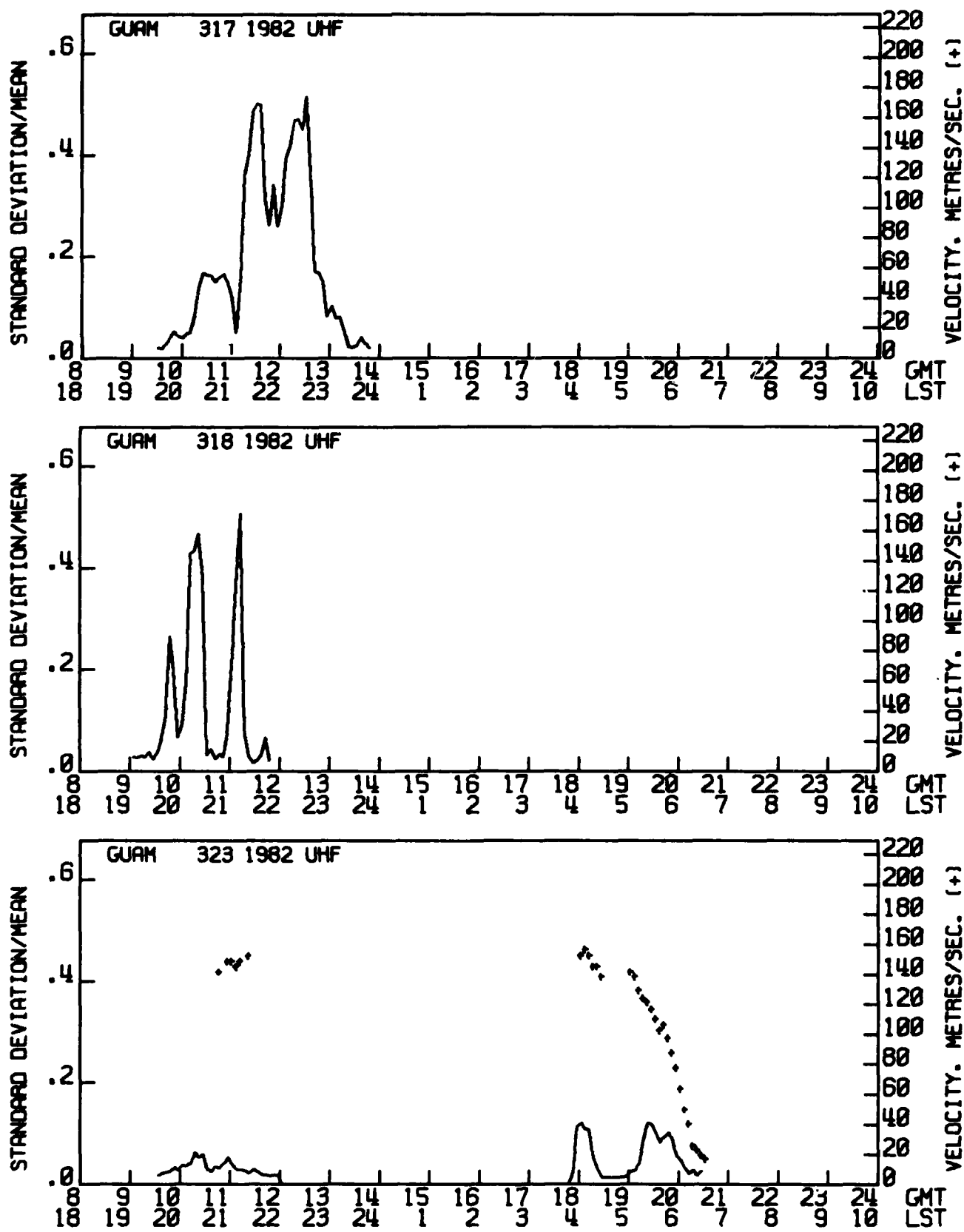


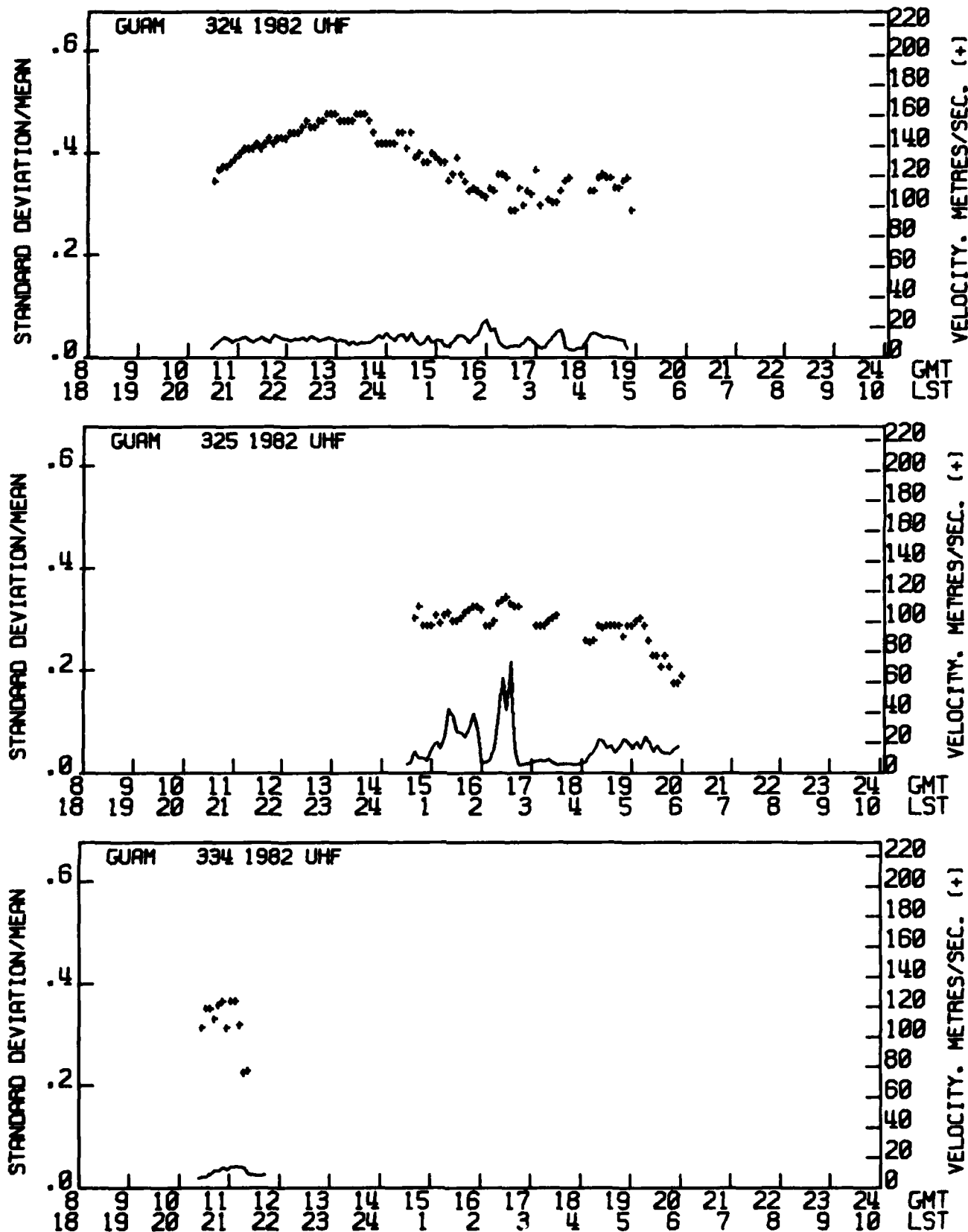


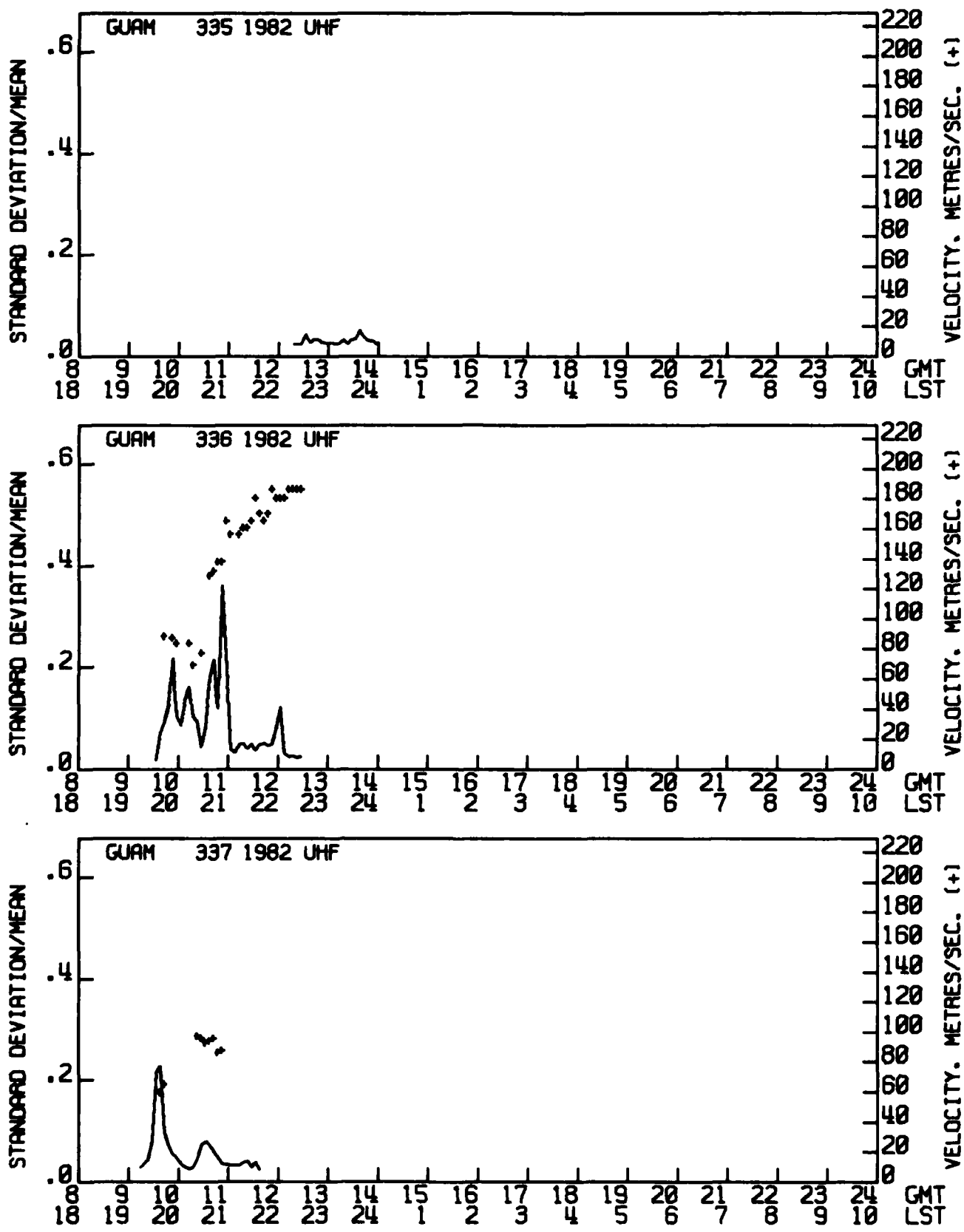


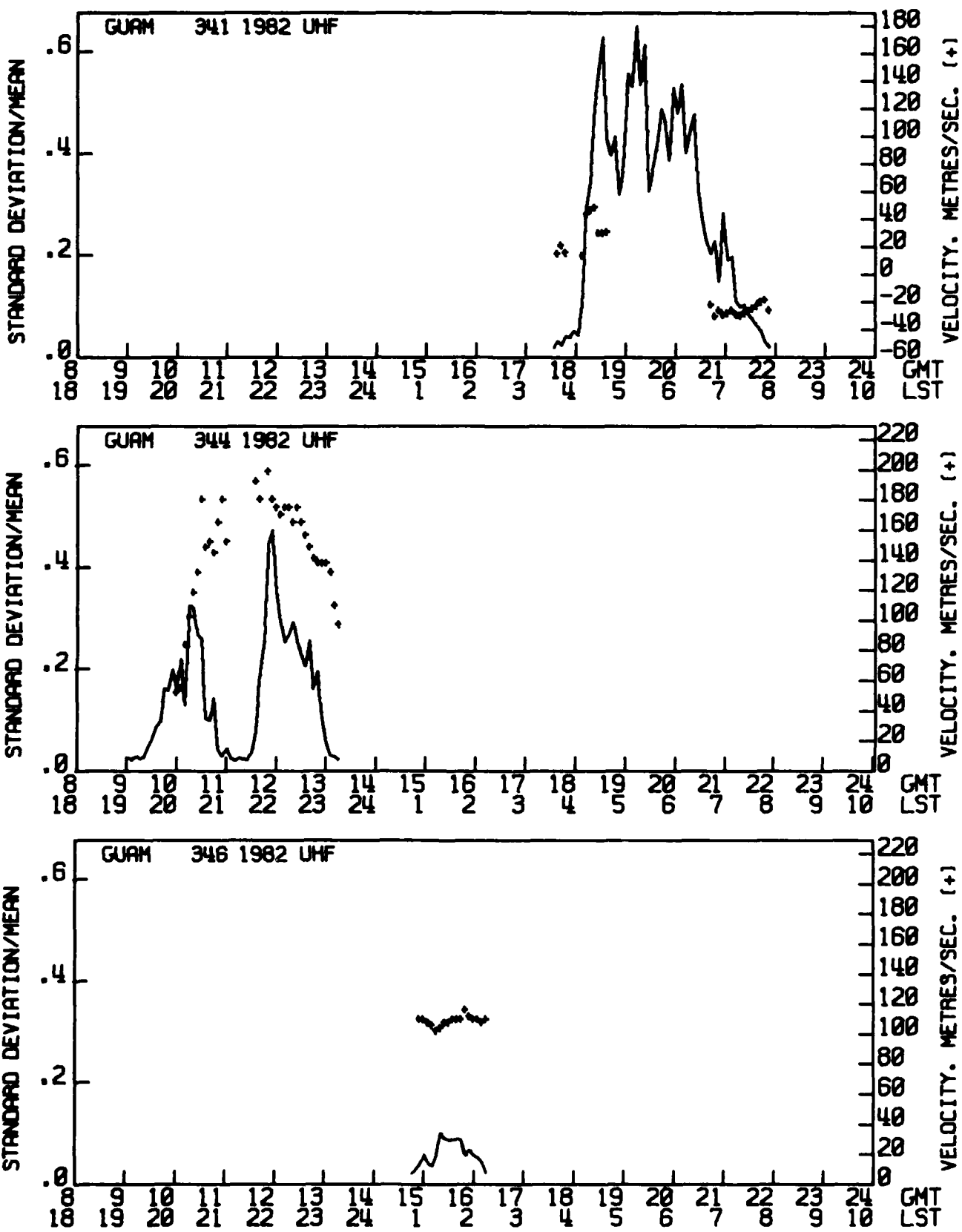


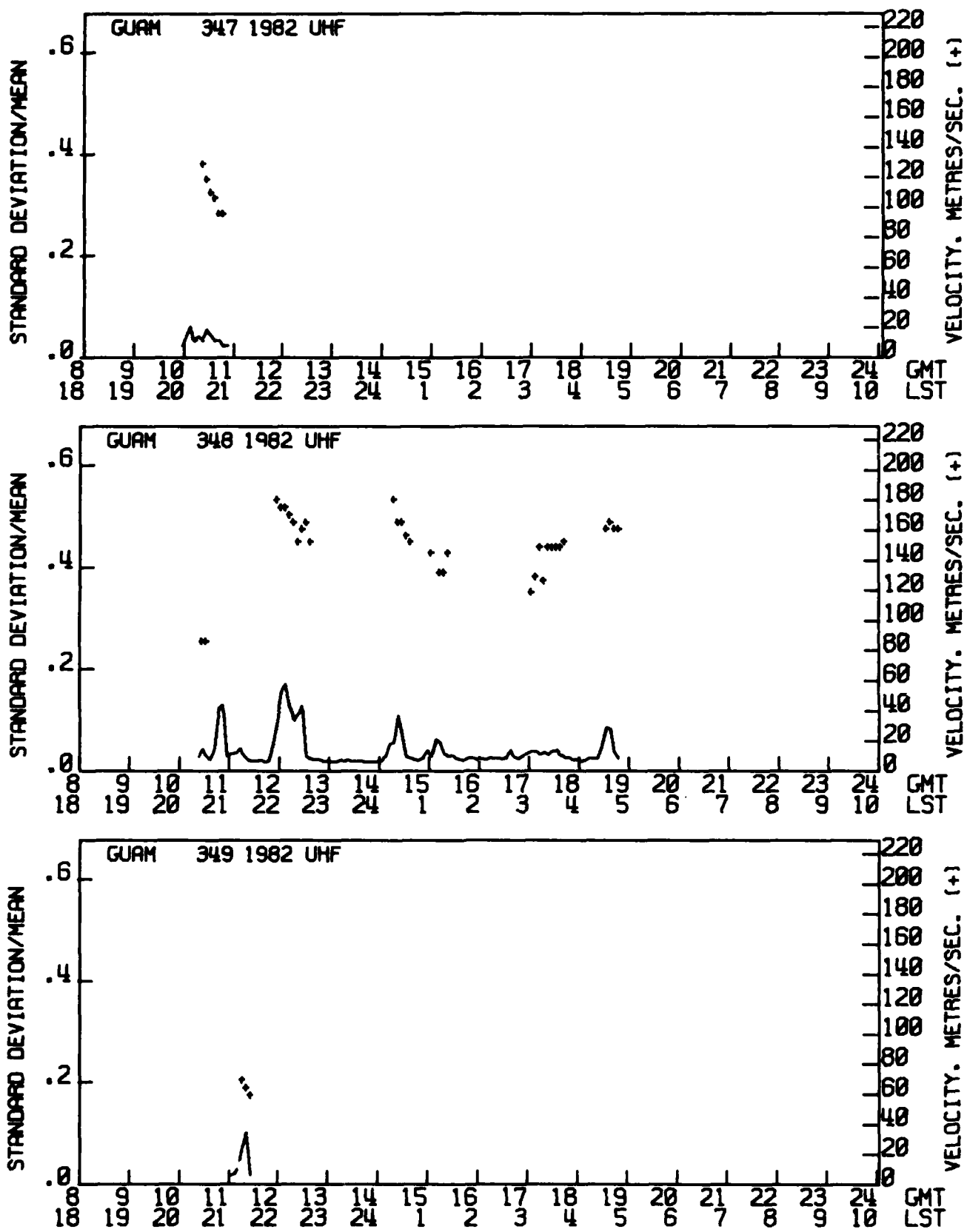


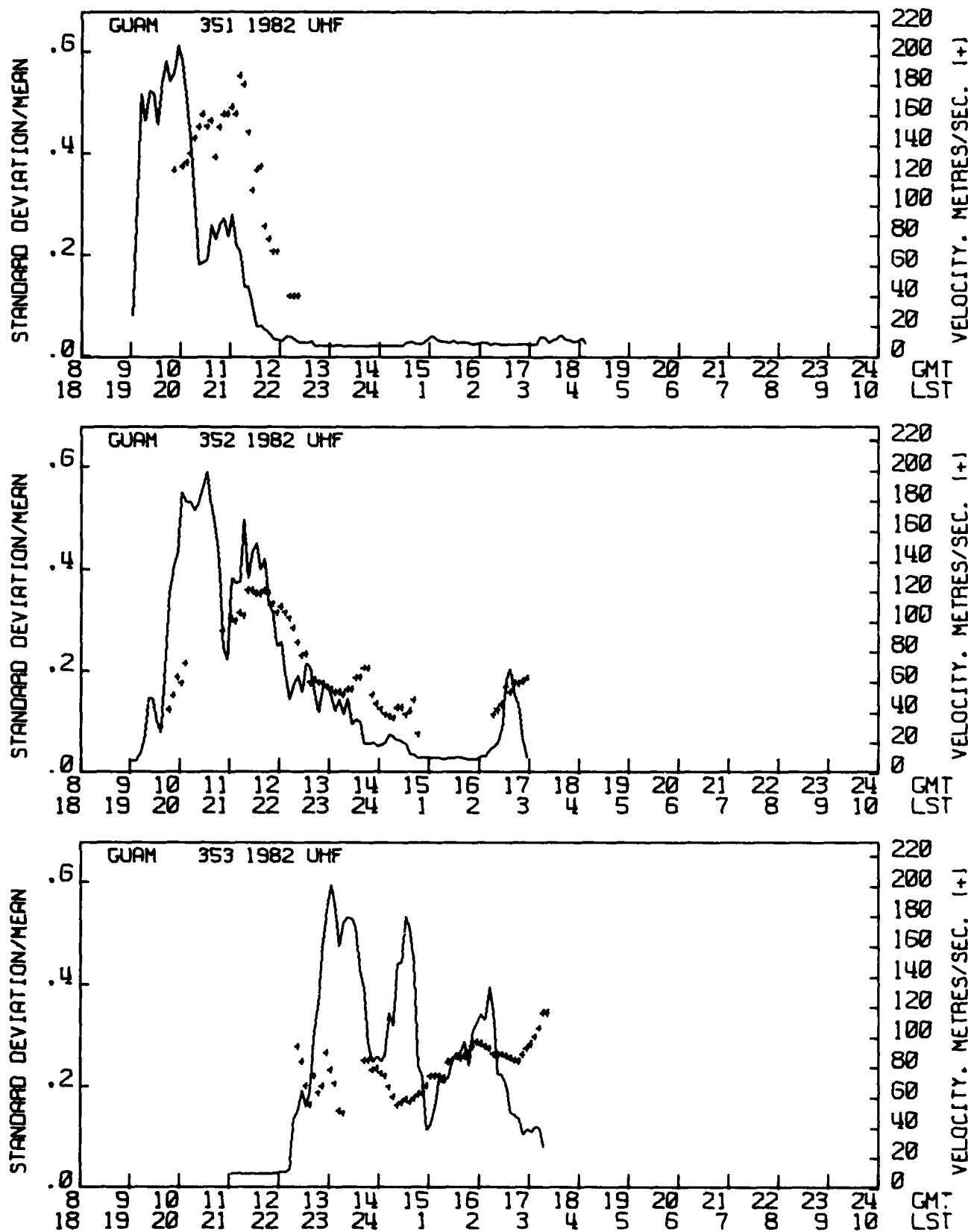


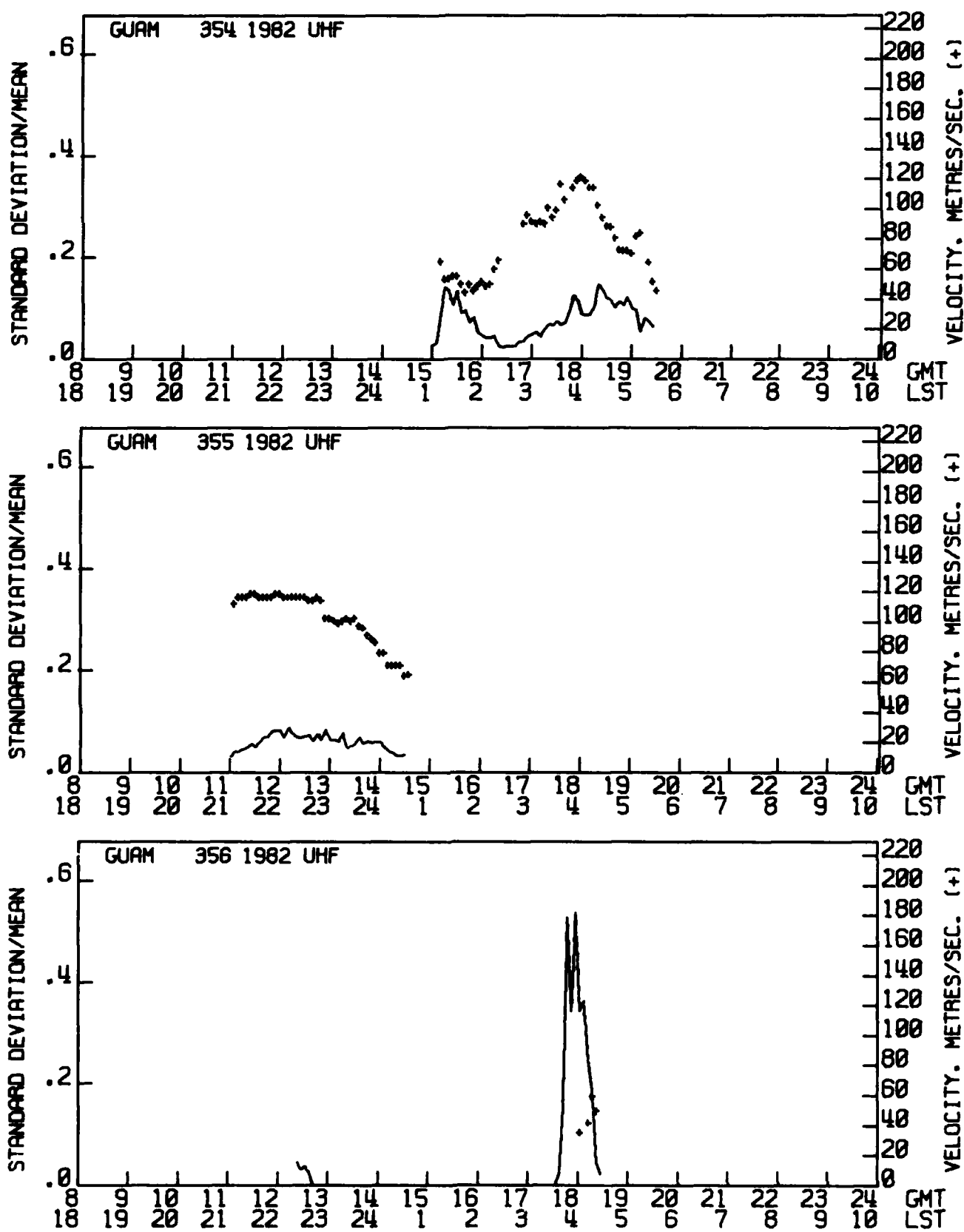


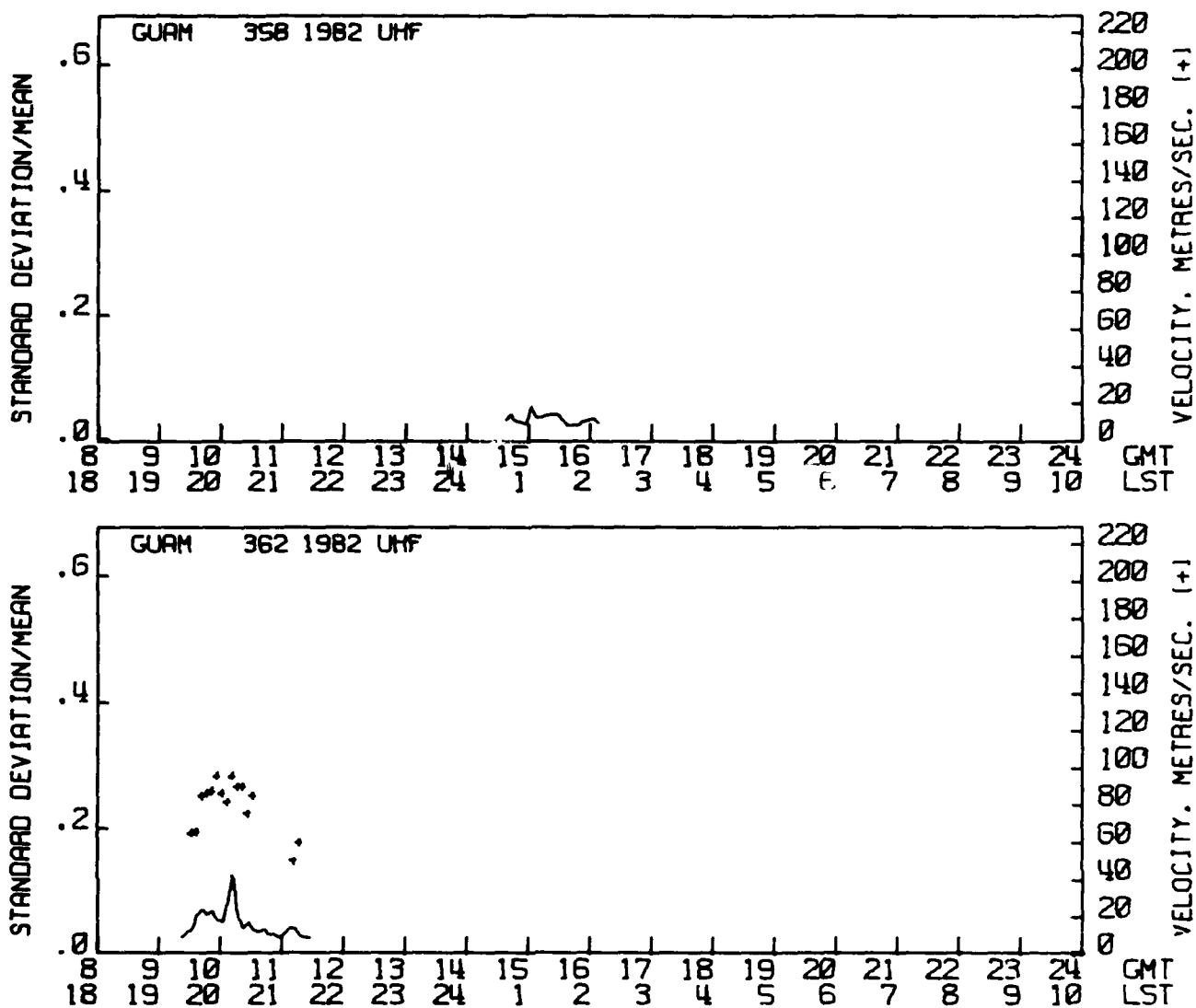


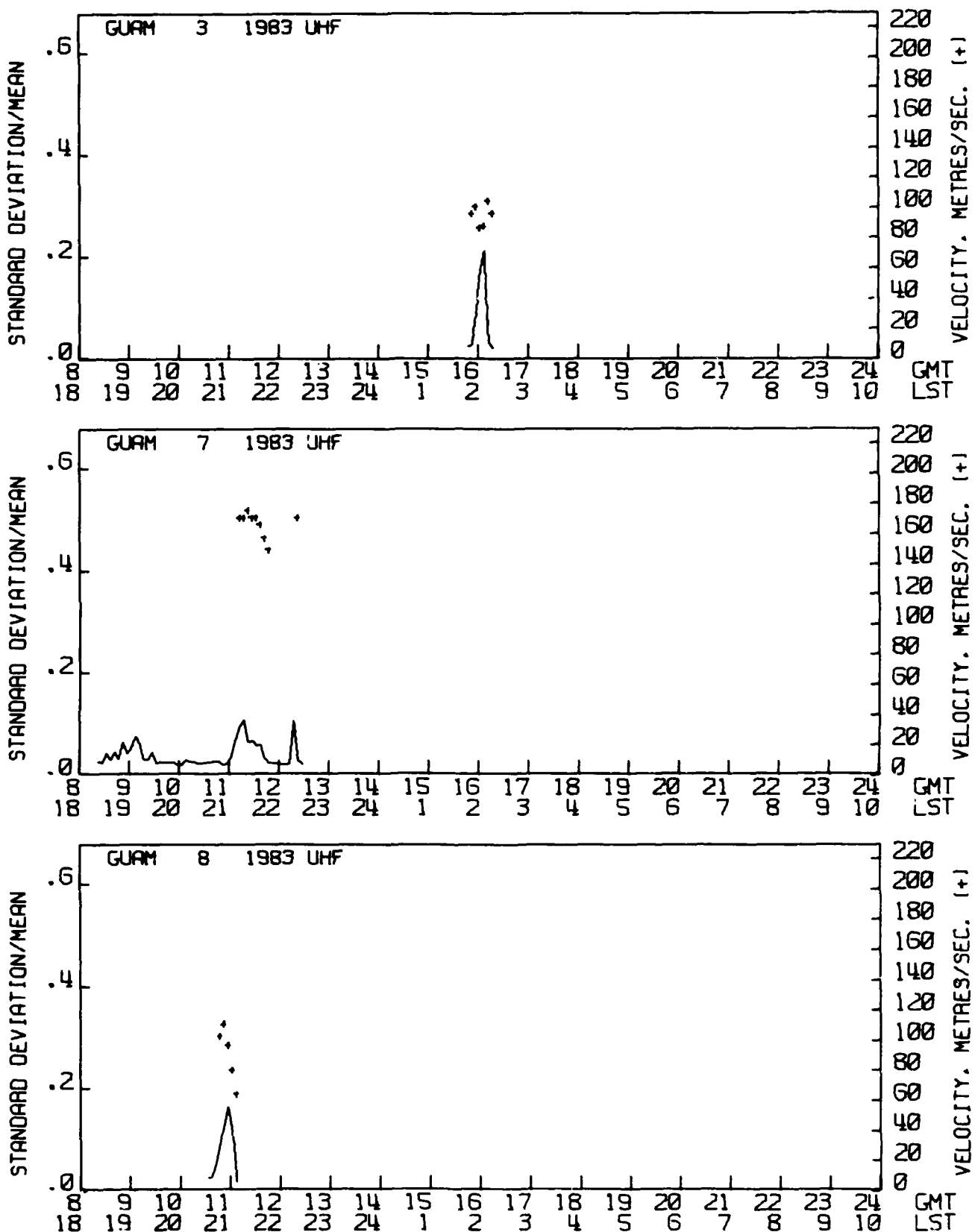












AD-A137 555

EQUATORIAL SCINTILLATION OF SATELLITE SIGNALS AND SOME
DRIFT CHARACTERISTICS OF THE SCINTILLATION(U) NAVAL
OCEAN SYSTEMS CENTER SAN DIEGO CA M R PAULSON

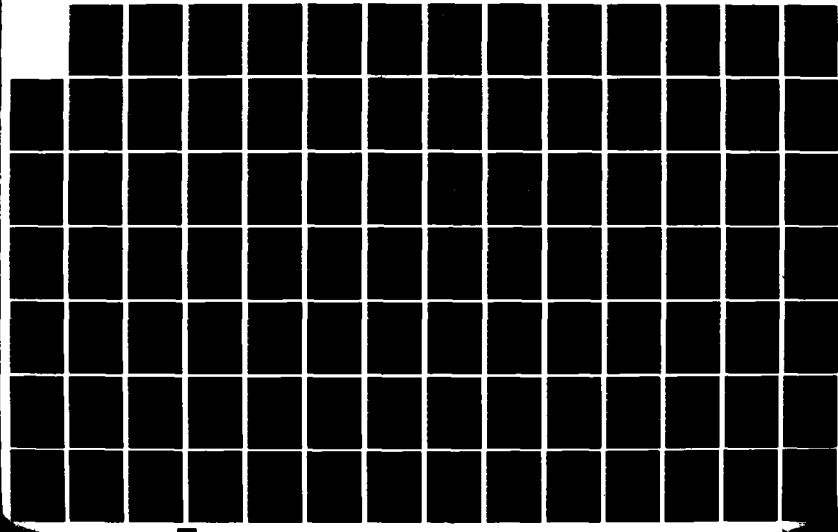
2/3

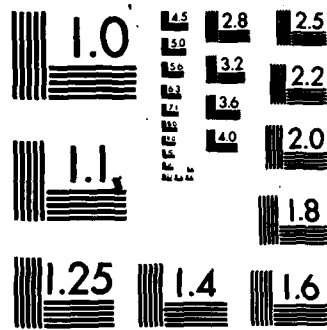
UNCLASSIFIED

15 OCT 83 NOSC/TR-911

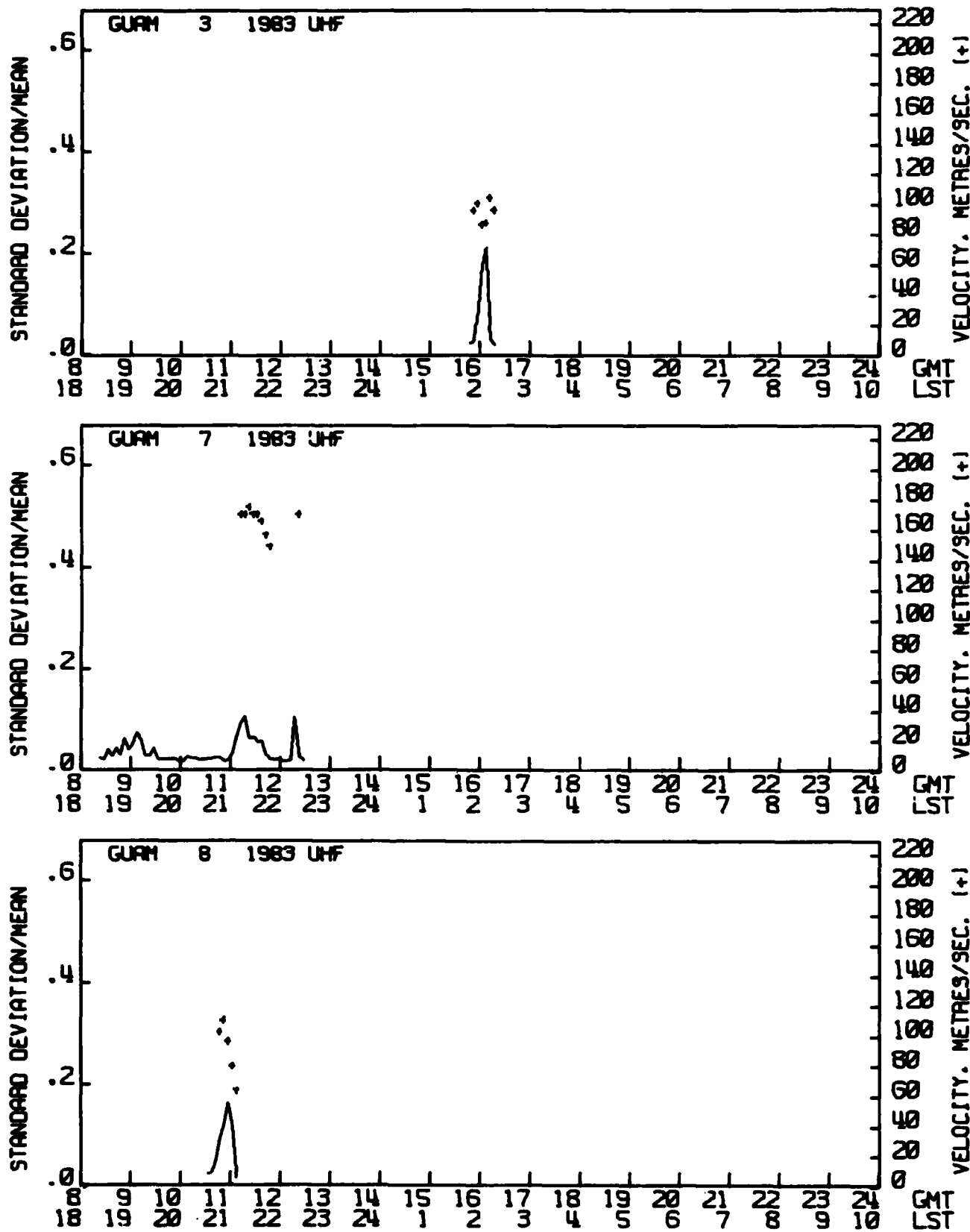
F/G 20/14

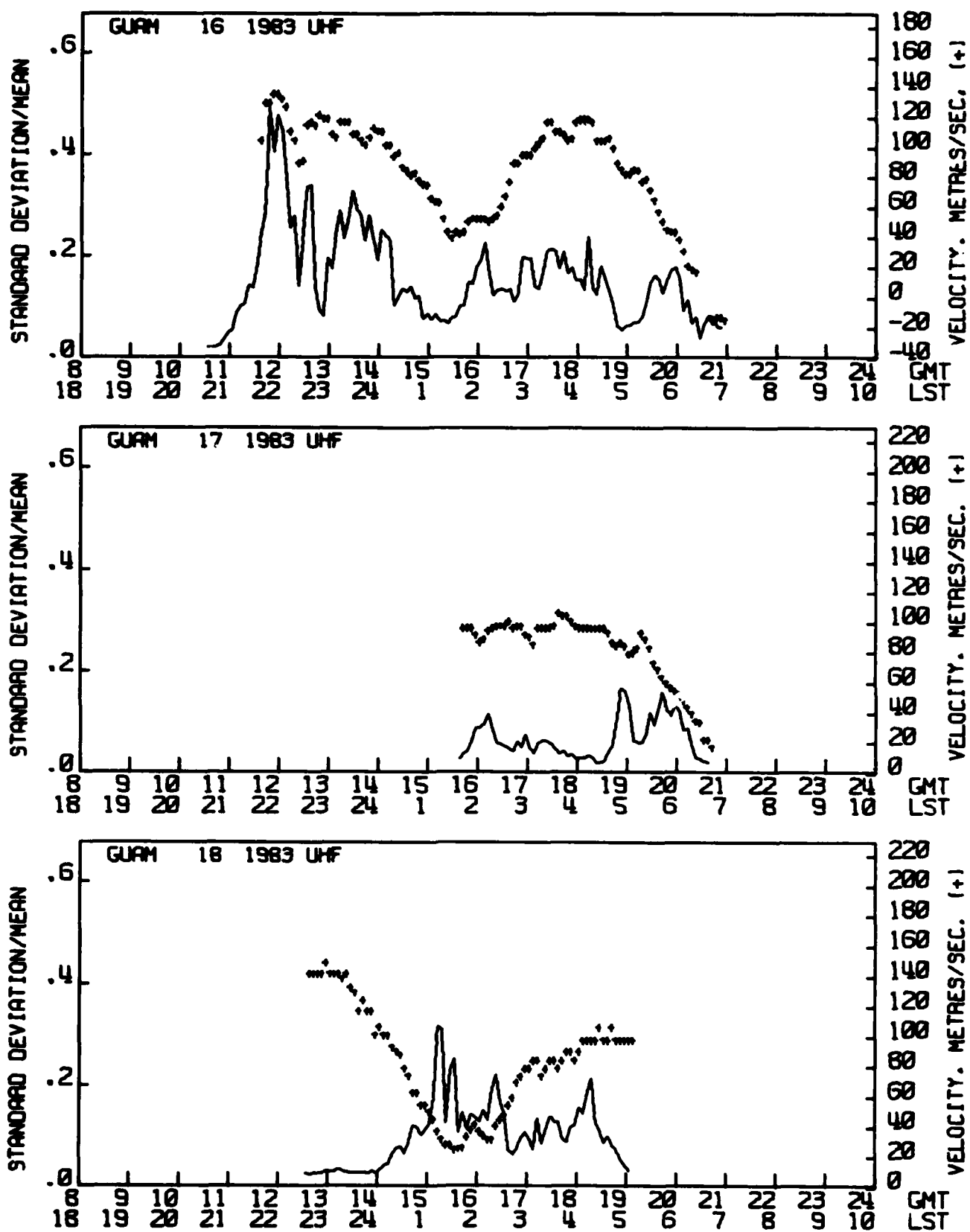
NL

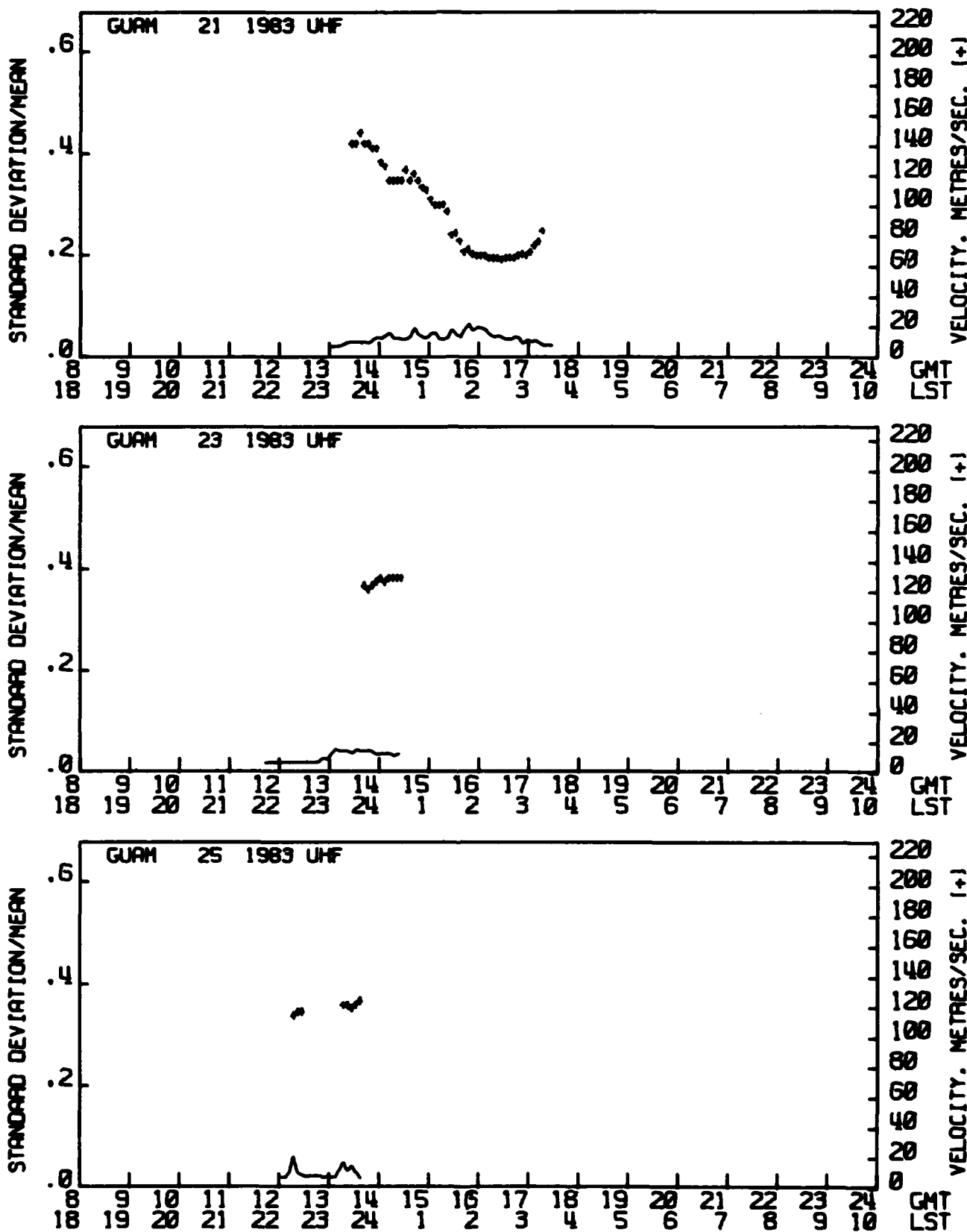


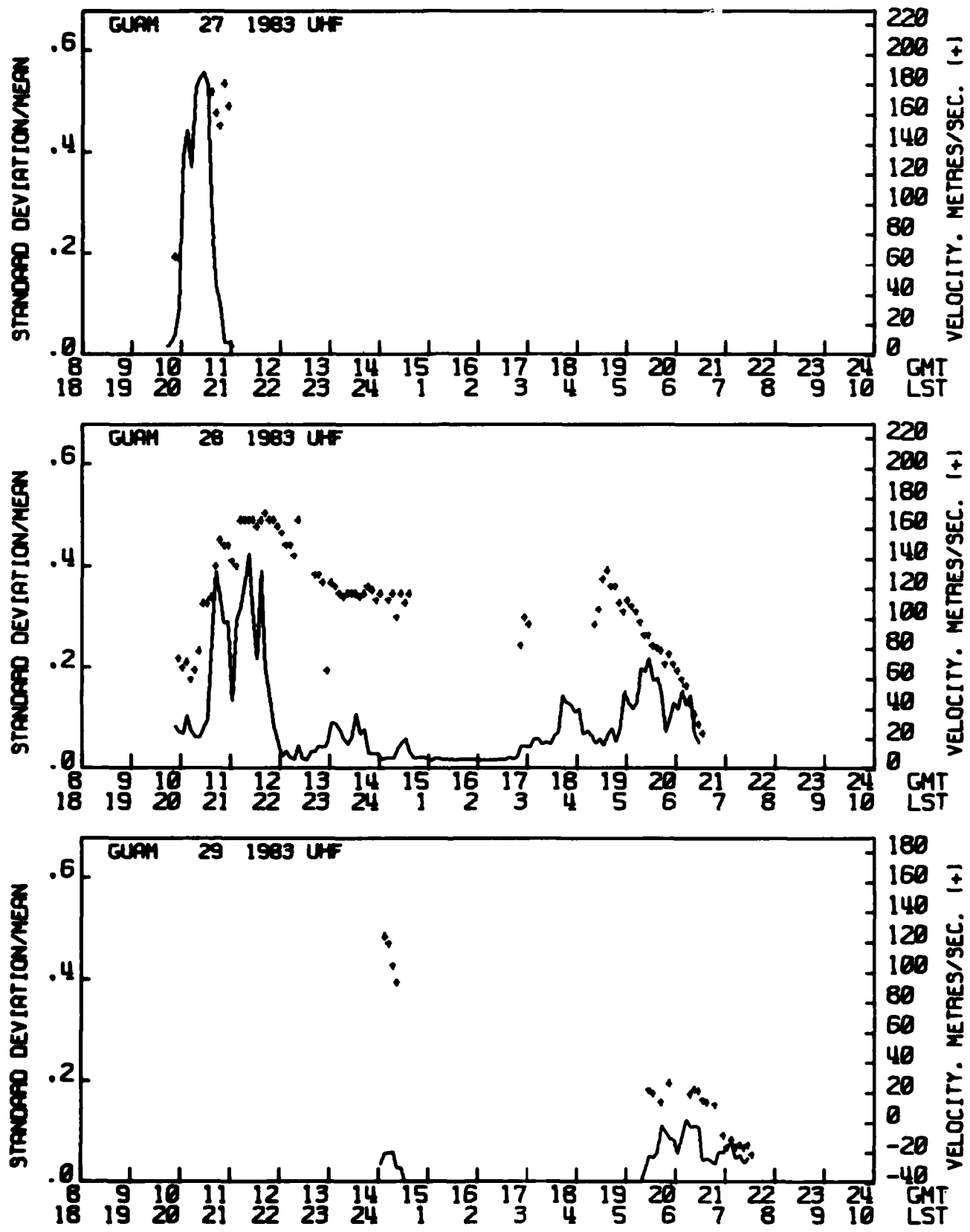


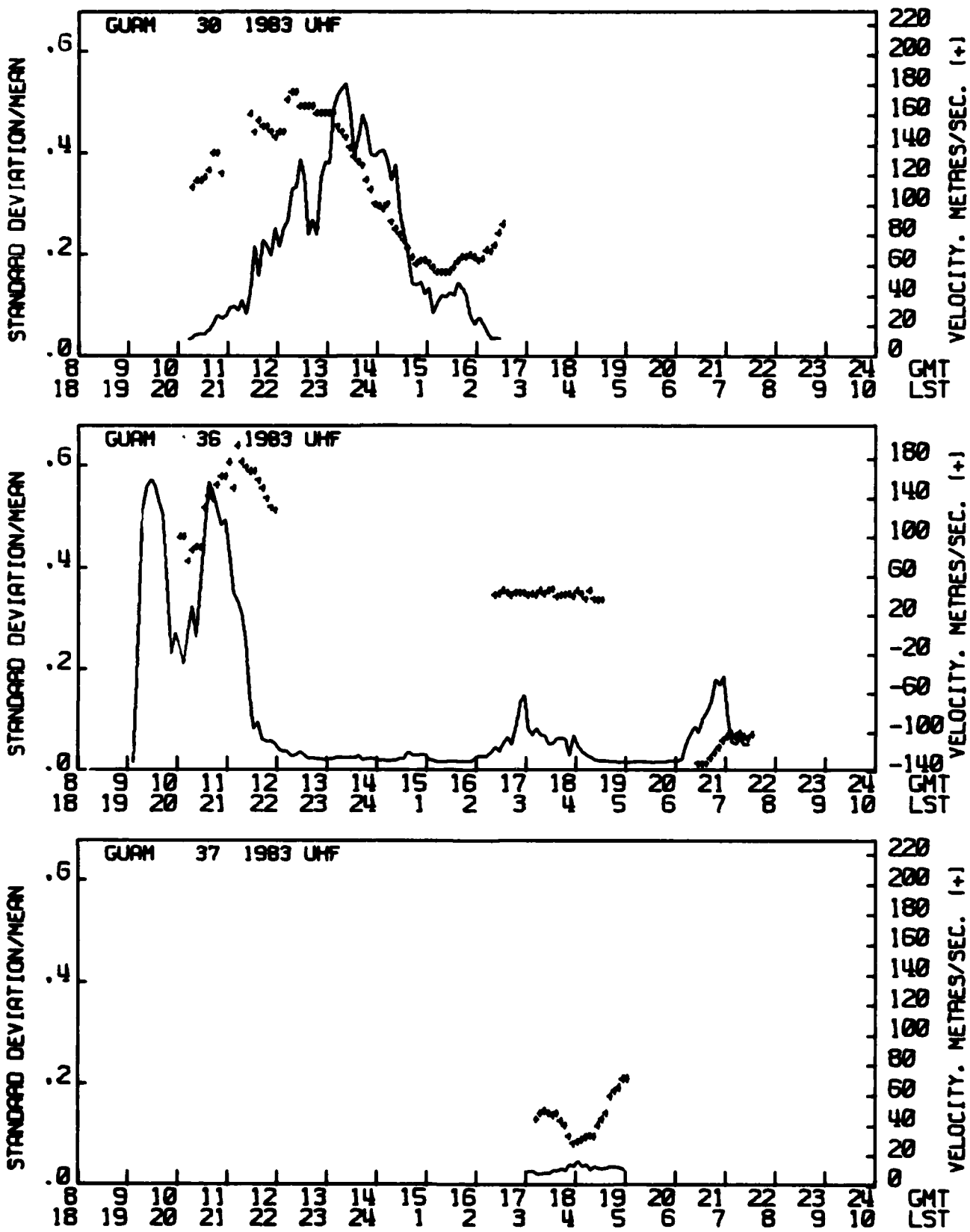
MICROCOPY RESOLUTION TEST CHART
NATIONAL BUREAU OF STANDARDS-1963-A

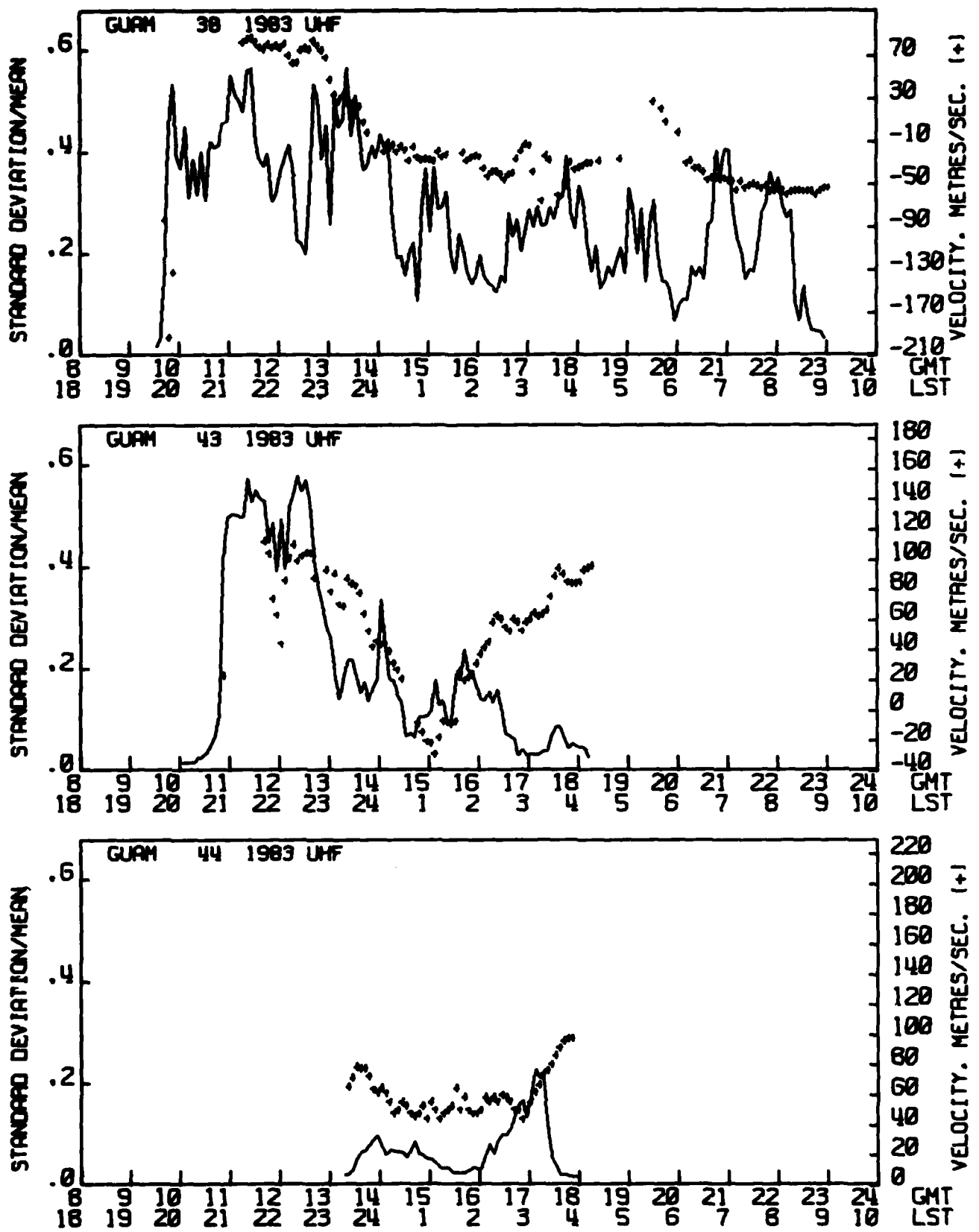


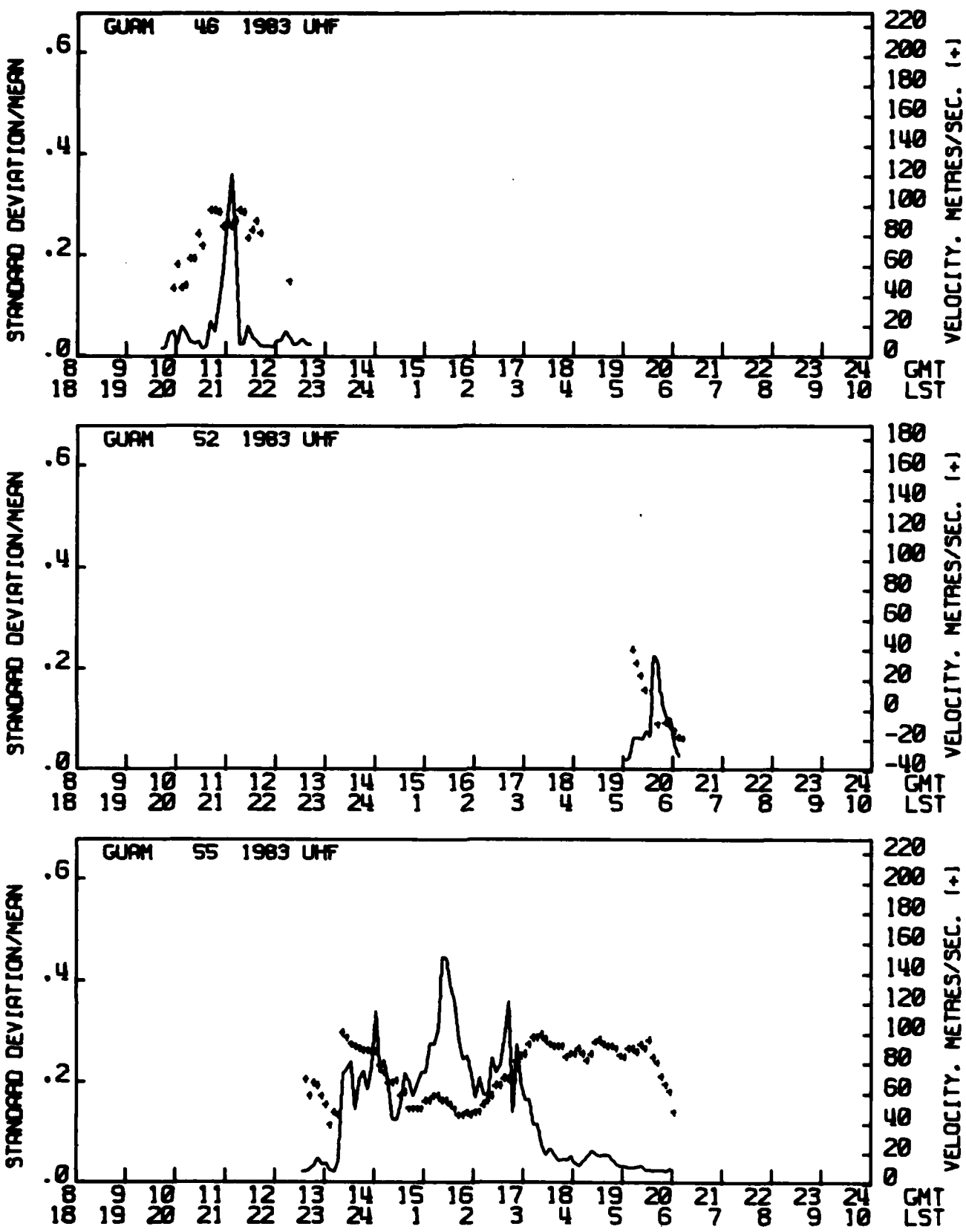


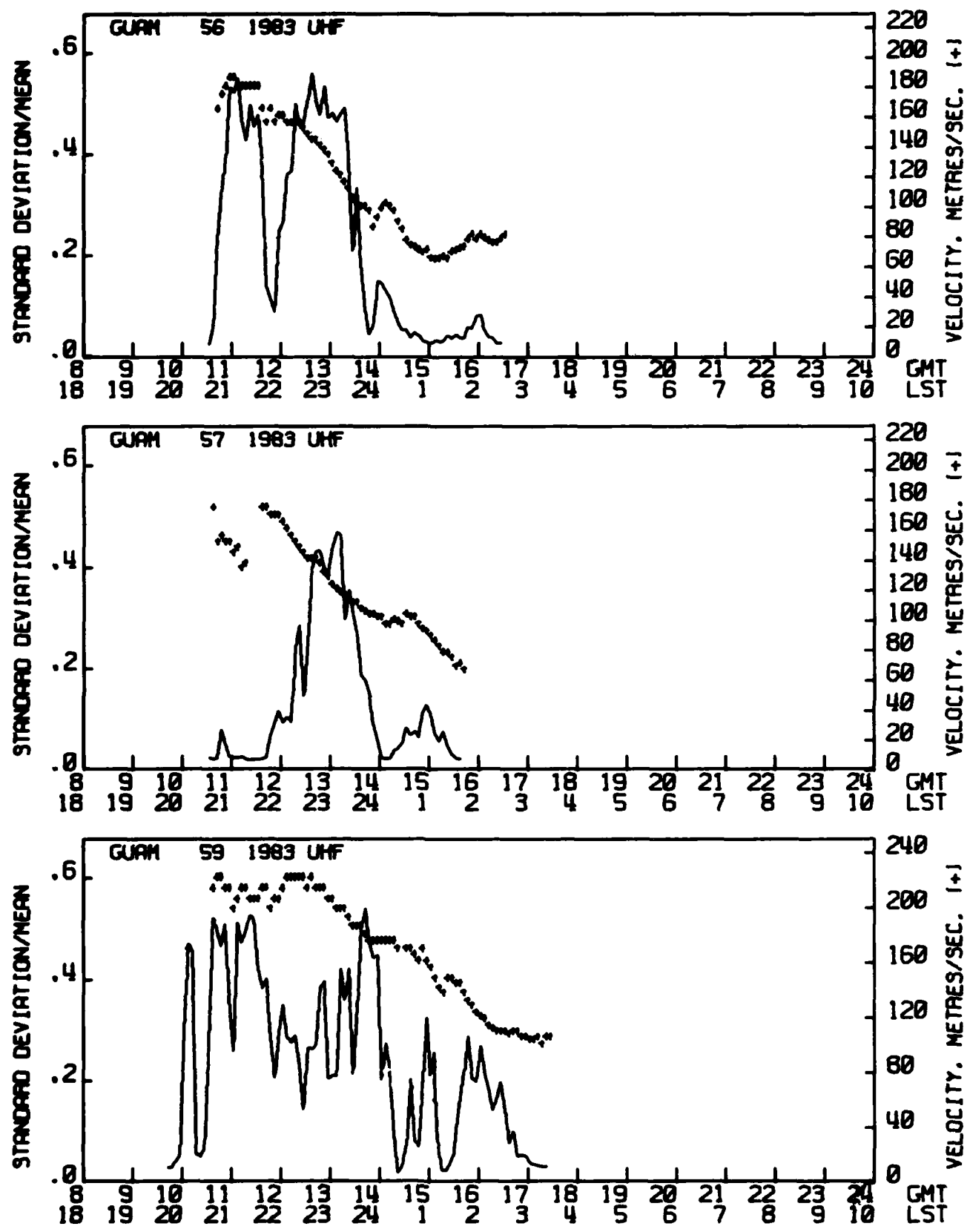


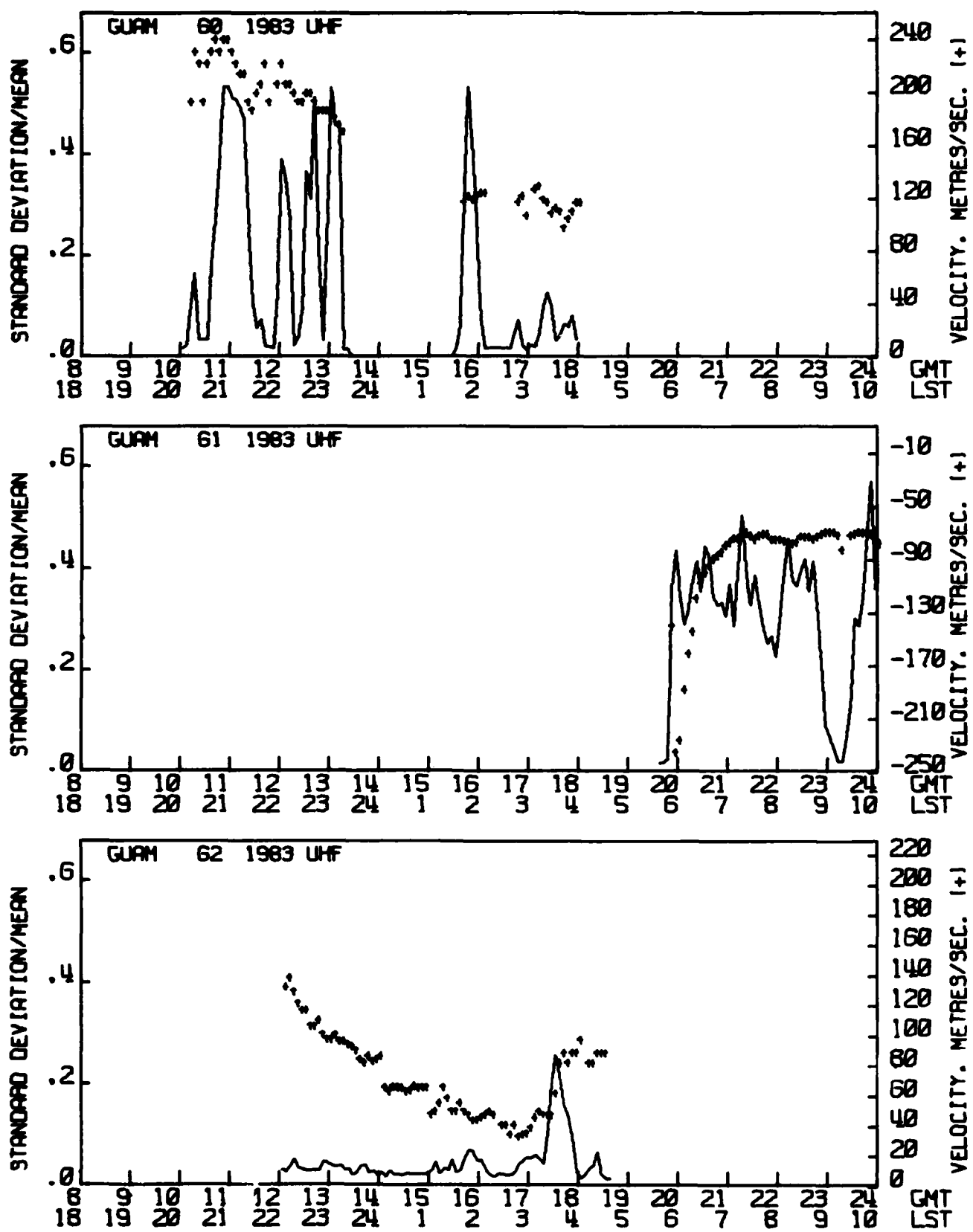


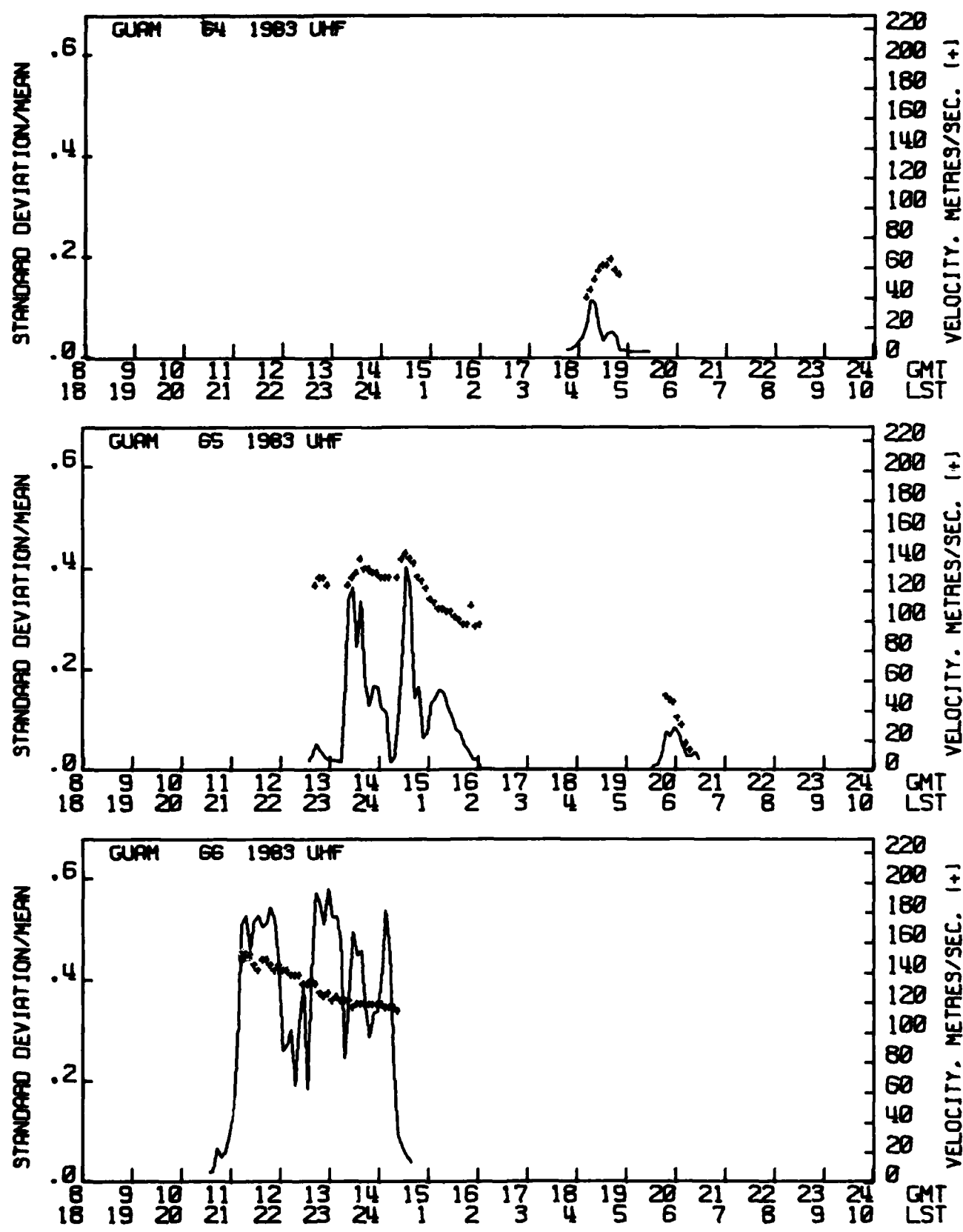


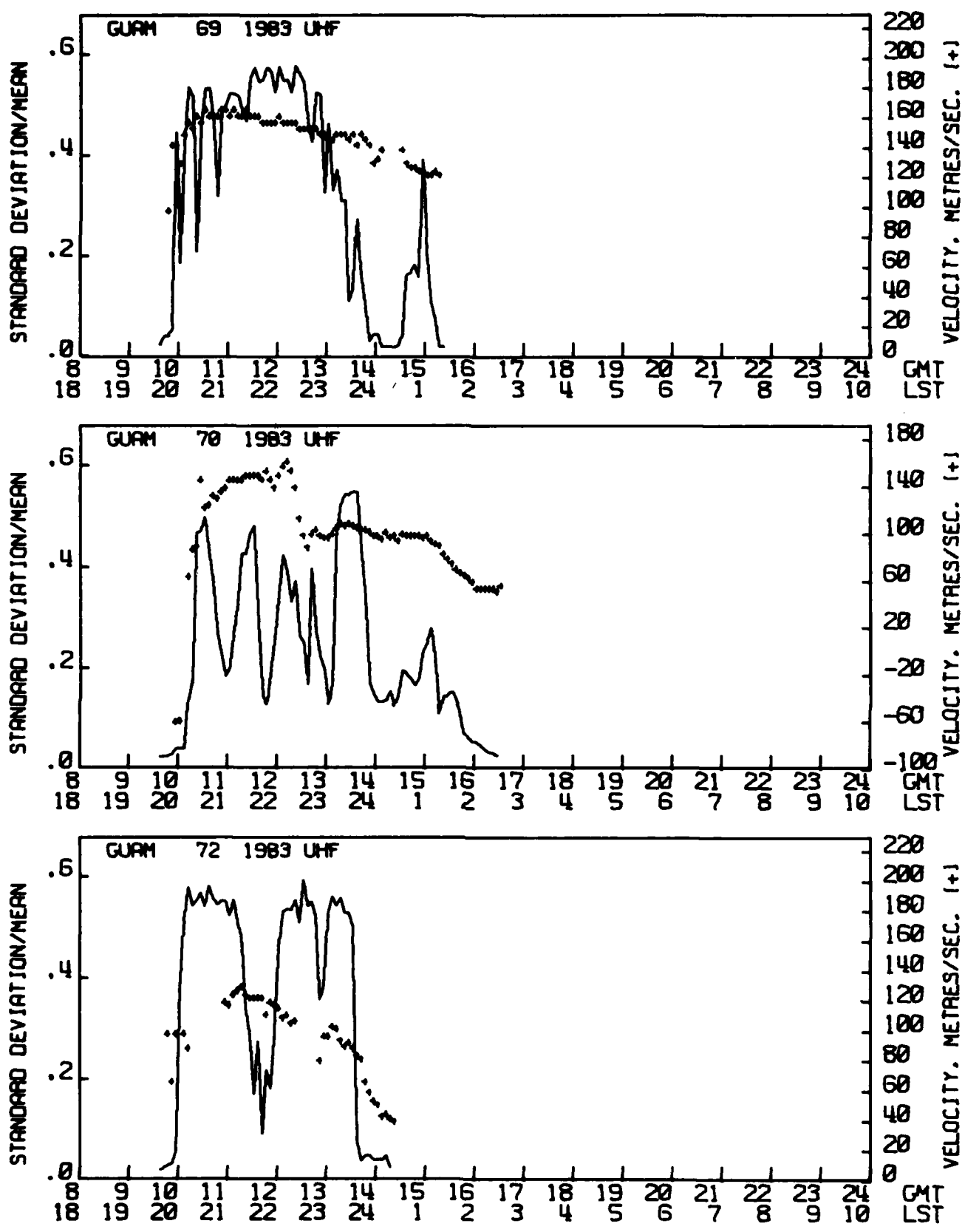


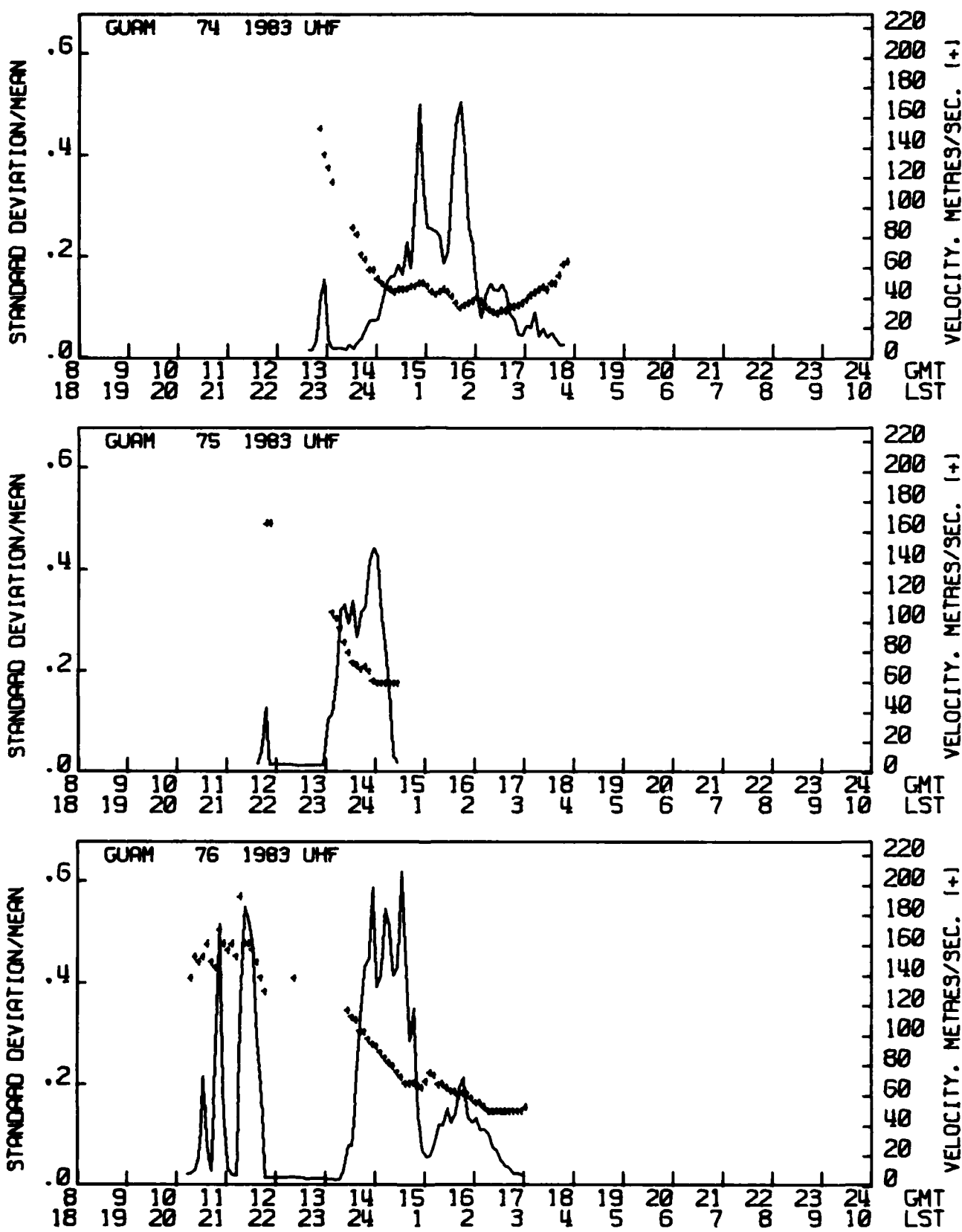


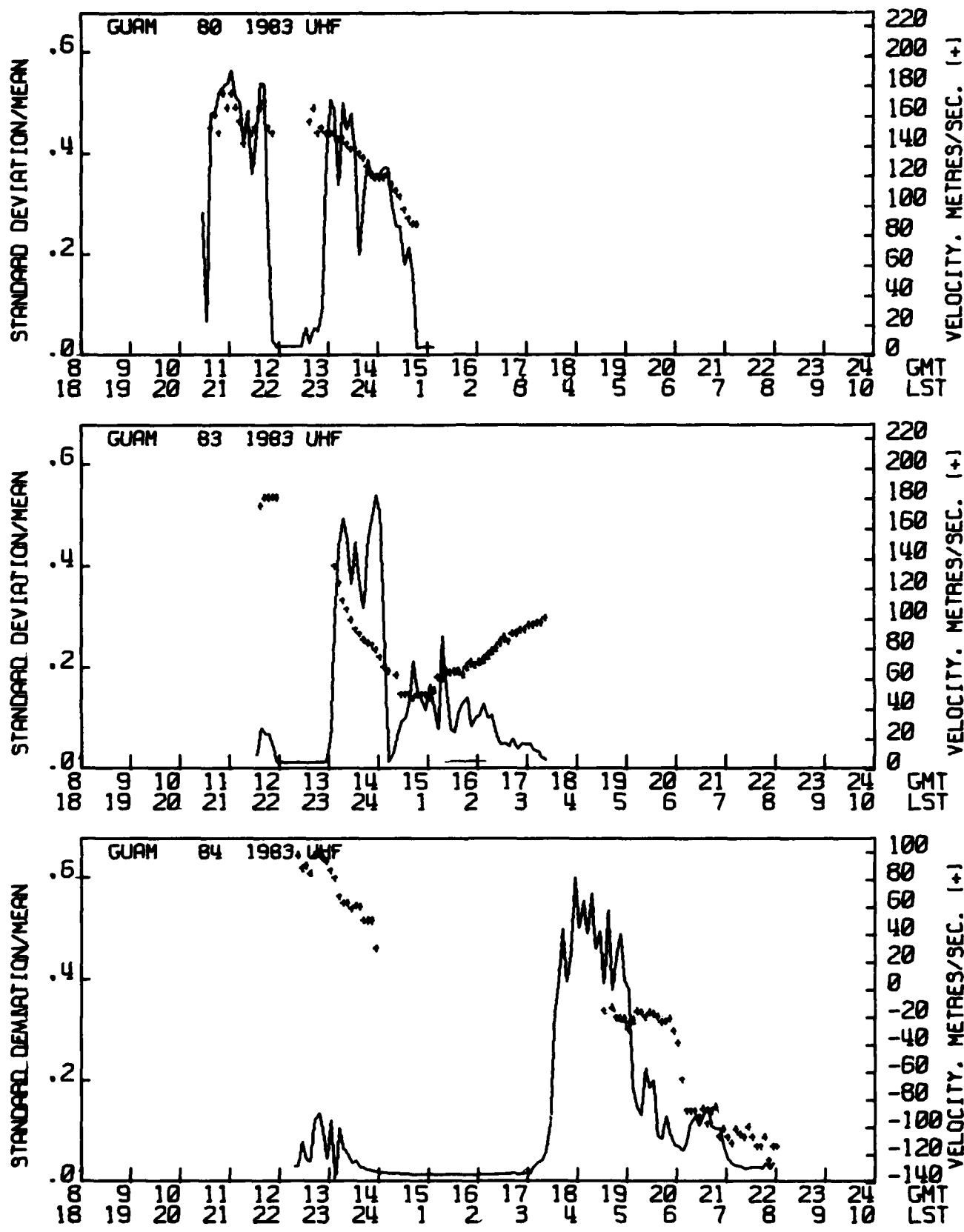


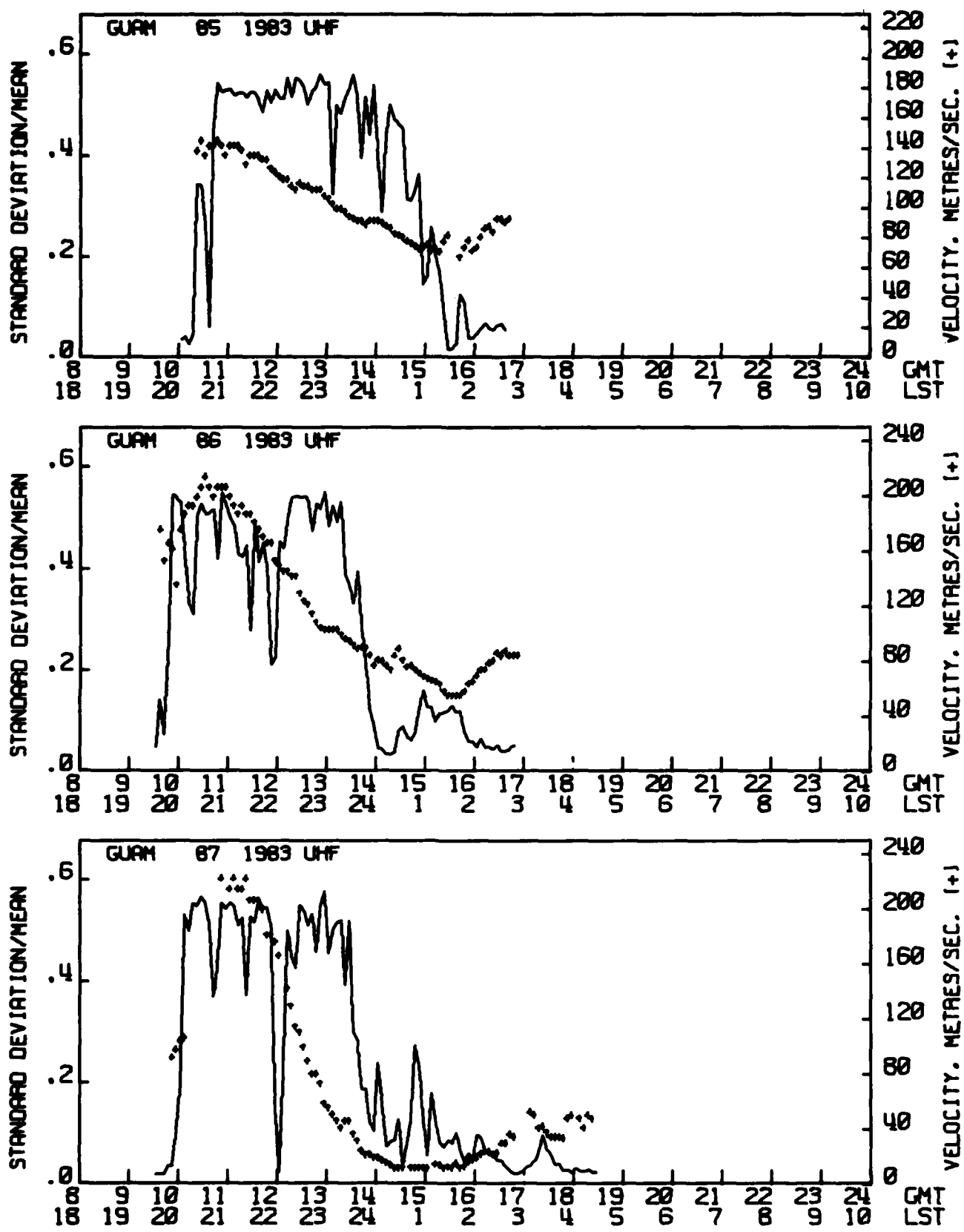


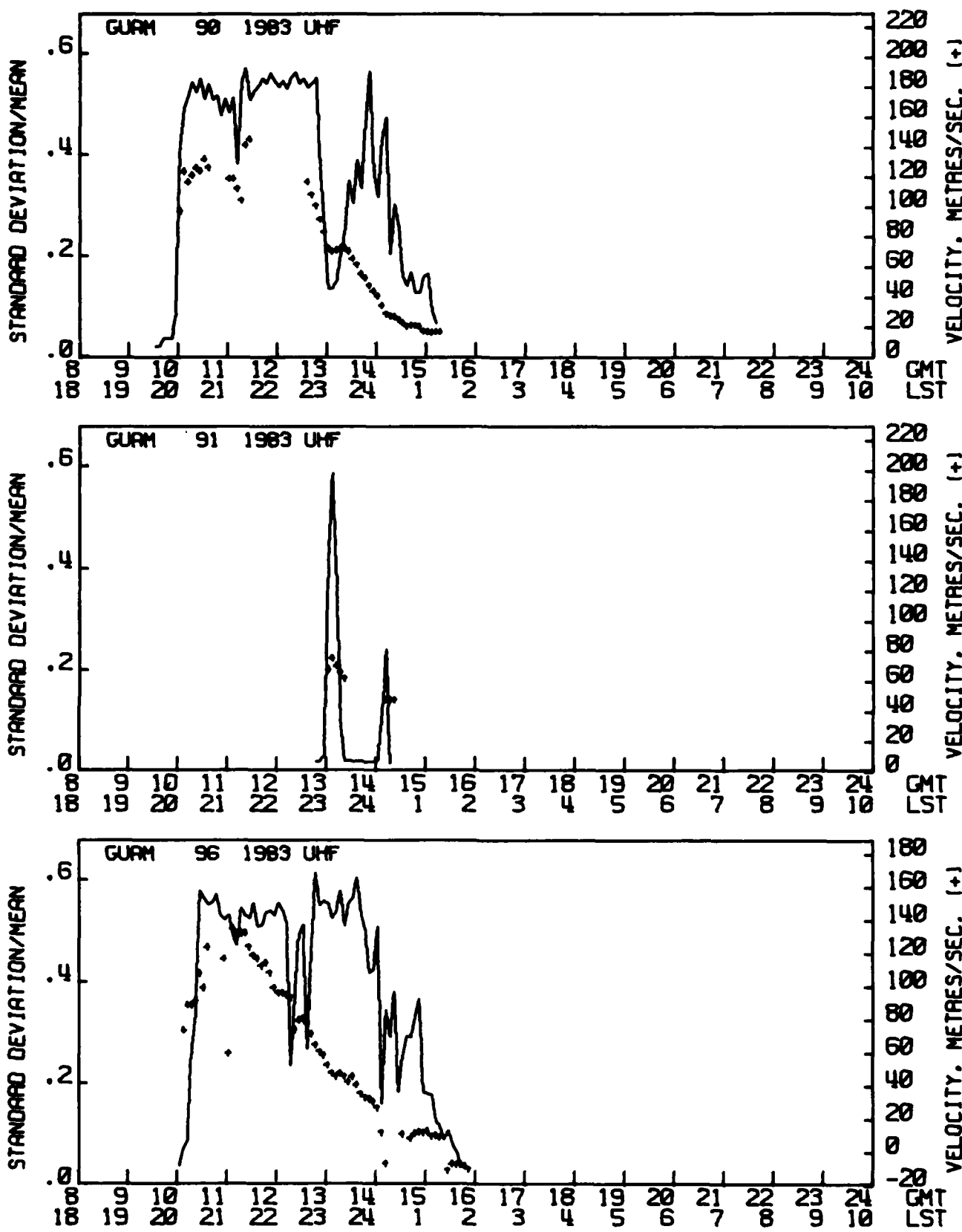


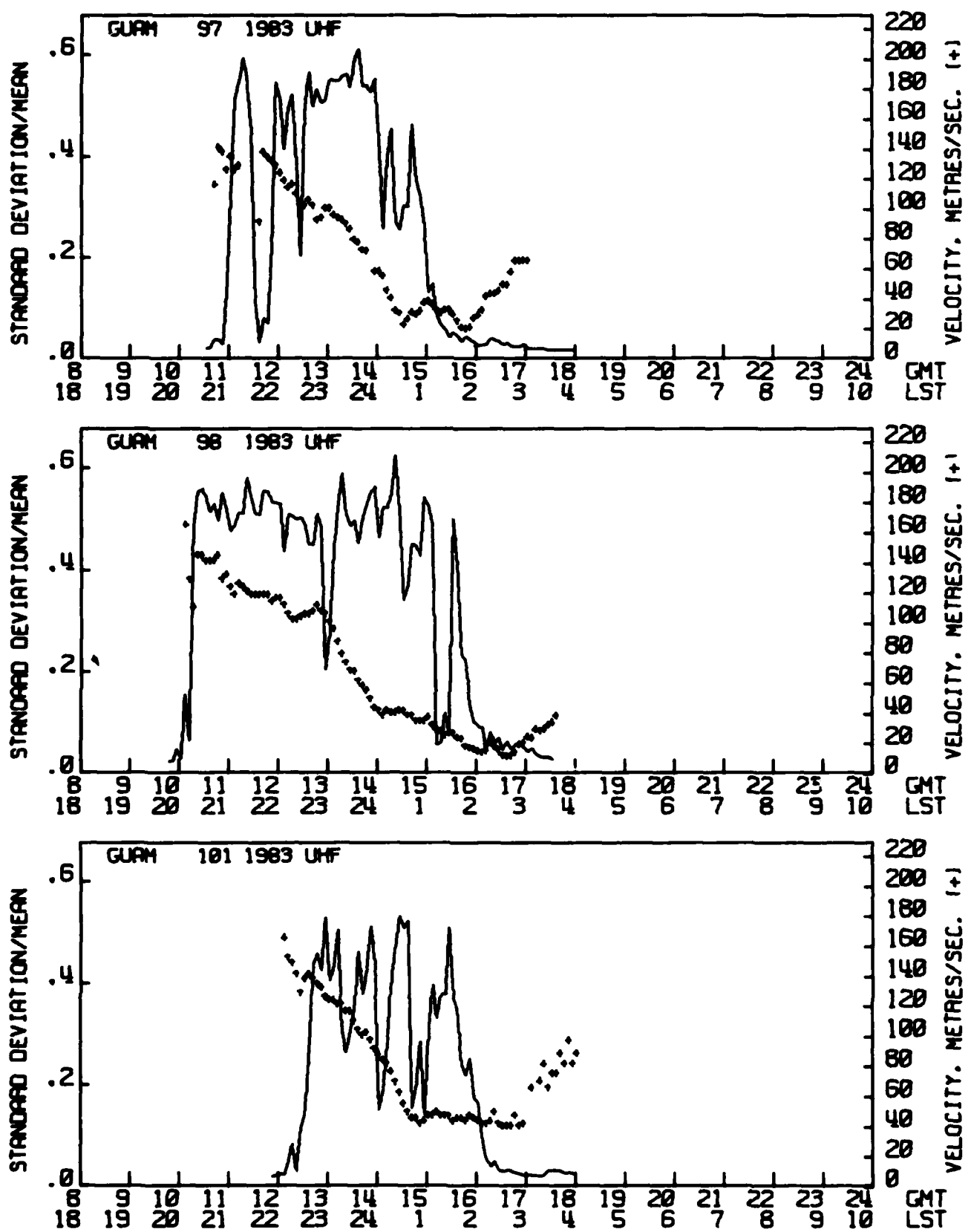


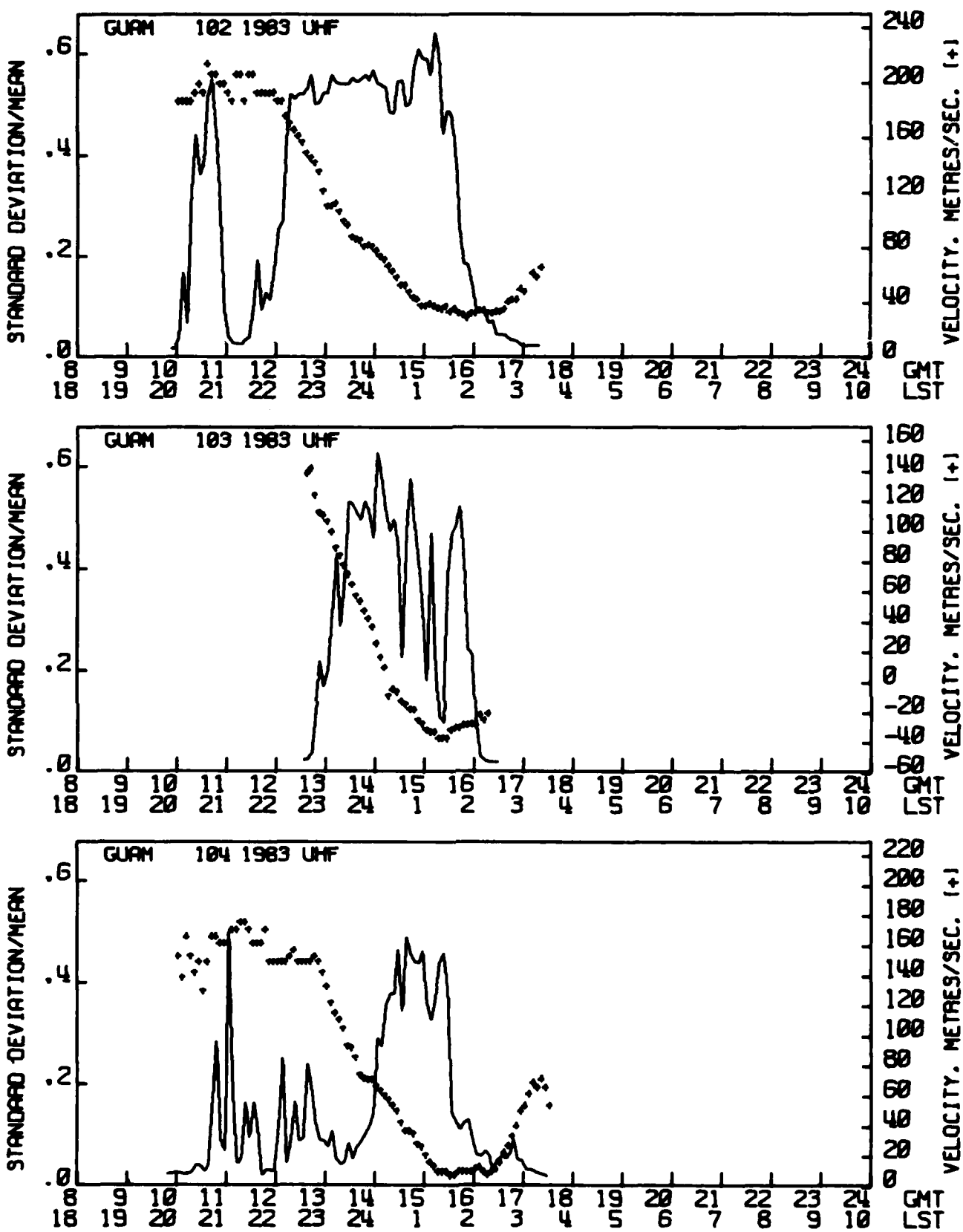


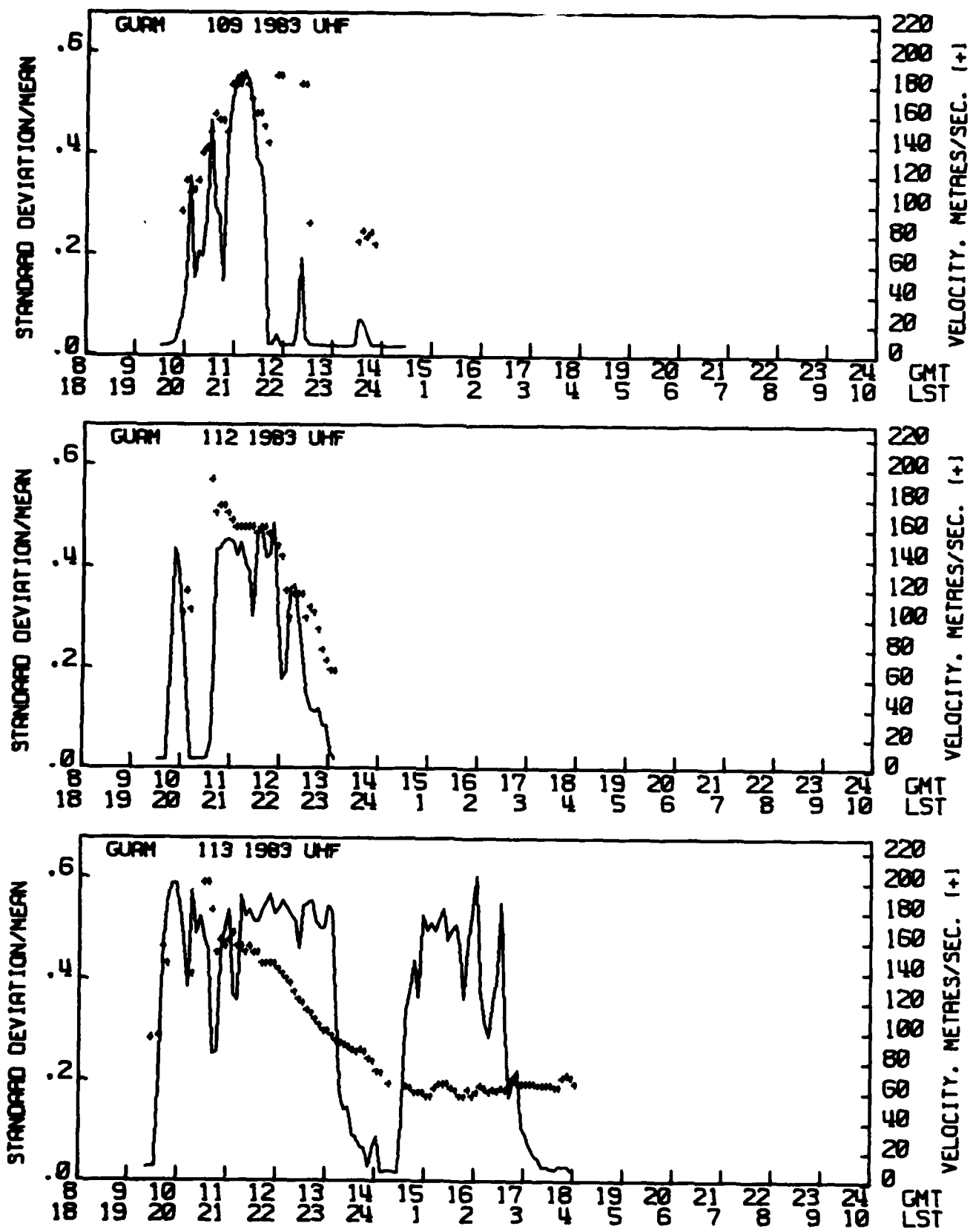


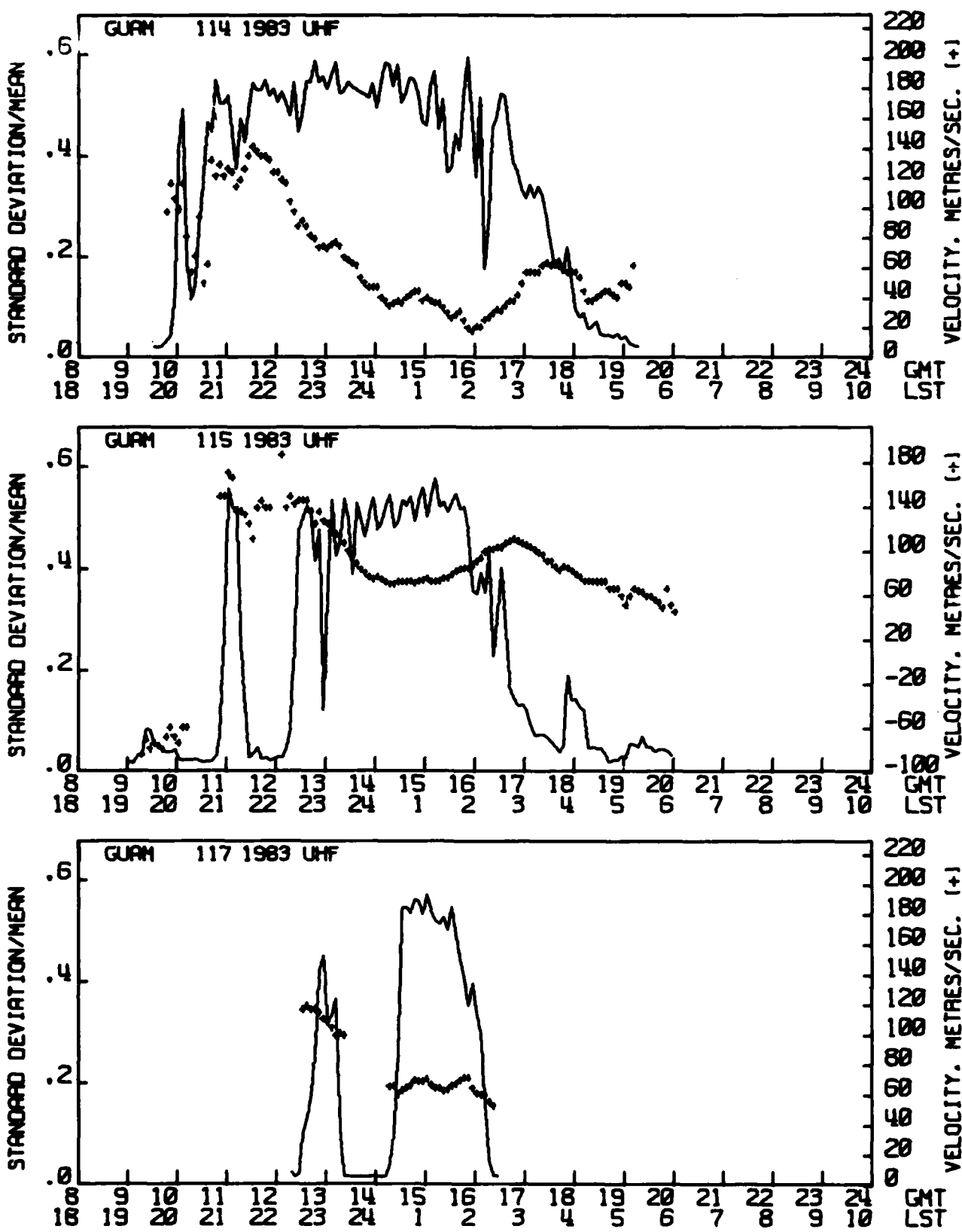


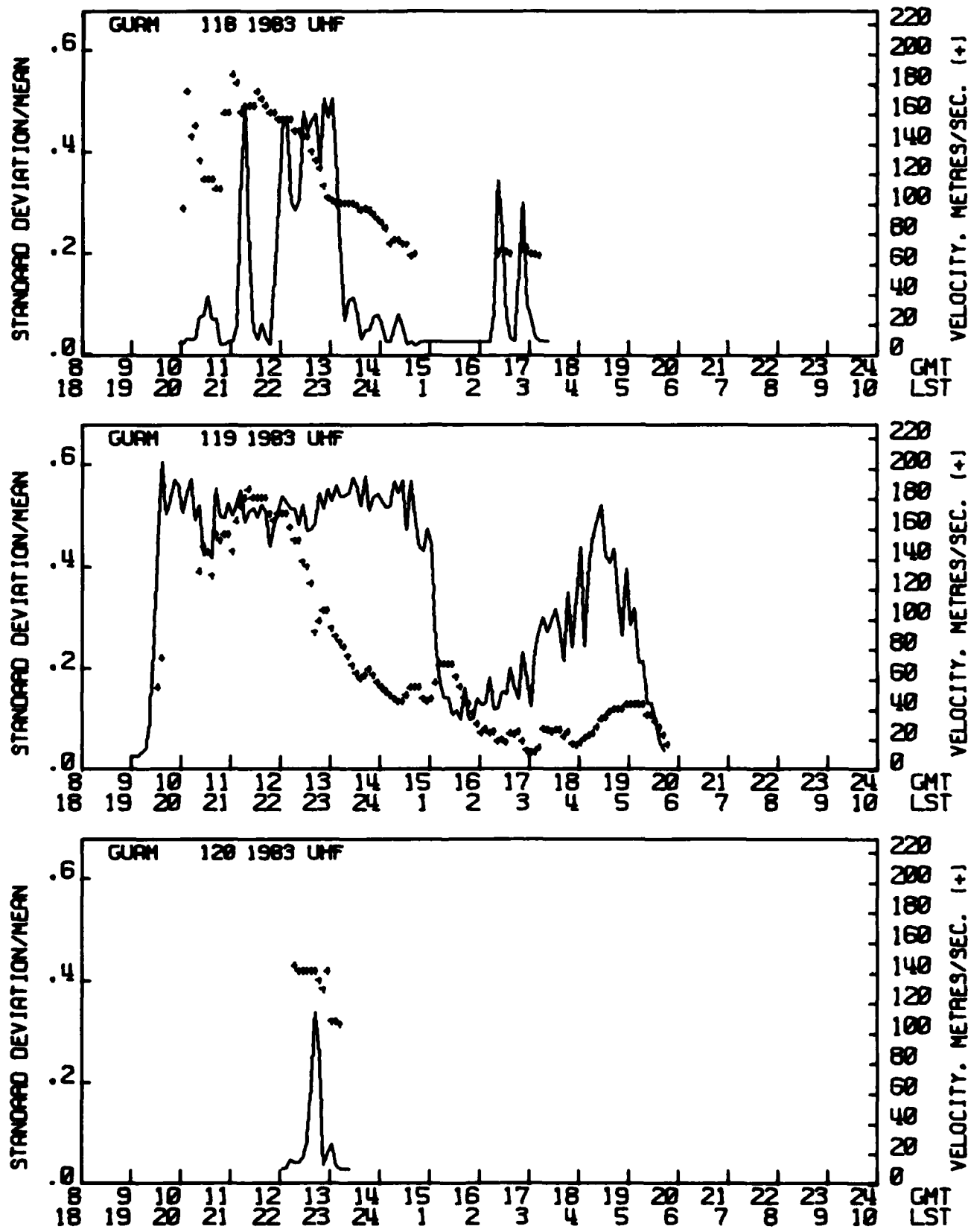


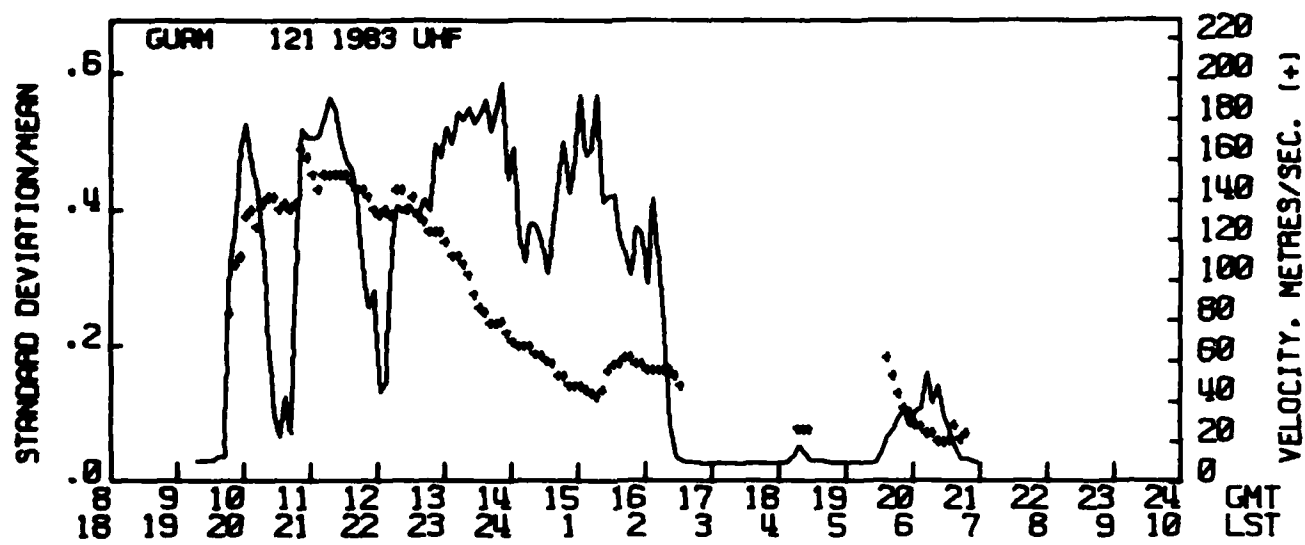






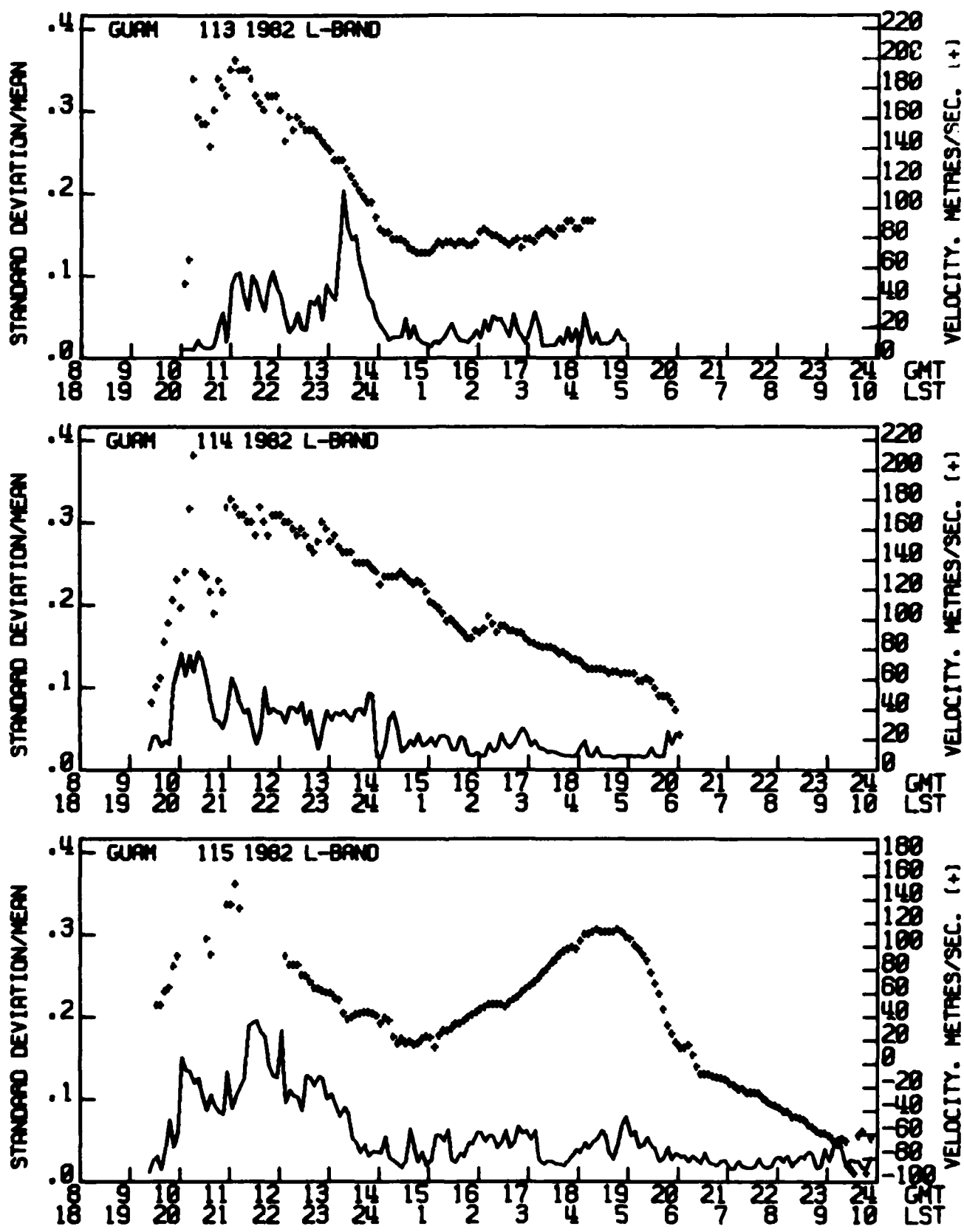


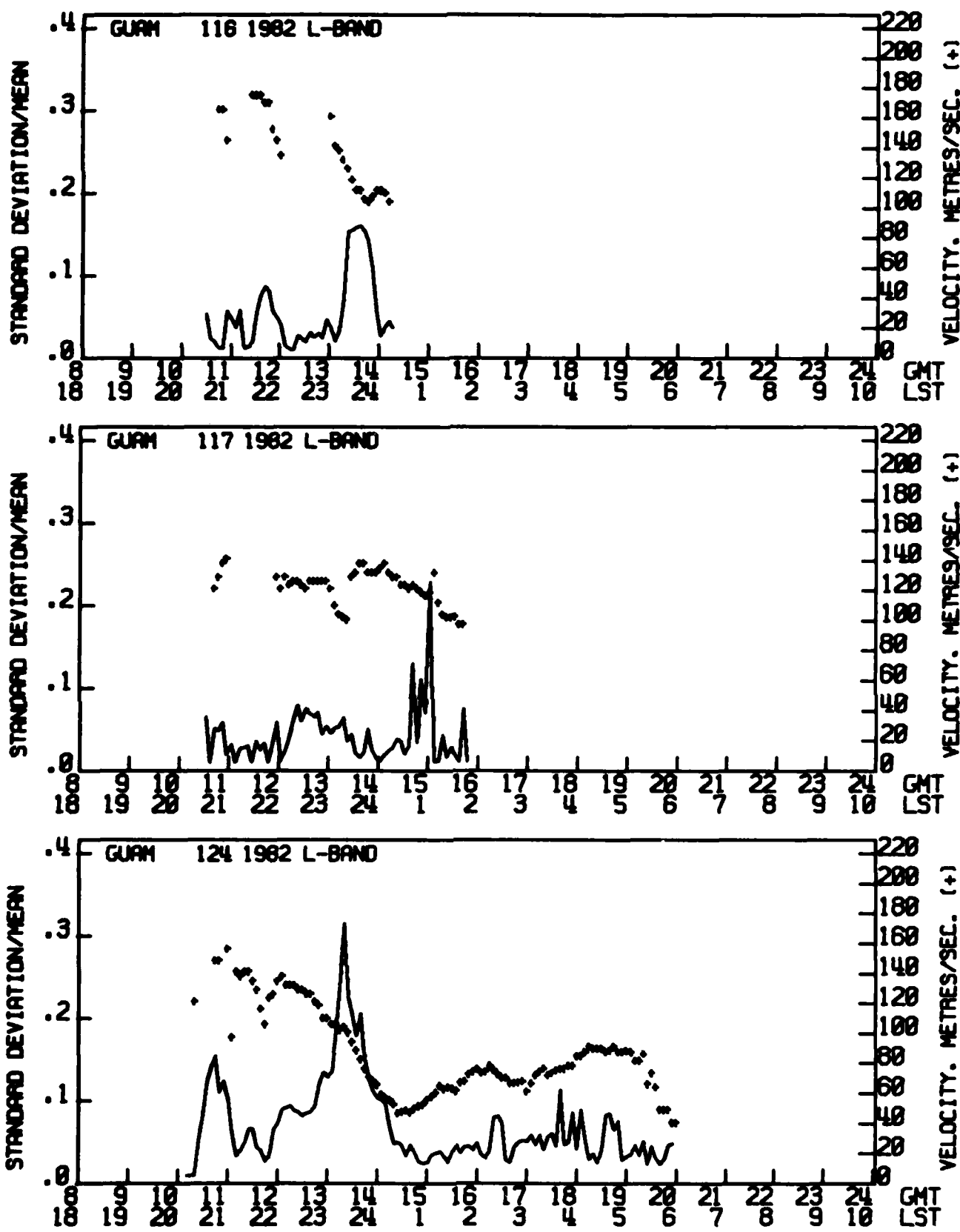


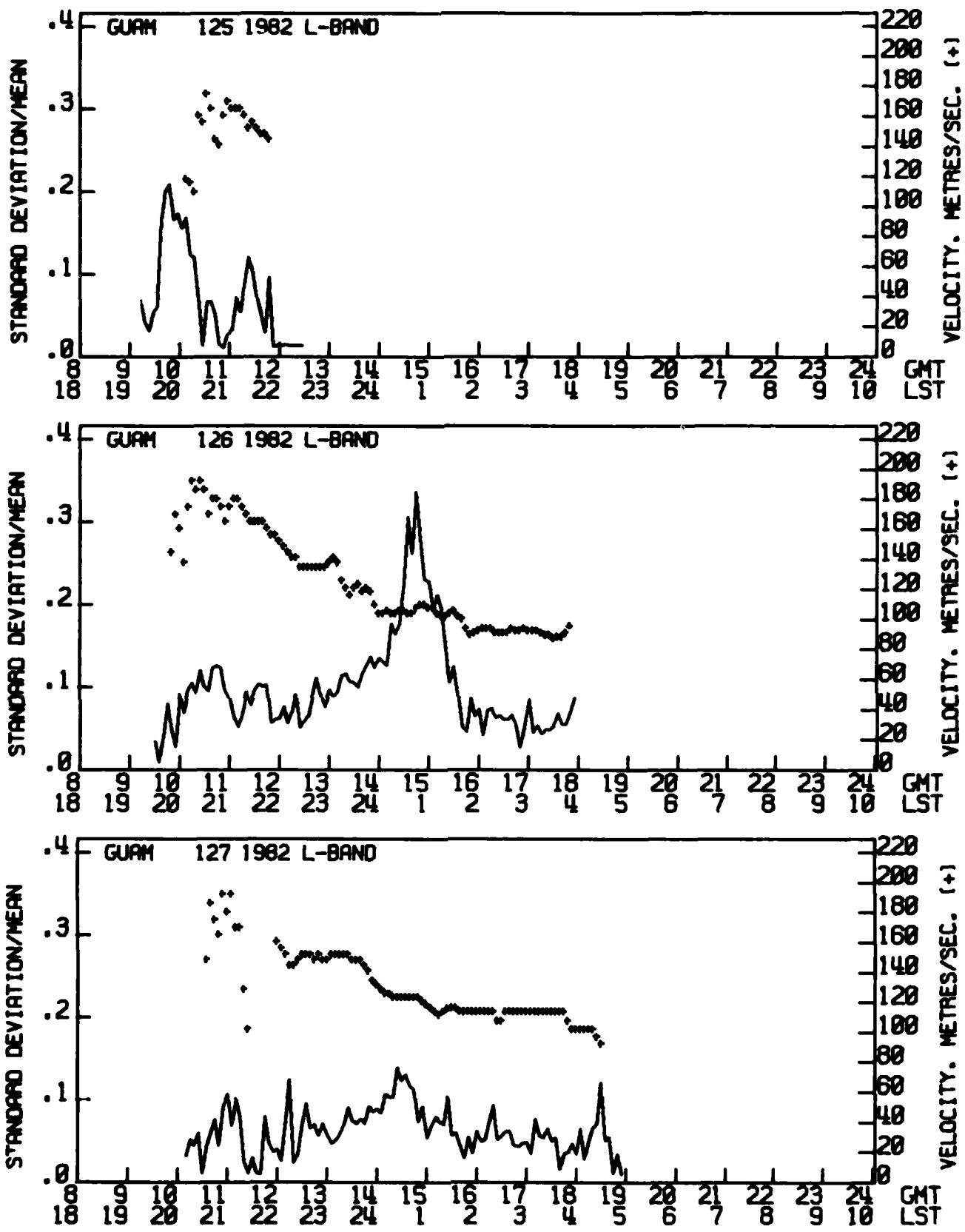


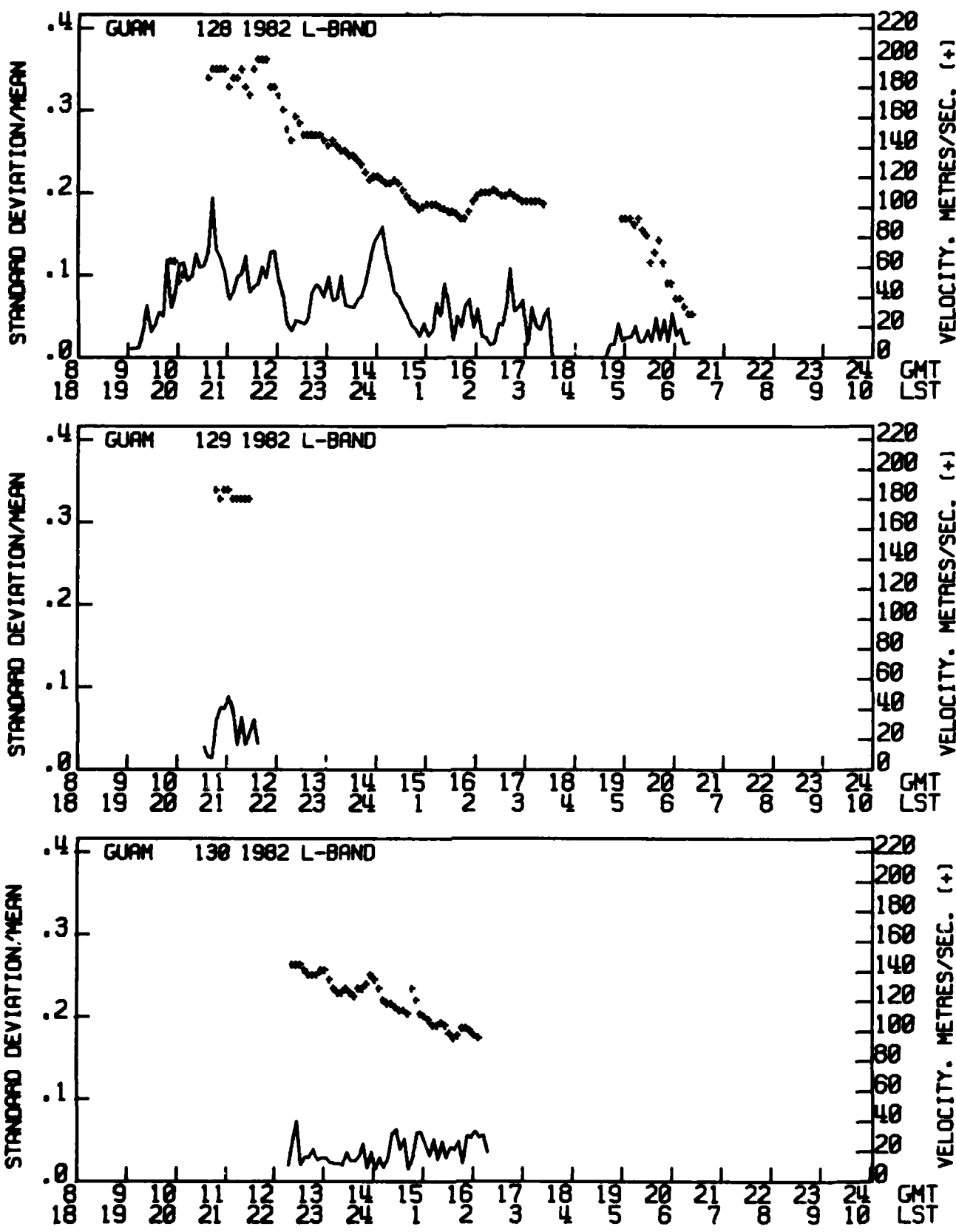
APPENDIX B

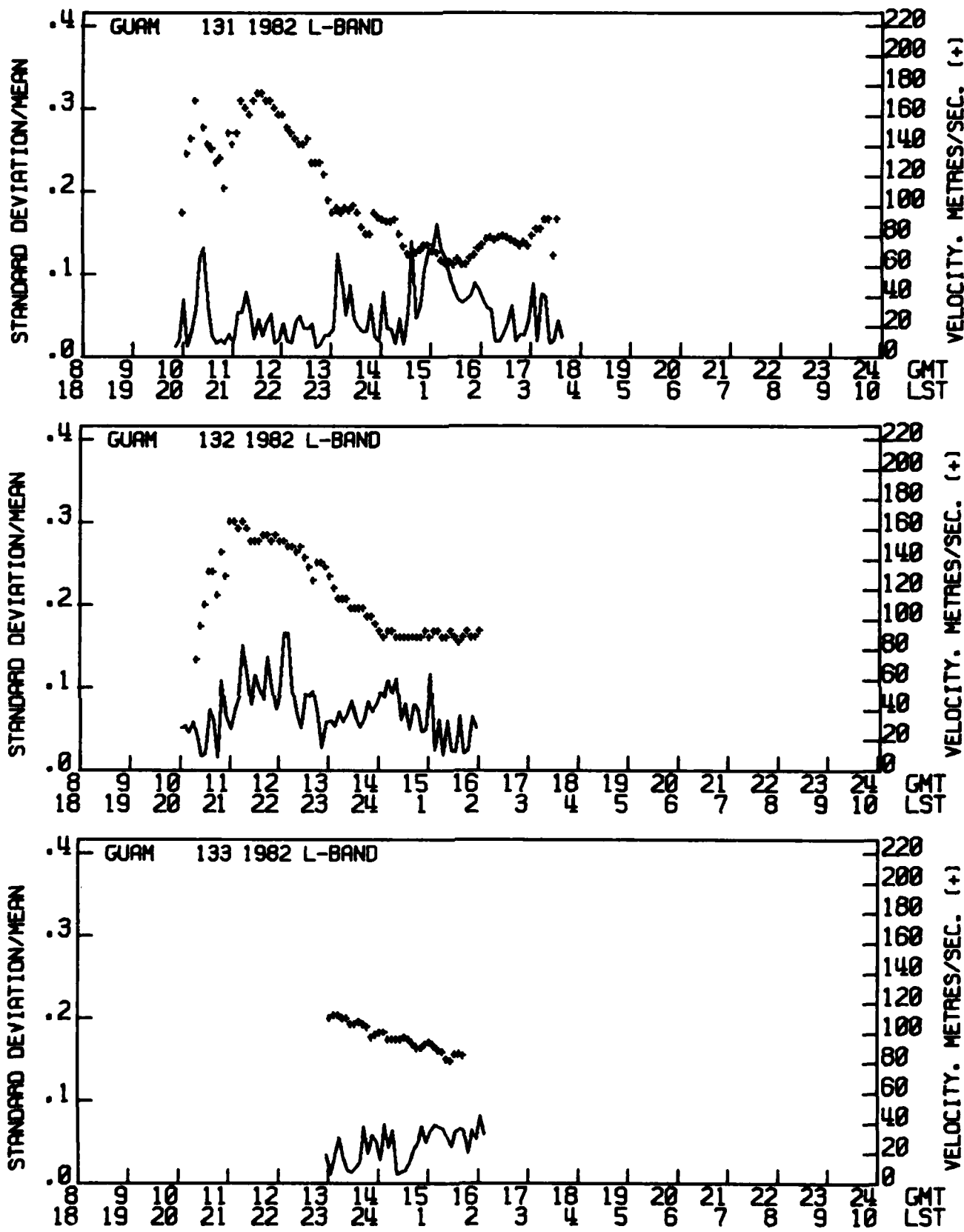
**PLOTS OF L-BAND SCINTILLATION INTENSITIES ALONG
WITH THE EAST-WEST COMPONENT OF DRIFT VELOCITIES
(POSITIVE VELOCITIES ARE EASTWARD DRIFT)**

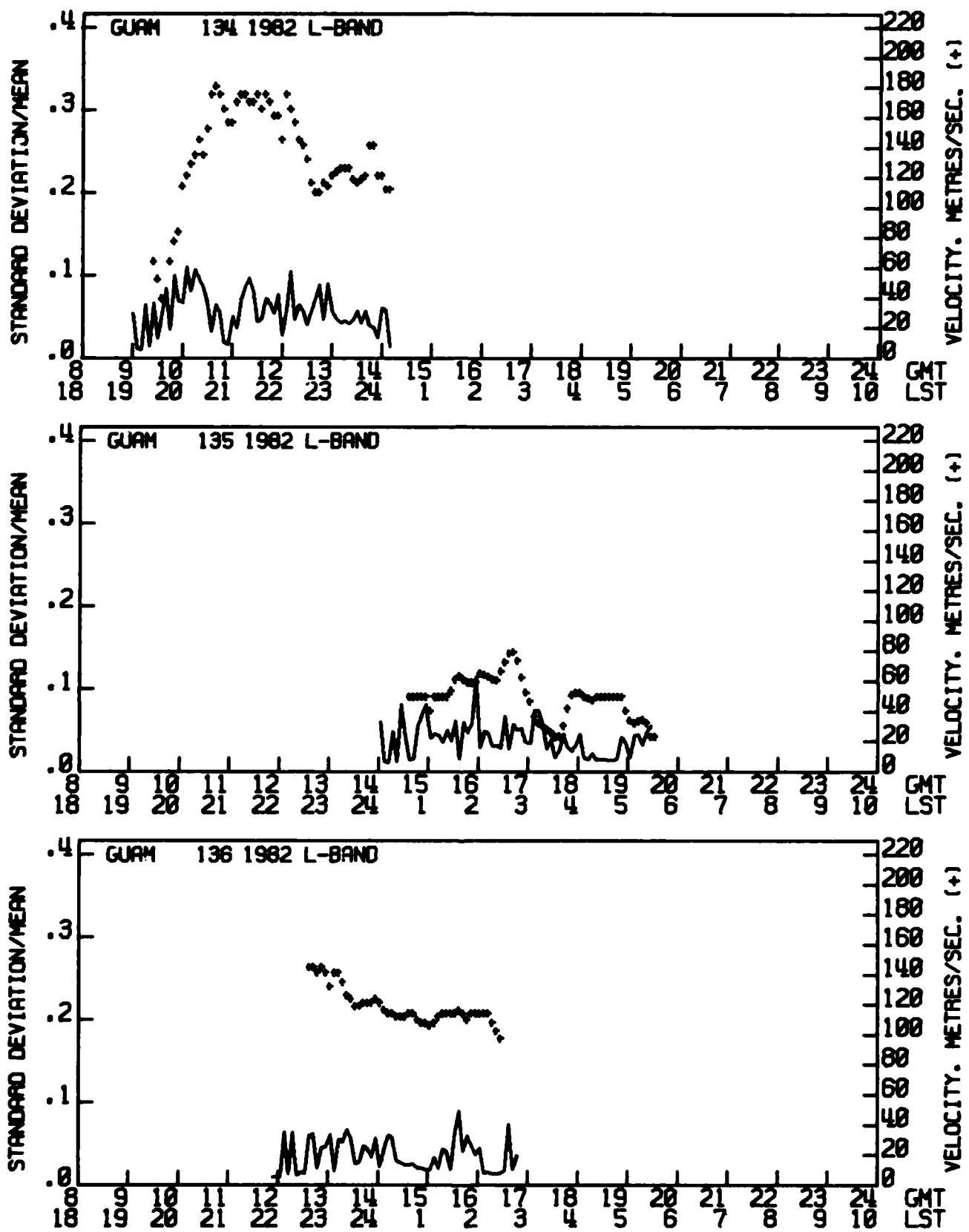


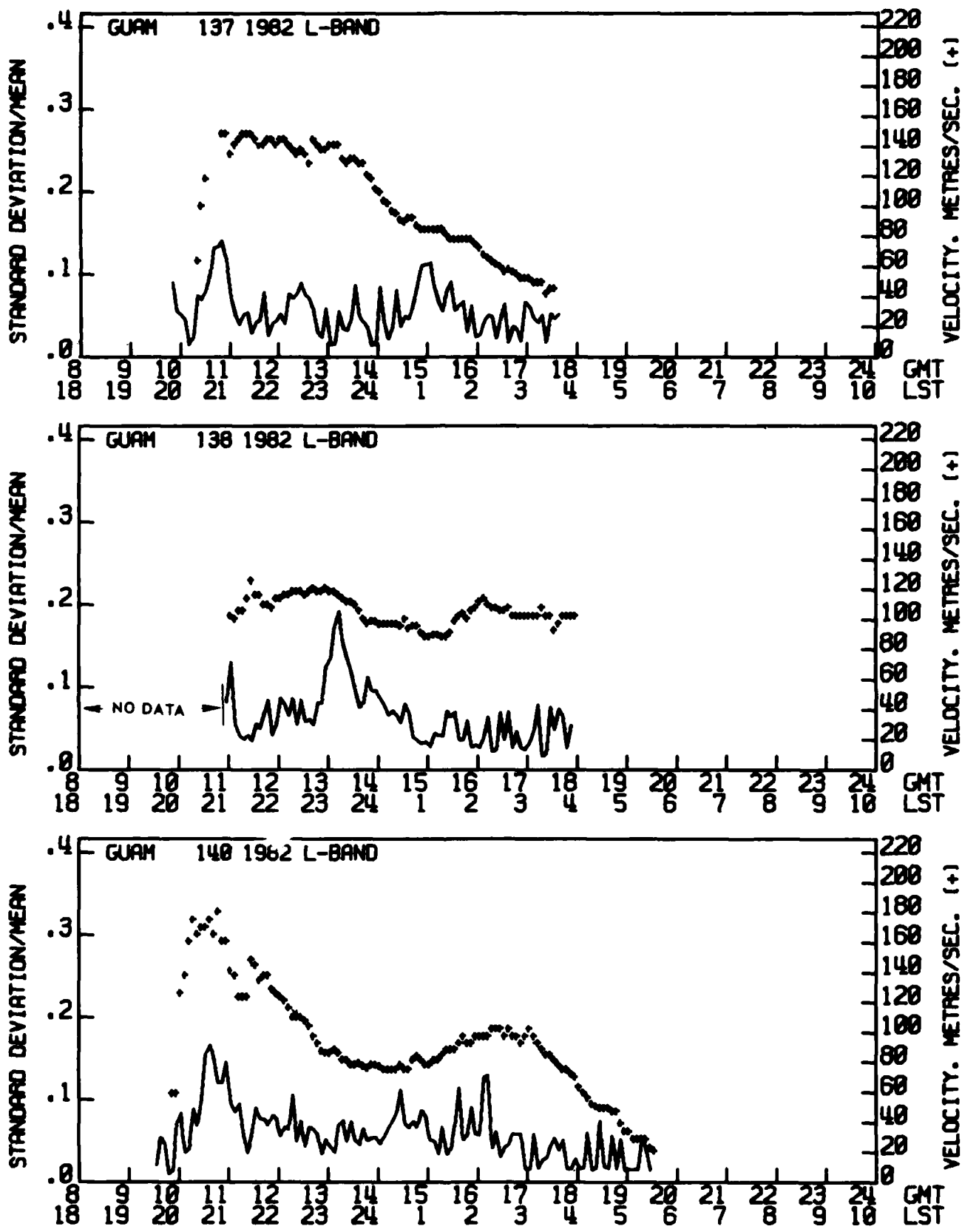


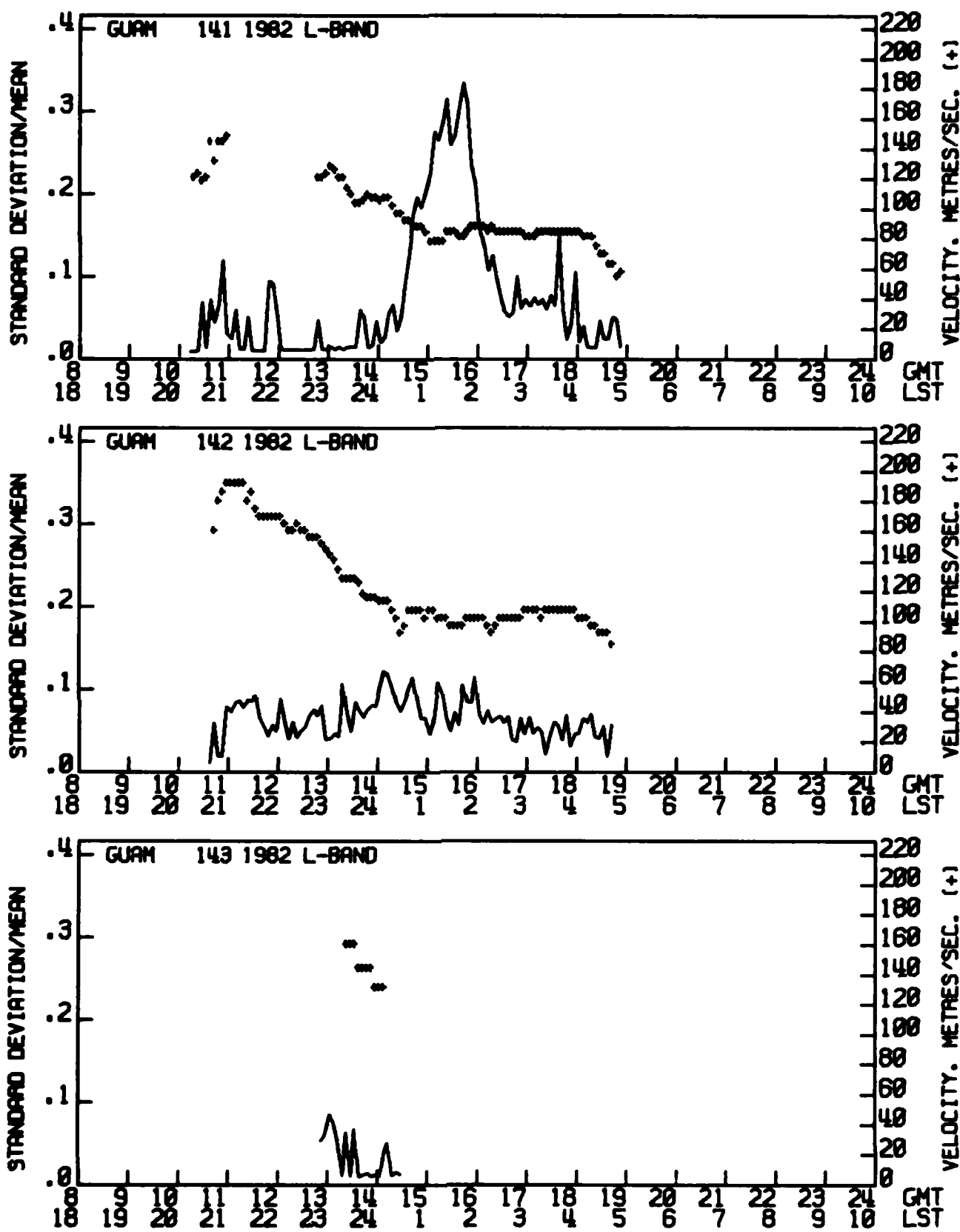


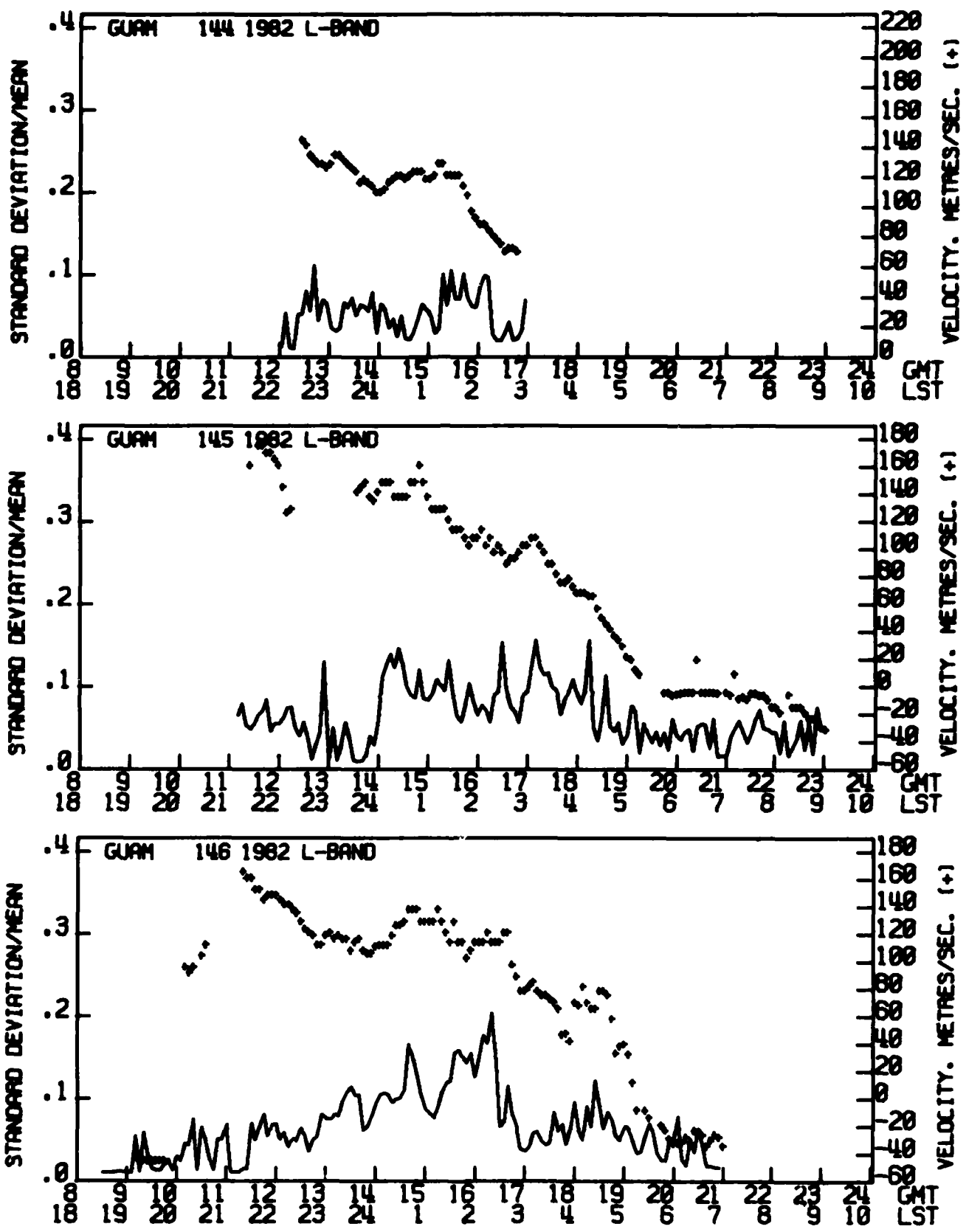


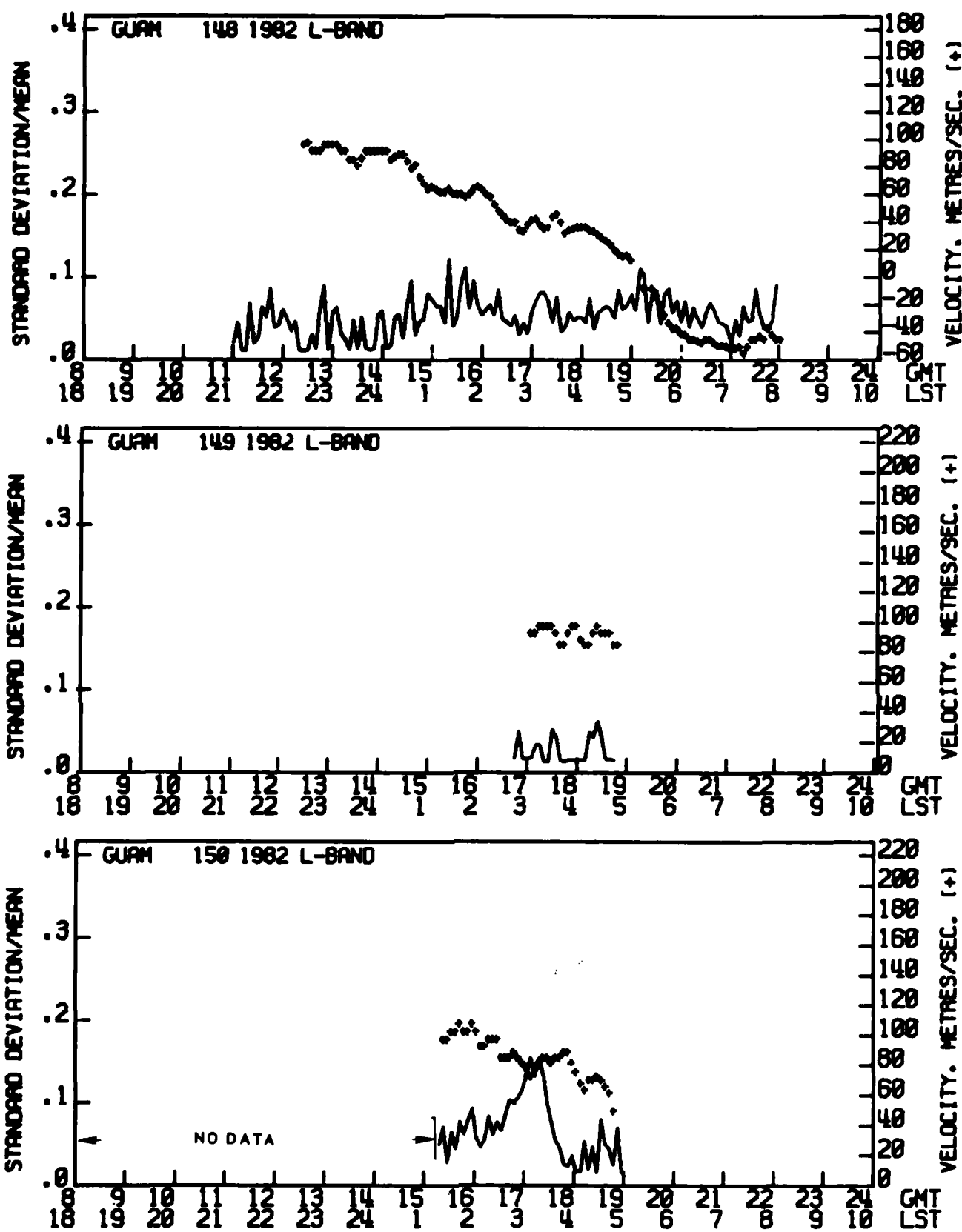


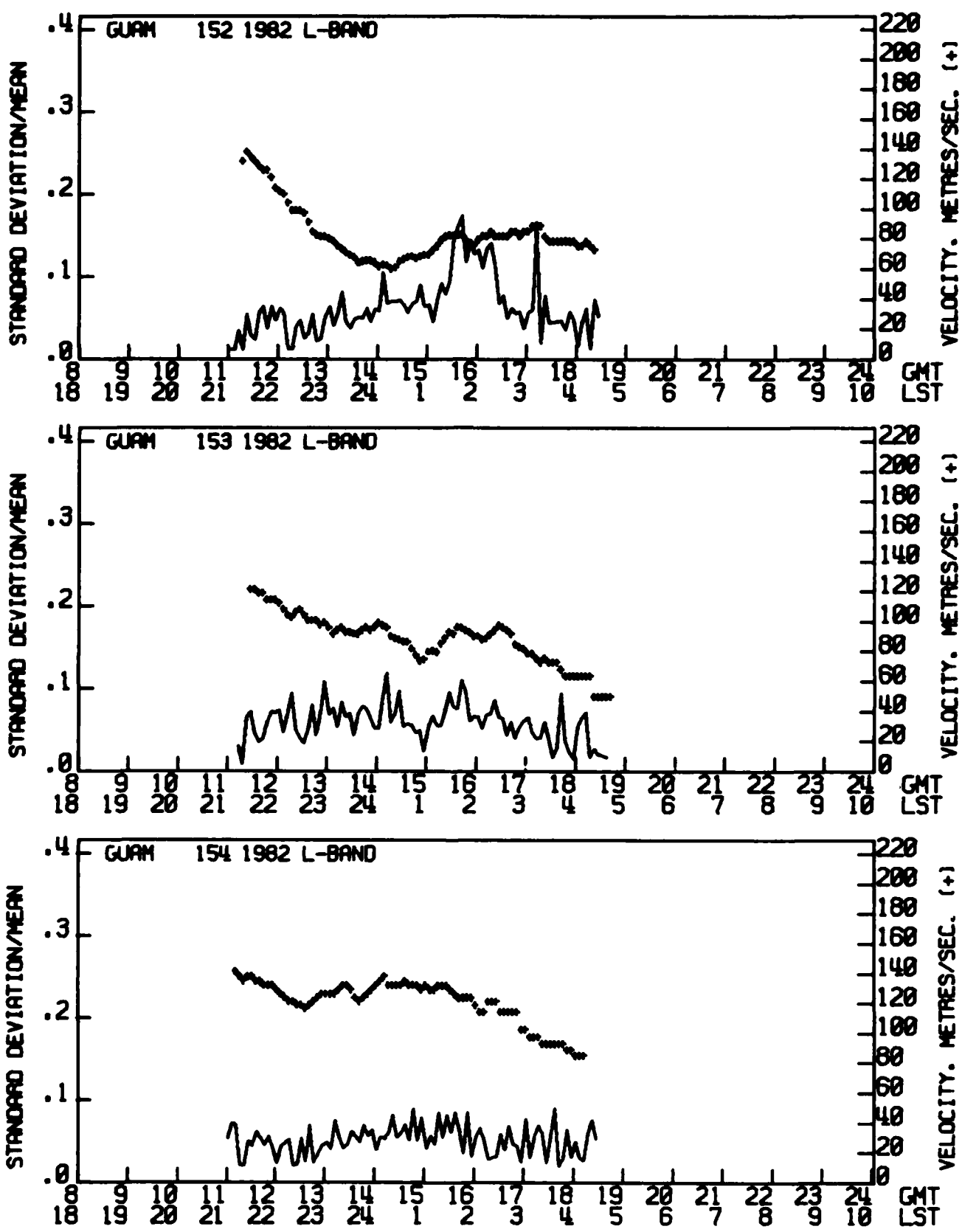


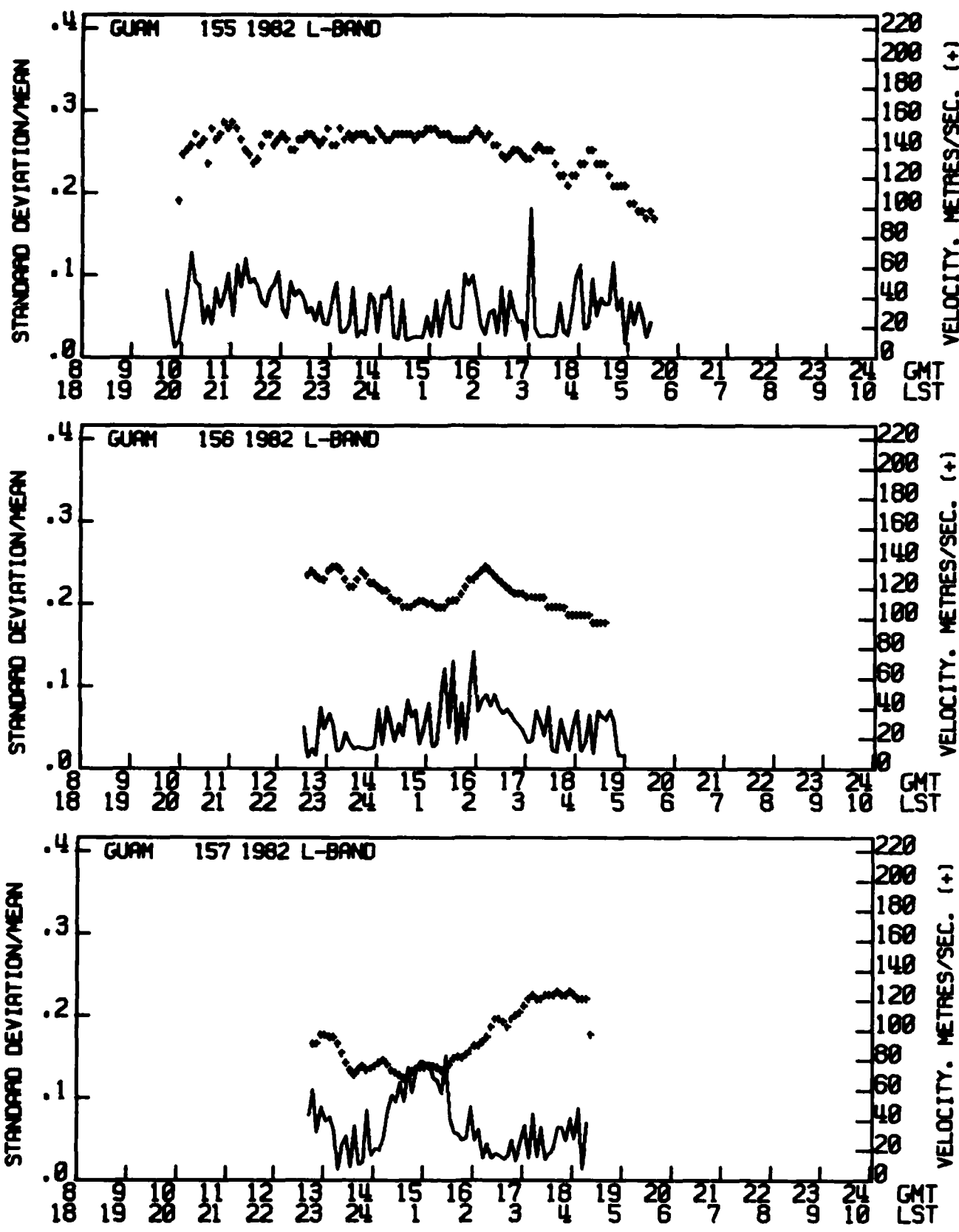


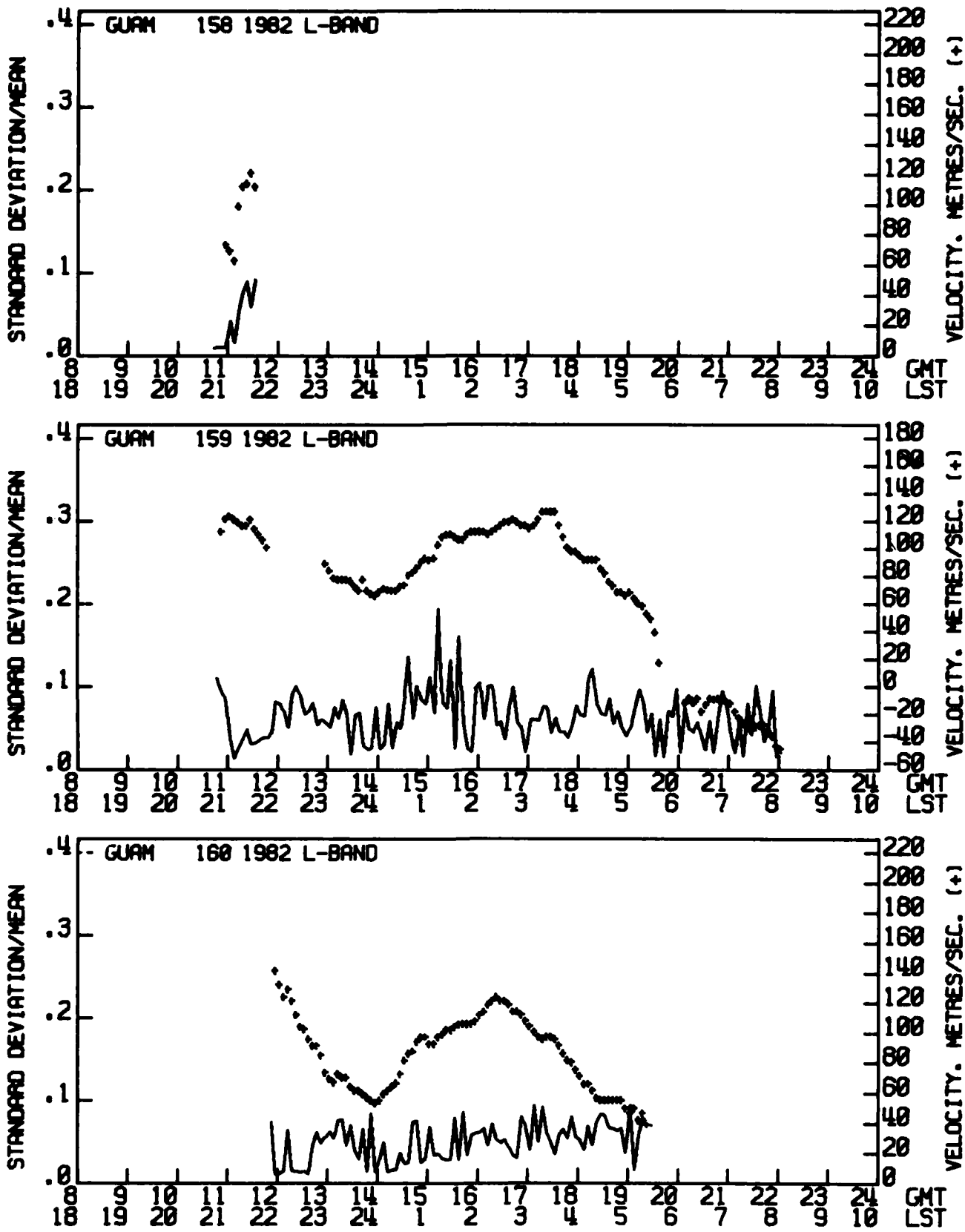


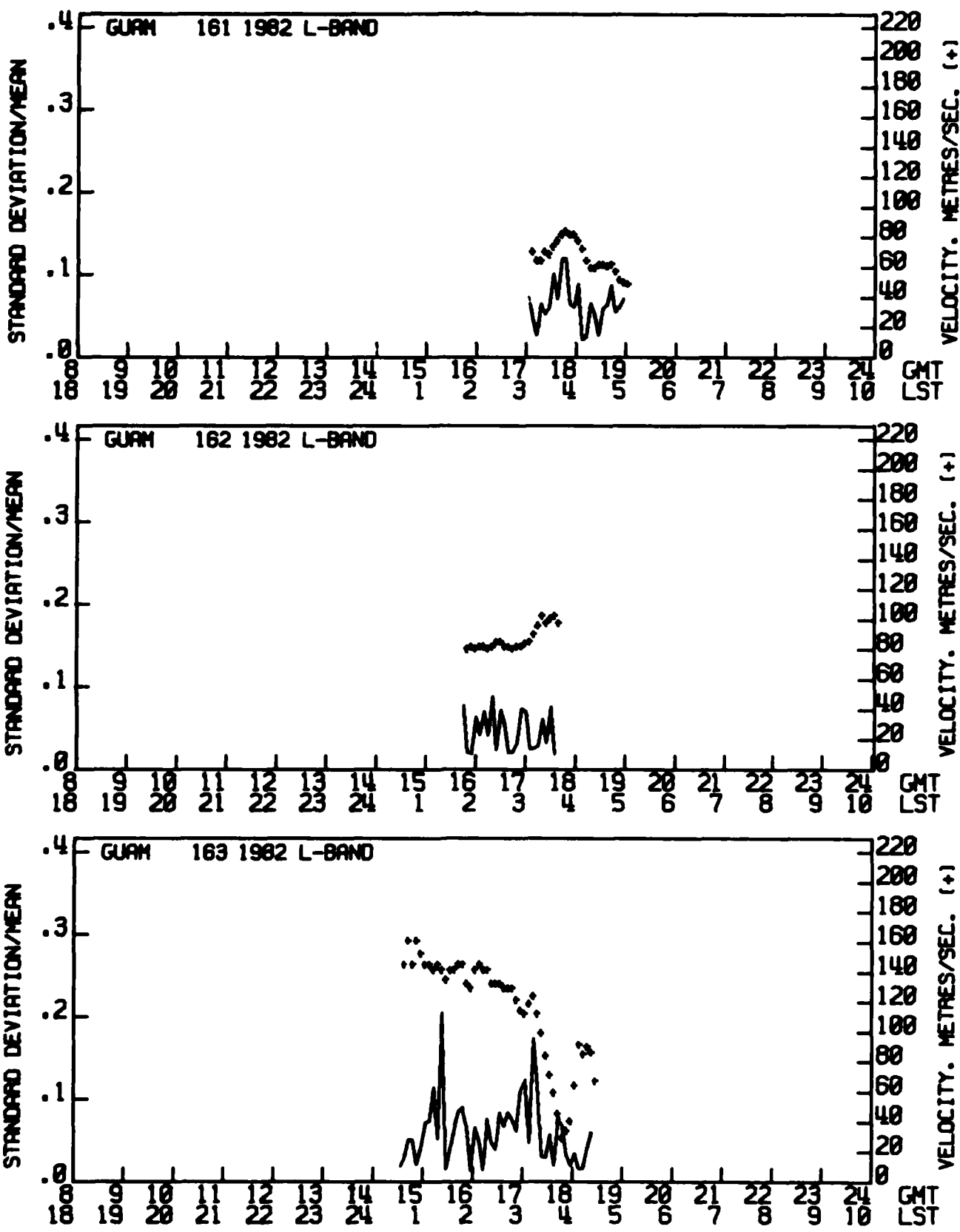


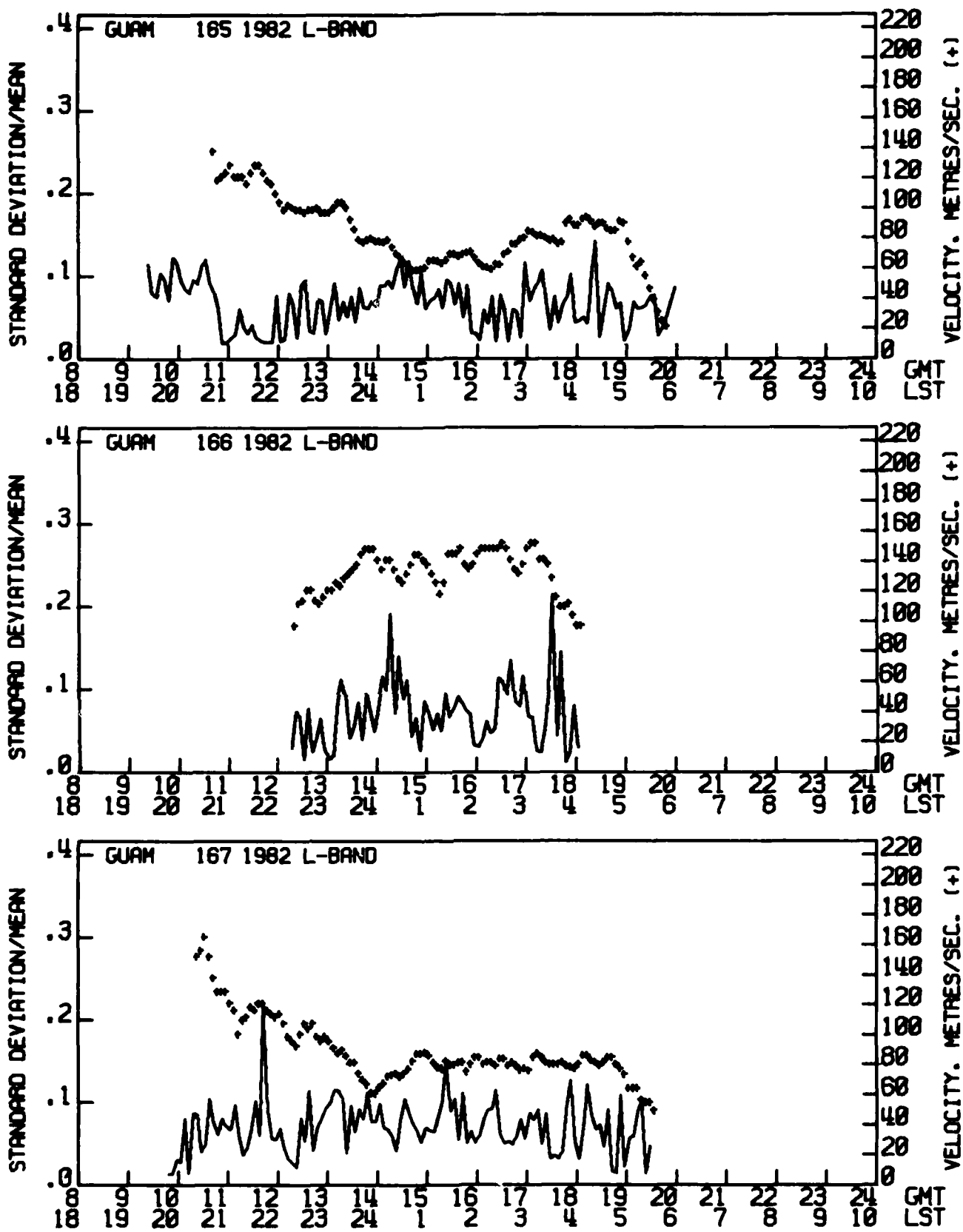


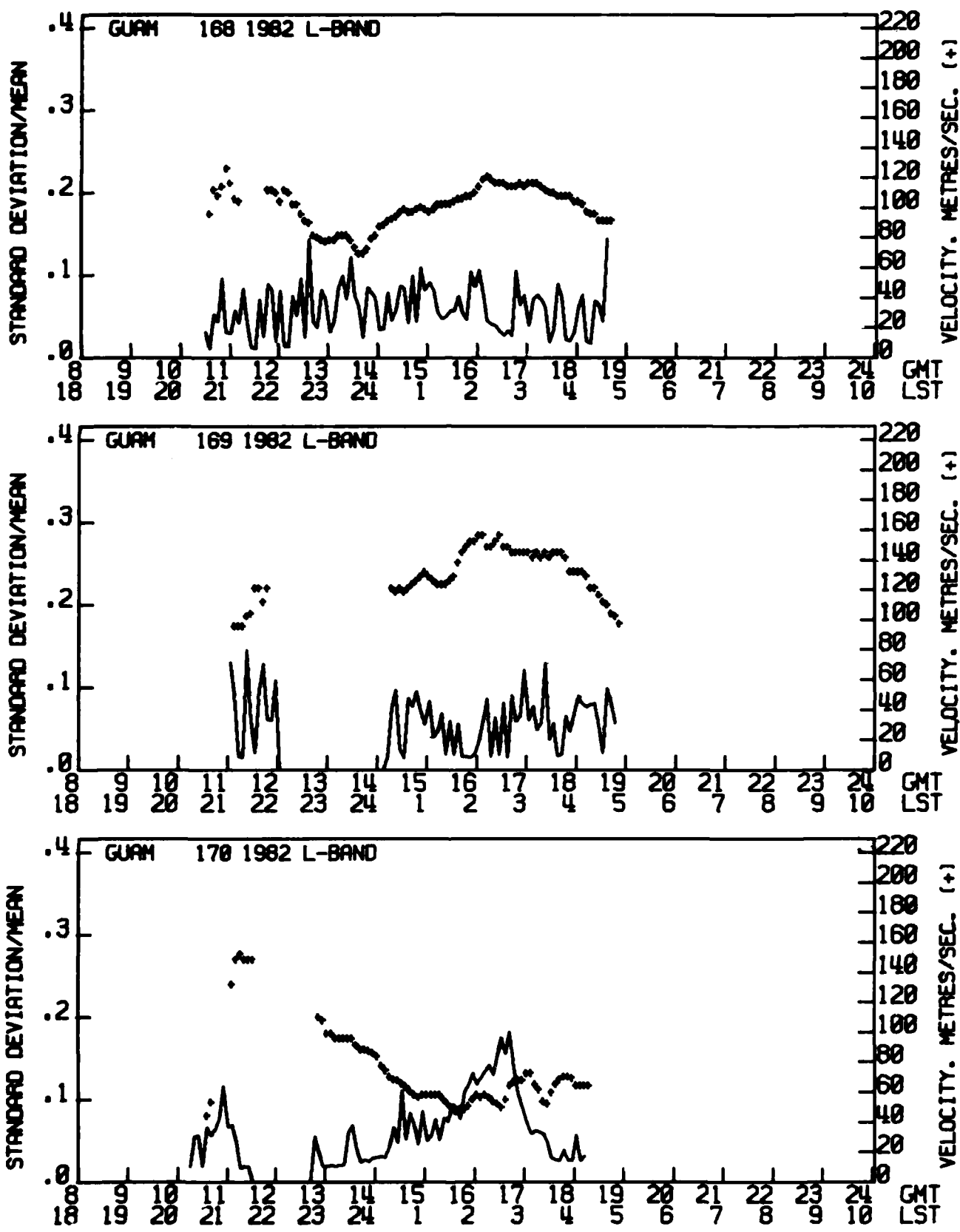


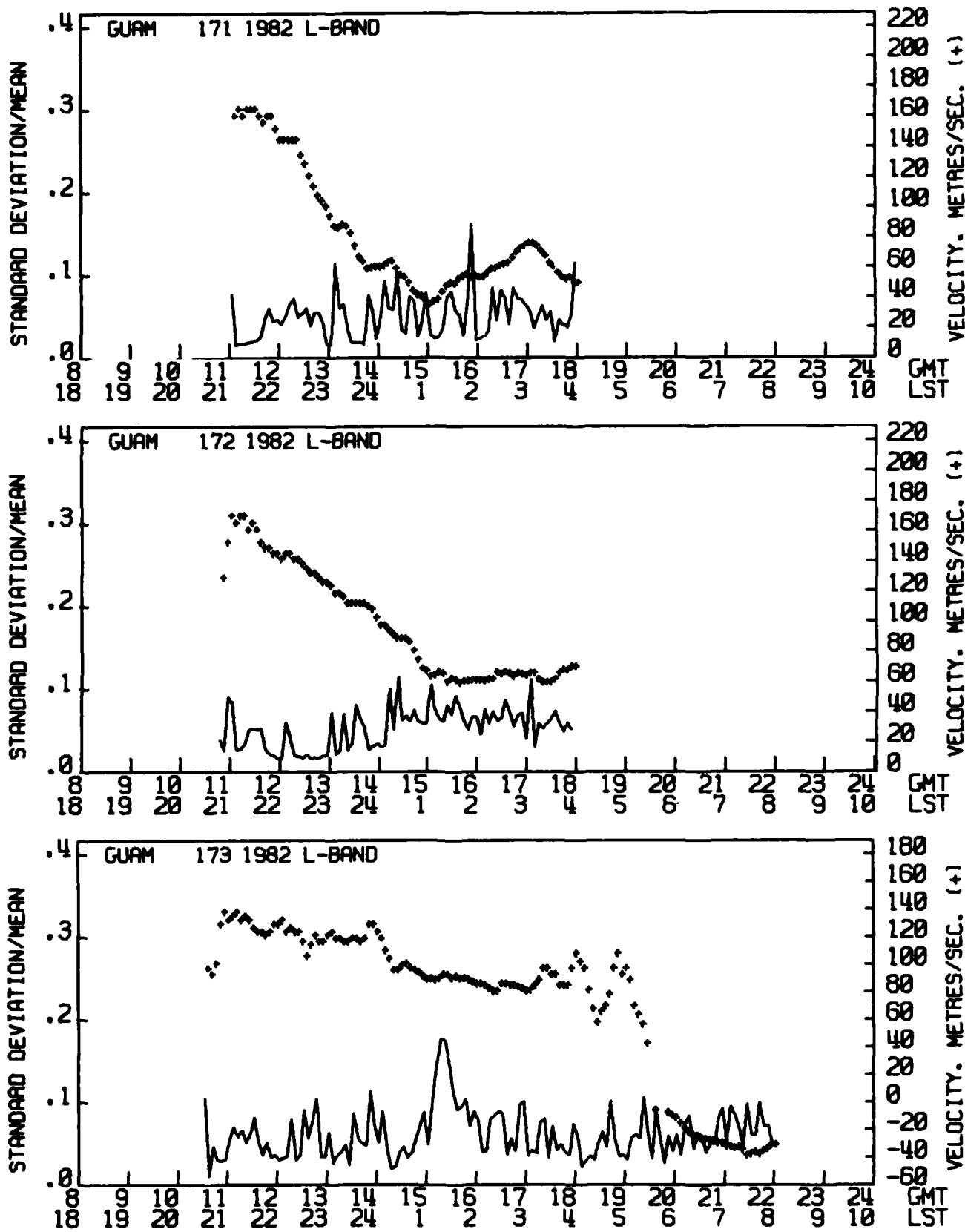


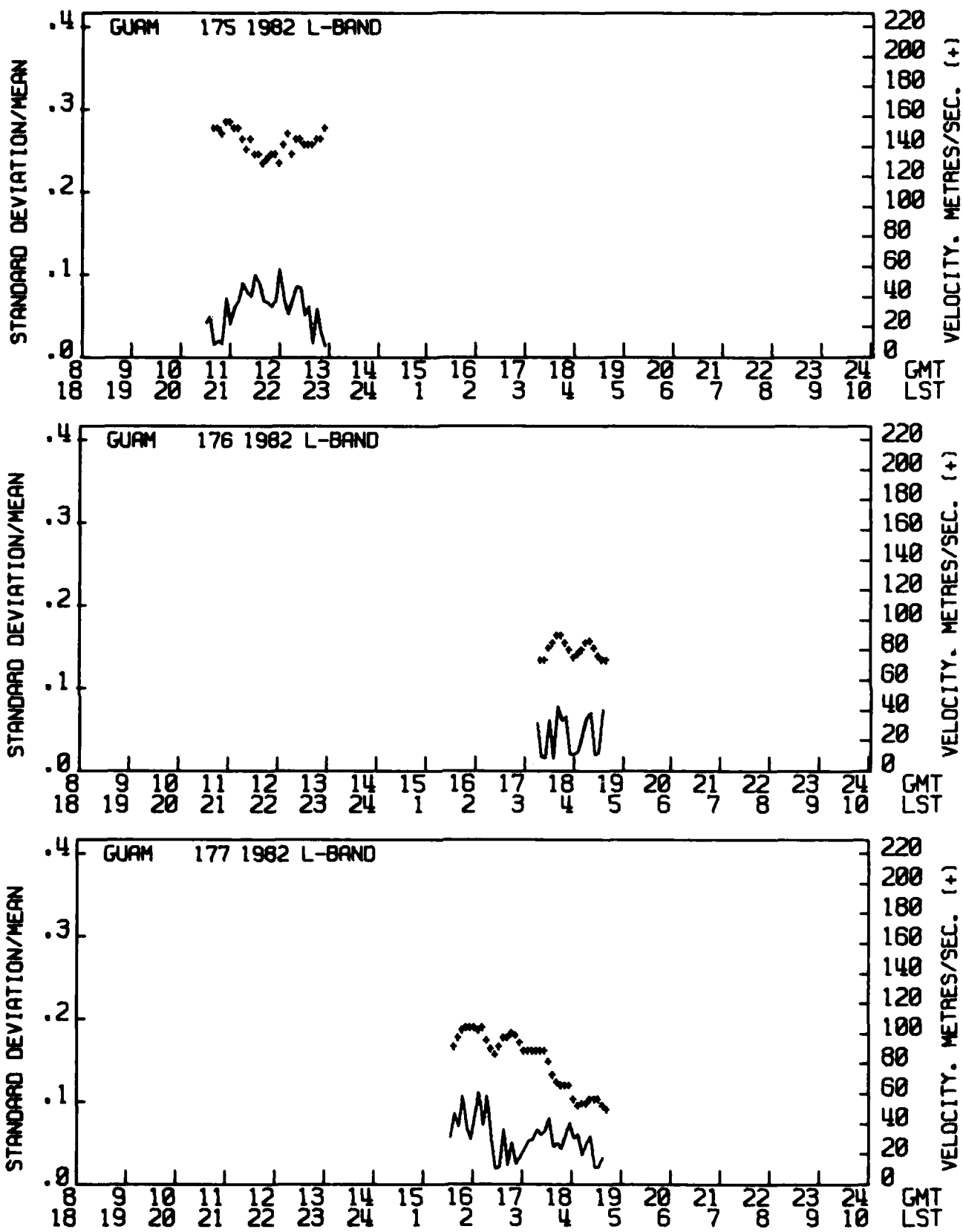


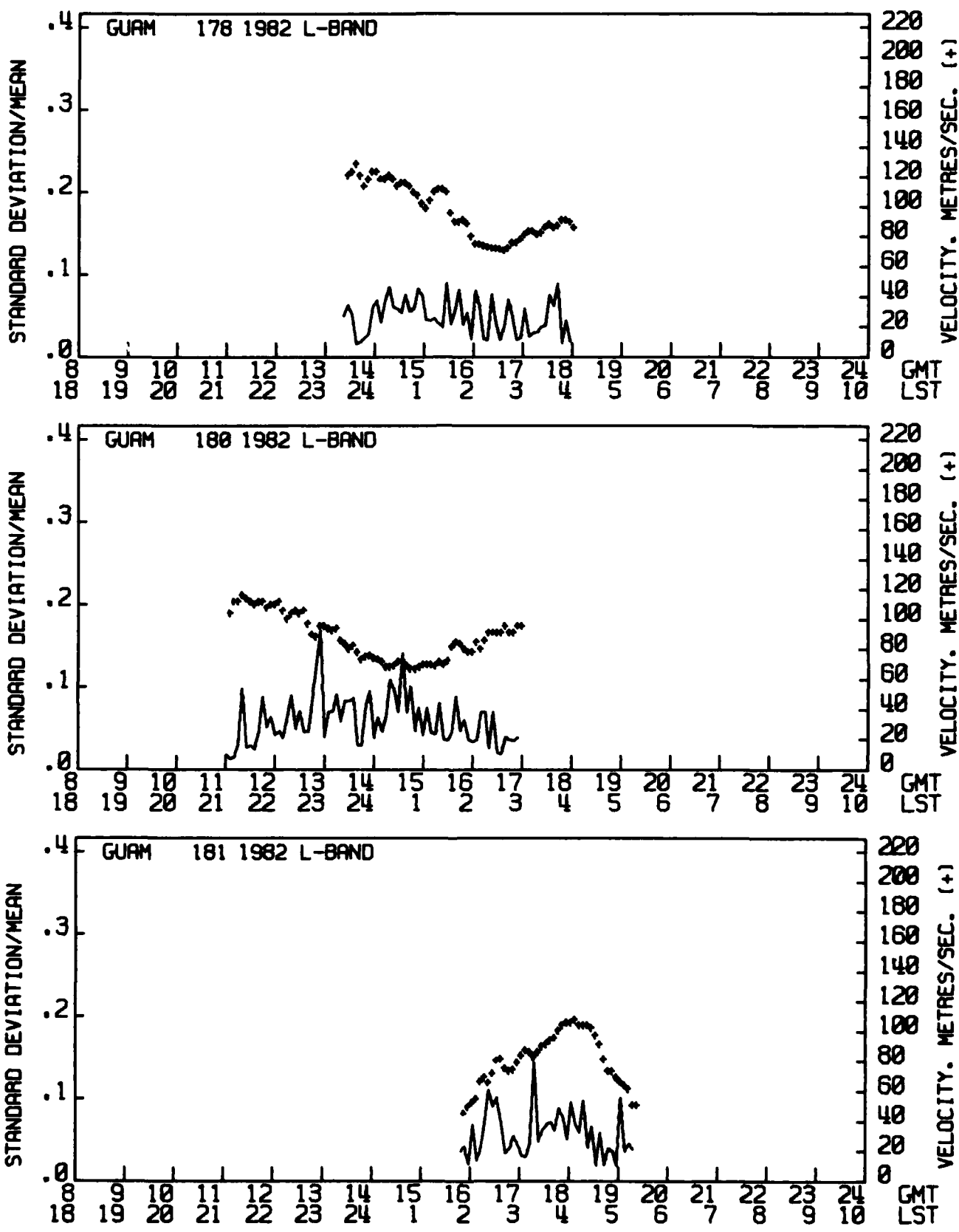


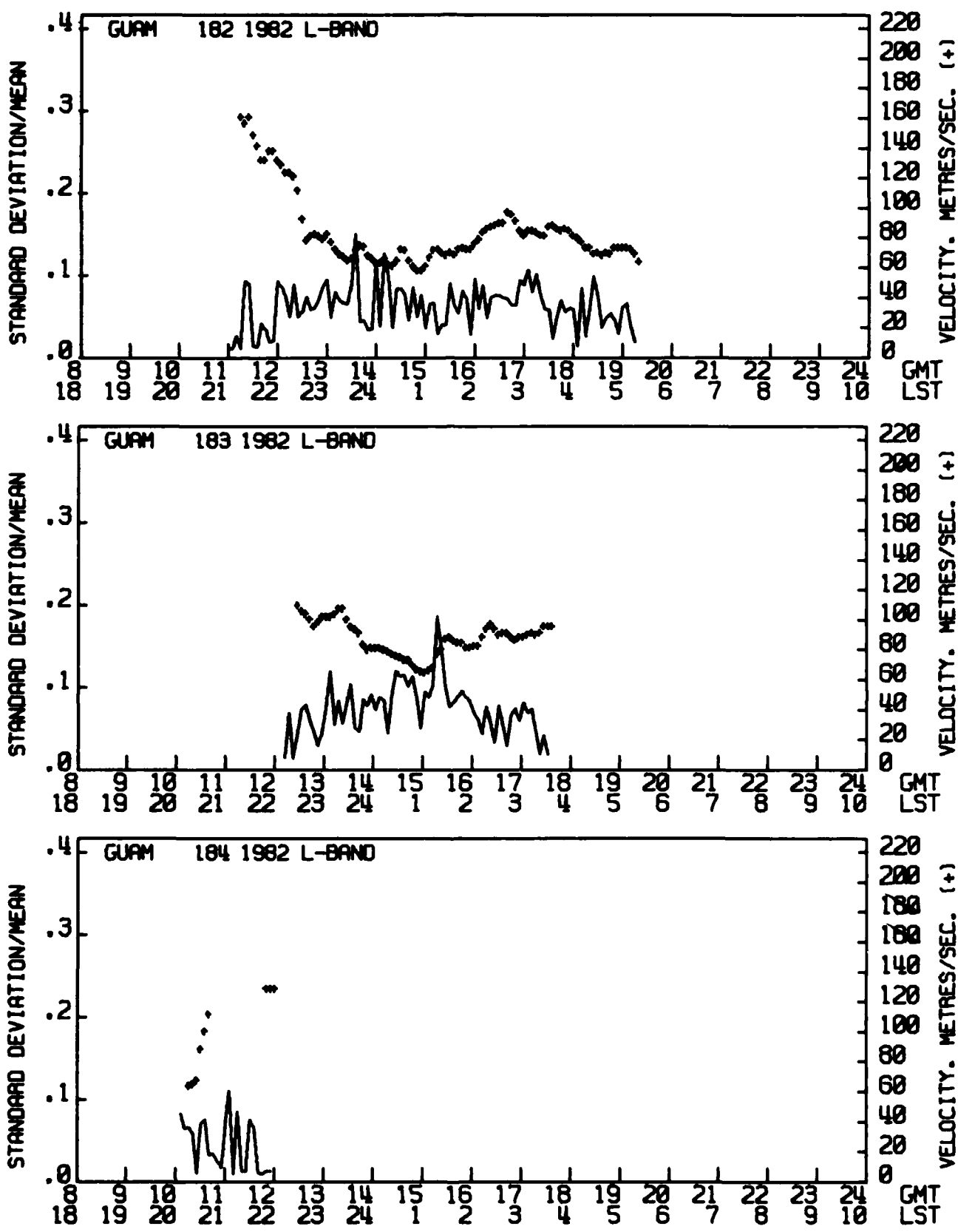


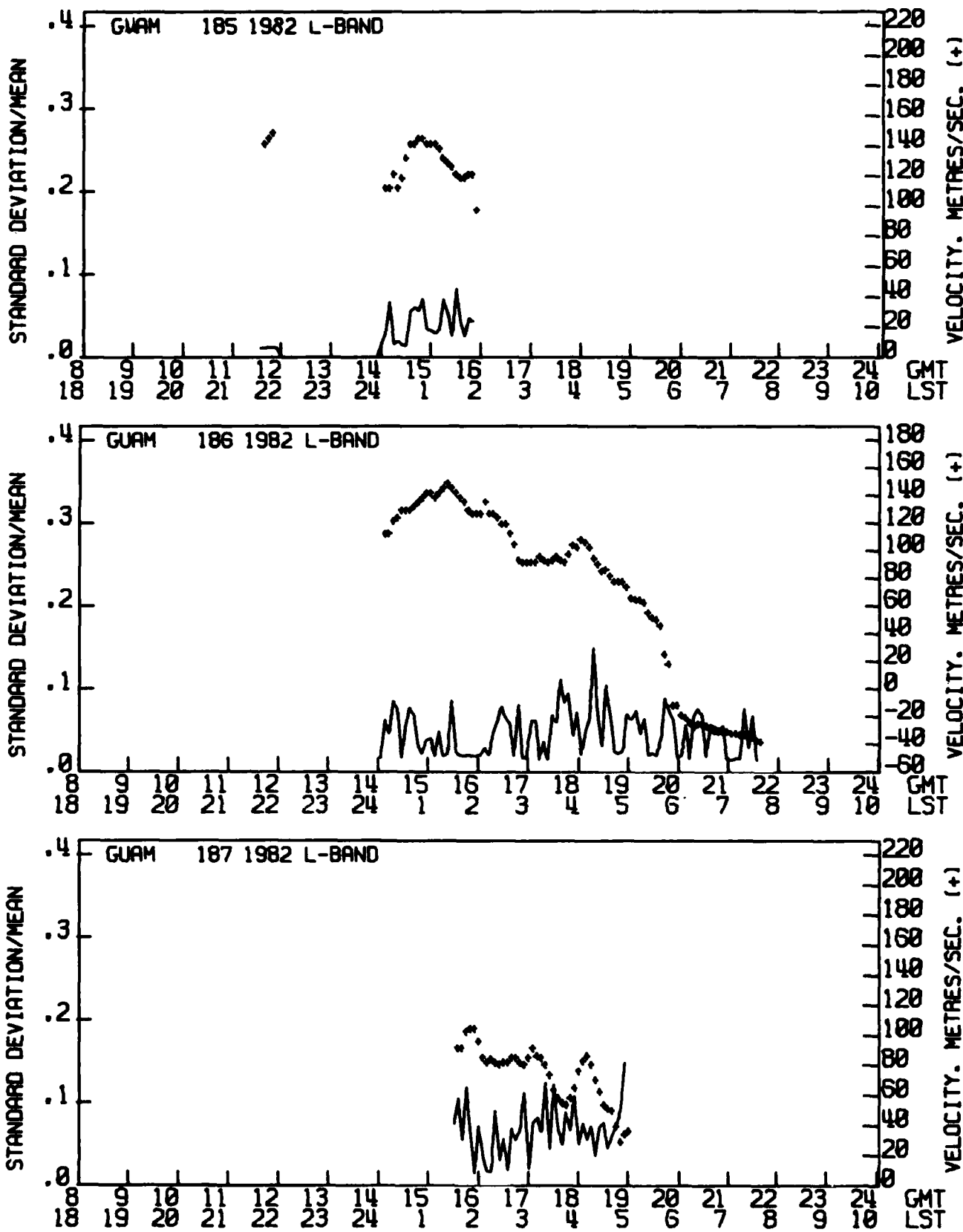


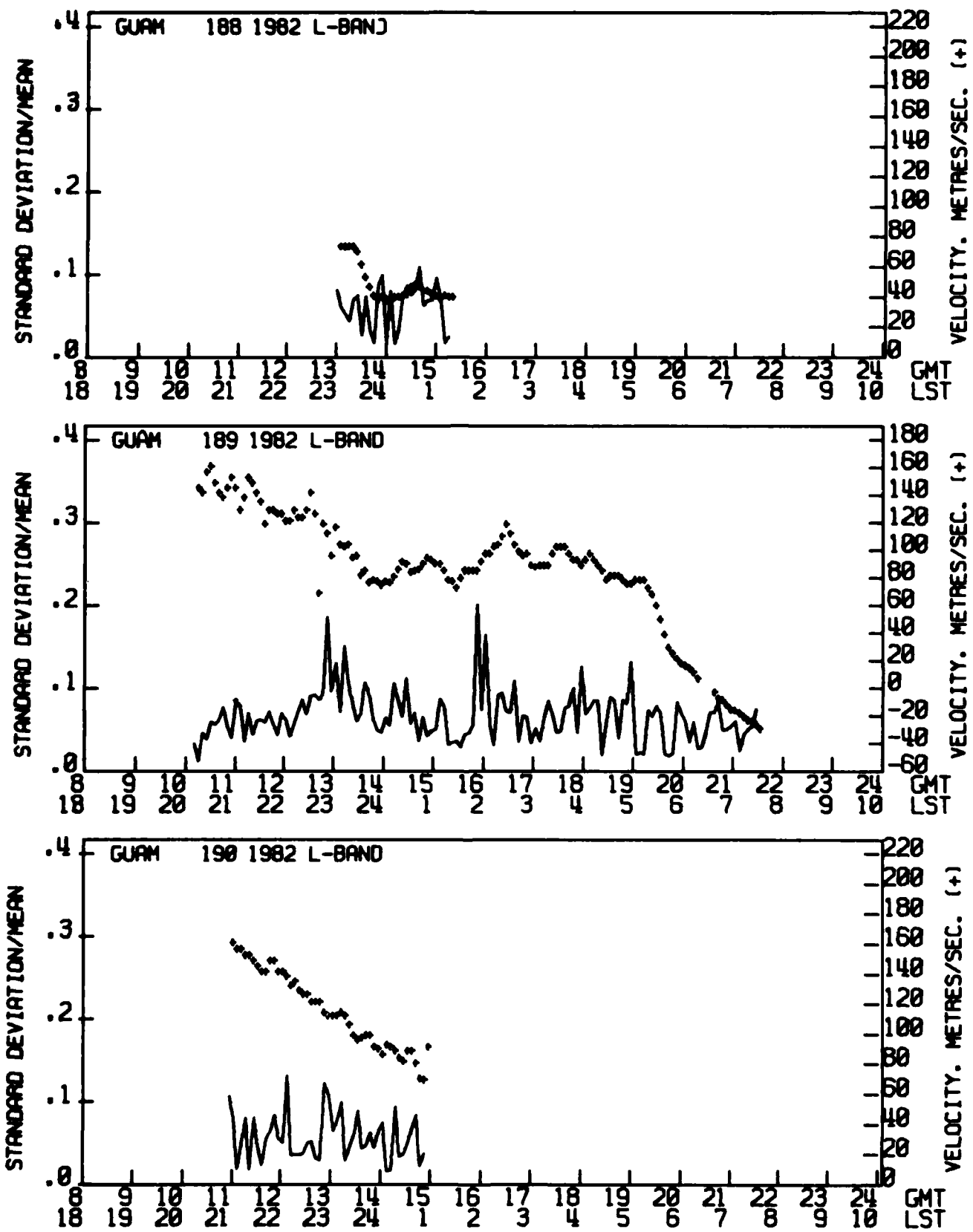


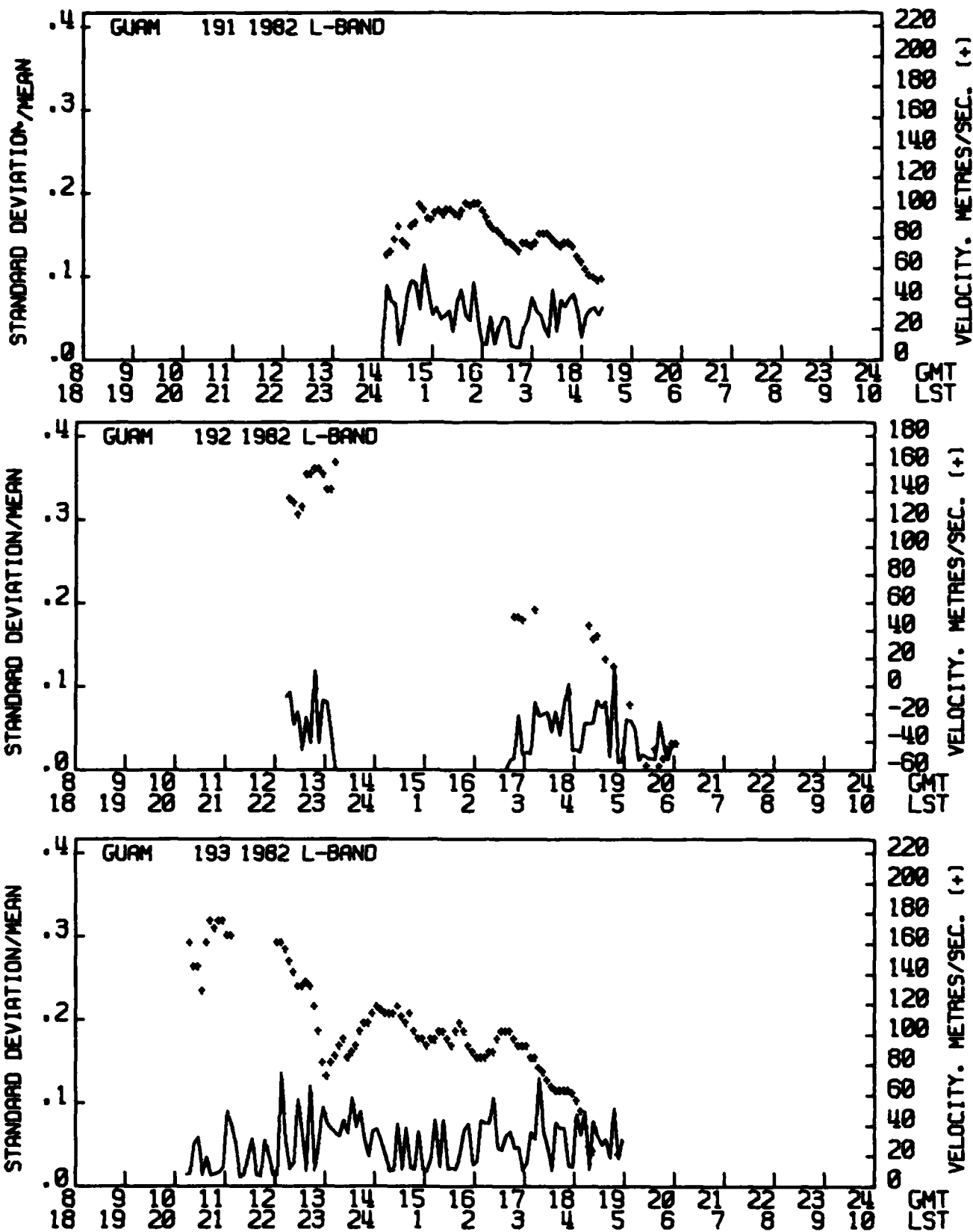


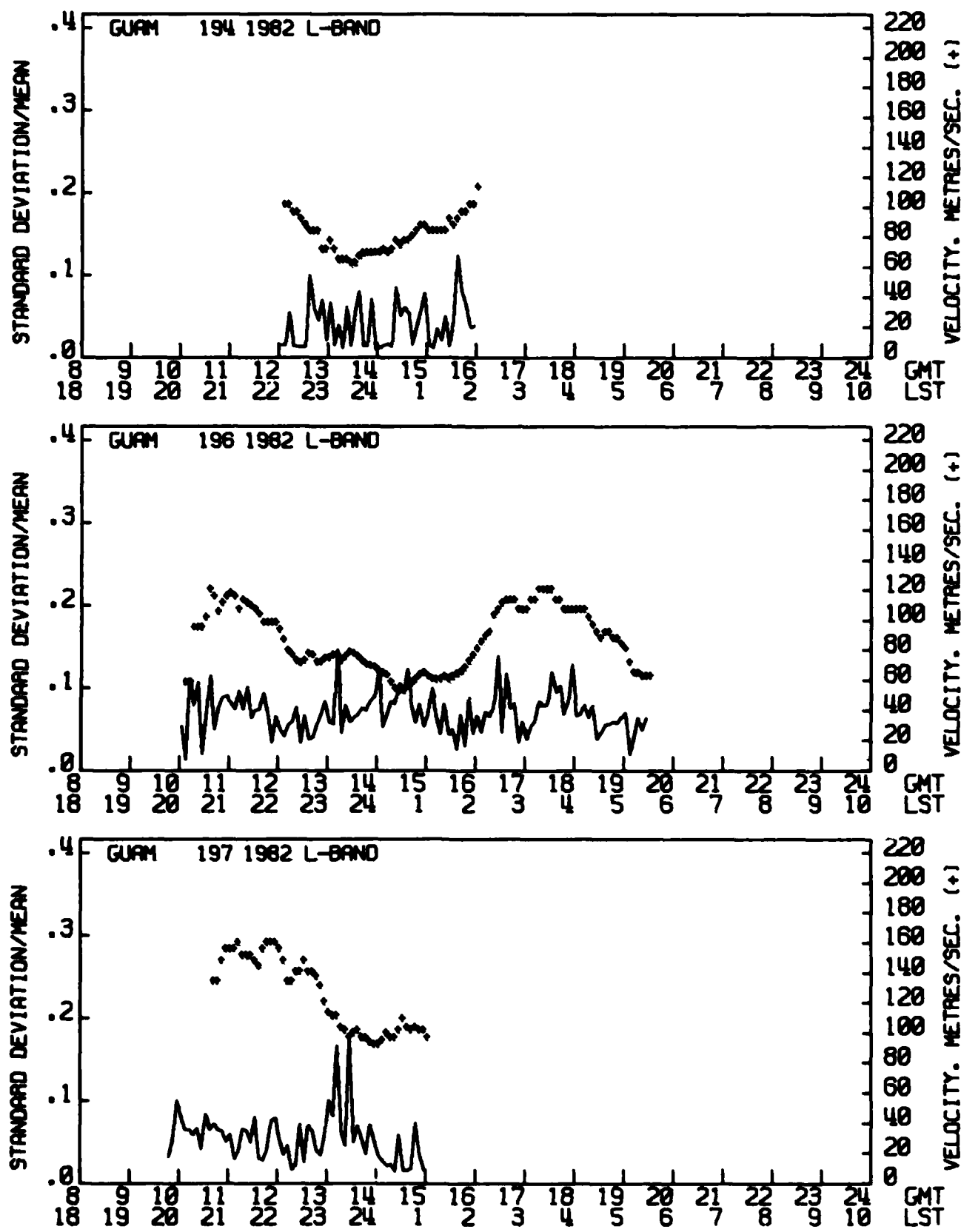


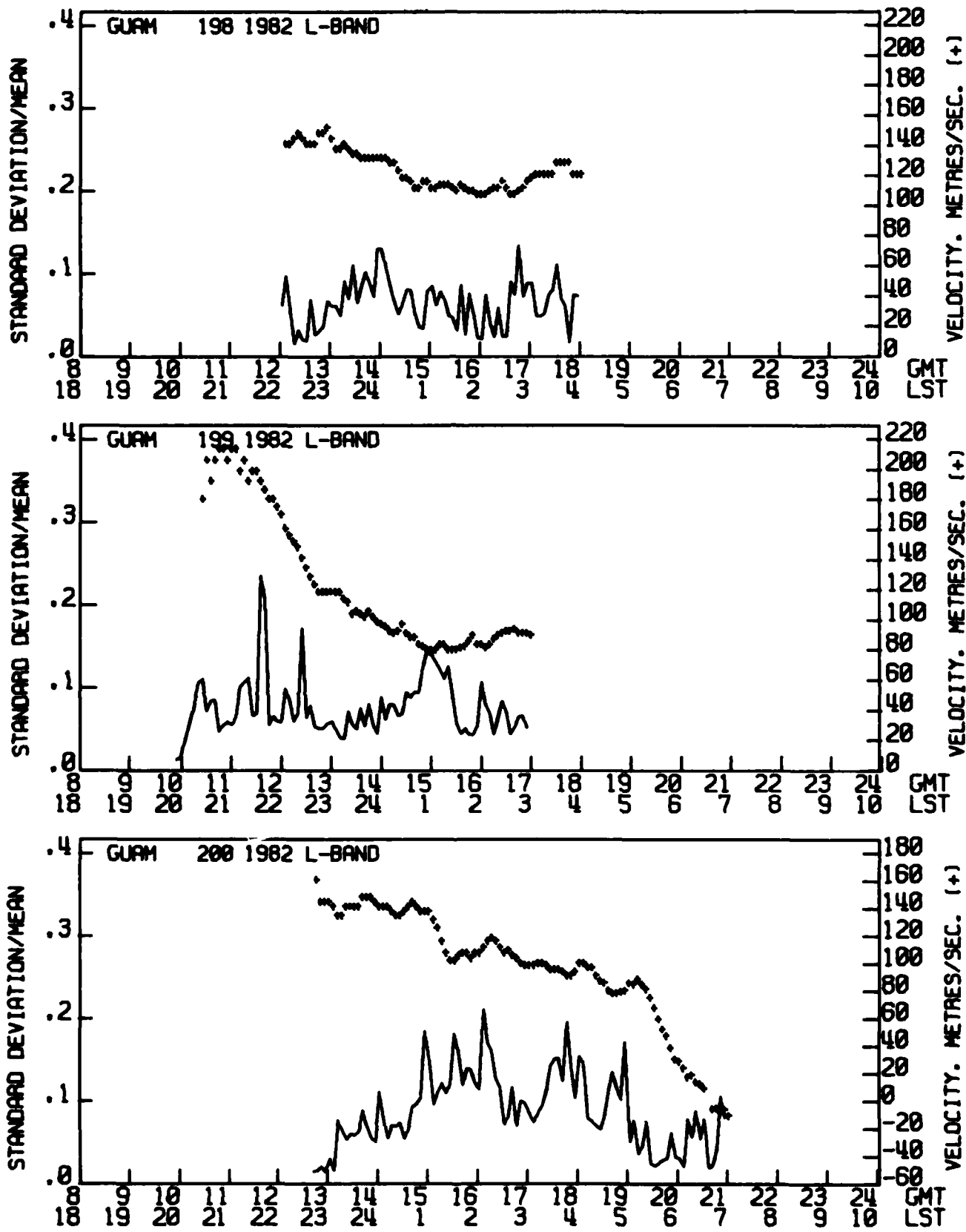


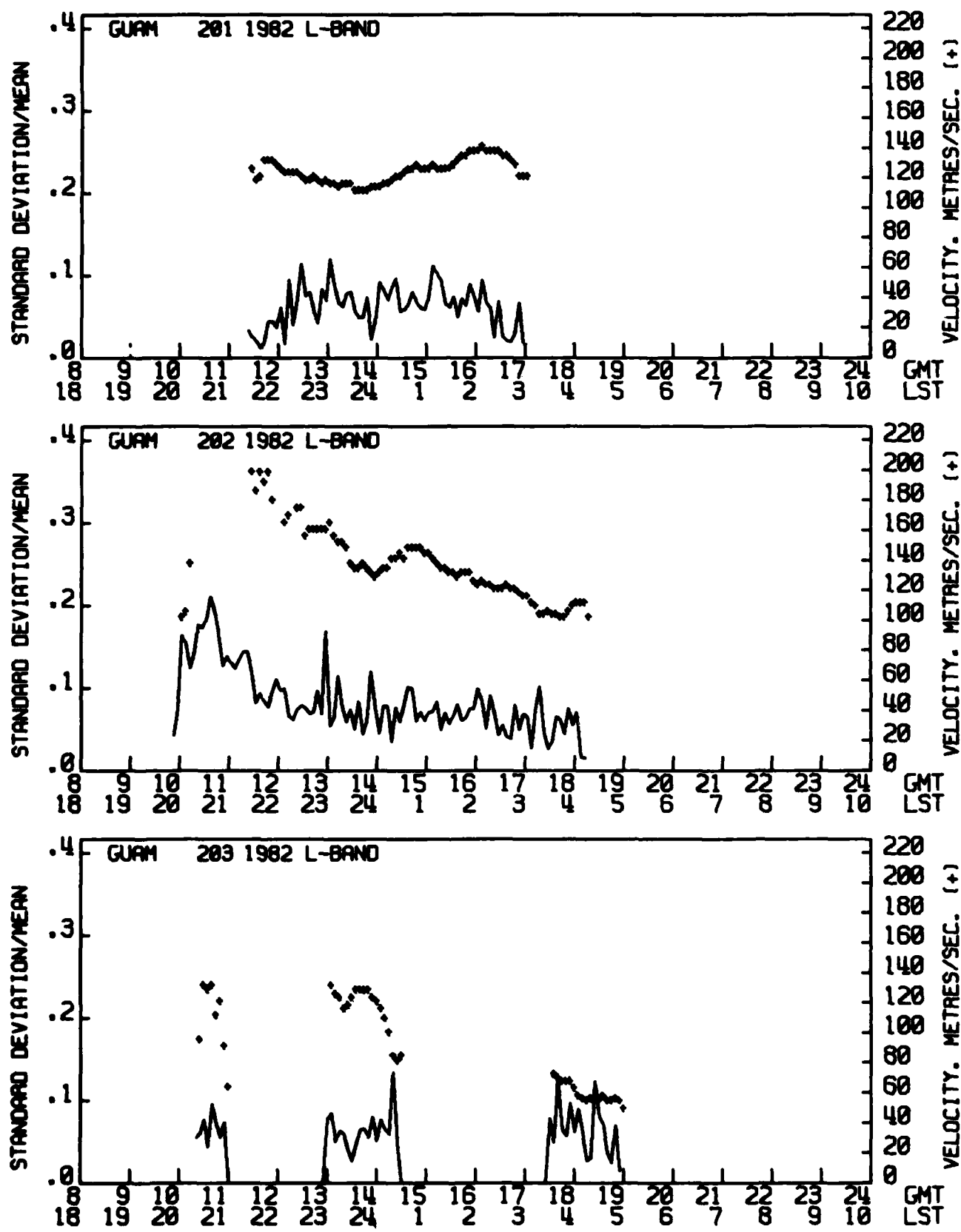


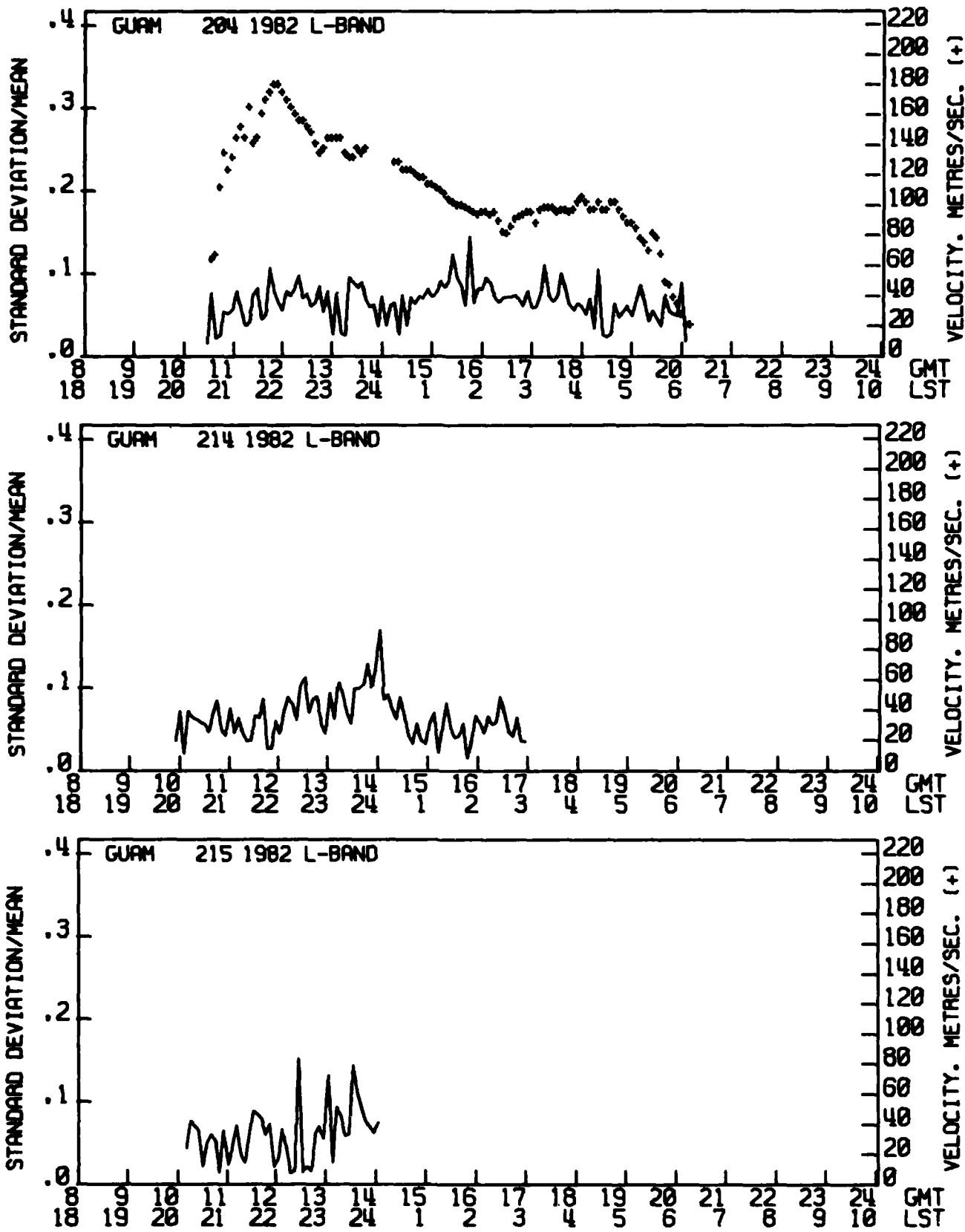


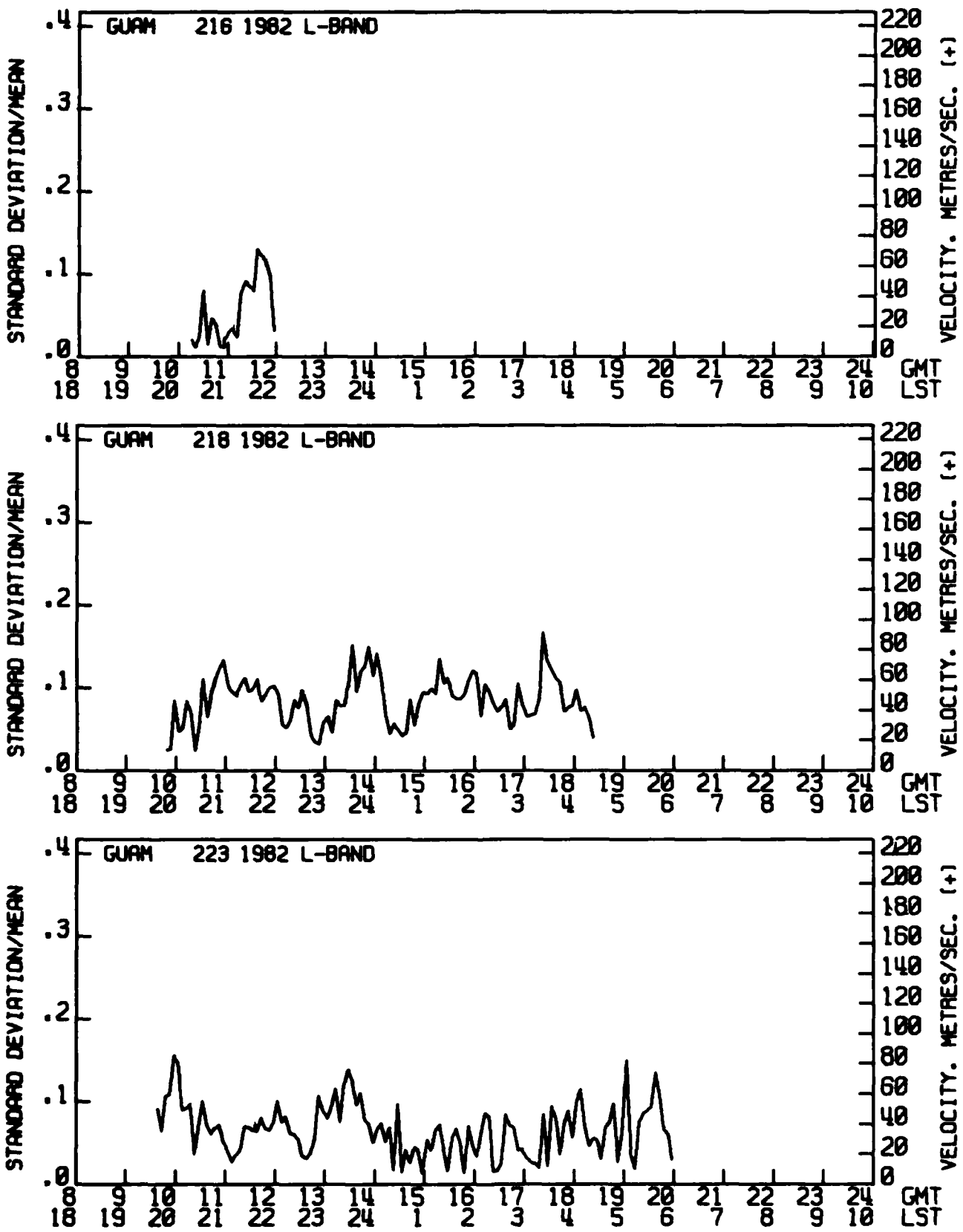


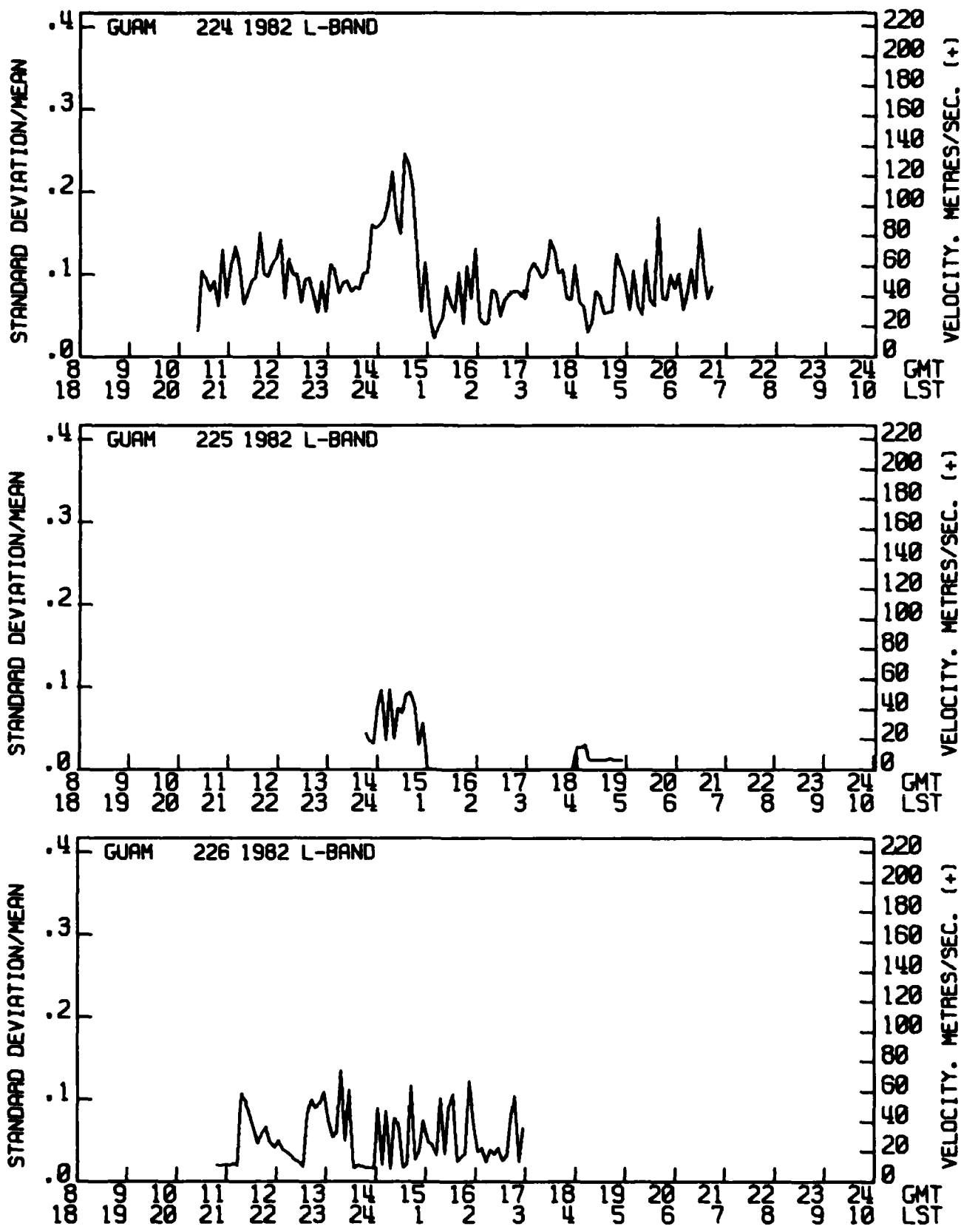


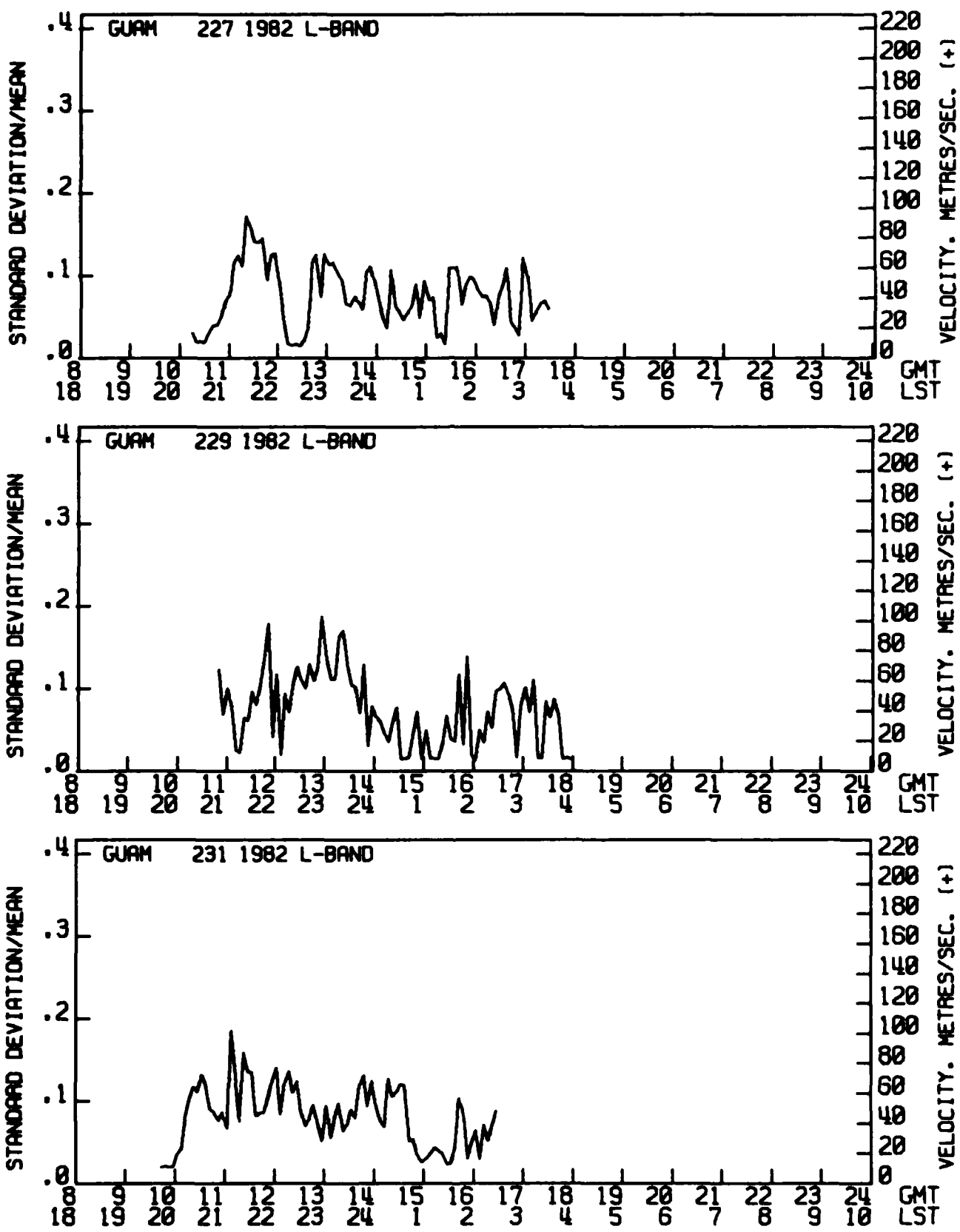


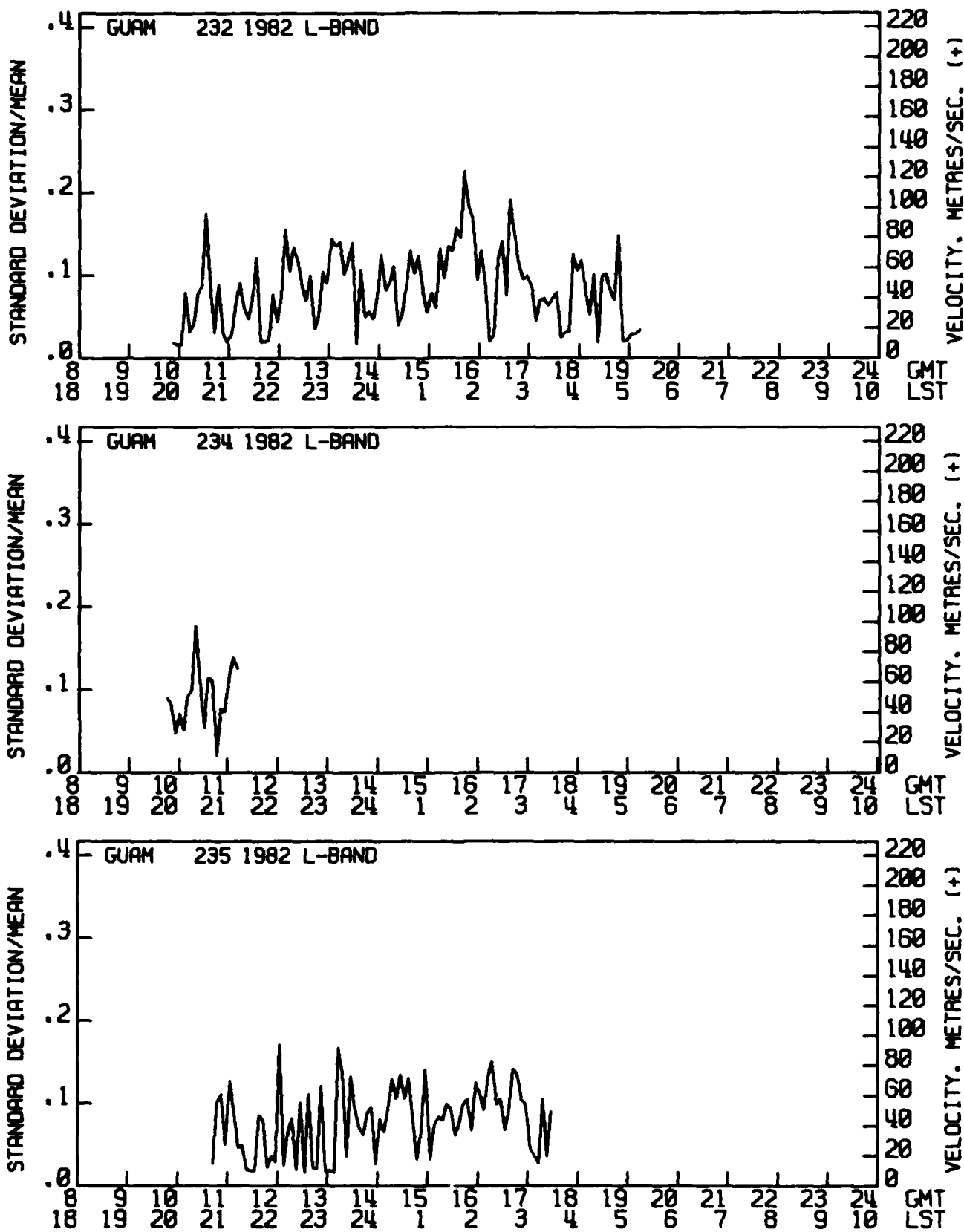


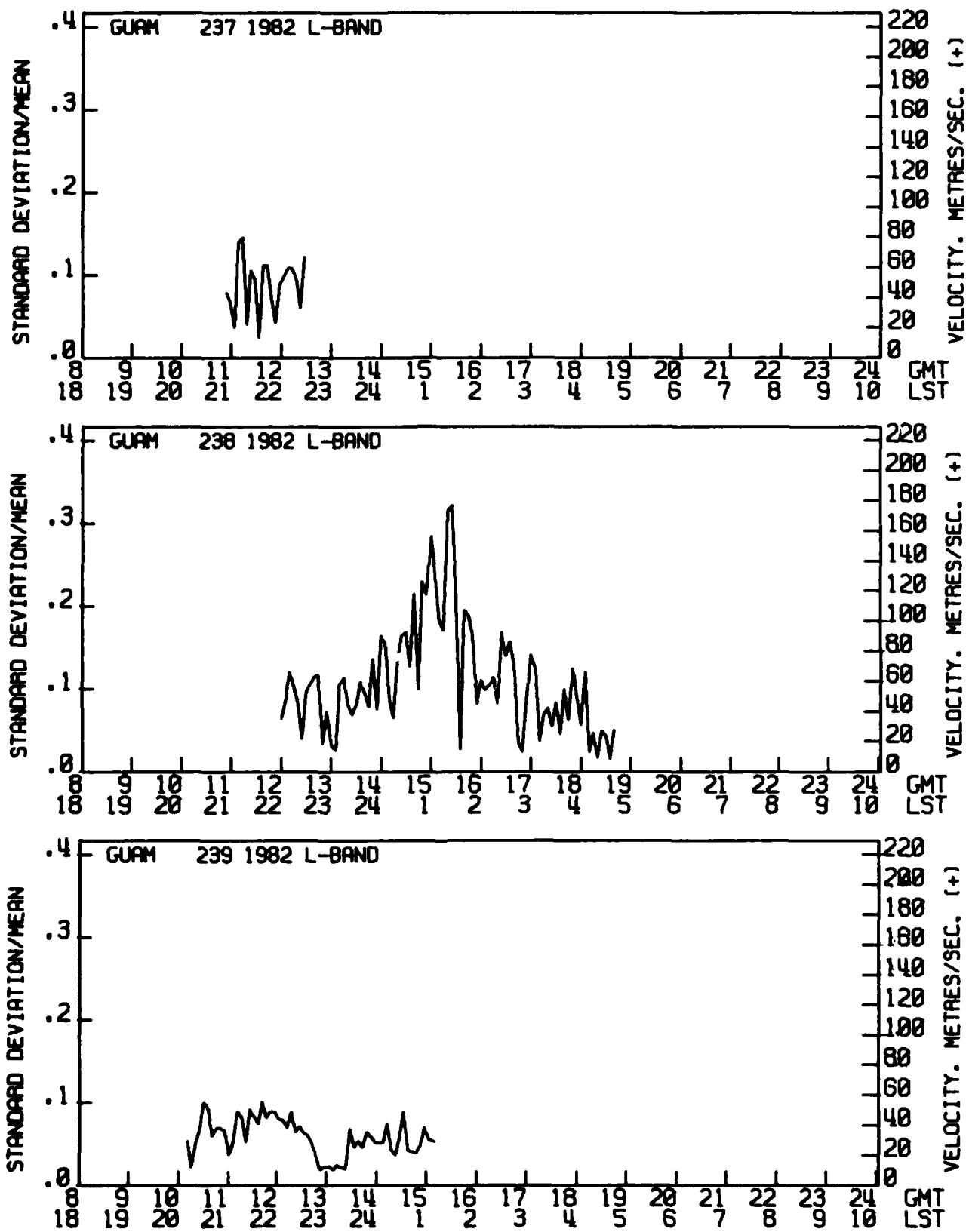


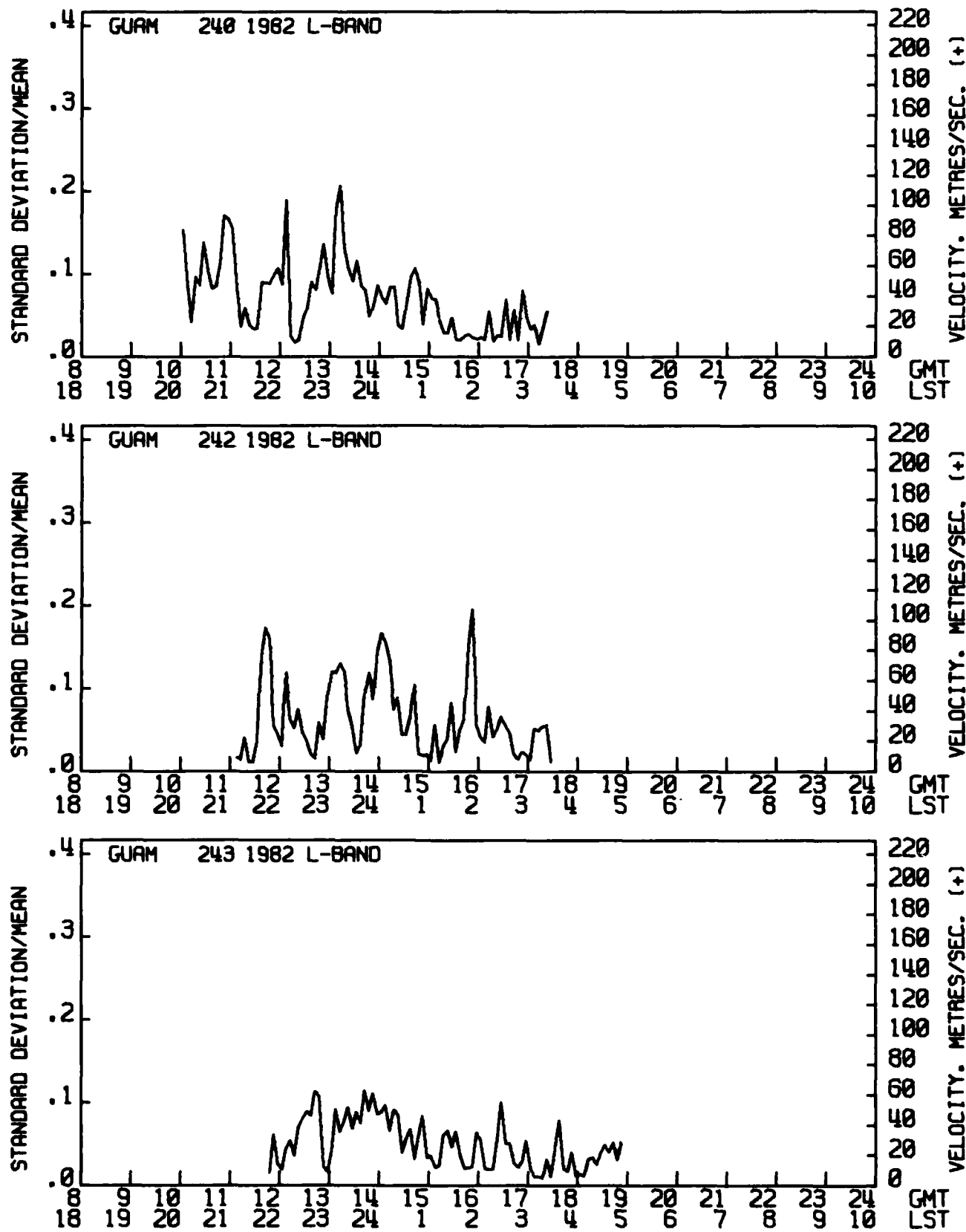


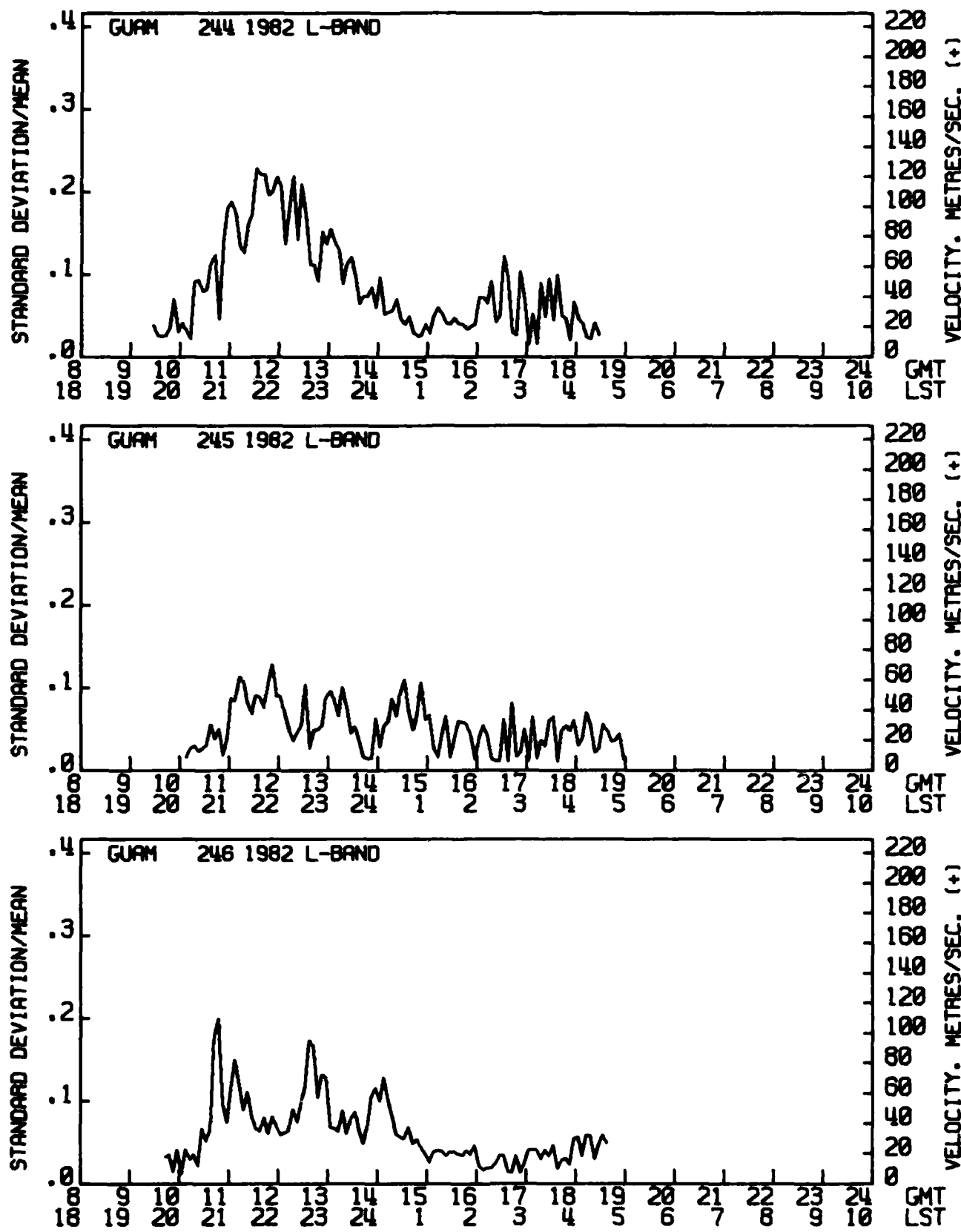


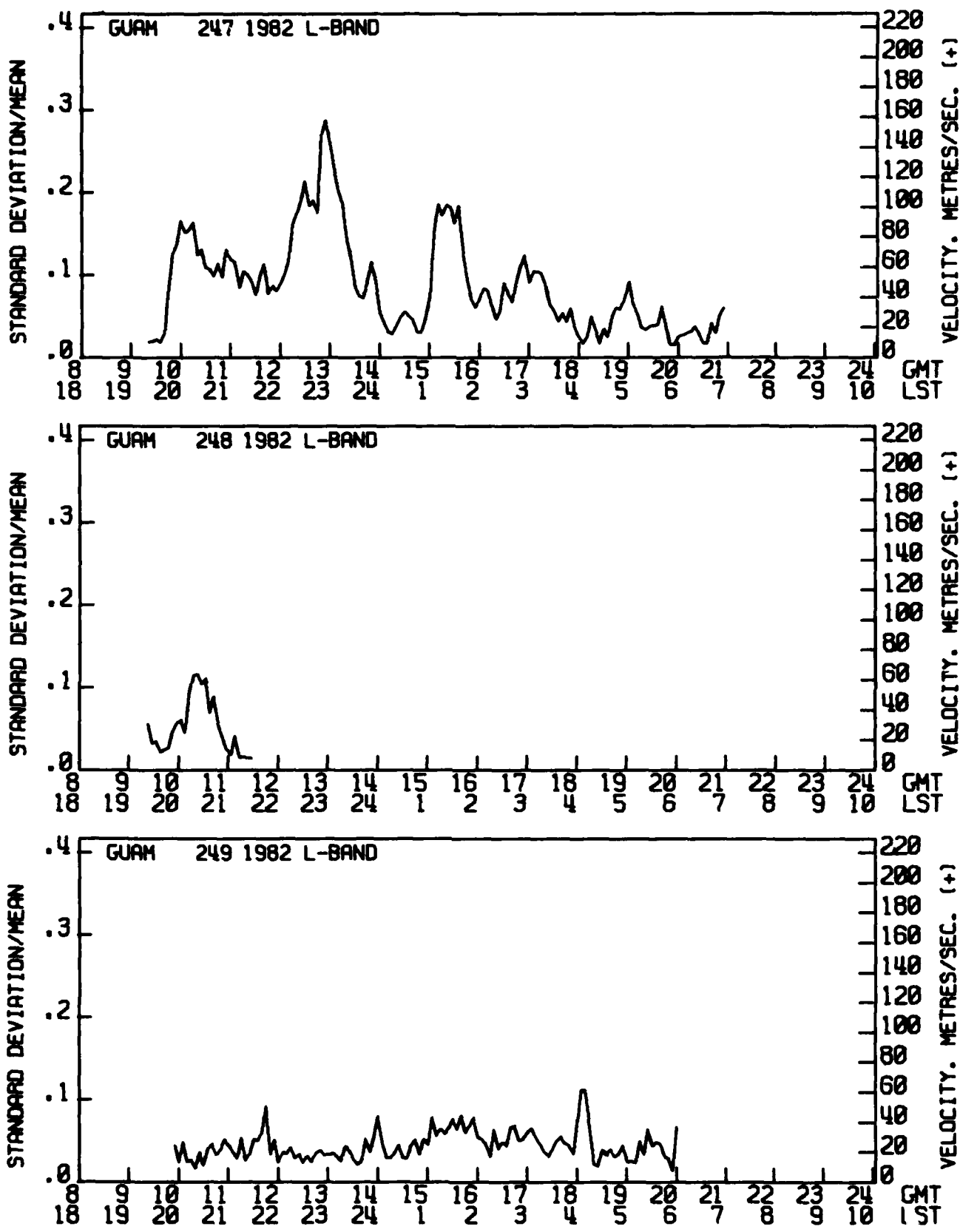


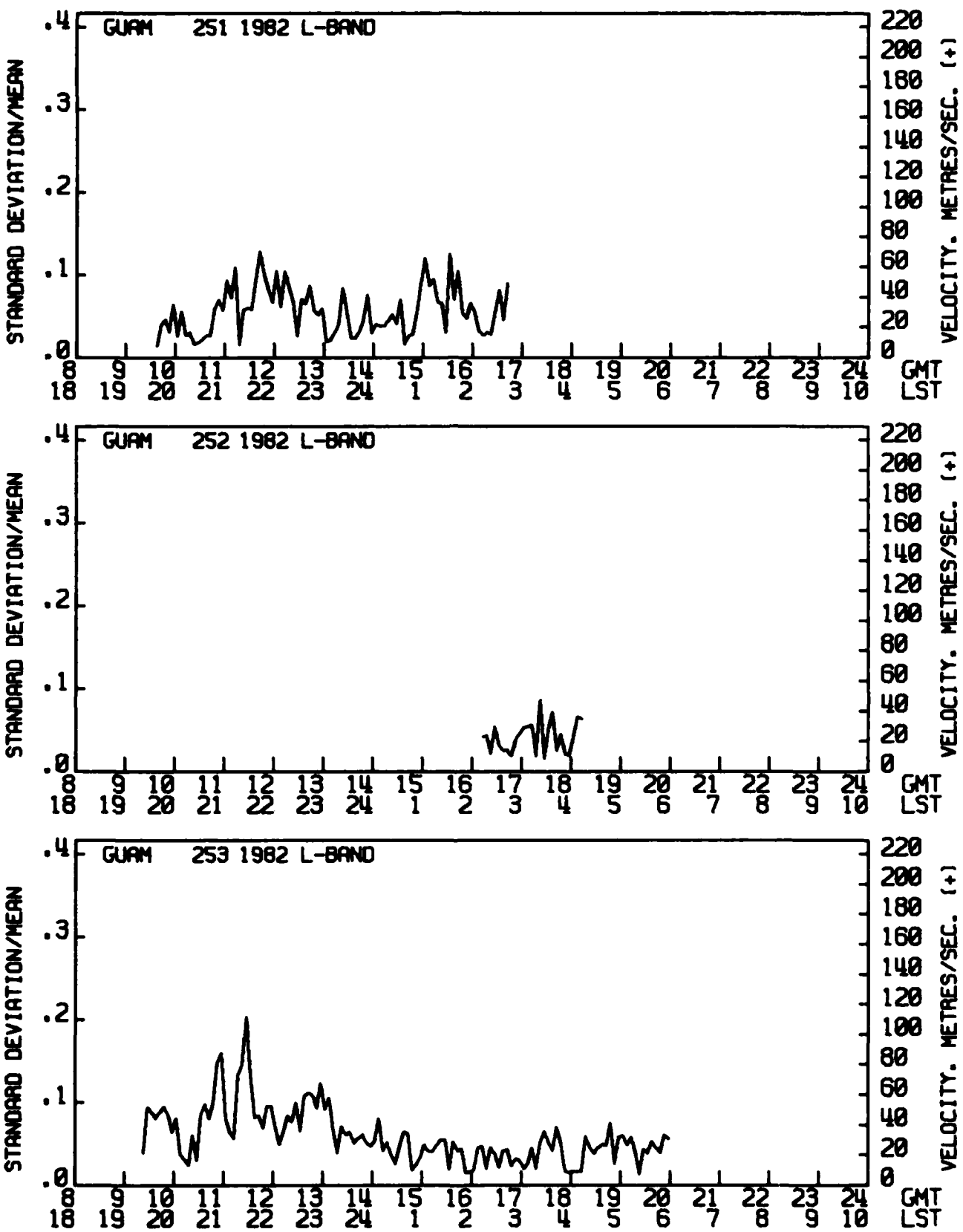


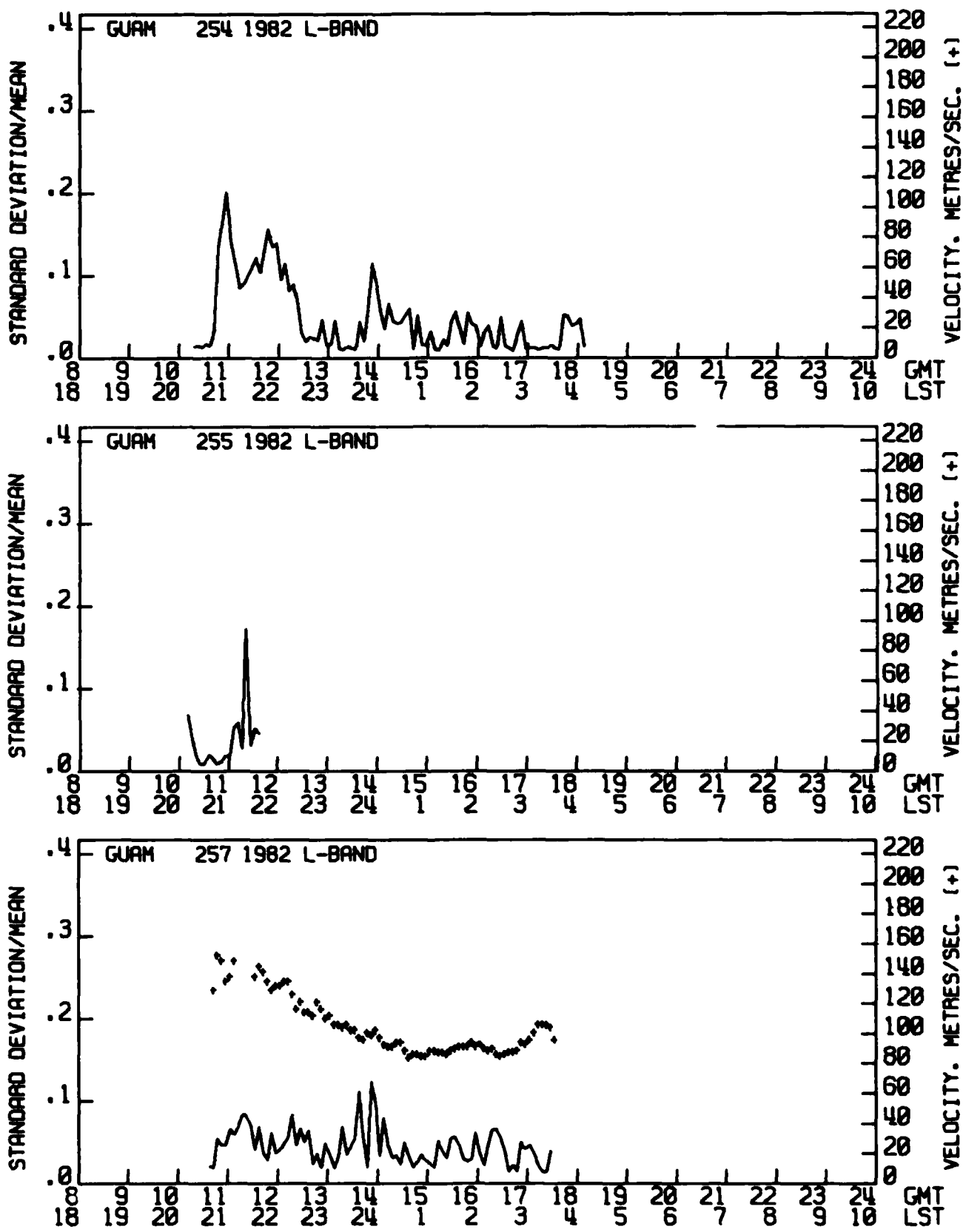


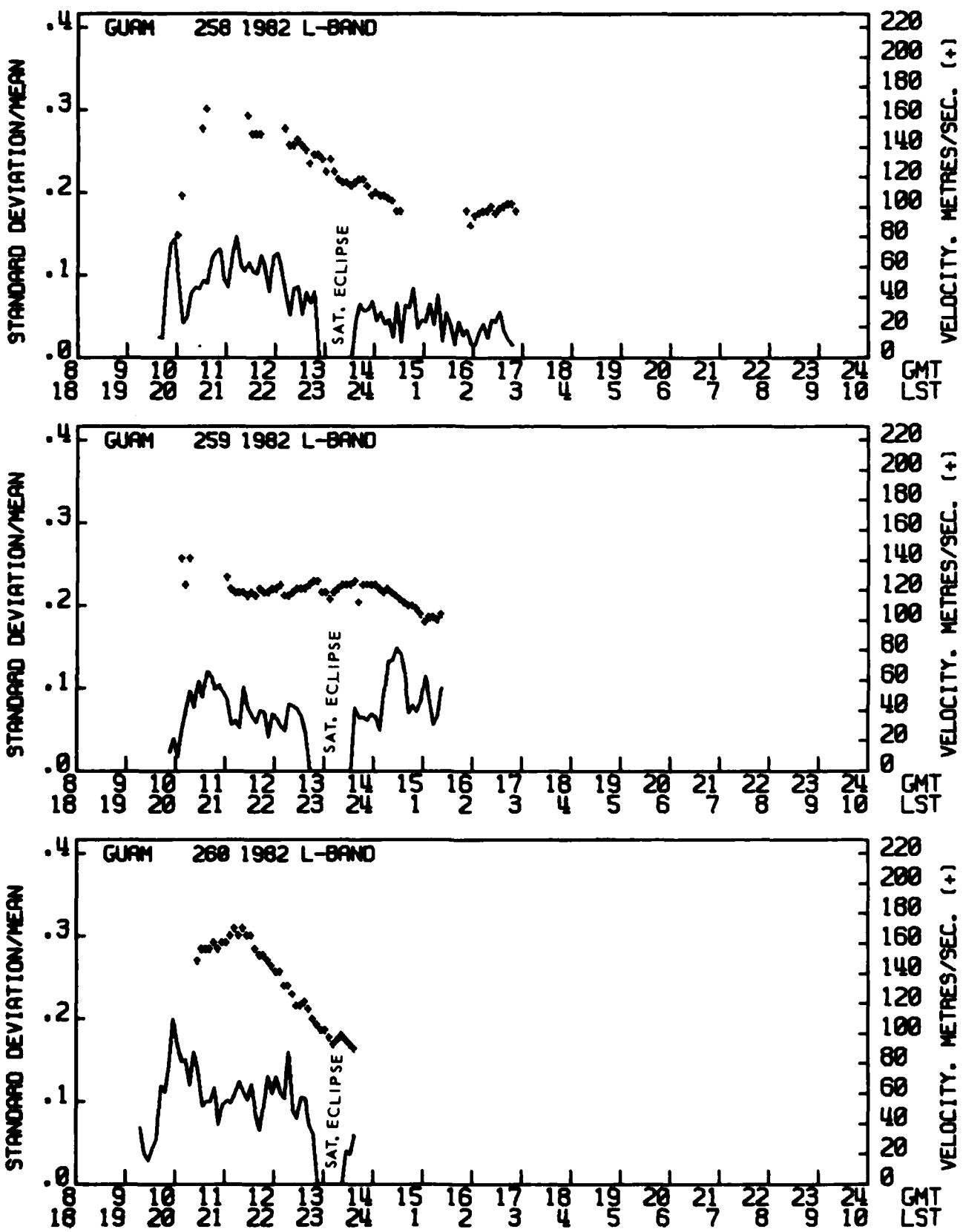


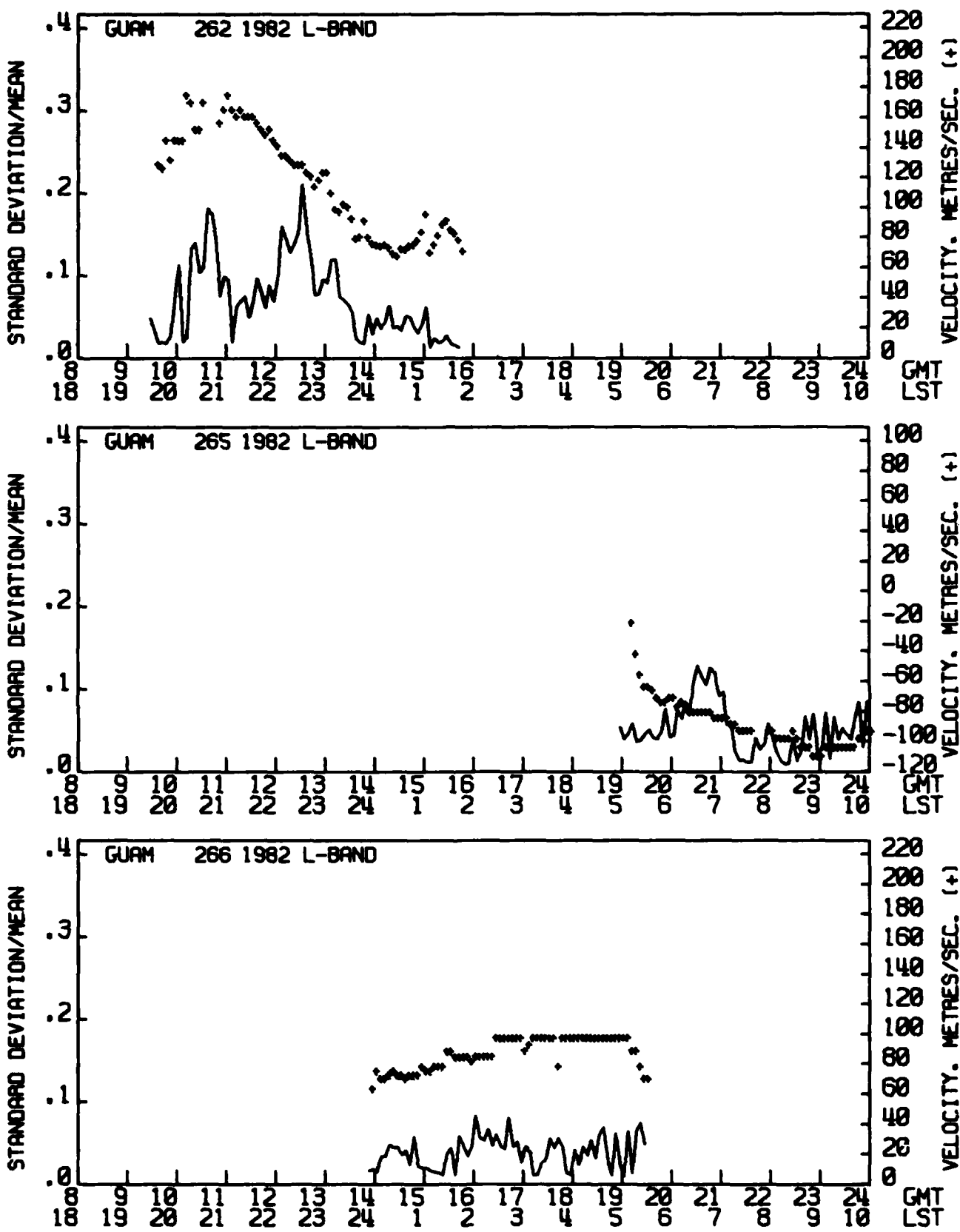


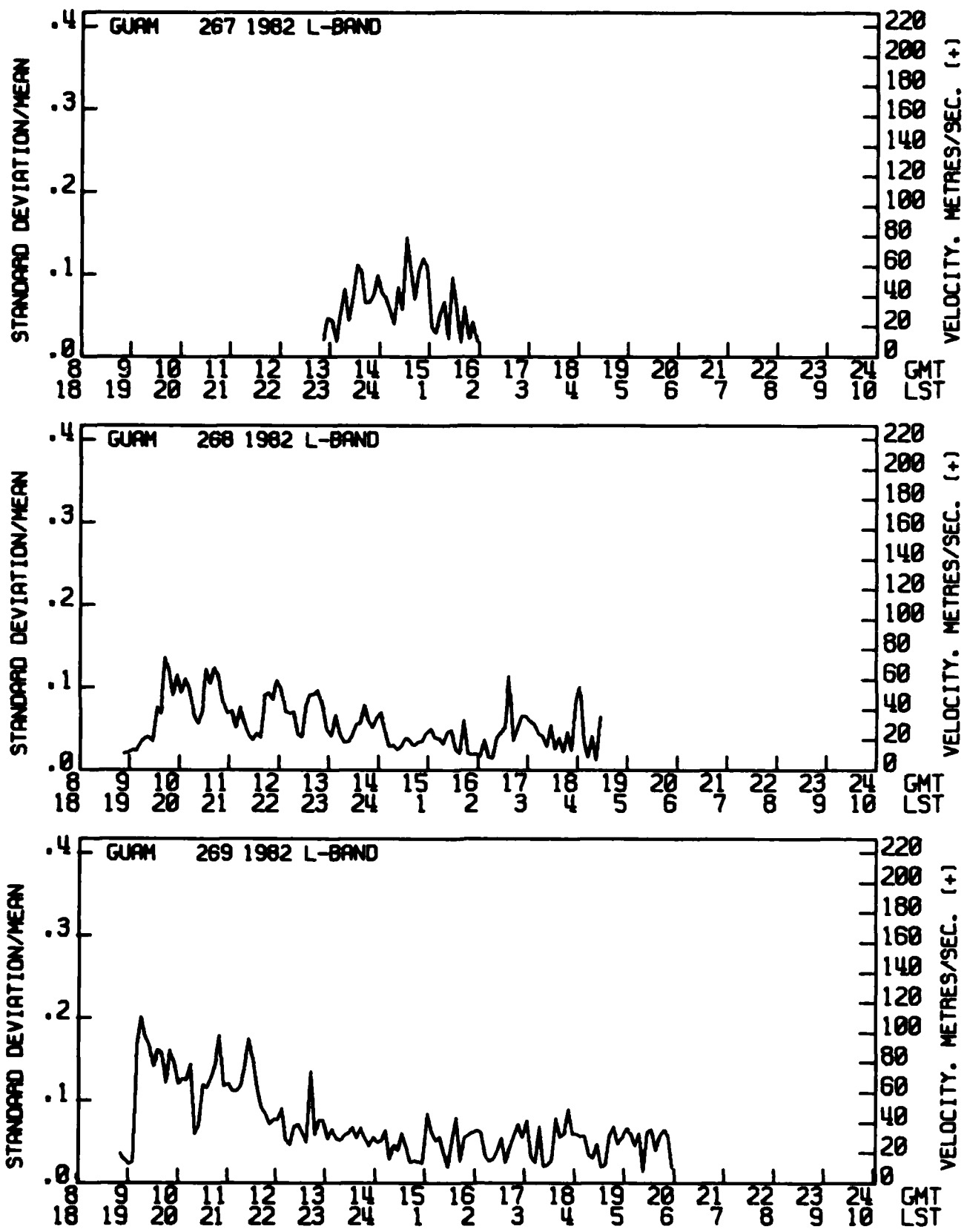


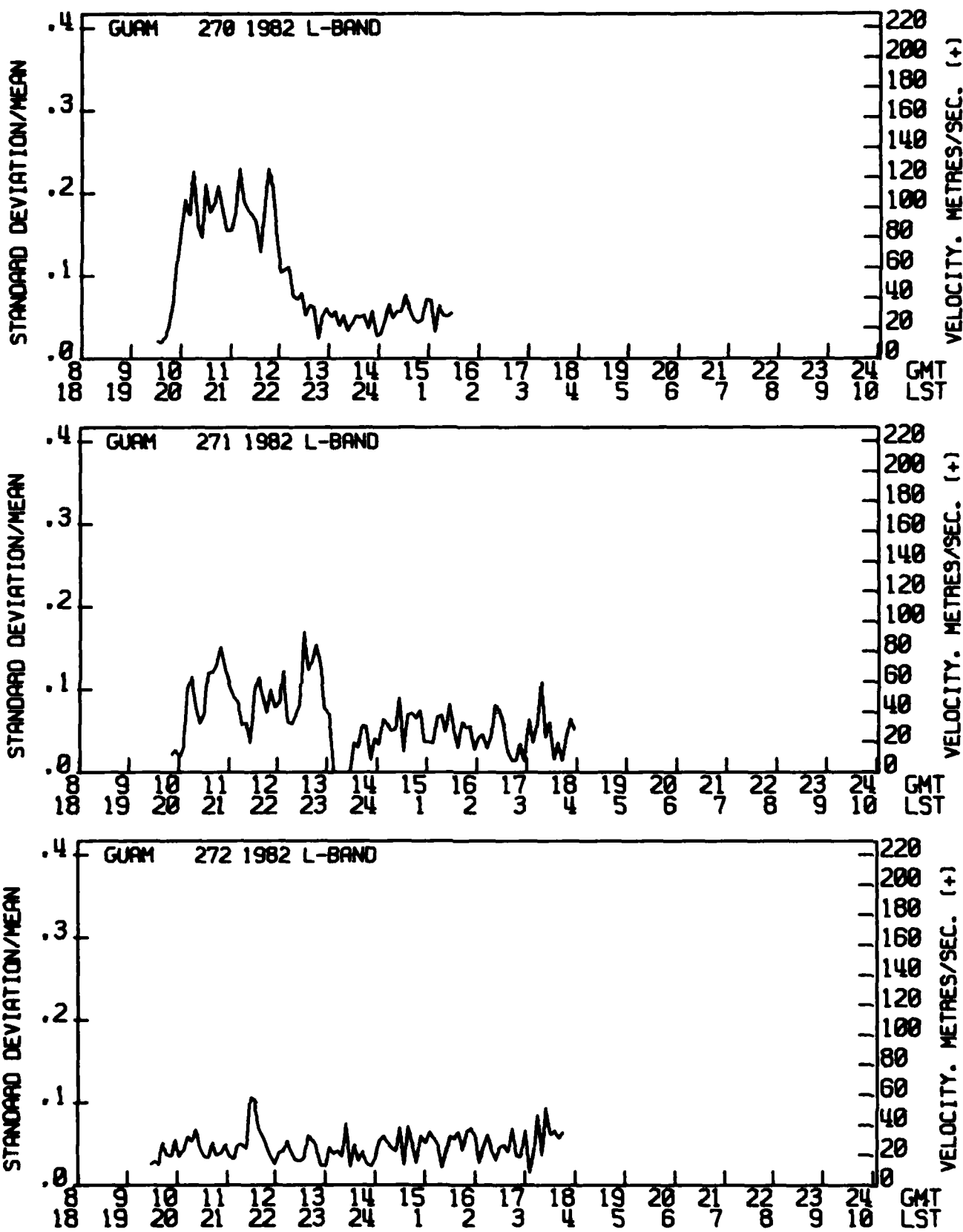


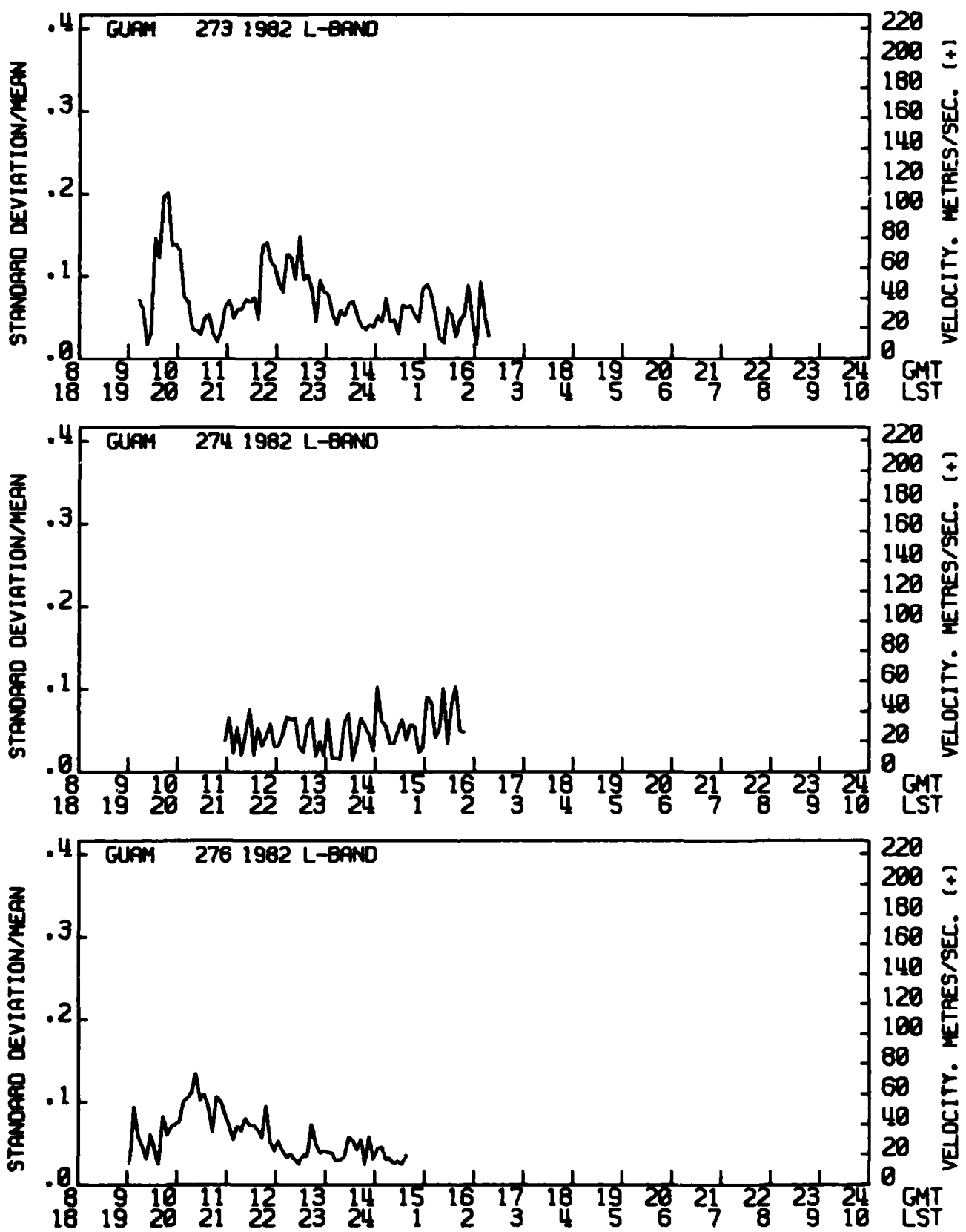


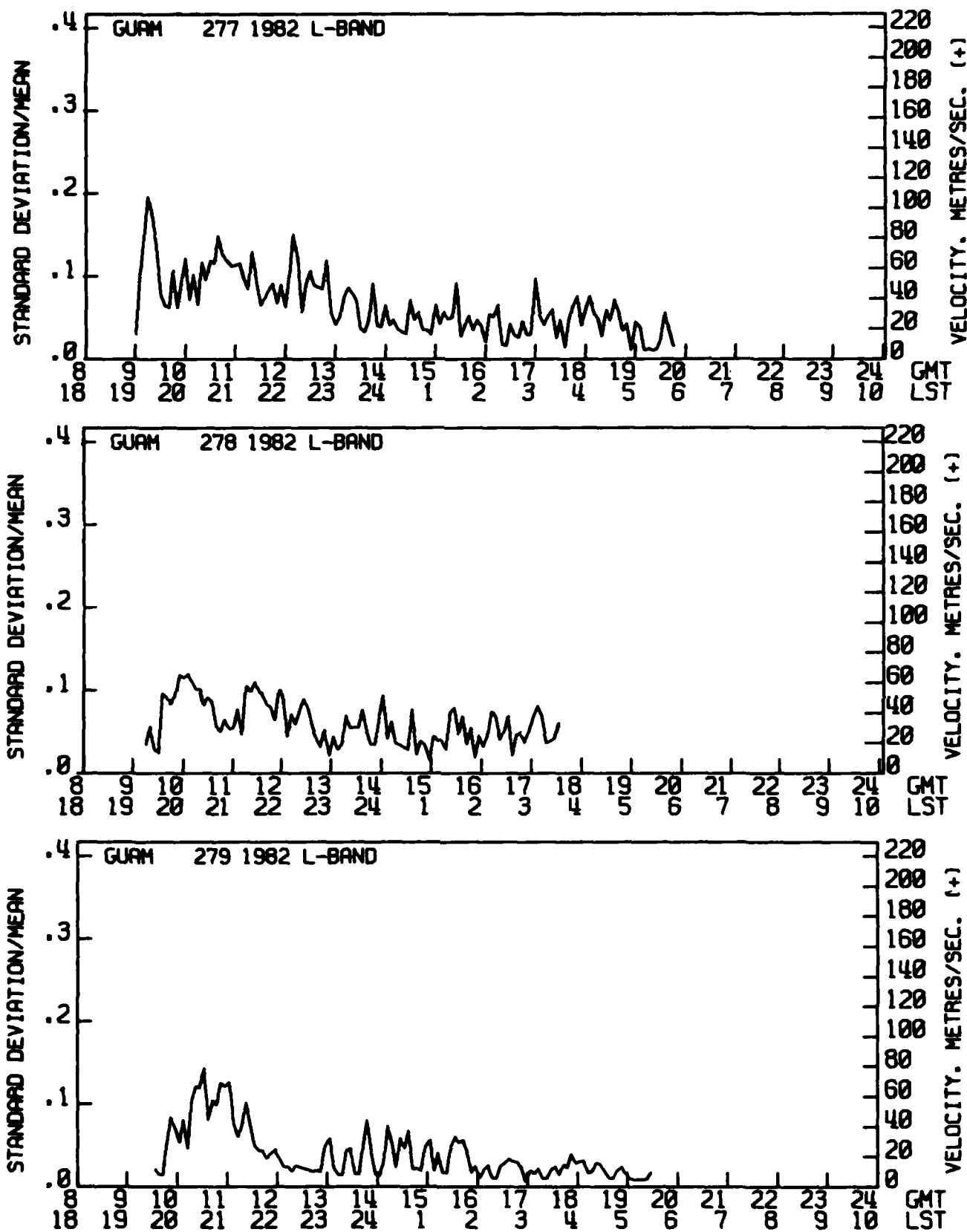


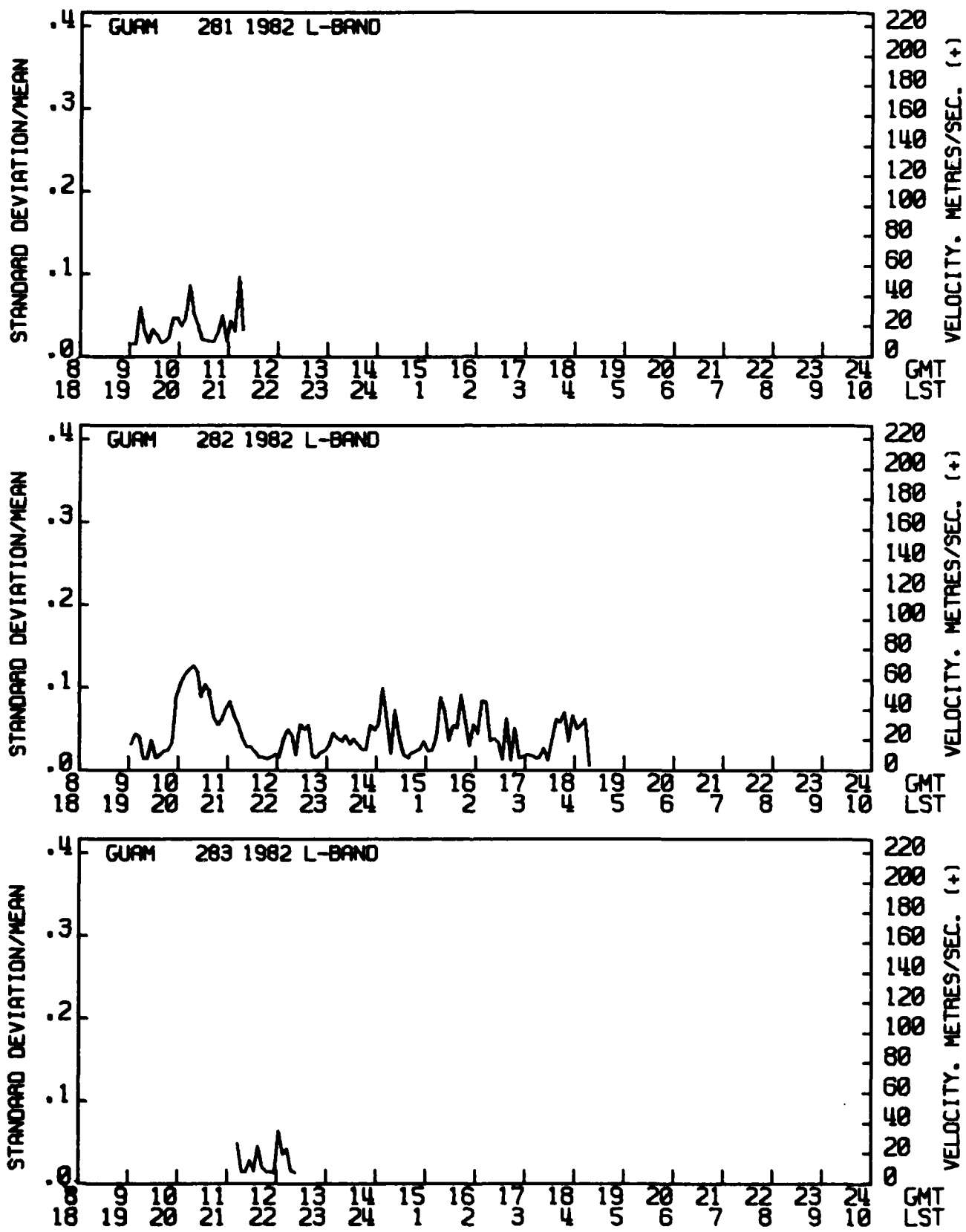


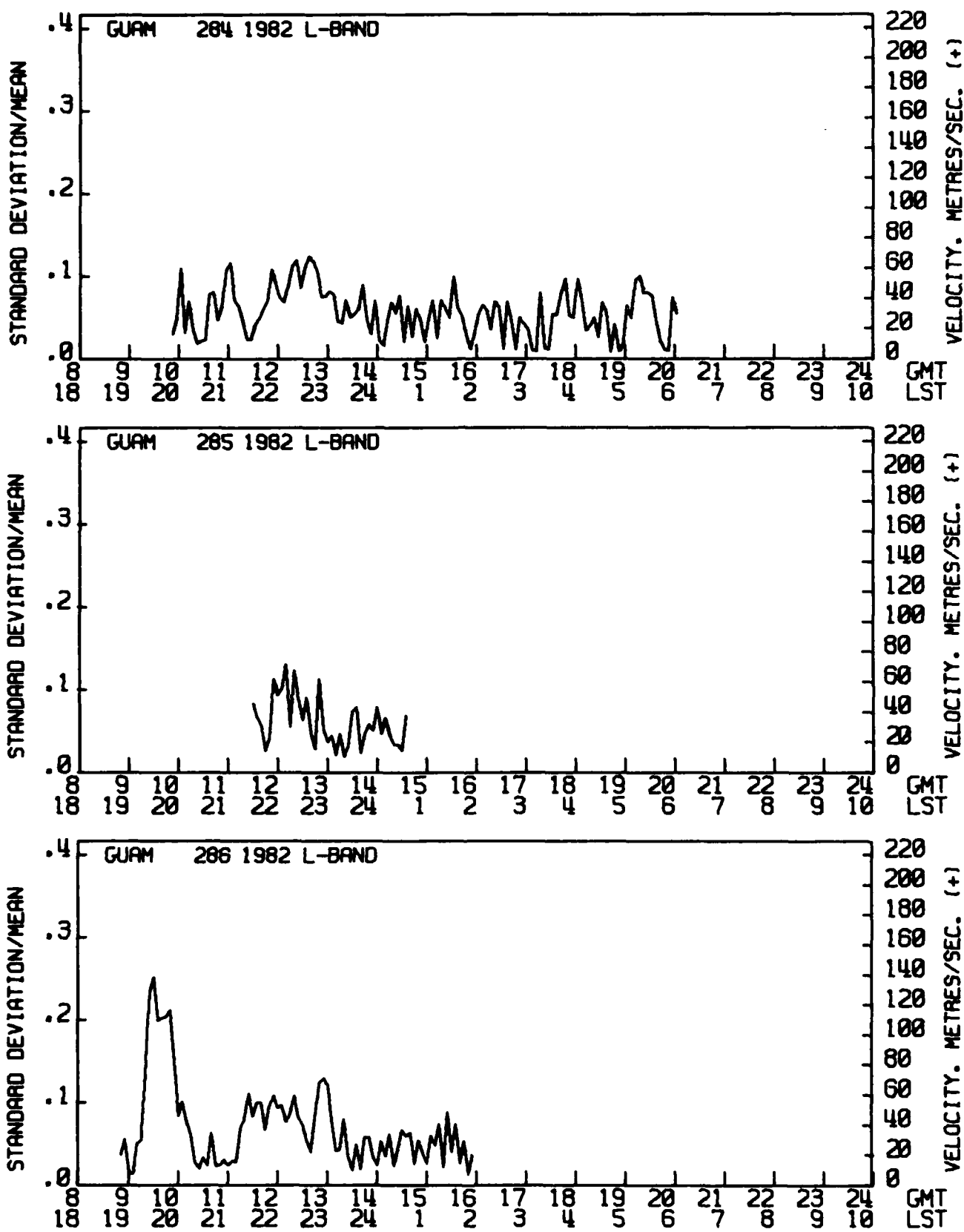


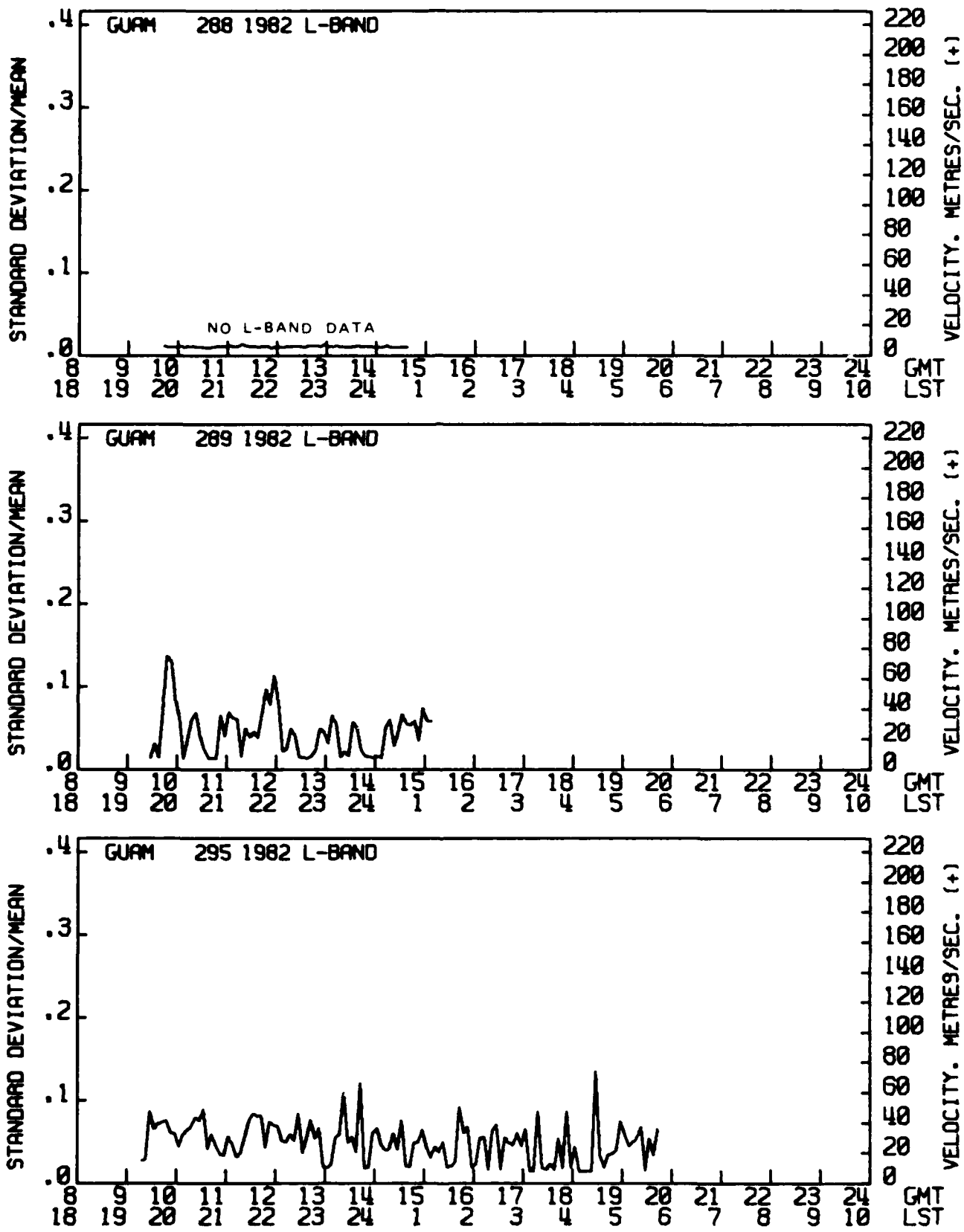


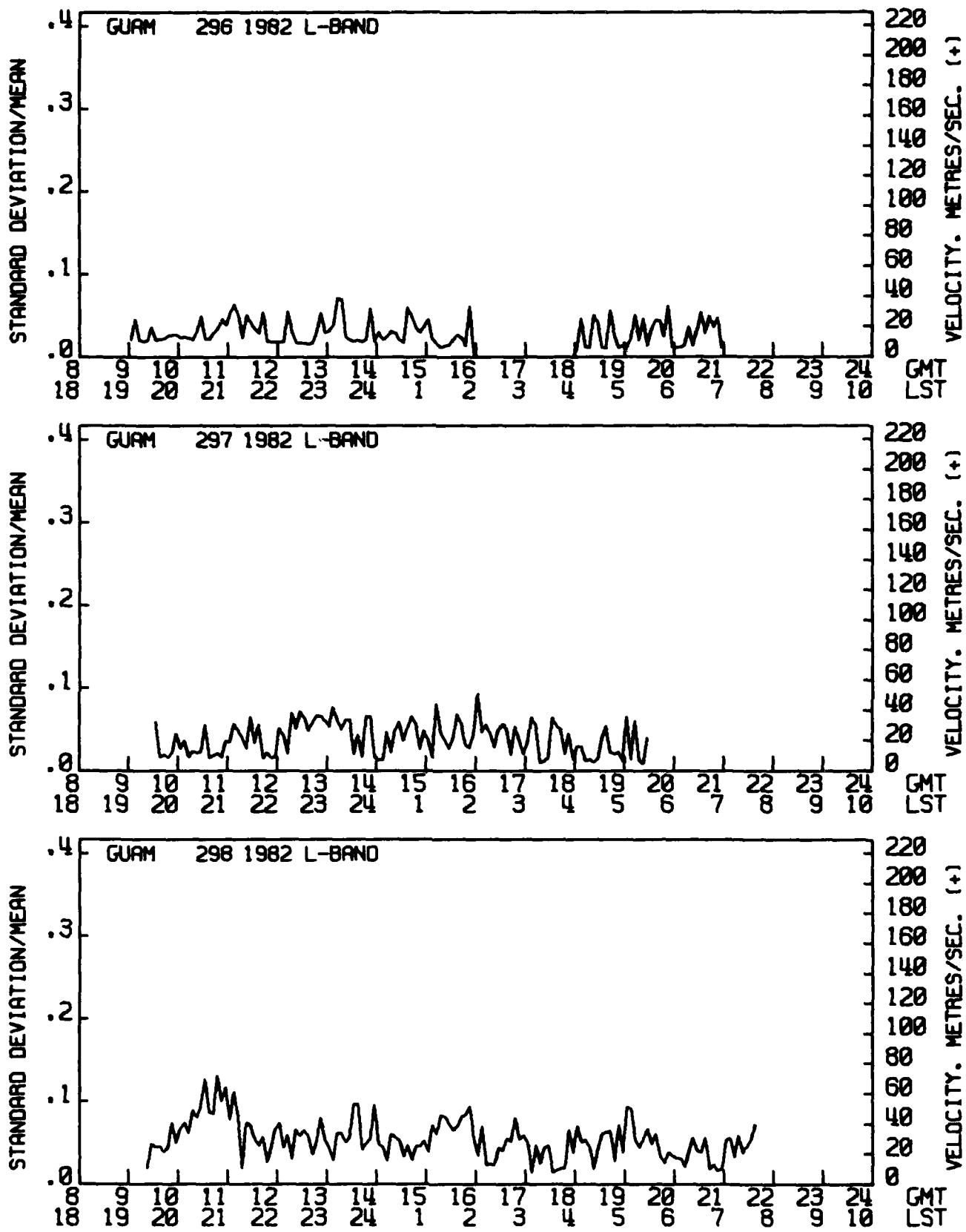


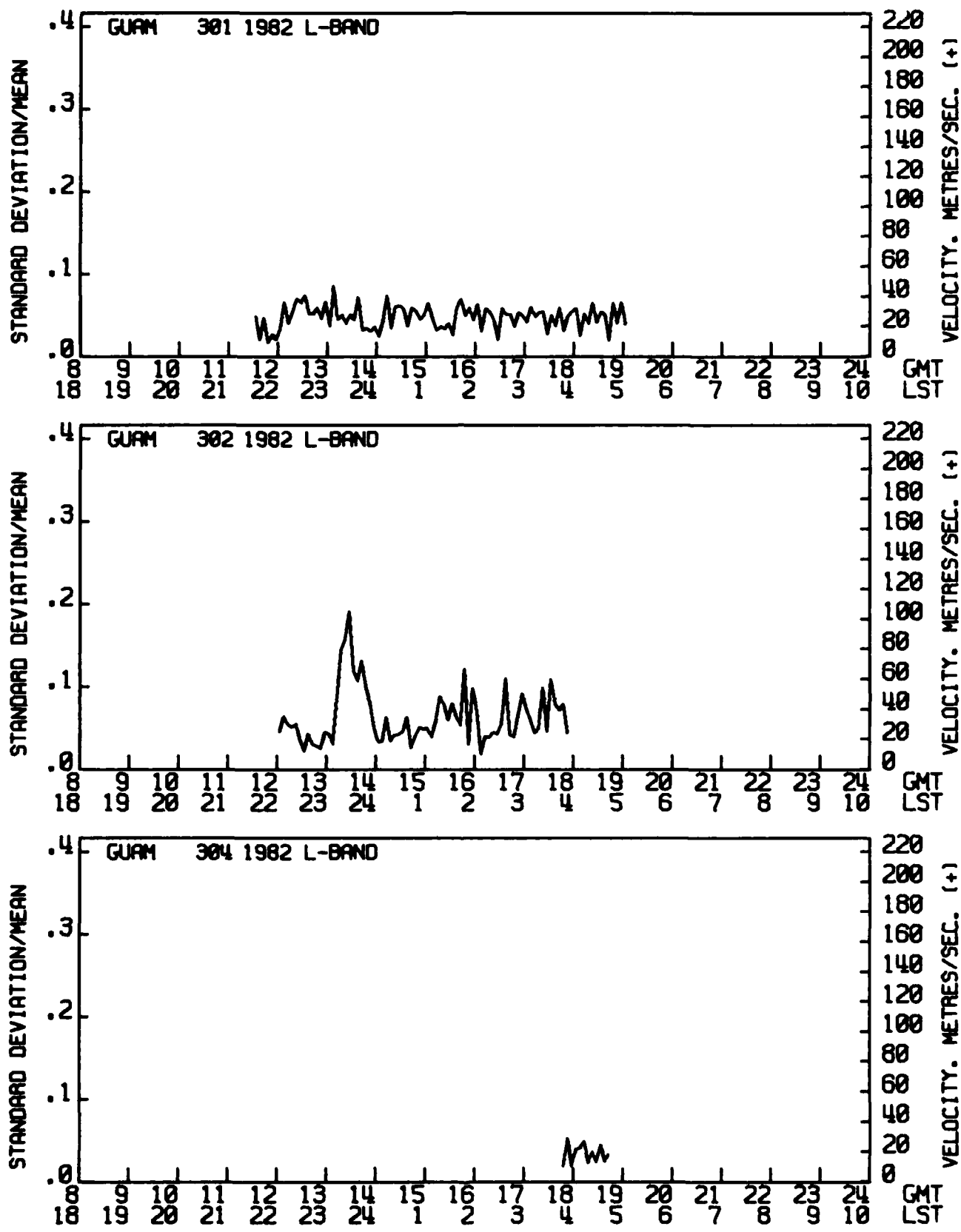


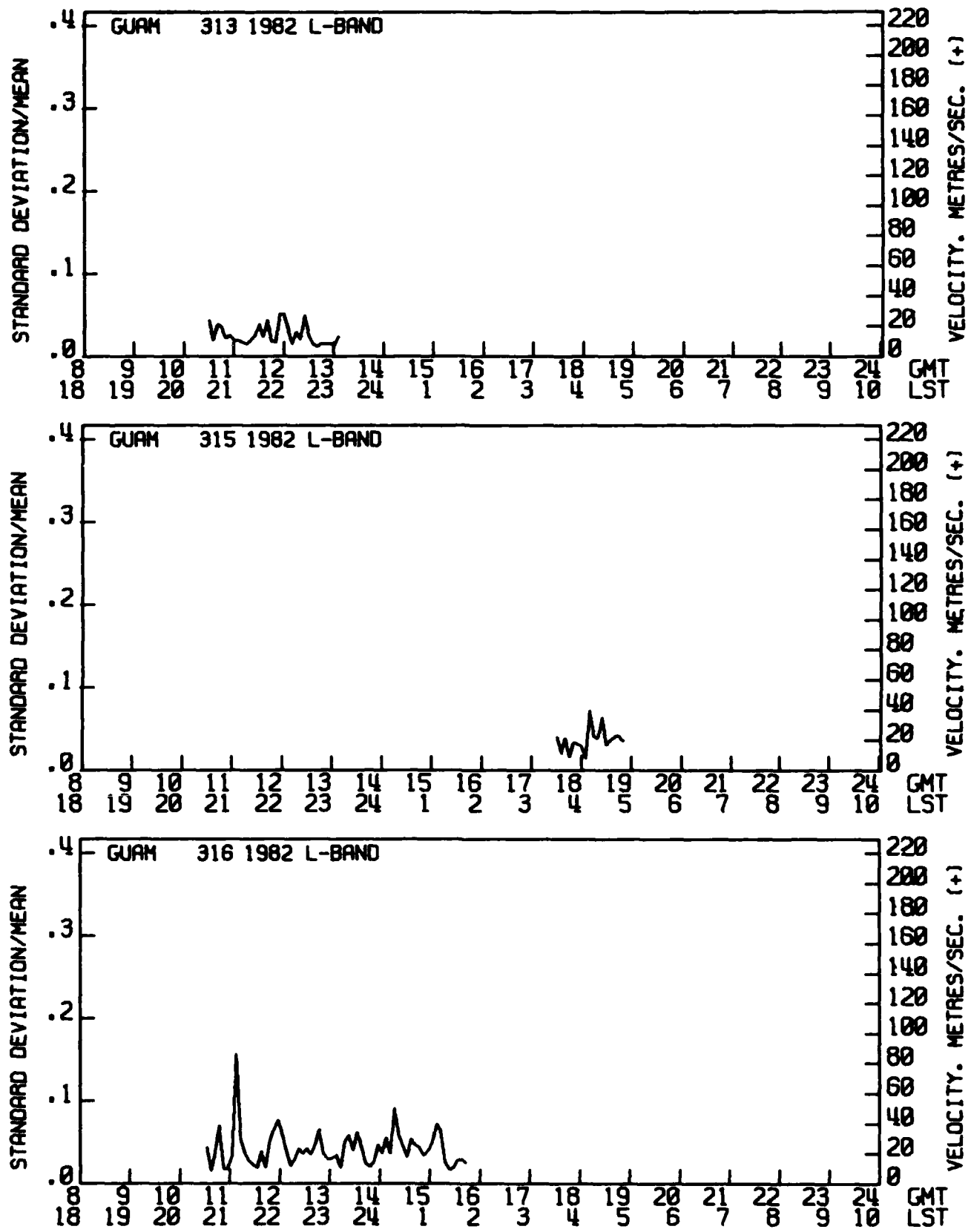


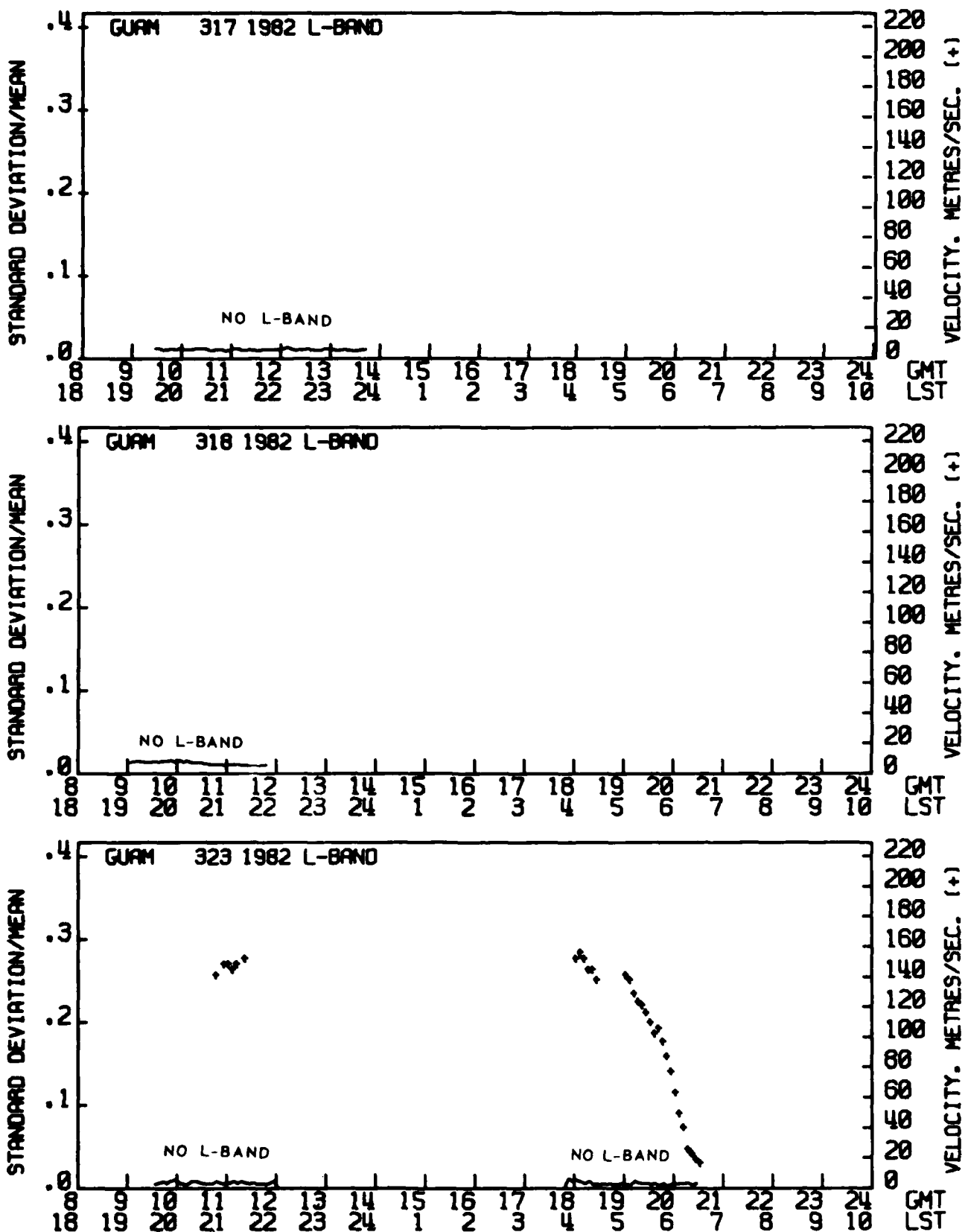


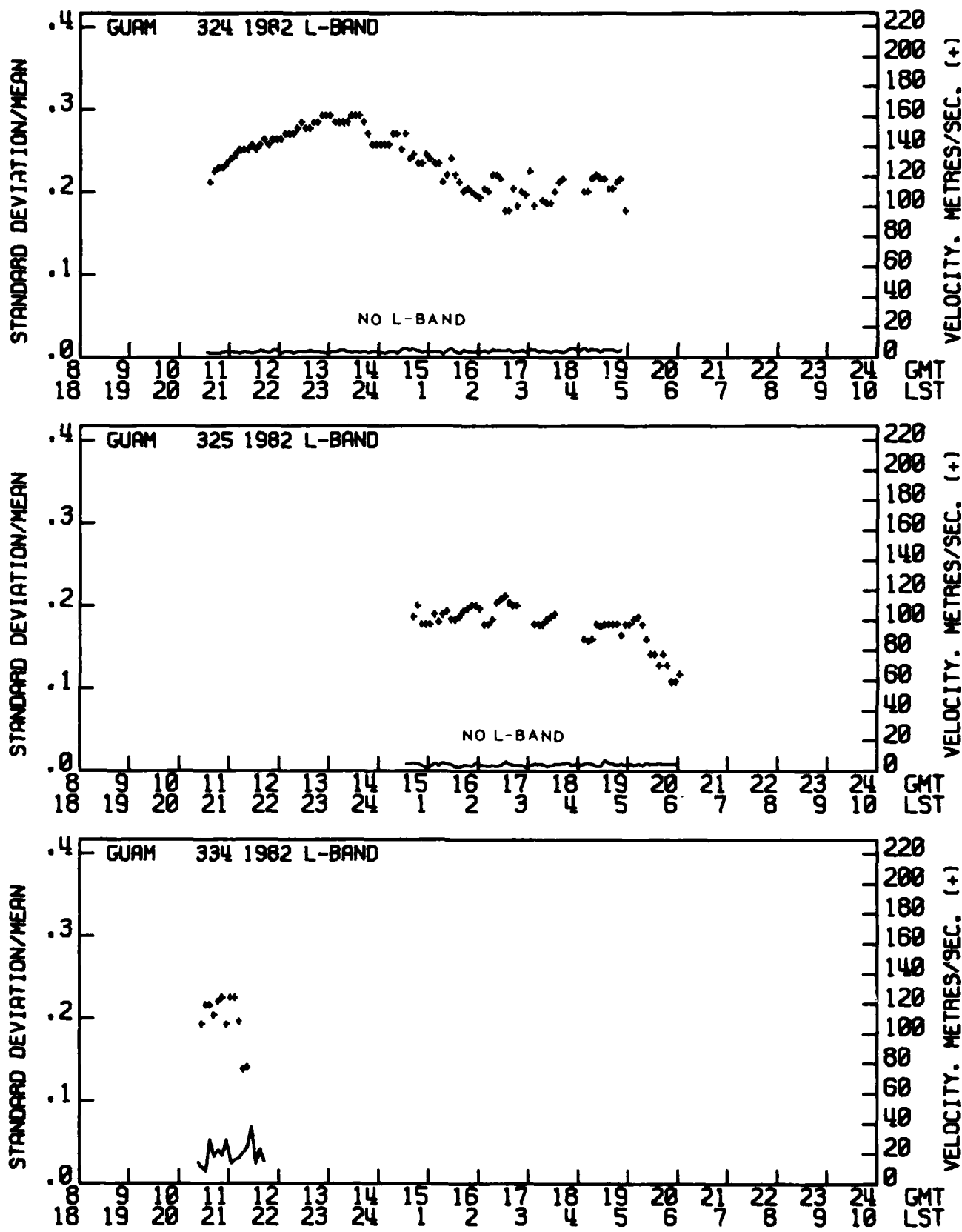


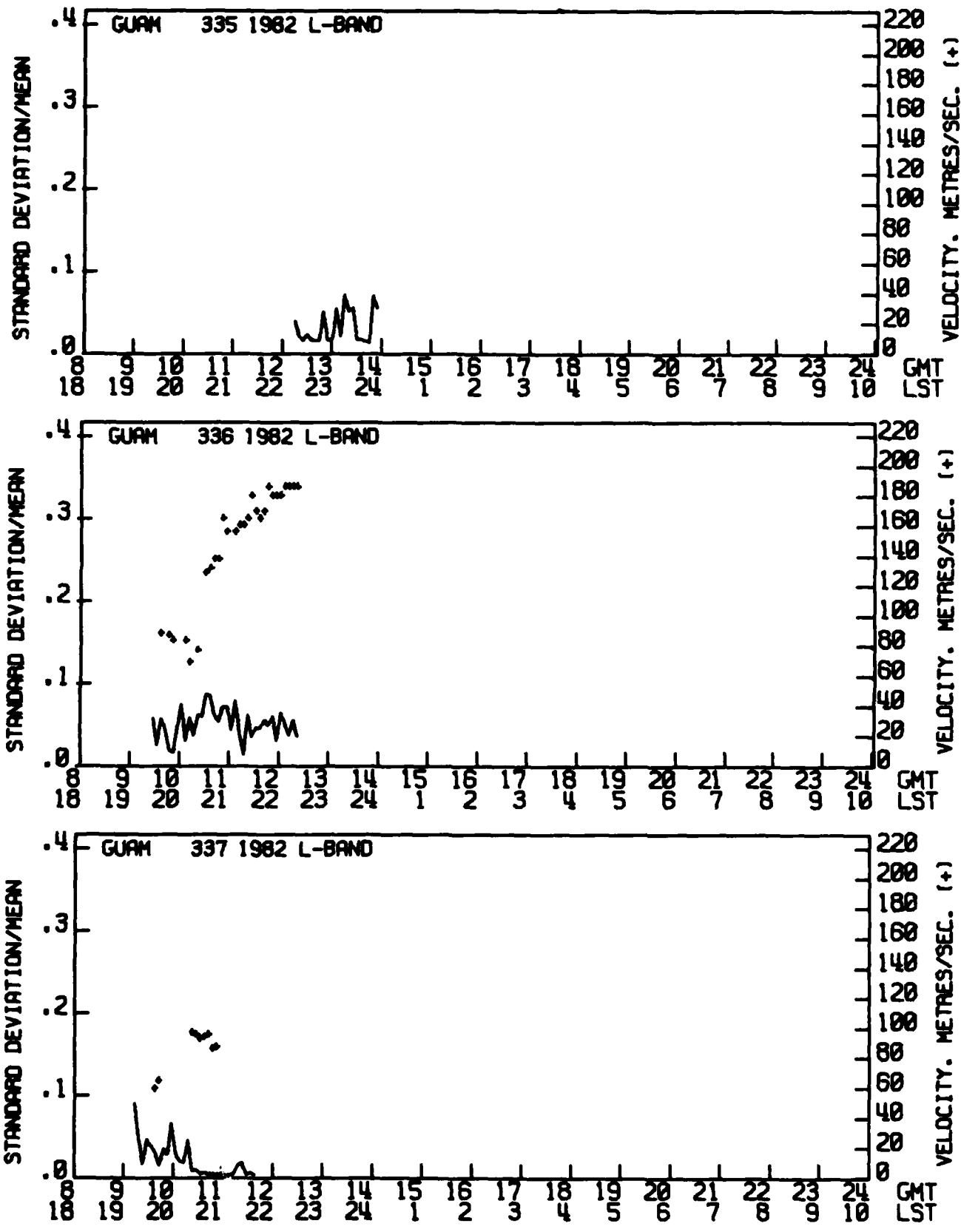


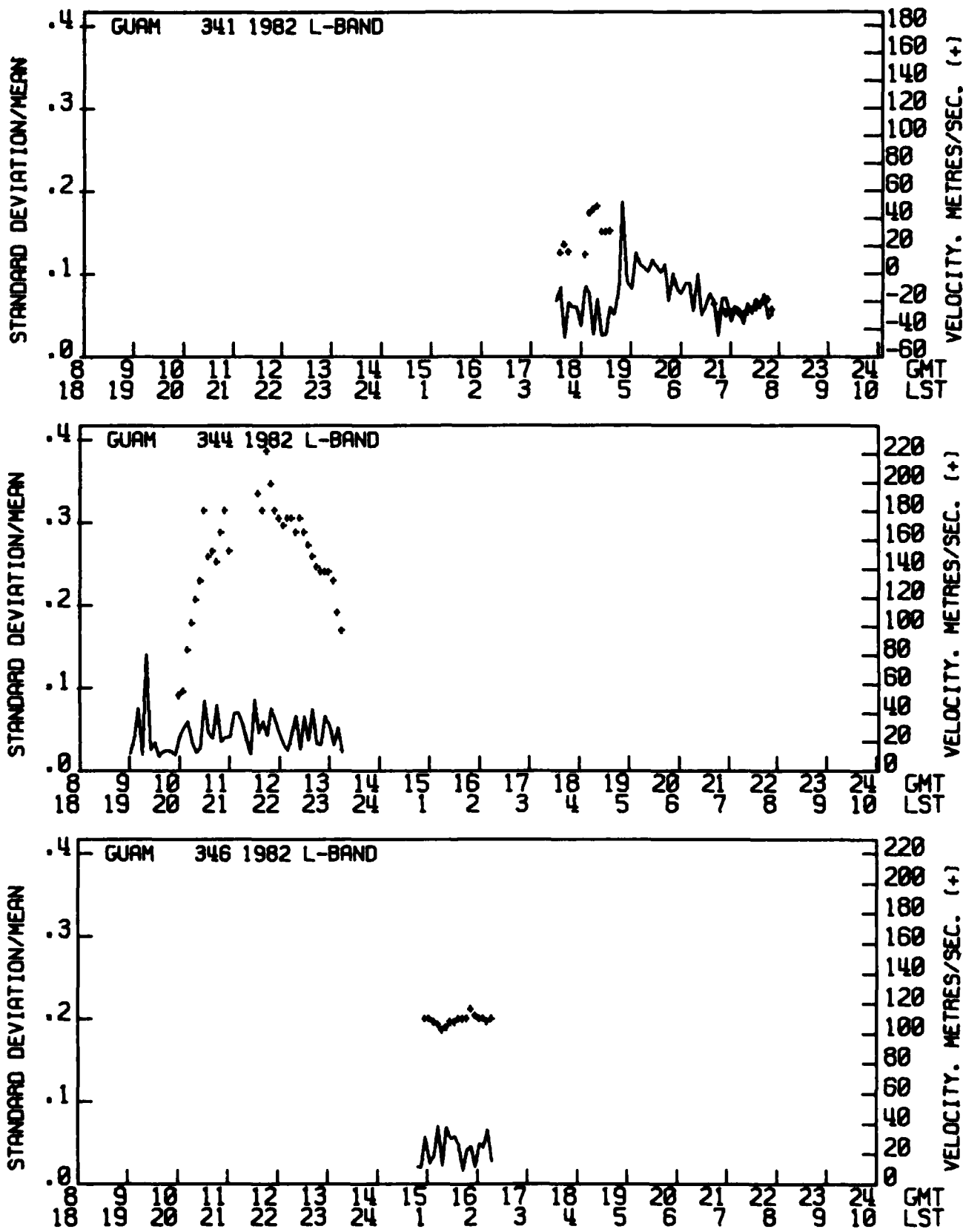


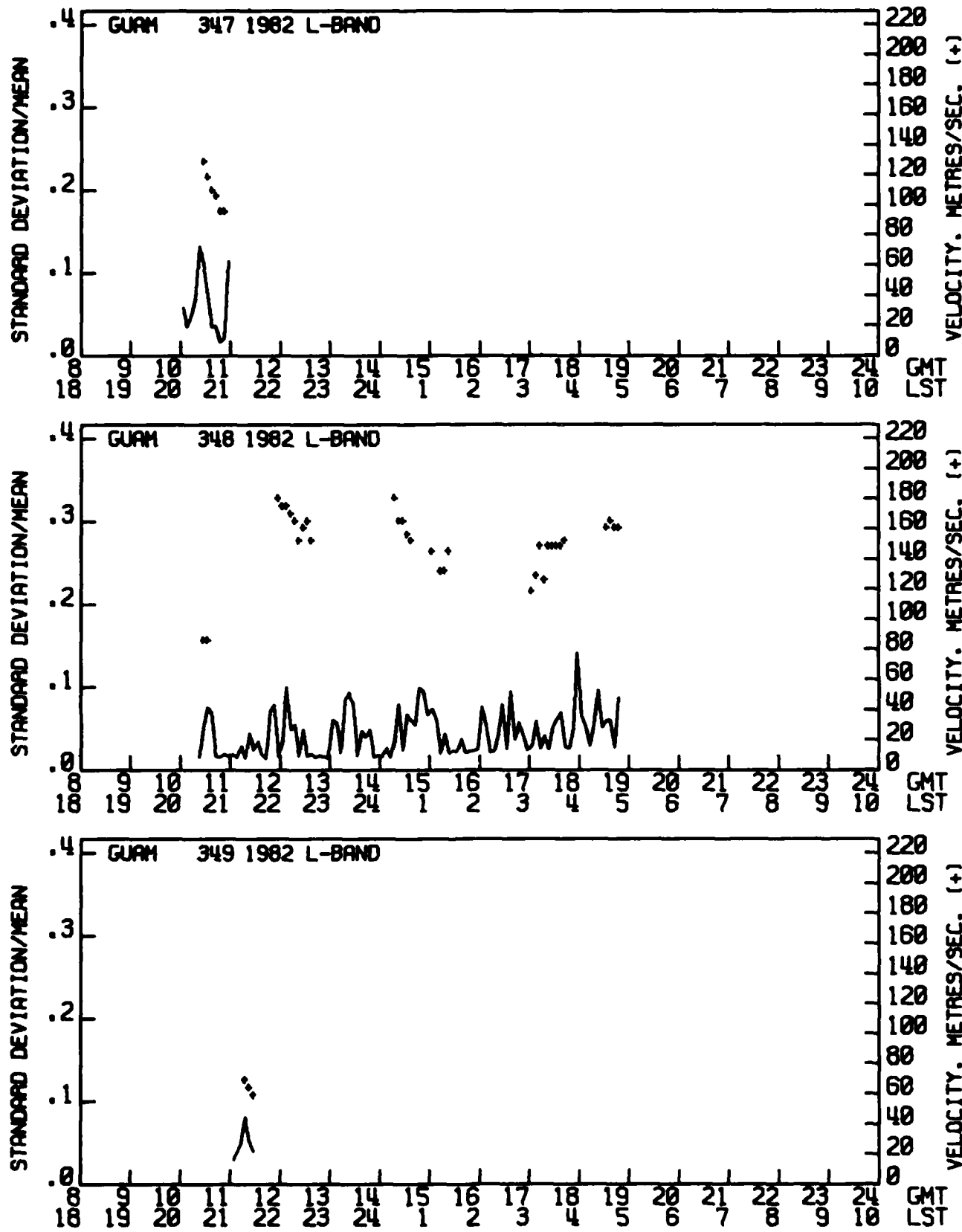


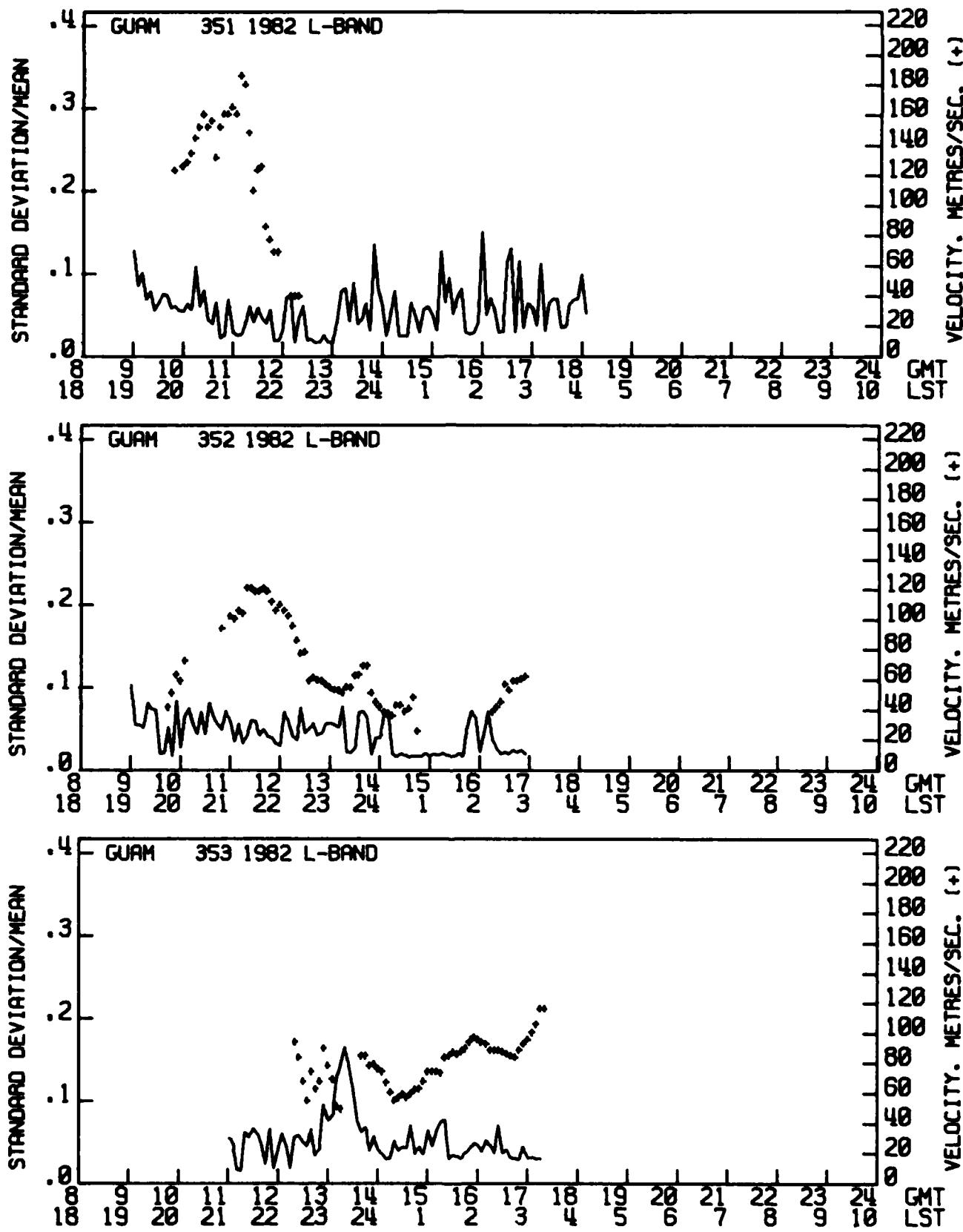


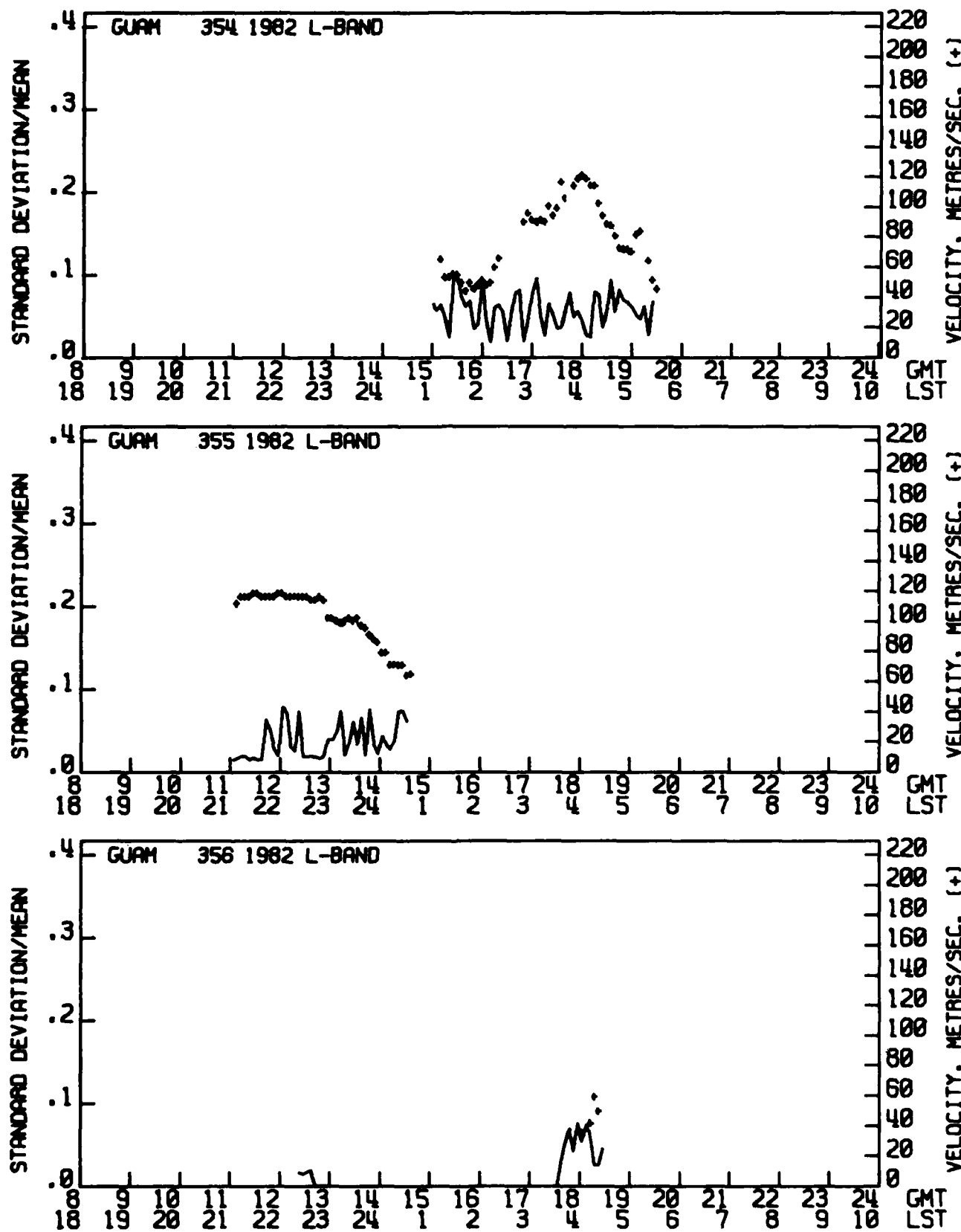


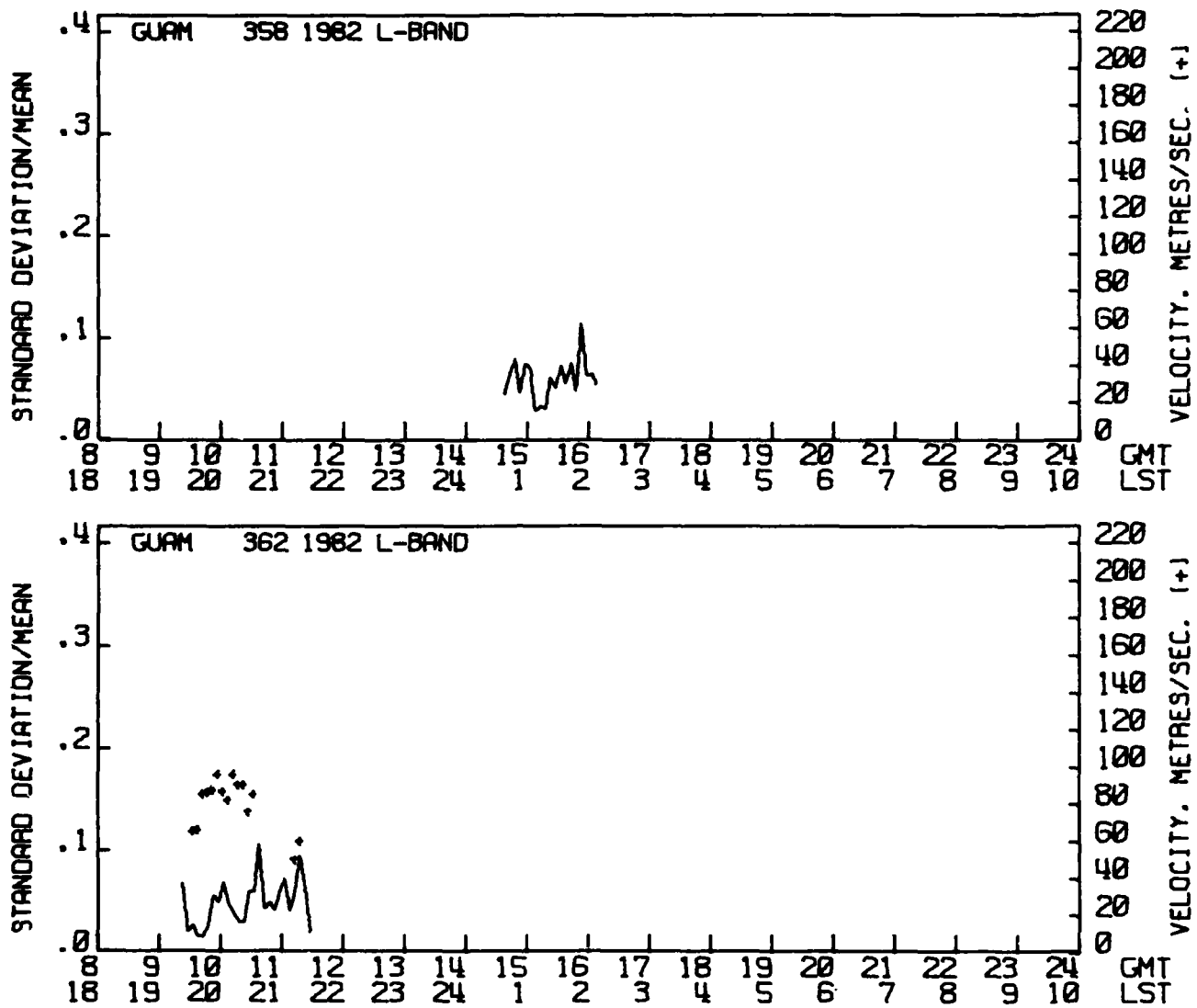


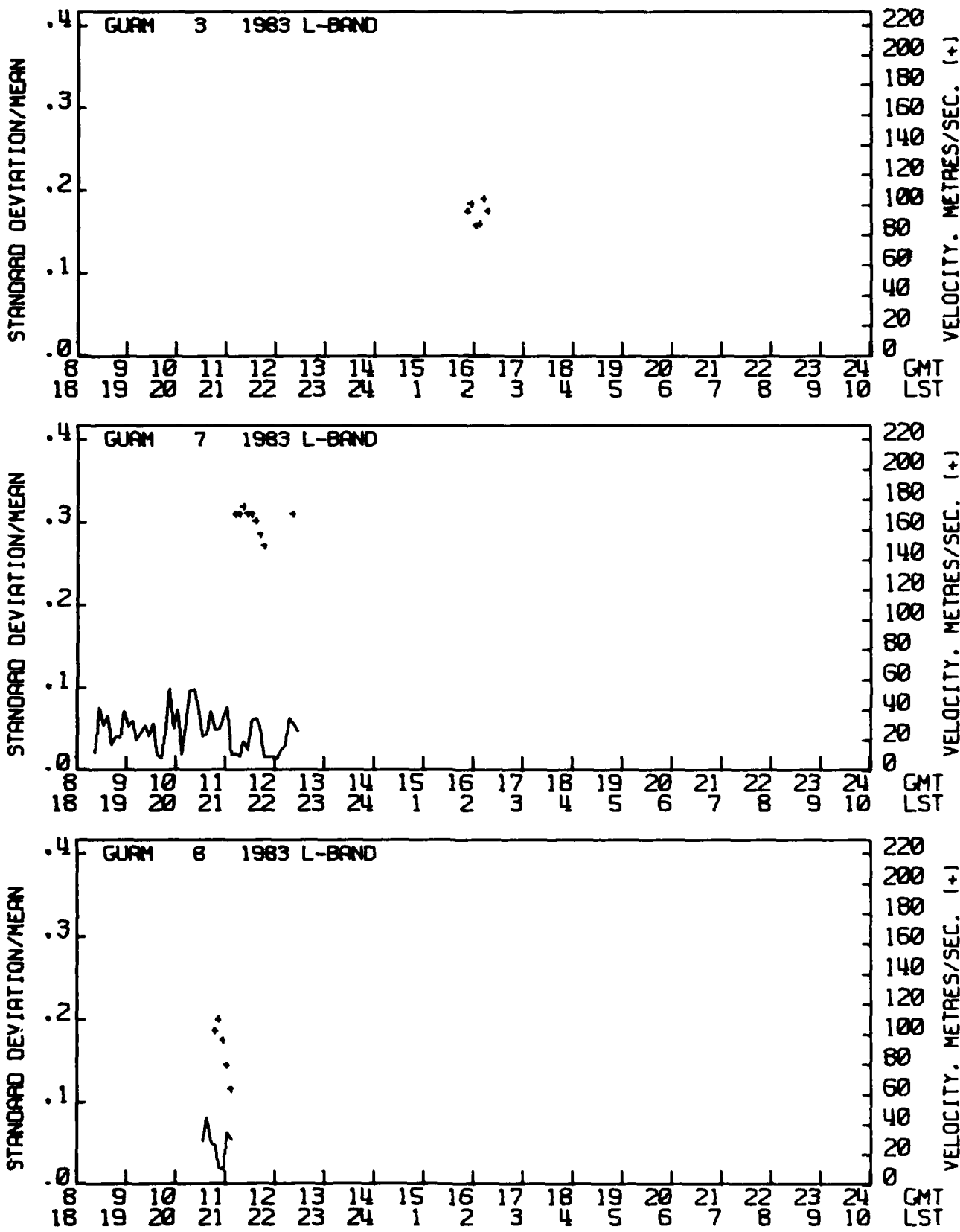


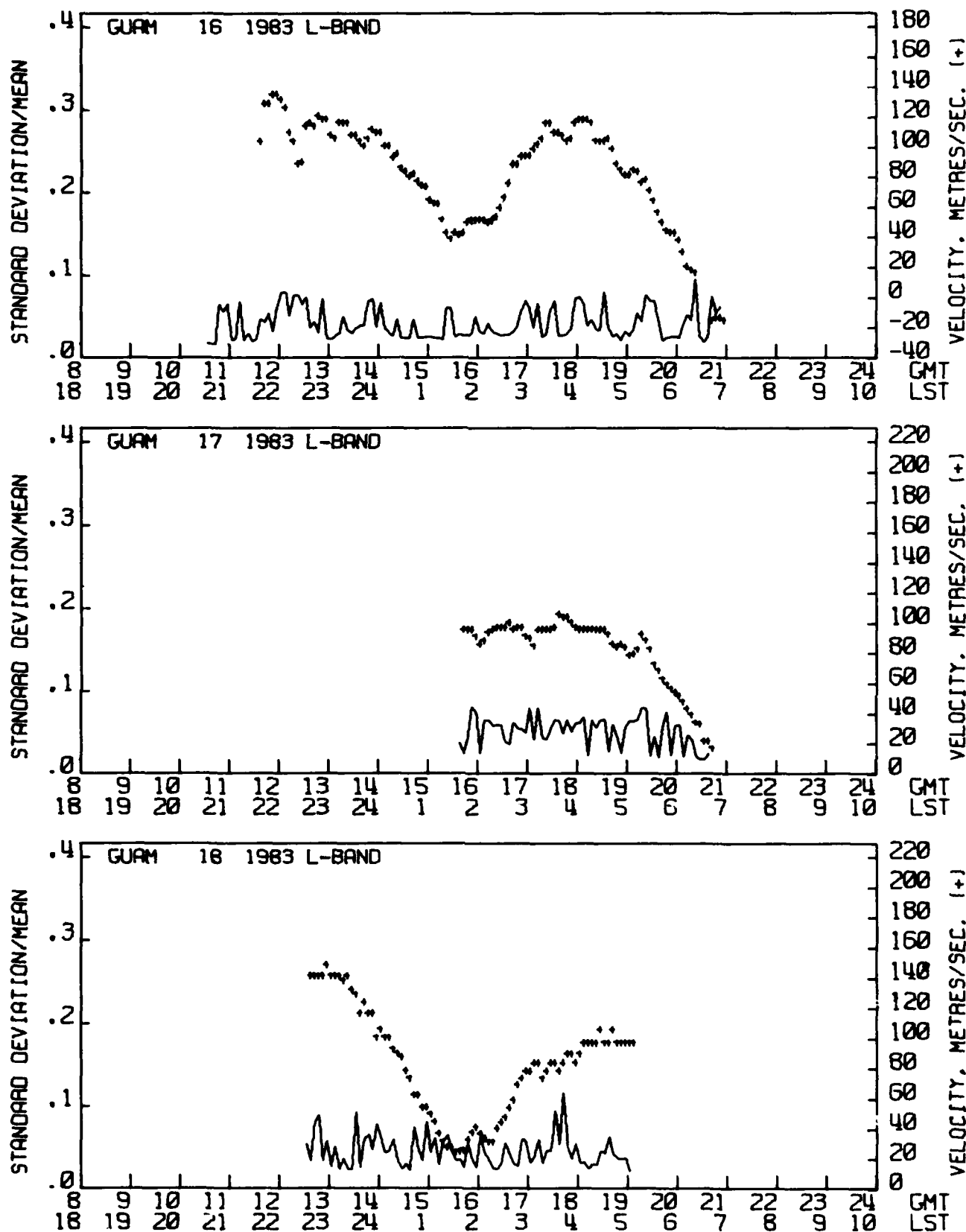


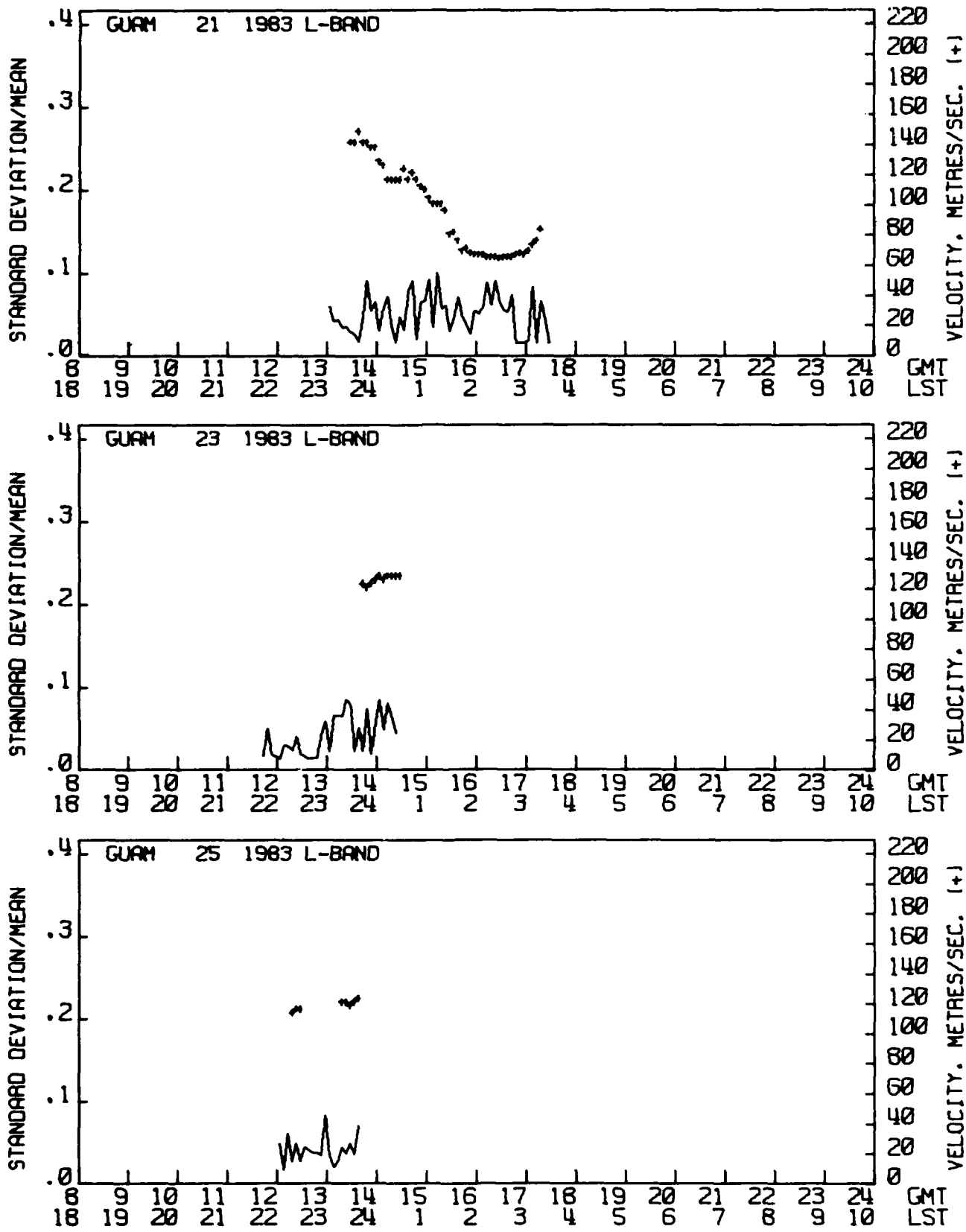


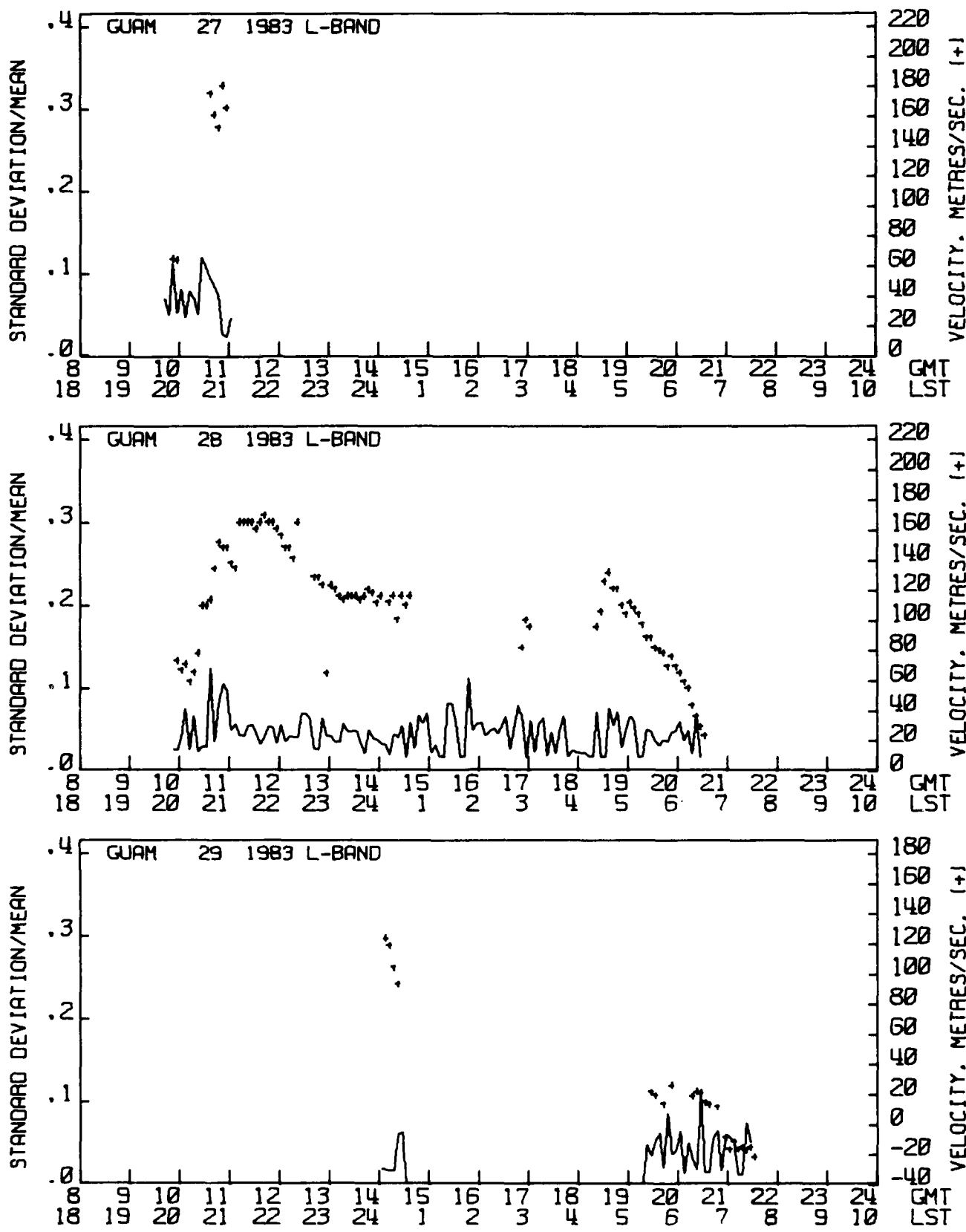


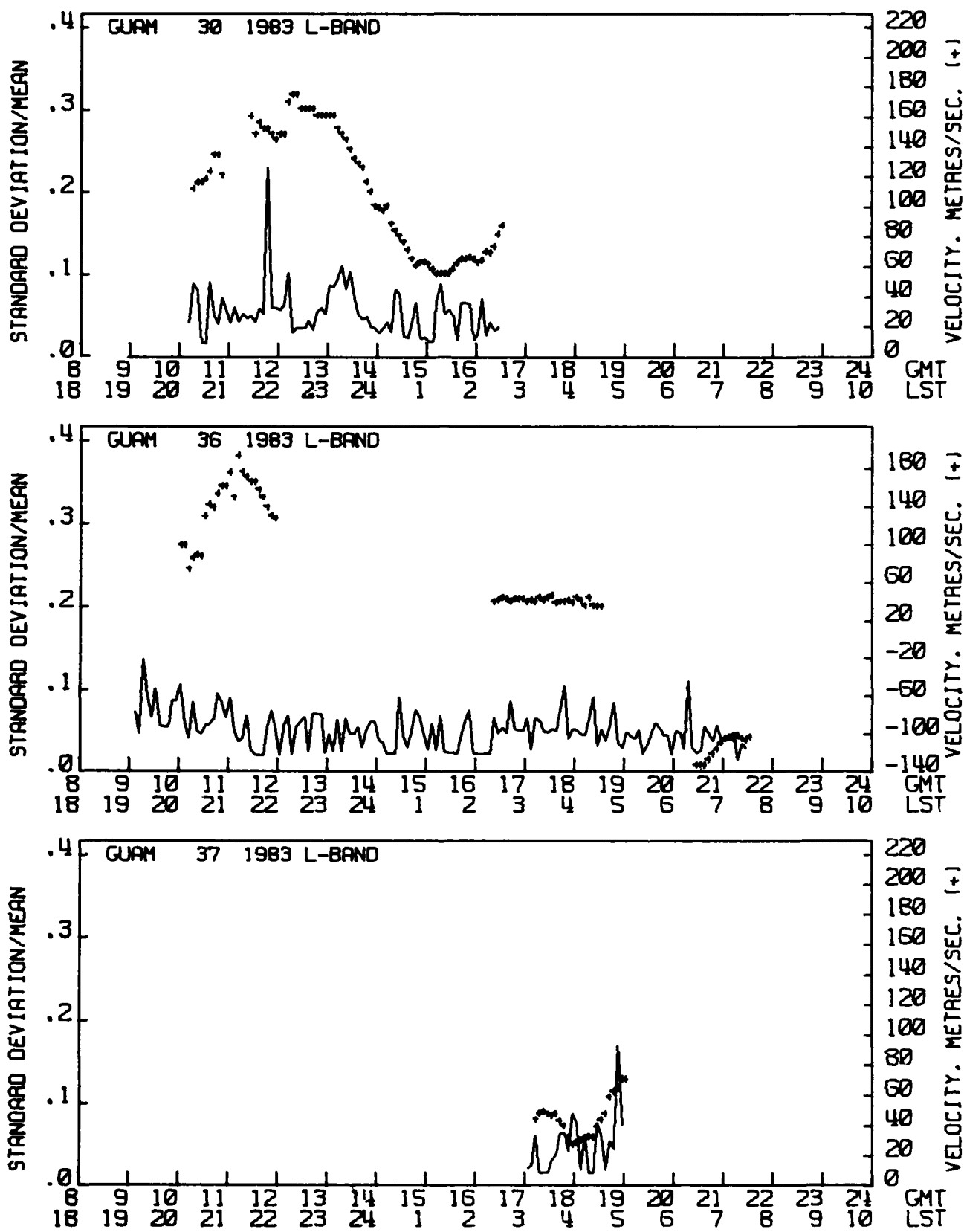


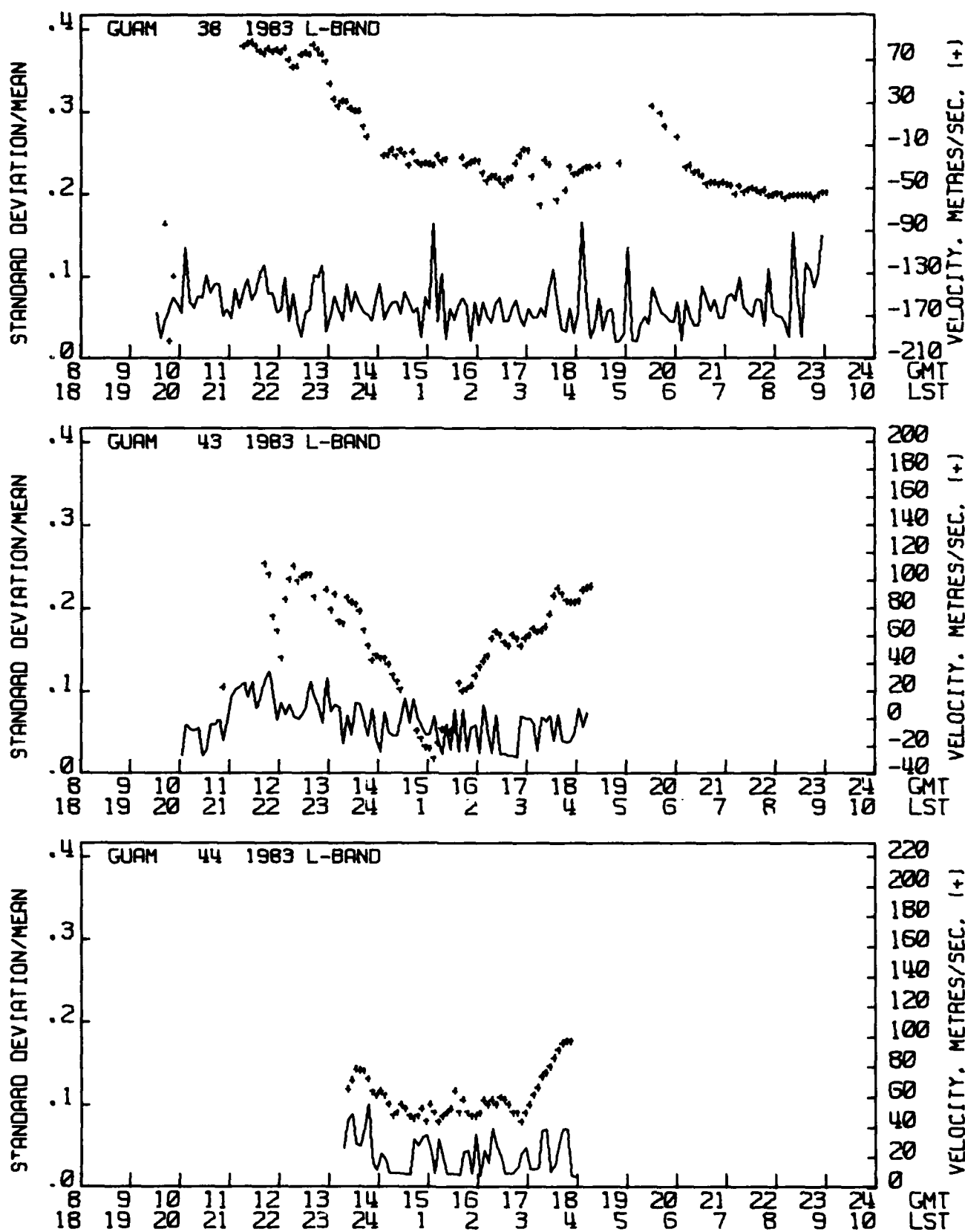


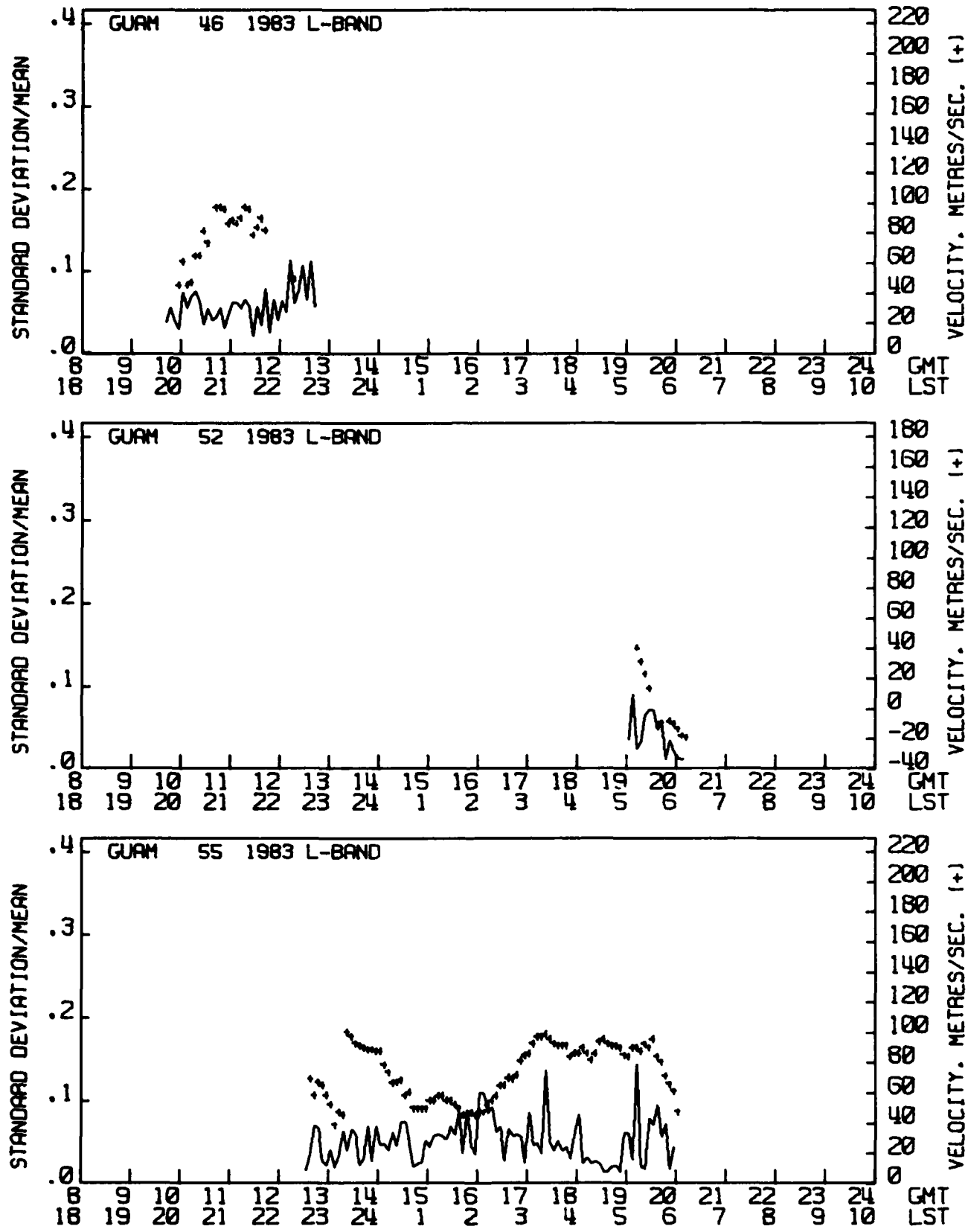


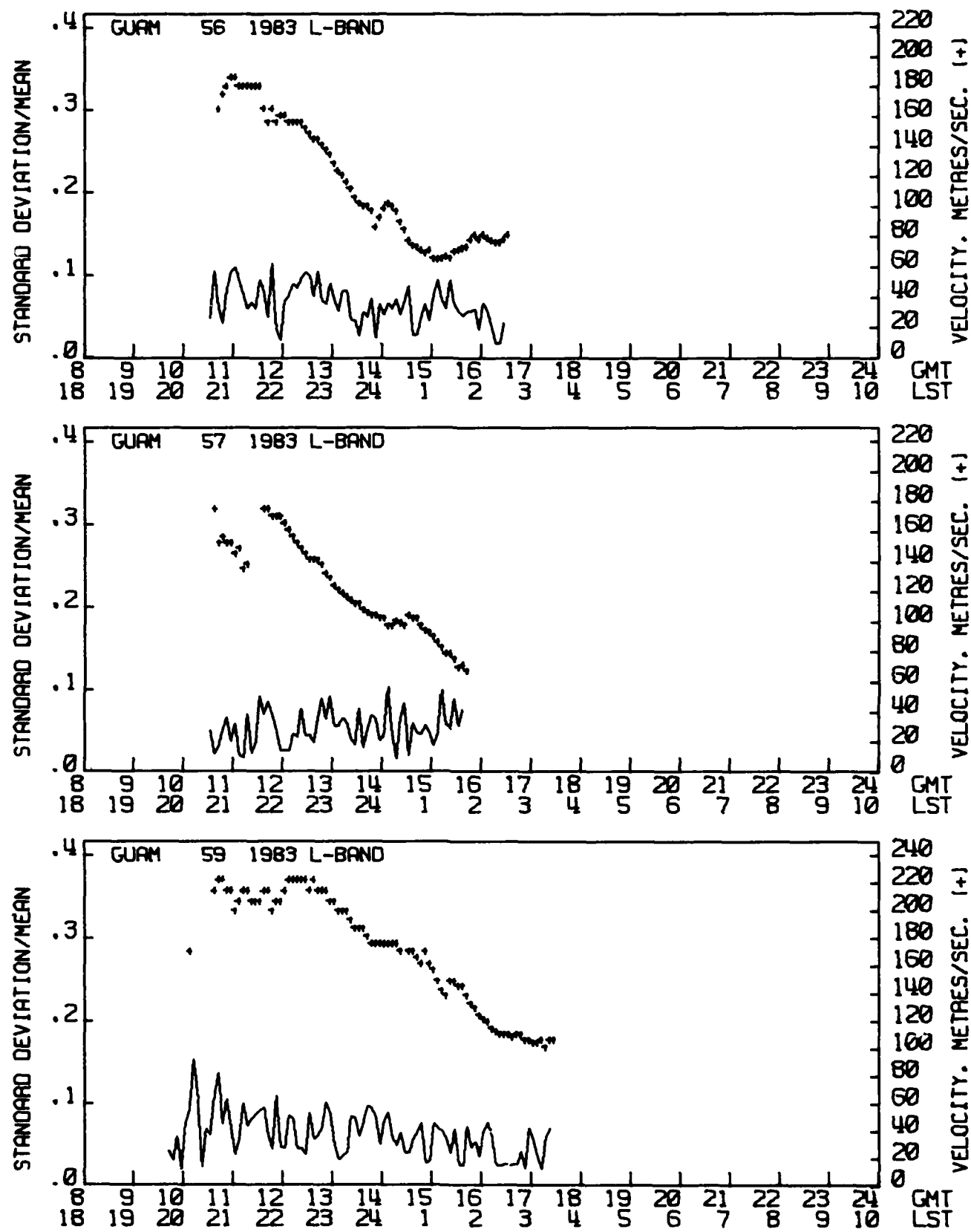


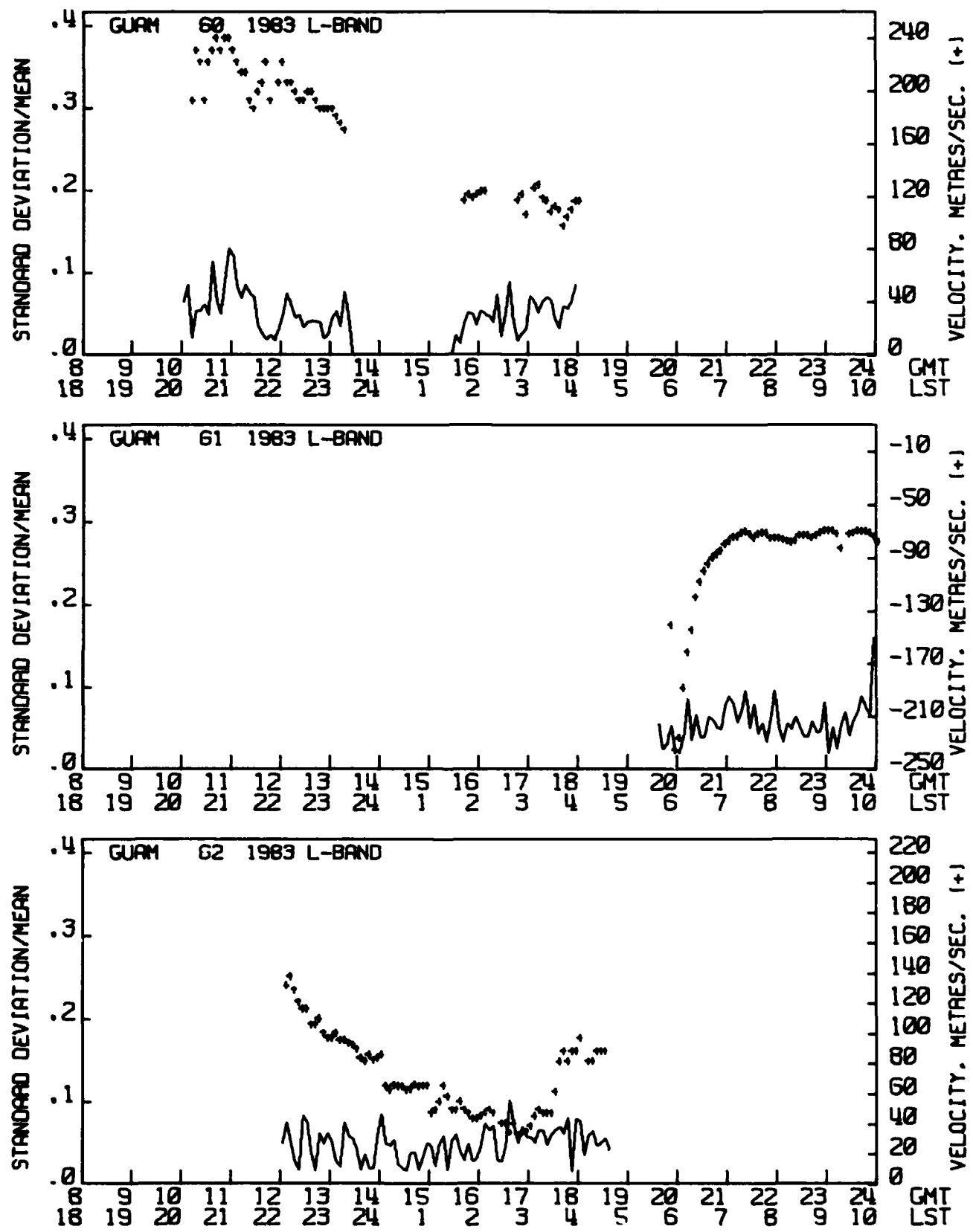


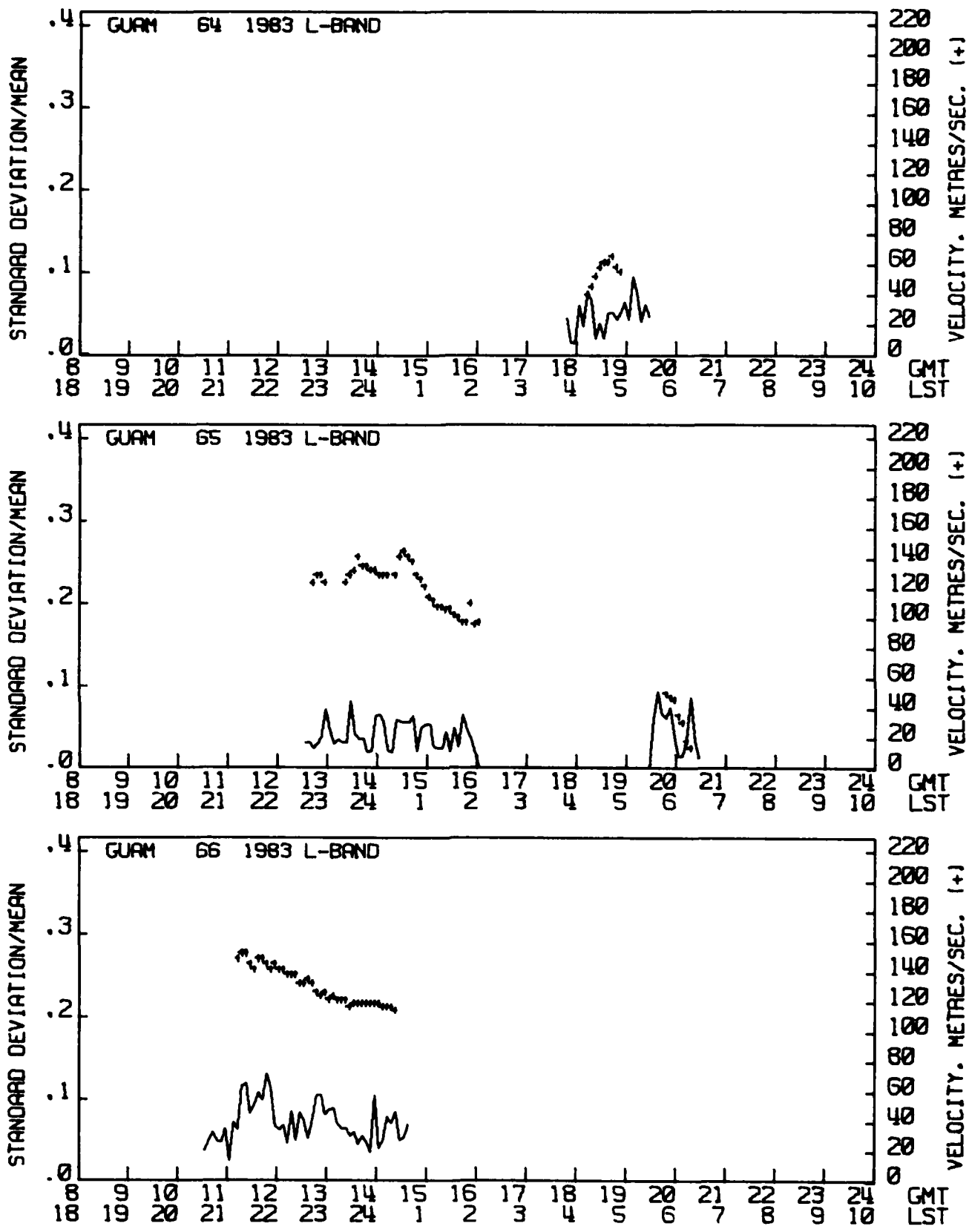


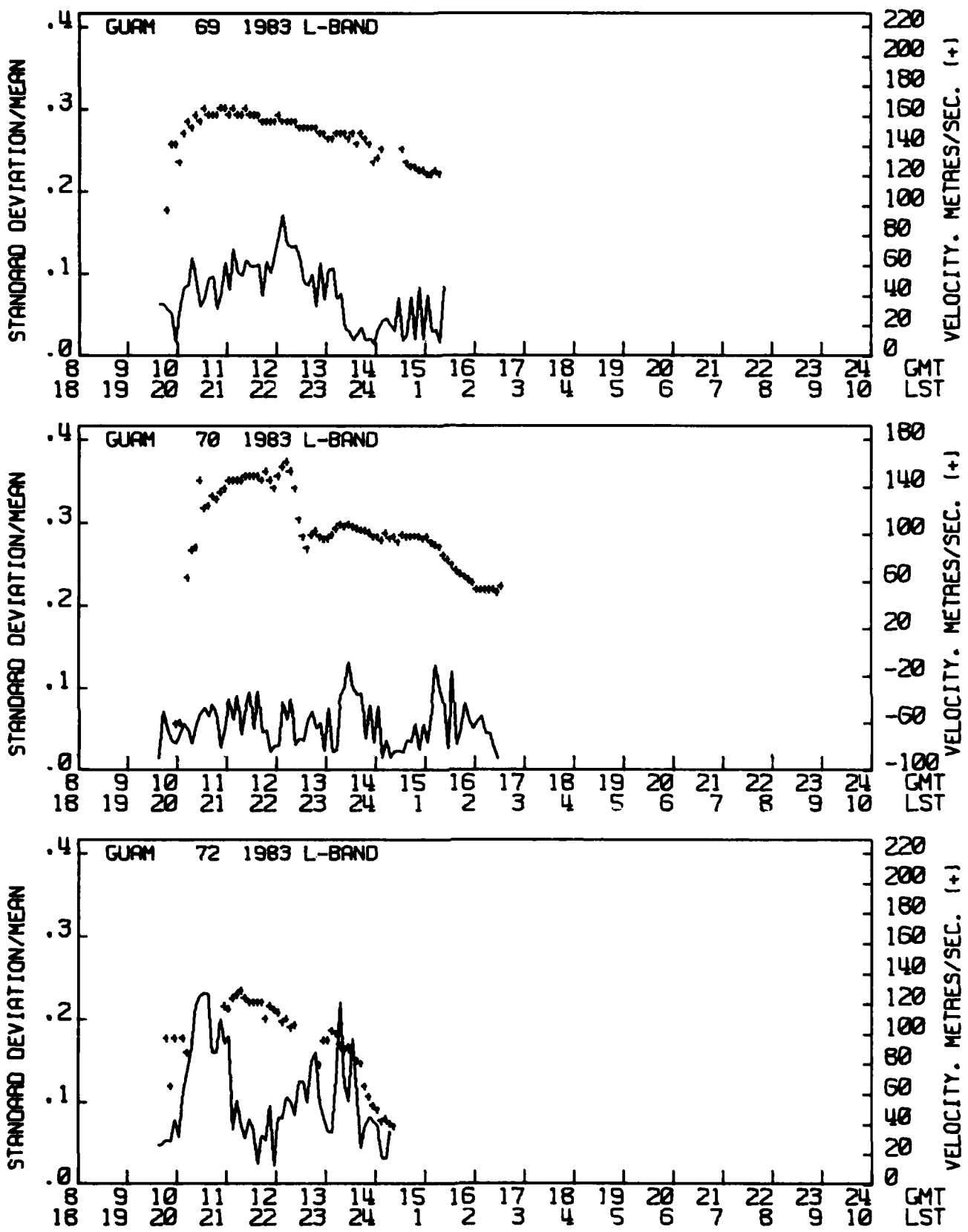


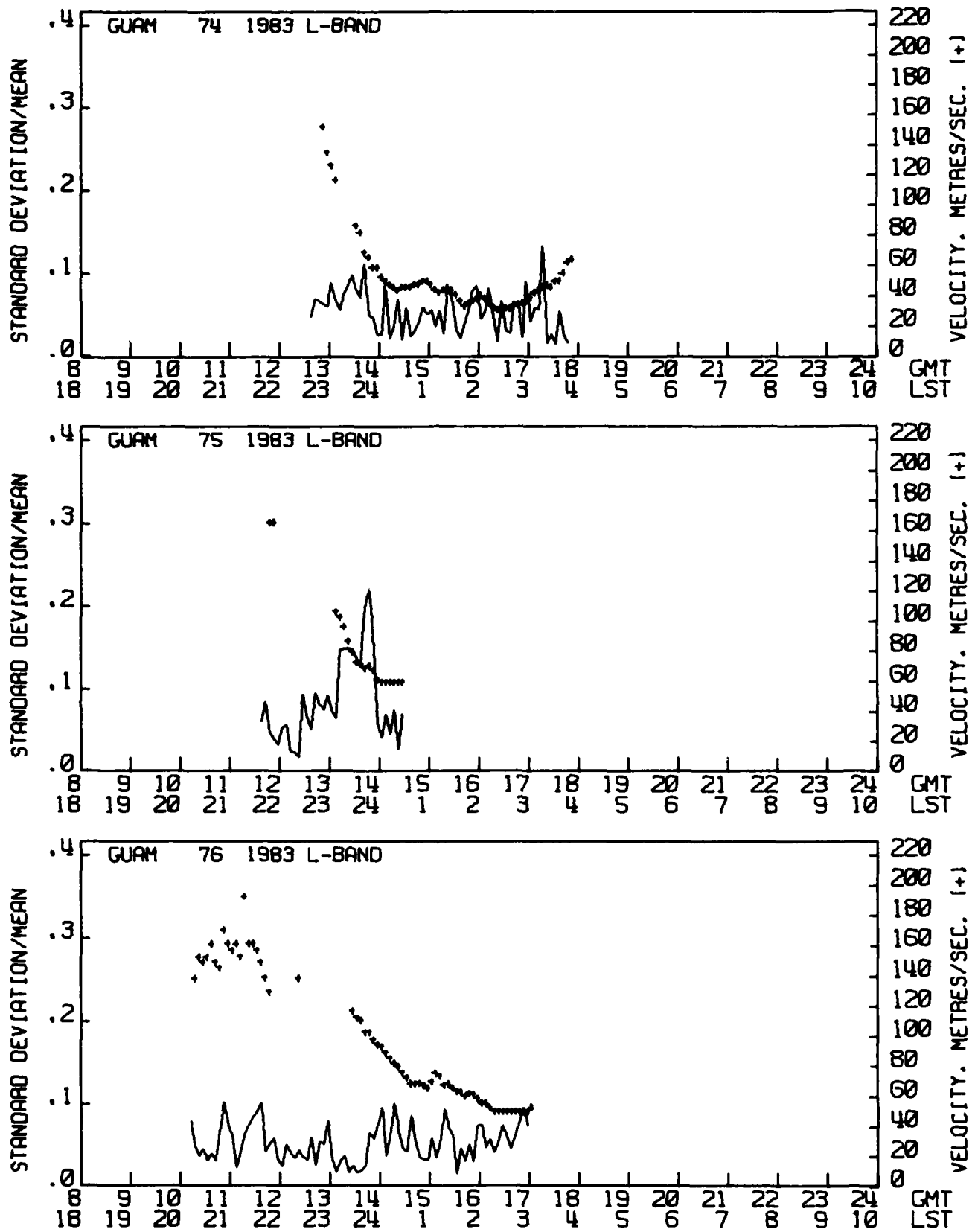


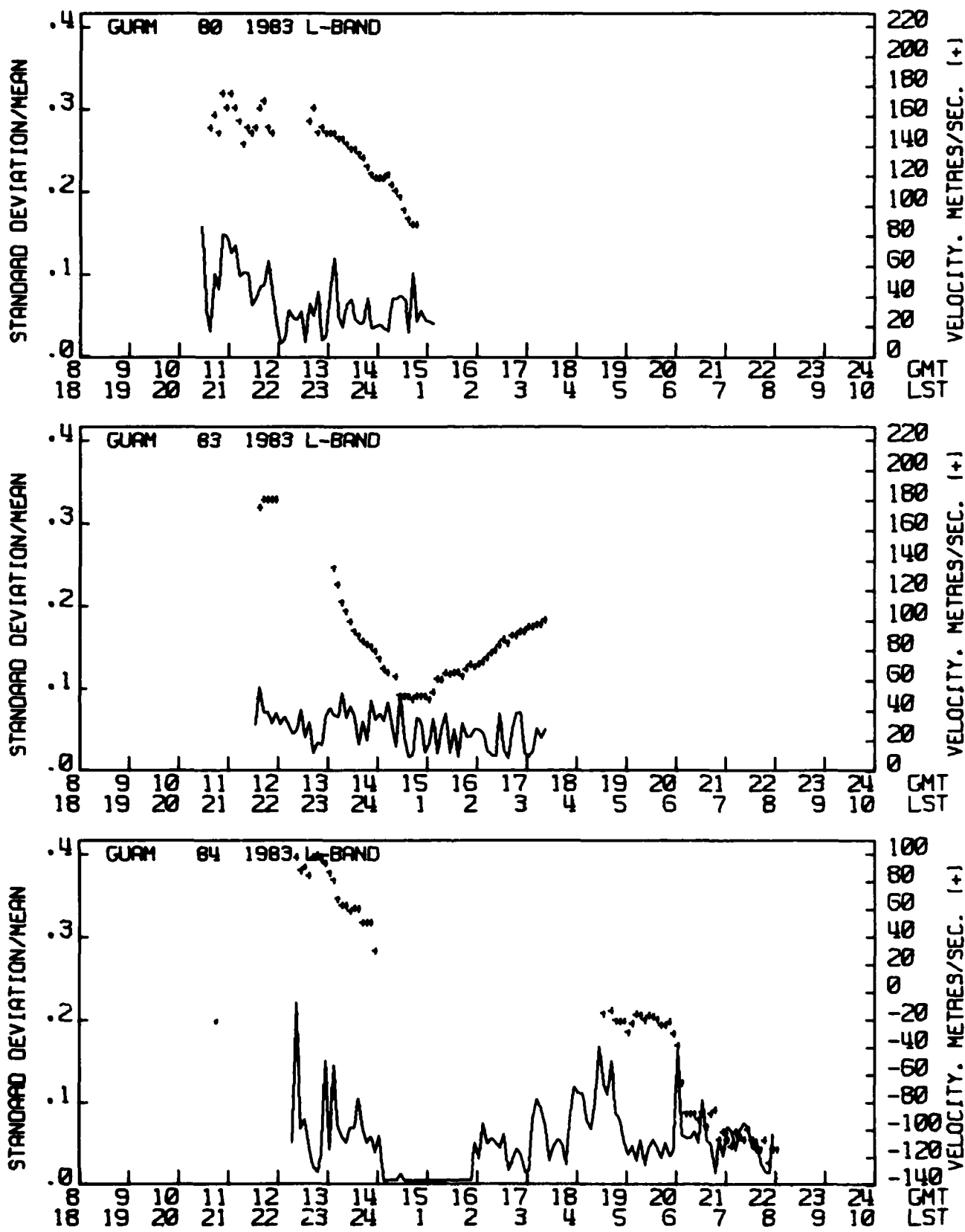


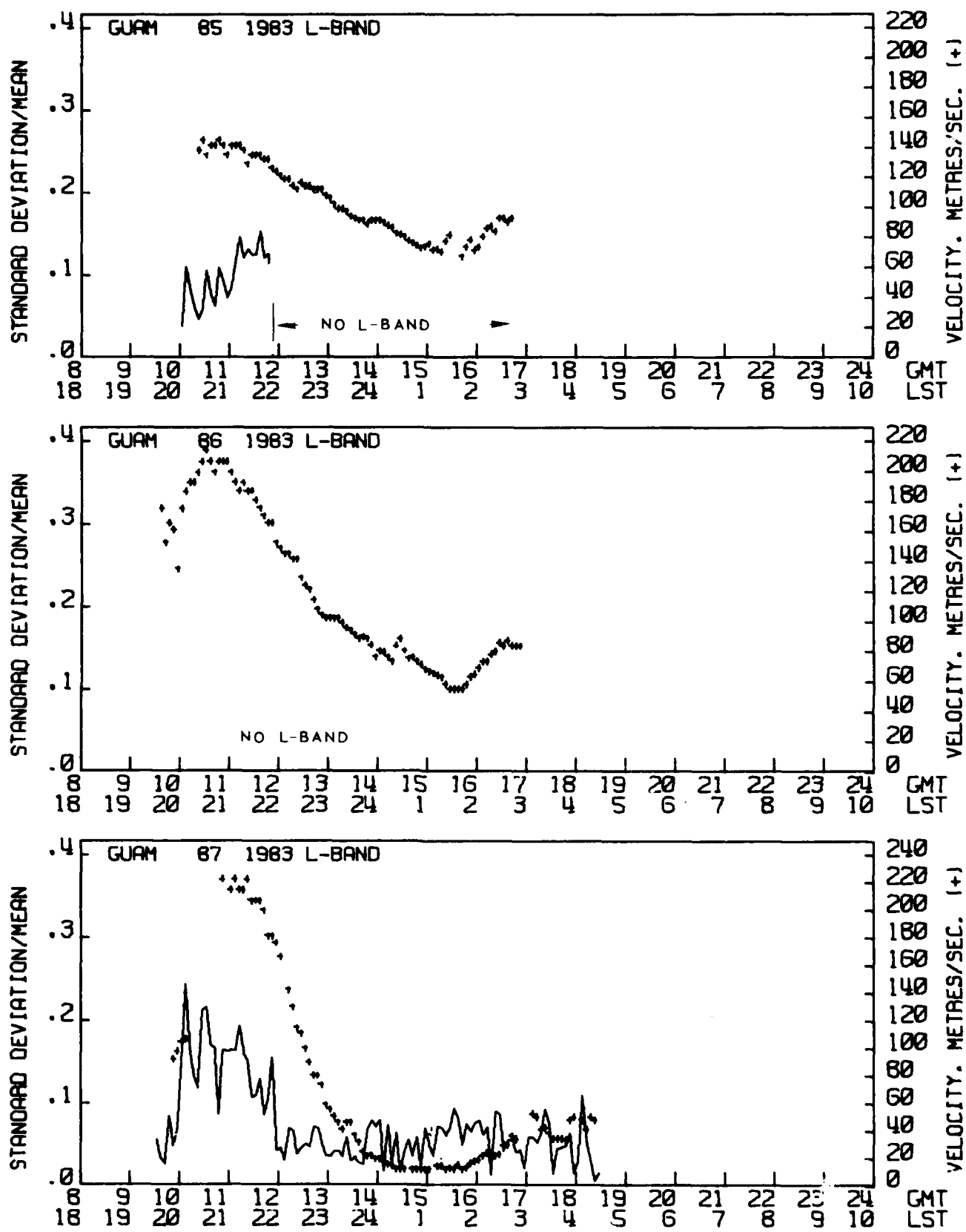


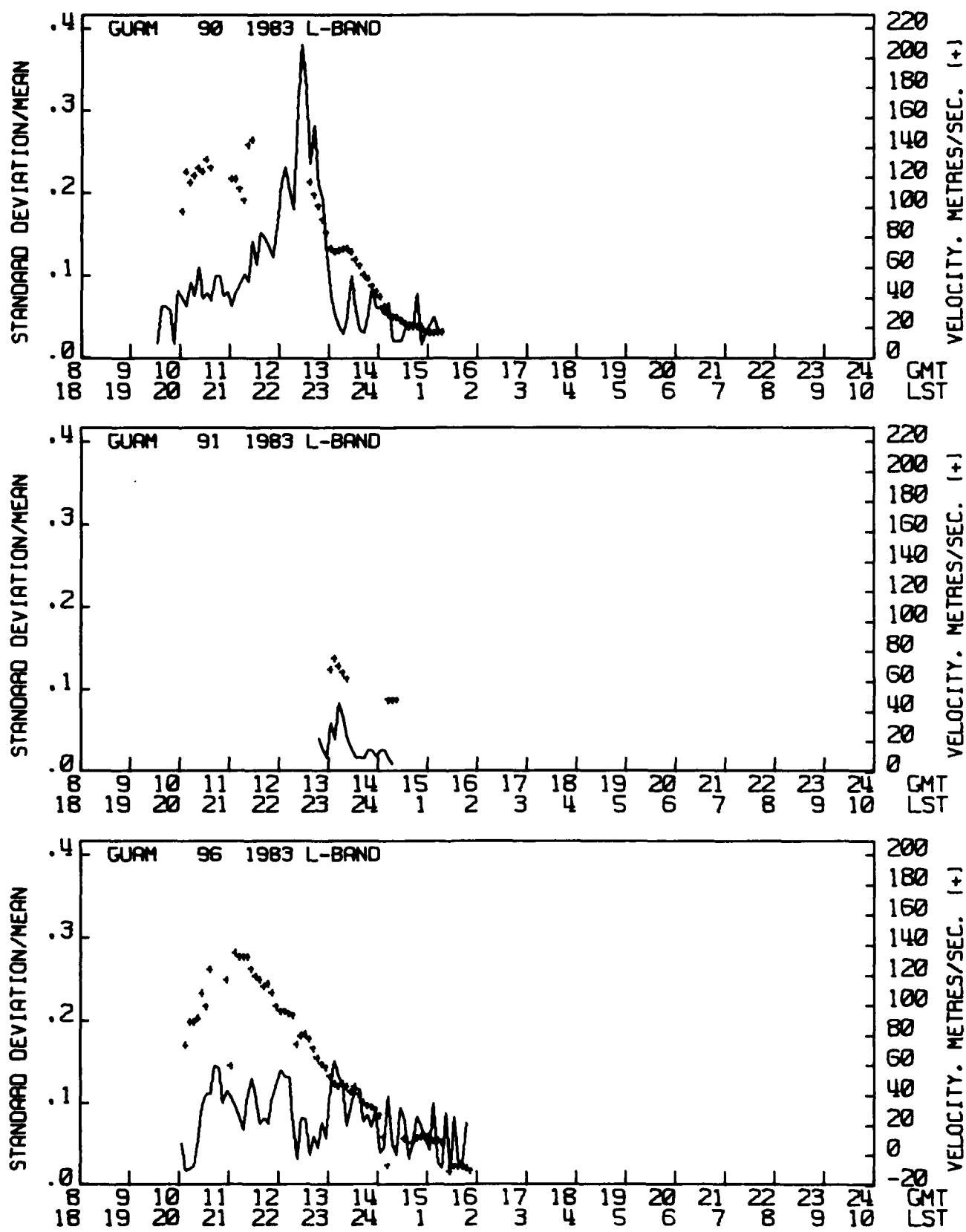


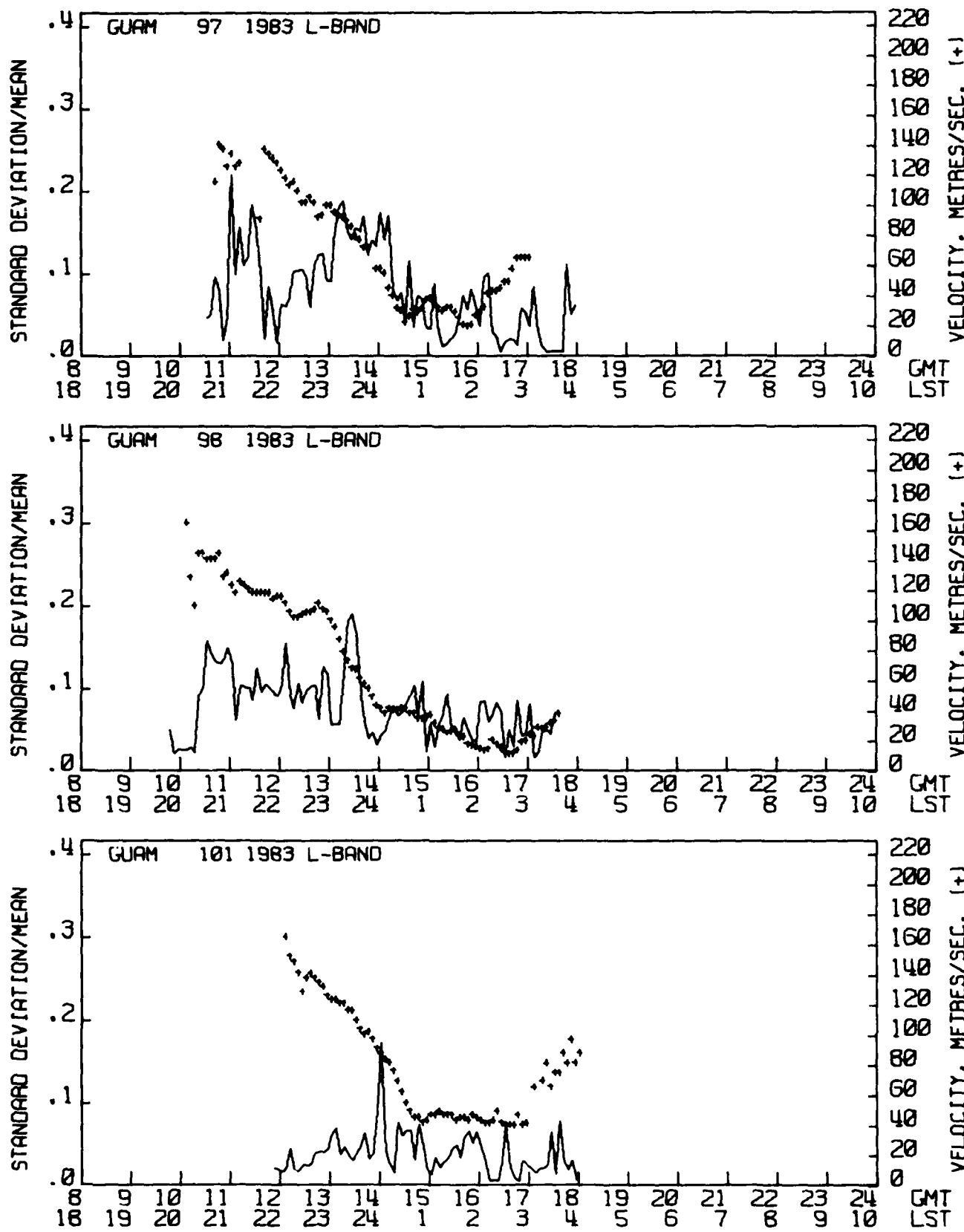


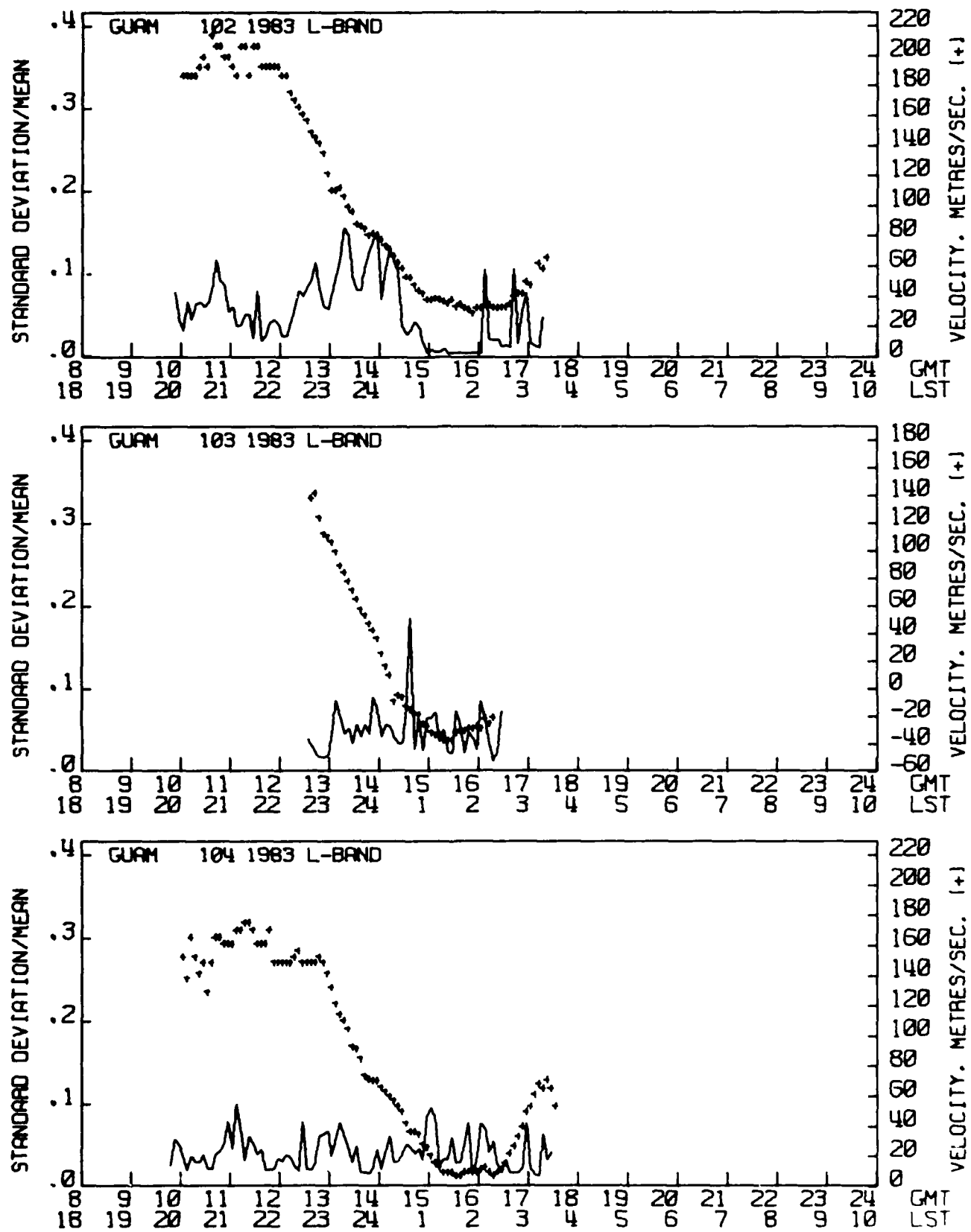












AD-A137 555

EQUATORIAL SCINTILLATION OF SATELLITE SIGNALS AND SOME
DRIFT CHARACTERISTICS OF THE SCINTILLATION(U) NAVAL
OCEAN SYSTEMS CENTER SAN DIEGO CA M R PAULSON

3/3

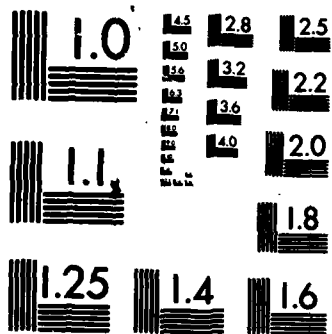
UNCLASSIFIED

15 OCT 83 NOSC/TR-911

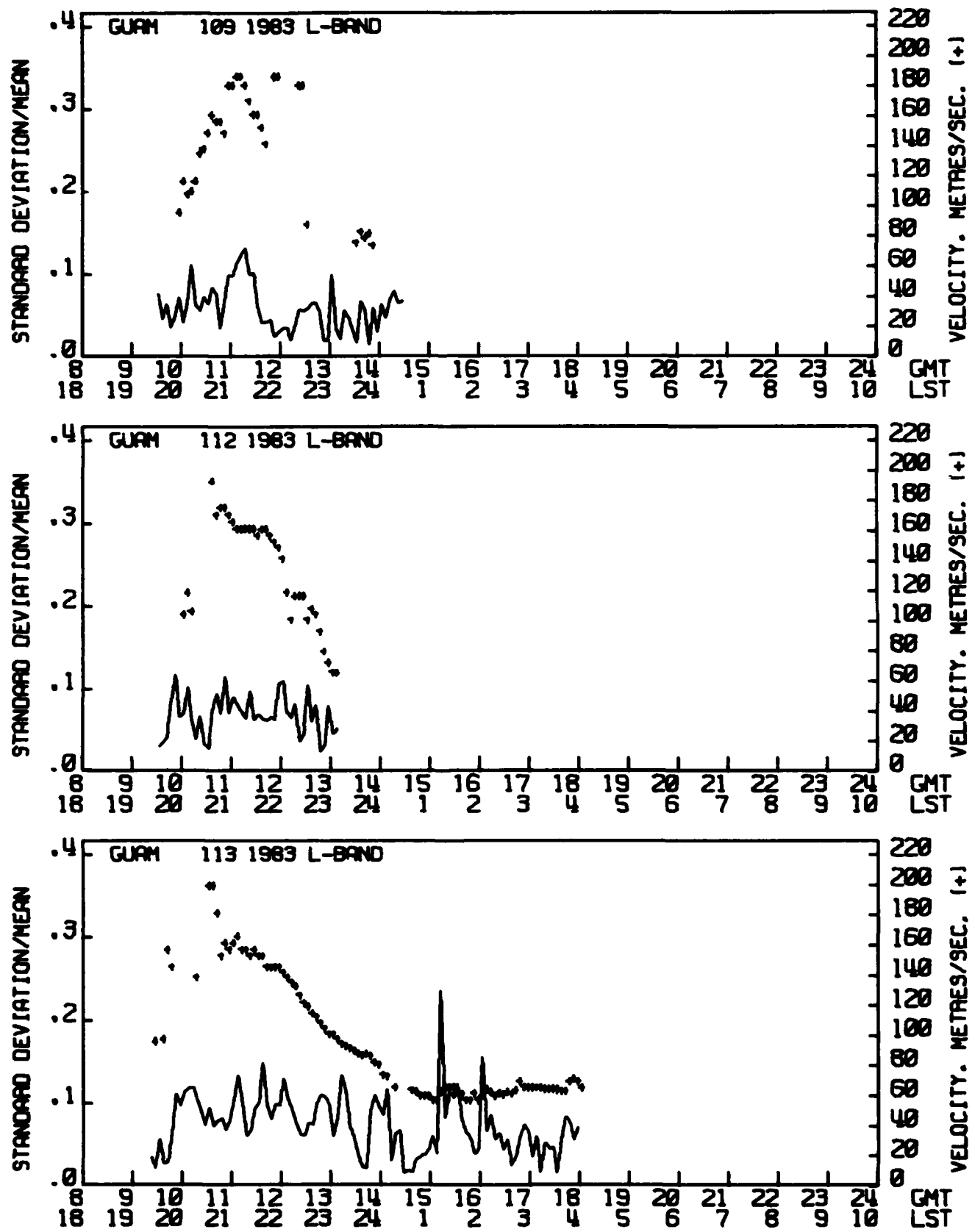
F/G 20/14

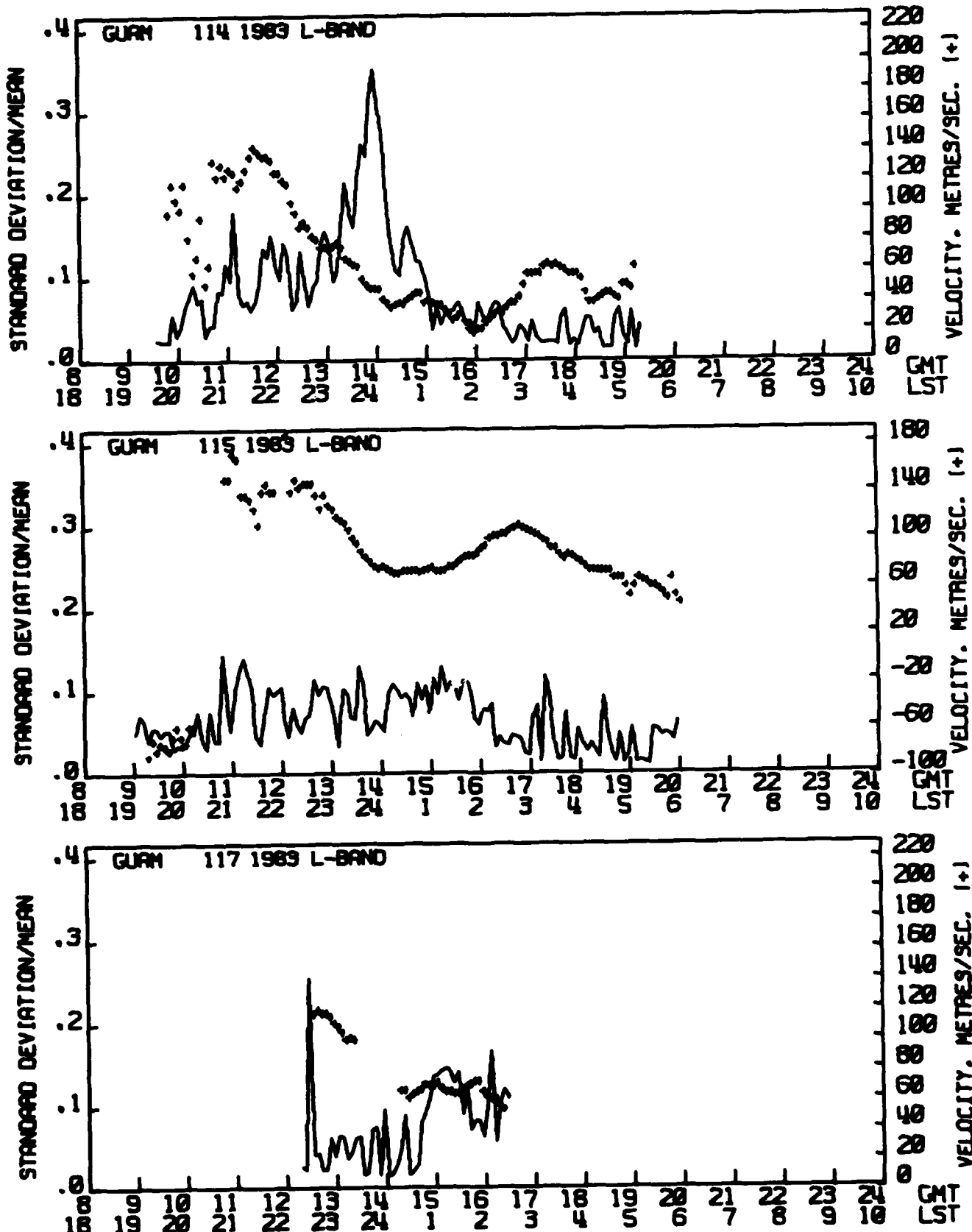
NL

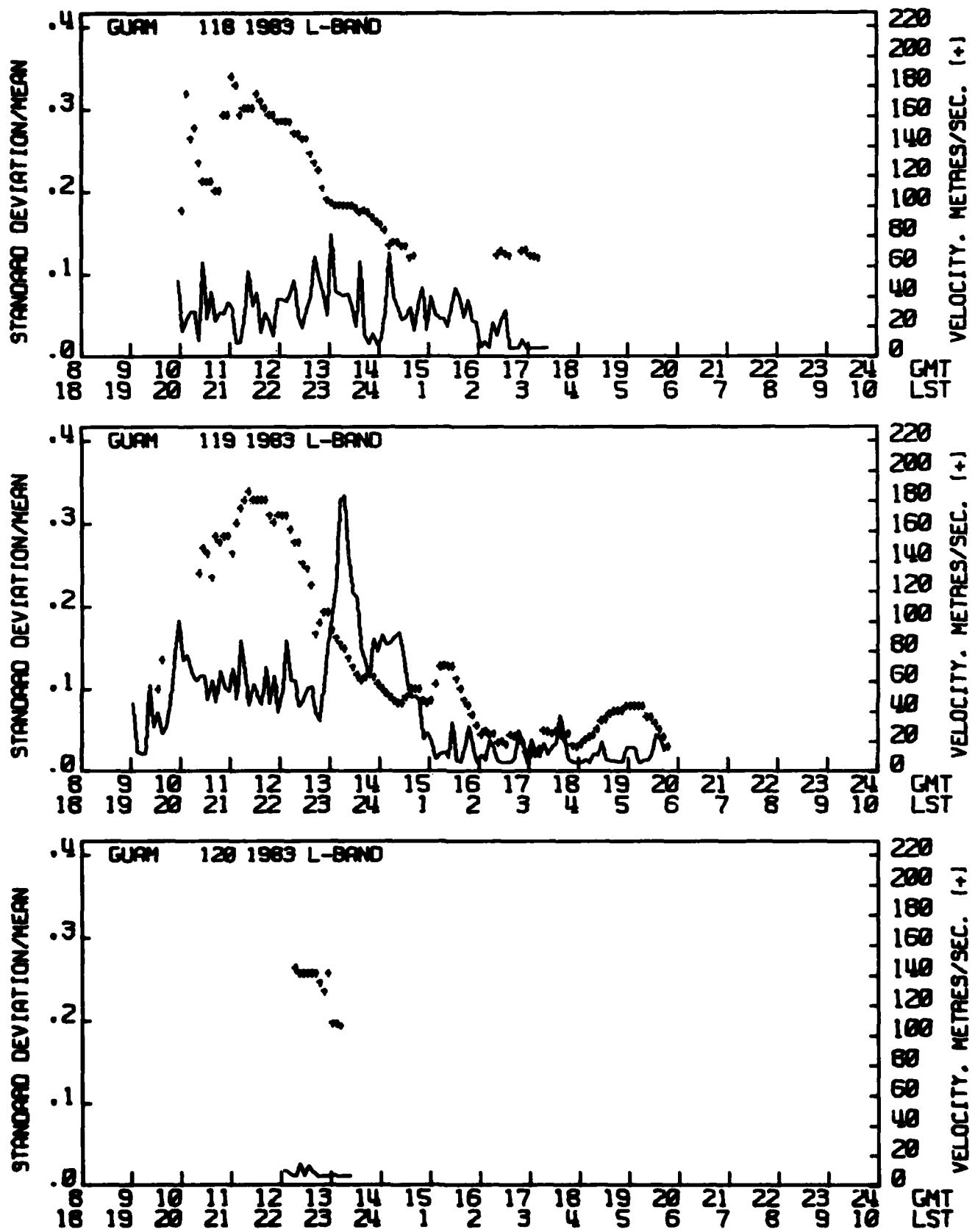


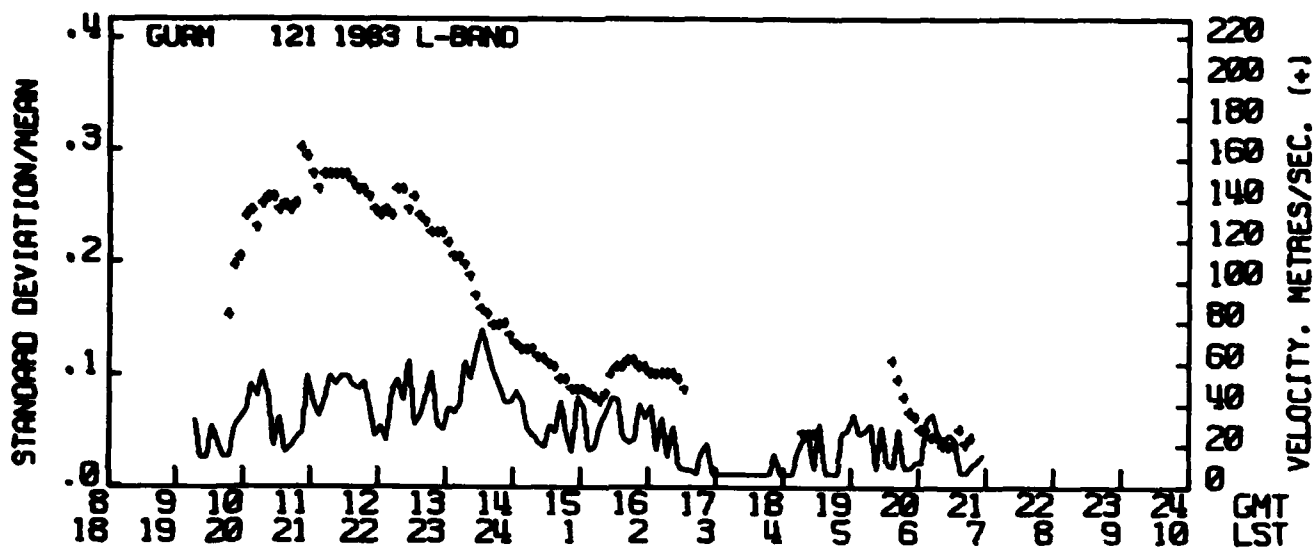


MICROCOPY RESOLUTION TEST CHART
NATIONAL BUREAU OF STANDARDS-1963-A









END

FILMED

3-84

DTIC